NOTE TO USERS

CHARACTERIZATION AND MECHANISM OF INFLUENZA A VIRUS INDUCED CELL DEATH

By

DEMETRIUS MATASSOV

A dissertation submitted to the Graduate Faculty in Biology in partial fulfillment of the requirements for the degree of Doctor of Philosophy, The City University of New York

2005

This manuscript has been read and accepted for the Graduate Faculty in Biology in Satisfaction of the dissertation requirement for the degree of Doctor of Philosophy.

1/24/05
Date

Chair of Examining Committee
Dr. Zahra Zakeri, Queens College

1/28/05
Date

Executive Officer
Dr. Richard L. Chappell

Dr. Timothy Short, Queens College

Dr. Cathy Savage-Dunn, Queens College

Dr. Richard A. Lockshin, St. John's University

Dr. Adolfo Garcia-Sastre, Mount Sinai School Of Medicine

Supervising Committee

The City University of New York

Abstract

CHARACTERIZATION AND MECHANISM OF INFLUENZA A VIRUS INDUCED CELL DEATH

By

DEMETRIUS MATASSOV

Advisor: Professor Zahra Zakeri

Virus induced host cell death is an important process as it contributes to the pathogenesis of the virus. Many viruses can induce cell death by interacting with the host's cell death machinery in different ways. The influenza virus is one such virus whose mechanism of induction of cell death has not been elucidated. The aim of this study was to characterize the type of cell death induced by the influenza virus and determine the cell death components that are activated and/or needed during influenza induced cell death.

Identifying the type of cell death induced by the virus is of great value as it can give insight to the pathways used by the virus to induce cell death. We started our study by characterizing the type of cell death in MDCK (Madin Darby canine kidney) and A549 human lung epithelial cells. We found that in both cell types influenza induced an apoptotic type of cell death albeit with different kinetics. Using UV inactivation of the virus we determined that the induction of cell death required the replication of the virus and not the mere attachment and internalization hence the extrinsic pathway alone may not be the activated target by virus attachment. In this line we showed that the Fas molecule, which is part of the extrinsic cell death pathway, is not necessary for virus induced cell death, but appears to enhance the killing.

We found that mitochondria, which are part of the intrinsic cell death pathway, are altered during influenza induced cell death and contribute to the demise of the cell. With the aid of different knockout cell lines we evaluated the need of certain cell death components associated with mitochondria during influenza induced cell death. Pro-apoptotic Bcl-2 family members BAK, BAX and BIM are not needed for cell death induction by the virus but enhance cell killing by the virus while the anti-apoptotic BCl-2 shows limited protection against influenza induced cell death. P53, another intrinsic cell death component, appears not to be required for cell death but can enhance its activation.

As to the activation of caspases we find that caspases are activated in both A549 and MDCK cells after virus infection, but are not required for the cell killing of the infected cells and are therefore dispensable. Lastly, we show that another class of proteases called cathepsins can affect the level of cell death as well as the replication of the virus.

We have shown from our data that both components of intrinsic and extrinsic pathways are involved in influenza induced cell death. We also show that when different parts of the pathways are deleted the virus still kills the cells perhaps by redirecting its use of other components of the same or other pathways. In addition some of the cell death components also affect the efficiency of viral replication. Our findings give support to the possibility that influenza virus is a good killer since it can use a multitude of different components of the cell death machinery.

ACKNOWLEDGEMENTS

I would like to thank my mentor Dr. Zahra Zakeri for all of her guidance and support during my doctorate education. For having the strength to put up with me and showing me the way of becoming an independent researcher. For being a friend I can turn to and a colleague with good advice.

I wish to thank my committee members: Dr. Timothy Short, Dr. Cathy Savage-Dunn, Dr. Adolfo Garcia-Sastre and Dr. Richard Lockshin for their time, support and input into my thesis. I especially would like to thank Dr. Richard Lockshin for everything he has done above and beyond for me.

I am thankful to my lab comrades: Carlos Penaloza, Ali Shirazian, Yixia Ye, Andleeb Hassam, and Monica Ramirez.

I would like to thank my friends for their support and guidance. They were all an integral part of me completing my thesis: William McIntosh, Tony Lee, Reid Covey, Harmit Kalia, Inez Silva and Nancy Pina.

Words cannot describe how grateful I am to my family's support during my Ph.D. education. Without them I would have not finished. I want to thank my sister Victoria, my brother George, my sister in-law Terri, my grandparents and most of all my mom and dad for their loving support, faith and patience. I truly owe everything to them. They sacrificed a lot for me to reach this point in my life and that is why I love them.

Last but not least Cathy has been source of love and inspiration for me that I am truly grateful. Words can't describe my thanks and love for her support during my thesis. Cathy has always stood by me and has been my foundation of hope. For that I will always love her.

I would like to dedicate this thesis to the loving memory of my beloved friend Eagle, my dog.

TABLE OF CONTENTS

LIST OF ILLUSTRATIONS

Page

Page

Page

Part I. Introduction:

Chapter 1. Biology of Influenza Virus

1.1. Viral Structure and Genome

1.2. Viral Proteins and Functions

1.3. Viral Replication Strategy

Chapter 2. Mechanisms of Cell Death

2.1. Importance of Cell Death

2.2. Different Types of Cell Death

2.2.1. Apoptosis or Type I Cell Death

2.2.2. Autophagic or Lysosomal or Type II Cell Death

2.2.3. Necrosis

2.2.4. Other Types of PCD

2.3. Pathways Involved in Cell Death

2.3.1. Extrinsic Pathway

2.3.1.1. Death Receptors and Their Action

2.3.2. Intrinsic Pathways

2.3.2.1. Mitochondria and Bcl-2 Family

2.3.2.2. p53

2.3.2.3. Caspases

2.3.2.4. Lysosomal proteases: Cathepsins

2.4.Virus Induced Cell Death

Part I. Introduction

Programmed cell death or apoptosis is an important process in that it helps remove unhealthy and diseased cells from an organism to maintain homeostasis. It occurs during embryogenesis and development of the immune system; and it is a normal host response to viral infections to ensure that viral progeny does not spread. There are many viruses that encode proteins that affect apoptosis in a positive or negative manner. Blocking apoptosis by a viral gene product ensures that the virus can maintain viral progeny production, thus establishing a persistent infection in a host. Viruses with anti-cell death abilities can maximize viral production by keeping the host cells alive and allow future propagation of the virus. In contrast, virus induced host cell death is an important process as it contributes to the pathogenesis of the virus. Different viruses may interact with cellular death machinery in different ways. Pro-cell death viruses can replicate quickly and spread easily so induction of cell death may not limit infections. The induction of cell death may also allow avoidance from the immune system by killing cells of the immune system. One virus that activates cell death is the influenza virus. Its importance stems from the fact that influenza viruses are recognized as serious worldwide pathogens for both humans and domestic animals. The molecular mechanism of influenza-induced cell death has not been resolved and is of central importance to this thesis. It appears that this induced cell death contributes to the cytopathogenic effects of the virus. Therefore, it is important to understand how influenza viruses regulate cell death. I will discuss later the importance and pathways of cell death in order to better analyze influenza induced cell death.

Chapter 1. Biology of Influenza Virus

Influenza virus is an enveloped virion with a segmented negative sense single stranded RNA (ssRNA) genome. Influenza viruses belong to the *Orthomyxoviridae* (from the Greek *orthos*, meaning standard, correct and *myxo*, meaning mucous) family, which has three genera: influenza A and B viruses, influenza C and the tick-borne Thogoto-like viruses (unnamed). Much of our discussion will be focused on type A influenza virus since it is an influential and widely studied pathogen. Influenza A viruses are further divided into subtypes based on the antigenic nature of their hemagglutanin (HA 1 – 14) and neuraminidase (NA 1 – 9) glycoproteins (reviewed in Fields et al, 1996).

1.1. Viral Structure and Genome

The influenza virus is an enveloped virus, meaning that the lipid envelope of the virus is derived from the plasma membrane of the infected host cell. The viruses are composed of 0.8% to 1% RNA, 70% protein, 20% lipid and 5% to 8% carbohydrate. Influenza virus particles are highly pleiomorphic, mostly spherical/ovoid, 80-120 nm diameter (reviewed in Compans and Choppin, 1975).

The outer surface of the influenza A particle consists of a lipid envelope from which project two types of glycoprotein spikes: a rod-shaped hemagglutinin, which is ~135Å trimer (HA), and a mushroom shaped neuraminidase, which is ~60Å tetramer (NA). The ratio of HA to NA is approximately 4-5 to 1. The third integral membrane protein is the M2 ion channel protein, for which biochemical evidence indicates a low

copy number present in the virion. The inner side of the envelope is lined by the matrix protein (M), which is the most abundant protein found in the virus. There is no stable lipid-free core other than the ribonucleoprotein (RNP) (Zabedee et al, 1985; Jackson et al, 1991; Hughey et al, 1992).

The 'RNP' (RNA + nucleoprotein) particles appear as flexible rods that exhibit loops at one end and a periodicity of alternating major and minor grooves, suggesting that the structure is formed by a strand that is folded back on itself and then coiled on itself to form a type of twin stranded helix or pan handled shape. The RNPs vary in length depending on the RNA segment (Duesburg, 1969; Pons et al, 1969; Rees and Dimmock, 1981).

The RNPs consist of four proteins and RNA. The nucleoprotein (NP) is the most abundant protein subunit in the nucleoprotein complex and binds to approximately 20 nucleotides. Associated to this complex are the three polymerase (P) polypeptides (PA, PB1 and PB2), which function as an RNA dependent RNA polymerase. The RNP complex in turn is the RNA dependent transcriptase complex (Inglis et al, 1976; Lamb and Choppin, 1976).

The influenza virus has a segmented negative sense ssRNA genome. Influenza A and B viruses each contain eight distinct RNA segments, whereas influenza C viruses contain seven RNA segments. Negative-stranded RNA genomes have to serve two functions: first as a template for synthesis of mRNAs and second as a template for synthesis of the antigenome (+) strand. Influenza viruses provide some remarkable examples of genome diversity: spliced mRNAs and overlapping reading frames (RF),

bicistronic mRNAs and overlapping RF and coupled translation of tandem cistrons (reviewed in Lamb and Choppin, 1983; here and elsewhere Lamb, 1989).

1.2. Viral Proteins and Functions

RNA dependent RNA polymerase complex

The three largest RNA segments (1-3) of influenza A encode three viral polymerase (P) proteins, PB2, PB1 and PA, respectively. The proteins were named based on their behavior on an isoelectric focusing gel: two proteins were basic (PB1 and PB2) and one acidic (PA). These viral proteins together form a complex that is called the viral RNA polymerase and have a variety of enzymatic activities. It appears that each P protein has its own karyophilic (nuclear transport) signal. The function of PB2 is to recognize and bind to the 7mGpppGpNm cap structure at the 5' end of the host cell mRNA molecule and to be used for the priming of influenza transcription. PB1 is responsible for chain initiation and elongation of the viral mRNA. The function of PA is not known (Inglis et al, 1976; Lamb and Choppin, 1976; Horisberger, 1980; Ulmanen et al, 1981; Winter and Fields, 1982).

Recently discovered was a novel 87-residue peptide encoded by the +1 reading frame of PB1 (Chen et al, 2001). This alternative reading-frame peptide designated PB1-F2 has several unusual features compared to other influenza gene products. PB1-F2 has a variable expression in individual infected cells, in some animal (especially swine) influenza virus isolates is absent, readily degraded by the proteasome complex and localizes to the mitochondria (Chen et al, 2001). N- and C-terminal deletion mutants and

site-directed mutagenesis of some basic residues of PB1-F2 revealed a domain from residues 46 to 75 important for mitochondrial localization (Yamada et al, 2004). Transfection of a plasmid encoding PB1-F2 into Vero, HeLa and MDCK cells had altered the overall mitochondrial morphology and lowered the inner mitochondrial membrane potential (Yamada et al, 2004). PB1-F2 had been shown to lead to the destabilization of mitochondrial membranes that leads to release of macromolecular and cell death (Gibbs et al, 2003, Chanturiya et al, 2004). PB1-F2 contains a mitochondrial targeting sequence (MTS) (predicted to form a positively charged amphipathic alpha-helix) and is able to form variably sized stable pores that are inserted into the inner mitochondrial membrane (Gibbs et al, 2003, Chanturiya et al, 2004).

Hemagglutinin Protein

The fourth RNA segment encodes the surface hemagglutinin (HA) glycoprotein. The HA molecule is a type I integral membrane protein that forms a homotrimeric spike of noncovalently linked monomers. It binds to sialic acid containing receptors on cell surfaces during viral attachment, fuses to plasma membranes during penetration in the cytoplasm and is a major antigenic determinant (Porter et al, 1979; Verhoeyen et al, 1980; Lamb, 1989; Nobusawa et al, 1991).

The HA molecule is synthesized as a single polypeptide, H_0, which is post-translationally modified by the addition of oligosaccharides and cleaved into two disulfide linked chains, H_1 and H_2. Cleavage is required for the virus to be infectious and is thus a critical determinant in pathogenecity and spread of infection. A precursor HA molecule that contains the sequence R-XK/R-R is cleaved by the intracellular furin

protease residing in the trans Golgi network (Klenk et al, 1975; Lazarowitz and Choppin, 1975; Klenk and Garten, 1994). Two bilayers of two opposing membranes are fused together by a mechanism requiring a low pH conformational change exposing the fusion peptide in HA (Skehel et al, 1986).

Nucleocapsid Protein

The nucleocapsid protein (NP) is the major structural protein that binds to the negative stranded viral RNA and forms the RNP. The protein is encoded on the fifth RNA segment of influenza A viruses. NP proteins are phosphorylated, but it is not clear what percentage of NP molecules is phosphorylated and whether phosphorylation is essential for function (Privalsky and Penhoet, 1977; Petri and Dimmock, 1981). NP molecules are transported to the nucleus after synthesis in the cytoplasm by the karyophilic signal contained within the protein (Lin and Lai, 1983). The mechanism of assembly is poorly understood. Both virion RNA (- strand) and template (+ strand) RNAs are associated with NP molecules, whereas the viral mRNAs are (+ strand) are not associated with NP molecules (Hay et al, 1977; Pons, 1971; Lamb, 1989).

Neuraminidase Protein

Encoded on RNA segment 6 is the neuraminidase (NA) class II integral membrane protein (Colman, 1989). It is the second glycoprotein of the influenza virion and a major antigenic determinant. NA catalyzes the cleavage of α-ketosidic linkage between a terminal sialic acid and adjacent D-galatose or D-galactosamine (Gottschalk, 1957). The role of NA in the influenza virus life cycle is still unclear. However, it has

been shown that HA removes sialic acid from HA, NA and the cell surface, thus blocking virus aggregation during budding (Palese et al, 1974).

The Matrix and M2 Proteins

RNA segment 7 of influenza A virus encodes two known proteins, the matrix protein (M_1) which lies inside the lipid envelope and constitutes the most abundant polypeptide in the virion, and the M_2 protein, which is a minor component of virions and has ion channel activity (Allen et al, 1980; Lamb and Lai, 1981). Three mRNA transcripts are derived from RNA segment 7: a colinear transcript encoding M_1 protein, a spliced mRNA encoding the M_2 protein and an alternatively spliced mRNA, which encodes a 9 amino acid peptide (Lamb et al, 1981).

The matrix protein underlies the viral lipid envelope and provides rigidity to the membrane. It is also believed that the matrix protein interacts with the HA, NA, and M_2 proteins and with the RNP structure. If the M_1 protein is not dissociated from the RNPs, then the RNPs will fail to be transported to the nucleus (Rees and Dimmock, 1981; Martin and Helenius, 1991).

The M_2 protein is a type III integral membrane protein that is abundant in infected cells but is underrepresented on the mature virion envelope. Once the virion is endocytosed and contained in an endosome, the M_2 protein functions by pumping hydronium ions into the virion, facilitating a conformational change that disrupts the protein-protein bonds holding the virion together (Lamb et al, 1985; Hay, 1992; Holsinger et al, 1994). The result is the dissociation of the matrix proteins from the RNPs.

Non-Structural Proteins

RNA segment 8 encodes two non-structural proteins, NS1 and NS2, where the NS2 mRNA is spliced out of the NS1 mRNA (Inglis and Almond, 1980; Lamb et al 1980; Lamb and Choppin, 1980; Lamb and Lai, 1980).

The NS1 protein is abundant in influenza virus-infected cells but it has not been detected in virions, hence the designation *NS* for *nonstructural* (Lazarowitz et al, 1971; Krug and Etkind, 1973). NS1 is a phosphoprotein that is translated early in infection and primarily located in the nucleus, but also appears late in the cytoplasm (reviewed in Fields et al, 1996). Several functions have been associated with the NS1 protein:

1. The NS1 protein inhibits pre-mRNA splicing by binding to specific splicing factors, e.g. U6 snRNP (Lu et al, 1994).
2. The NS1 protein inhibits mRNA transport out of the nucleus by binding to polyA (Alonso-Caplen et al, 1992; Fortes et al, 1994).
3. The NS1 protein stimulates viral mRNA translation by binding to the 5' untranslated region (UTR) of the viral mRNAs (de la Luna et al, 1995).
4. The NS1 protein inhibits *in vitro* dsRNA-mediated activation of dsRNA-activated protein kinase (PKR) by binding to dsRNA (Lu et al, 1995).
5. NS1 may be an auxiliary virulence factor, playing a crucial role in inhibiting interferon-mediated antiviral responses of the host (Garcia-Sastre et al, 1998).

Two functional domains required for regulating nuclear export of mRNA have been identified in the NS1 protein. A domain near the N-terminal end of NS1 (residues 19 through 38) was shown to be the RNA-binding domain. This domain is not arginine-rich as in some RNA-binding domains and does not even have a high net positive charge. The second NS1 functional domain, which is located in the C-terminal end, can be presumed to be the effector domain that interacts with host nuclear proteins. Influenza viruses can tolerate large C-terminal deletions of NS1 protein, suggesting that the effector domain is not essential for viral replication (reviewed in Fields et al, 1996).

Recent evidence has shown that influenza A viruses expressing C-terminally deleted forms of the NS1 protein (NS1-81 and NS1-110) have a reduction in the accumulation of virion RNA and the synthesis and accumulation of late virus proteins (Falcon et al, 2004). These results indicate that the NS1 protein is essential for nuclear and cytoplasmic steps during the virus cycle (Falcon et al, 2004).

It has been proposed that the NS1 protein has the ability to suppress transcription of interferon-stimulated genes (ISG) and IFNα production. Support for the argument comes from a virus that has the entire NS1 protein deleted (delNS1). It is able to replicate in STAT1 (Signal Transducer and Activator of Transcription 1) knockout mice but unable to grow in wt mice, MDCK cells and eggs. STAT proteins are involved in the induction of interferon in cells. However, delNS1 has the ability to grow in Vero (Green monkey kidney) cells that are adapted to serum-free media. These cells have a genetic defect in interferon production (Emeny and Morgan, 1979). It has been demonstrated that tumor cells resistant to interferon alpha (IFNα) (correlated with a reduction in expression of STAT1) are susceptible to oncolysis by the infection of the delNS1 influenza virus

(Muster et al, 2004). The use of this mutant virus can be exploited to kill human IFN-resistant melanoma cells (Muster et al, 2004).

A mutant NS1 protein defective in the amino-terminal region containing the dsRNA binding was made by substituting alanines for two basic amino acids within NS1 (R38 and K41) that were previously found to be required for RNA binding (Donelan et al, 2003). The recombinant influenza A virus showed increased IFN-beta production in MDCKS cells (Donelan et al, 2003).

Altered NS1 proteins with an impaired RNA-binding function or insertion of a longer foreign sequence did not replicate in murine lungs but was able to induce a Th1-type immune response with high titers of virus-specific serum and mucosal immunoglobulin G2 (IgG2) and IgA, but with lower titers of IgG1 (Ferko et al, 2004). On the contrary, replicating viruses elicited high titers of serum and mucosal IgG1 but less serum IgA. The mutant viruses also induced a rapid local release of proinflammatory cytokines such as interleukin-1beta (IL-1beta) and IL-6 (Ferko et al, 2004). The generation of the mutant RNA binding domains created replication-deficient viruses that were good for making influenza virus vaccines.

Further support of the function of NS1 comes from the inhibition of dsRNA-activated protein kinase (PKR). IFN is able to induce the activation of PKR. In the presence of dsRNA PKR becomes activated and phosphorylates eIF2α. As a result, protein synthesis within the cell is globally blocked. NS1 protein binds to dsRNA and subsequently blocks the activation of dsRNA-activated PKR *in vitro*. For this reason it was suggested that one of the mechanisms employed by the influenza virus to evade the antivirus effects might involve the NS1 protein. This hypothesis might explain why

influenza transfectant viruses containing large deletions in the NS1 protein are capable of replicating efficiently in the interferon deficient Vero cell lines but not in normal host cells.

The lethal H5N1 influenza viruses, unlike other human, avian, and swine influenza viruses, were found to be resistant to the anti-viral effects of interferons and tumor necrosis factor alpha (Seo et al, 2004). This resistance was associated to the action of the NS1 protein and may explain a mechanism for highly virulent viruses (Seo et al, 2004).

New evidence has shown that the NS1 protein of human influenza A virus has an RNA silencing suppression activity in plants, similar to RNA silencing suppressor proteins of plant viruses (Bucher et al, 2004, Delgadillo et al, 2004). NS1 has also been shown to bind to small interfering RNA molecules (siRNAs) and enhance viral pathogenicity (Bucher et al, 2004). The data shows a potential role for NS1 in counteracting innate antiviral responses in mammals by sequestering siRNAs (Bucher et al, 2004, Delgadillo et al, 2004).

It has been proposed that the NS2 protein functions as a nuclear exporting protein, where it facilitates the export of RNPs from the nucleus (O'Neill et al, 1998). As a result it is designated NEP, for nuclear export protein. It has also been found that the NS2 protein is not a non-structural protein but exists in virions and is associated with the M1 protein (Richardson and Akkina, 1991; Yasuda et al, 1993).

Knowing the functions and structures of the various influenza proteins can give insight to how the virus can activate and modulate the components of the cell death pathways. The different interactions by the individual influenza proteins with the host

proteins can provide information to the induction of cell death. For example, PB1, PB2, PA, NP and NS1 are synthesized early during an infection and could be possible inducers of cell death in the infected cells.

1.3. Viral Replication Strategy

Influenza viruses bind to sialic acid residues present on cell surface glycoproteins or glycolipids via the receptor-binding site in the distal tip of the HA molecules. Different influenza viruses have different specificities for sialic acid linked to galactose by α2,6- or α2,3- linkages, and this is dependent on specific residues in the HA receptor-binding pocket. Interaction of HA with sialic acid is of fairly low affinity, but high avidity is probably achieved by multiple low-affinity interactions.

Influenza viruses enter cells by a process of engulfment called *receptor-mediated endocytosis*. Following internalization, the vesicle fuses with endosomes, where uncoating of influenza virus is dependent on the acidic pH of this compartment. For the influenza virus RNPs to penetrate into the cytosol, they have to cross the membrane of the virion and that of endosomes (Matlin et al, 1982; Marsh and Helenius, 1989).

Negative-strand RNA viruses encode and package their own RNA-dependent RNA transcriptase, but mRNAs are synthesized only after the virus has uncoated in the infected cell. Viral replication occurs after synthesis of the mRNAs and requires synthesis of viral proteins. Among the RNA viruses, influenza virus is very special in that all of its RNA synthesis–transcription and replication–takes place in the nucleus of the infected cell.

Genome segments are transcribed by the 3 polymerase polypeptides associated with each genome segment. During the initial phase of influenza infection (~2h), active host DNA synthesis is required and the replication of the virus is prevented by UV exposure, but not thereafter (Abraham, 1979). The reason is that in the initial step of replication PB2 attaches to the m^7GpppXm cap of host mRNAs. This structure is cleaved from the host mRNA by PB2, and serves as a primer for viral RNA synthesis where 11-15 nucleotides (complementary to the conserved sequence at the 3' end of the vRNA) are added by PB1, after which PB2 dissociates from the growing strand; these structures can be isolated from infected cells. PB1 + PA then complete the synthesis of the (+) sense strand (Fields et al, 1996; Mikulasova et al, 2000; Neumann et al, 2004).

Two classes of (+) sense RNA are made in infected cells:

- Incomplete, 3' polyadenylated transcripts that are exported to the cytoplasm and serve as mRNAs (due to the presence of a specific polyadenylation sequence ~20nt from the 5' end of the (-) sense vRNA template strand)

- cRNA = complete, non-polyadenylated (+) sense copies of the (-) sense vRNA (made by readthrough of the polyadenylation signal) which serve as template for the synthesis of progeny (-) sense vRNAs.

In addition to stealing caps, influenza virus mRNAs make use of another aspect of host cell nuclear function, namely, the splicing machinery. Influenza virus mRNA

transcripts provide one example of splicing of RNA that is not transcribed from DNA by RNA polymerase II. Similar splicing of RNA is seen in the Borna virus.

Most of the proteins made (e.g. HA, NA) remain in the cytoplasm or become associated with the cell membrane. However, the NP protein migrates back into the nucleus, where it associates with newly-synthesized vRNA to form new nucleocapsids. These nucleocapsids migrate back out into the cytoplasm and towards the cell membrane (mechanism unclear). The level of free nucleoprotein (NP) is thought to control whether mRNA or cRNA is produced because later in infection there is lots of NP, and mRNA synthesis stops but cRNA synthesis continues. NP is thus a crucial switch in the replication cycle between expression and assembly. Shut-off of host cell protein synthesis is complete by about 3 hours post infection (Fields et al, 1996; Neumann et al, 2004).

The packaging mechanism responsible for sorting eight distinct genome segments into each virus is not known. However, it has been found that greater than eight RNA segments can be packaged into a virus with the exact number of extra RNA segments not known. In addition, there is some evidence that the sorting of genome segments is not a purely random process (Duhaut and McCauley, 1996). Under conditions in which virions are limiting vRNAs compete for packaging but do so in a nonspecific manner and each influenza A virus virion must package an average of 9 to 11 vRNAs (Bancroft and Parslow, 2002). The first step described in the process of viral RNA packaging appears to be the recognition of a specific RNA packaging signal by the virus's nucleocapsid (N) protein (Narayanan et al, 2003). Influenza A viruses with deleted HA and NA cytoplasmic tails showed reduced vRNA to protein content and altered morphology

indicating that the HA and NA cytoplasmic tails affect not only virion morphology but also proper genome packaging (Zhang et al, 2000).

Influenza viruses are released from the infected cell by budding off the host plasma membrane and not from the cell lysing. Approximately 4h after infection, patches of M1 protein form on the cell membrane, which appears to thicken, incorporating HA and NA on the outside of the membrane. The nucleocapsid segments are incorporated into the particle as it buds out through the membrane. NA is thought to have a role in release of budding particles, since budding is inhibited by anti-NA antibodies. Host-cell membrane proteins appear to be excluded from virions. Virus particles are gradually released from the surface of the cell over a period of several hours before the cell eventually die. The molecular process of how the virus kills the cell is not known and is under current debate. The death of the cell is the focus of this research. There are still many questions on how the virus is able to induce cell death in the infected cell. Before one can understand the induction of viral induced cell death a general understanding of cell death is needed and will be discussed below.

Chapter 2. Mechanisms of Cell Death

2.1. Importance of Cell Death

Cell death is an important biological process that serves as a major mechanism for the regulation of cell numbers and as a defense mechanism to remove unwanted and potentially dangerous cells (Rossi and Gaidano, 2003; Debatin, 2004). Failure of cells to die is seen in some cancers and autoimmune disorders. Conversely, an abnormal increase in cell death is observed in neurodegenerative disorders and ischemic injury. Therefore, an understanding of the regulation of the machinery of cell death is of great value. Since the theme of this thesis involves virus-induced cell death an understanding of the importance, types and pathways of cell death will enable better insight into this topic of research. We begin our discussion on the importance of cell death during development, homeostasis and pathogenesis.

Cell death during the development of the nervous and immune system allows the removal of superfluous cells and the proper functioning of these systems. During vertebrate brain development, nerve growth factor withdrawal induced cell death allows the appropriate connections between neurons to occur and helps with the formation of the overall architecture of the nervous system network (Oppenheim, 1991). In the immune system, the death of the majority of developing B cells removes cells with improper gene rearrangements, anti-self expression or lack of stimulation by interleukins (Gercel-Taylor et al, 2002).

In all normal tissues, cell proliferation and cell death are finely balanced and any disruption alters the homeostasis. Blood and skin cells, for instance, are constantly renewed by their respective progenitor cells; but this proliferation has to be compensated by cell death. The activation of cell death allows an organism to control the cell number and the tissue size, and to protect itself from harmful cells that threaten homeostasis (Barisic et al, 2003). An example of this delicate balance is seen during differentiation of hemopoietic stem cells to mature erythrocytes (Testa, 2004). Cells during differentiation become progressively sensitive to erythropoietin, which controls both the survival and proliferation of erythroid cells. The immune system is another example of this delicate balance between cell proliferation and cell death. B cell death ensures that newly produced B cells have functional receptors and do not recognize self-antigens with high avidity. Cell death is triggered in lymphocytes when the pool of survival factor signals (e.g., IL-3 and IL-4) is limited (Khaled and Durum, 2002). This process has been termed "clonal abortion" (von Boehmer, 1994).

As cell death is critical for the development and maintenance of homeostasis in healthy tissues, its dysregulation can lead to pathogenesis and disease. For example, excessive levels of cell death contribute to neurodegenerative disorders (Ross and Poirier, 2004; Bossy-Wetzel et al, 2004) such as Alzheimer's disease (Campion et al, 1995), Huntington's disease (Sawa et al, 2003; Browne and Beal, 2004) and spinal muscular atrophy (Morris, 2000); to vascular diseases (Jaeschke and Lemasters, 2003; Eefting et al, 2004) and AIDS (acquired immunodeficiency syndrome), in the case of human immunodeficiency virus (HIV) (Krzyzowska et al, 2000). During an HIV infection, an elevation of cell death in both CD4+ and CD8+ cells occurs due to T cell activation,

which leads to an impairment in the immune system and AIDS (Galati et al, 2002). In contrast, reduced levels of cell death lead to the development of cancer (Green and Evan, 2002; Vogelstein and Kinzler, 2004; Zhivotovsky and Kroemer, 2004), autoimmune diseases such as lupus (White and Rosen, 2003; Sheriff et al, 2004) and rheumatoid arthritis (Liu and Pope, 2004), persistent infections such as by adenovirus (Braithwaite and Russell, 2001; Lichtenstein et al, 2004) and herpes virus (Aubert and Blaho, 2001; Goodkin et al, 2004) and other diseases.

Cells possess an intrinsic ability to self-destruct by the activation of a cell suicide program. Most cells maintain the program in readiness and activate cell death in response to specific, often pathological, stimuli. As mentioned above cell death is important during development, homeostasis and removal of unwanted and potentially dangerous cells, such as potentially cancerous cells, self-reactive lymphocytes, or cells that have been infected by viruses.

A dying cell can display a variety of different morphological and biochemical characteristics that are distinct from each other, indicating that there are different types of cell death. These different types of cell death will be discussed in more detail below.

2.2. Different Types of Cell Death

As mentioned above cell death plays an important role during development, homeostasis and pathogenesis. Cell death can be triggered by a variety of stimuli, including withdrawal of essential growth factors, treatment with glucocorticoids, γ-irradiation, certain pathogens and activation of certain external receptors (Rossi and

Gaidano, 2003). With the activation of cell death cells can undergo different types of death involving many different death pathways, recognized by their distinct morphological and biochemical characteristics.

Cell death has been morphologically differentiated into physiological cell death and necrosis (Kerr, 1969; Kerr et al, 1972; Searle, 1975; Wyllie et al, 1980; Wyllie, 1987). Physiological cell death, a very well controlled process, has been most often referred to as programmed cell death (PCD) (Lockshin, 1969). The term PCD implies a predictable sequence of steps in target cells under a genetic control. Classically its morphology has been divided into two types, i.e., apoptosis or type I cell death, and lysosomal or type II cell death (Kerr, 1965; Kerr, 1971; Schweichel and Merker, 1973; Clarke, 1990; Zakeri et al, 1993; Okada and Mak, 2004).

2.2.1. Apoptosis or Type I Cell Death

Type I or classical apoptotic cell death is characterized by morphological changes that include the rapid condensation of the cytoplasm and nuclear chromatin, resulting in DNA and chromatin fragmentation as well as blebbing of the cell membrane surface, followed by the formation of apoptotic bodies, phagocytosis, and secondary lysosomal degradation of fragments by phagocytes or neighboring cells (Kerr et al, 1965; Kerr, 1971; 1972). During apoptotic cell death, the dying cell begins to round and reduce in volume and size, while the plasma membrane still maintains its integrity (Kerr et al, 1972). Apoptosis is usually associated with the activation of nucleases that degrade the chromosomal DNA into large (50 to 300 kilobases) and subsequently into very small

oligonucleosomal fragments (Wyllie, 1980; Wyllie et al, 1984). These small fragments when electrophoresed on an agarose gel give the hallmark DNA laddering pattern that occurs during classical apoptosis (Cohen et al, 1994). During nuclear condensation in a dying cell, the chromatin condenses and begins to migrate along the nuclear membrane by a process called nuclear margination (Wyllie, 1980; Wyllie et al, 1981; Ziegler and Groscurth, 2004).

Another hallmark of apoptosis is the activation of a class of cysteine proteases called caspases, which are responsible for propagating the cell death signal within the cell, the degradation of certain cellular proteins, and reorganization of the cytoskeleton. During apoptosis, depolarization and cleavage of actin, cytokeratins, lamins and other cytoskeletal proteins typically occurs (Bursch et al, 2000). The cleavage of poly(ADP-ribosyl) polymerase (PARP) has also been shown to be an important marker for caspase activity, specifically for caspase-3 activity (Soldani and Scovassi, 2002). Cell death can occur even when caspases are inhibited but the lack of caspase activity abolishes the apoptotic changes in a cell; classical apoptosis is caspase-dependent (Leist and Jaattela, 2001; Glassford et al, 2002). The involvement of these and other proteases will be discussed in more detail below.

Mitochondria, in addition to their role in respiration, are also involved in initiation and execution of apoptosis, an activity that is controlled by Bcl-2 (B-cell lymphoma-2) family proteins (Singh, 2004) as will be discussed in more detail below. Mitochondrial function appears to be critical in some cells for executing a death program, and activation of these cellular organelles is a crucial step for coordinating and integrating several upstream and downstream apoptotic pathways (Schultz and Harrington, 2003).

During the later stages of apoptosis dying cells begin to fragment and form apoptotic bodies that are taken up by neighboring cells by the process of phagocytosis (Duvall et al, 1985; Savill and Fadok, 2000). The lipid distribution between the outer and inner leaflets of the plasma membrane enclosing the apoptotic bodies is critical for elimination of these cellular remnants. Phosphatidylserine, normally present in the inner leaflet and excluded from the outer leaflet, is exposed in the outer leaflet of apoptotic bodies. The presence of phosphatidylserine in the outer leaflet (as detected by Annexin V) marks apoptotic bodies for elimination by phagocytic cells (Duvall et al, 1985; Fadok et al, 1992; reviewed in Savill and Fadok, 2000). Thus, the process of apoptosis does not elicit an inflammatory response.

Apoptosis is biochemically defined as an energy-requiring process since energy is needed to propagate the signal and achieve the apoptotic morphology in a cell (Nicotera et al, 2000; Lang-Rollin et al, 2003). However, in situations where the required energy is not found the whole apoptotic process can halt and continue via a different mechanism (for review, see Zakeri and Lockshin, 2002). It appears also that a requirement for macromolecular synthesis and *de novo* gene transcription (Wyllie et al, 1984; Lockshin and Zakeri, 1992) has been identified.

2.2.2. Autophagic or Lysosomal or Type II Cell Death

For many years apoptosis has been of great interest to the scientific community, and much has been learned about its mechanism. However, PCD is confined not only to apoptosis: morphological and biochemical data suggest that autophagic, type II or

lysosomal cell death is important in PCD as well (Lockshin, 1973; Schweichel and Merker, 1973).

Autophagic cell death is a phylogenetically old phenomenon, as it has been observed in the slime mold *Dictyostelium discoideum* (Cornillon et al, 1994), in *C. elegans* (Hall et al, 1997), and in other invertebrates and vertebrates. Autophagy occurs usually in quiescent or postmitotic cells that are large and have massive cytoplasm, such as muscle (Beaulaton and Lockshin, 1977), larval midgut (Lee et al, 2002) and glandular tissues at metamorphosis (Jochova et al, 1997). Activation of autophagic PCD results in the massive elimination of many cells during a developmental program or cell injury.

The characteristics of autophagic cell death appear distinct from apoptosis although many apoptotic changes eventually develop. One of the most prominent features of autophagic PCD is the formation of numerous large vacuoles in the cytoplasm of dying cells. These autophagic vacuoles are formed as a result of a fusion between late autophagasomes and lysosomes (Cuervo, 2004). 3-methyladenine (3-MA) blocks the formation of autophagic vacuoles and the eventual death of cells like tamoxifen treated human mammary carcinoma cells (MCF-7) (Bursch et al, 1996), gastric and glioma cells overexpressing Ras (Chi et al, 1999), neuronal cells deprived of NGF (Xue et al, 1999), and kidney cells exposed to bacterial toxins (i.e. Shiga and diphtheria toxins) (Seglen and Jordan, 1982; Sandvig and van Deurs, 1992). As in type I PCD (apoptosis), the membrane stays intact and cell death does not elicit an inflammatory response.

Another very prominent characteristic is the degradation of cytoplasmic components prior to any nuclear changes (i.e. condensation and fragmentation of the nuclei), which usually occurs at the late stages of death (Bursch et al, 2001; reviewed in

Marino and Lopez-Otin, 2003; Wang and Klionsky, 2003; Cuervo, 2004). Autophagic PCD is exemplified by the labial gland of *Manduca sexta* and intersegmental muscle of silkmoths (Lockshin and Williams, 1965; Lockshin and Beaulaton, 1974; Beaulaton and Lockshin, 1977; Halaby et al, 1994; Zakeri et al, 1995). Biochemical evidence suggests that the state of the cytoskeleton in dying cells exhibits different fates according to the type of death. In autophagic PCD the cytoskeleton is redistributed but mainly preserved as seen in MCF-7 cells treated with tamoxifen as compared to in apoptotic cells where the cytoskeleton is completely depolymerized (Bursch et al, 2000). Even though there are drastic cytoplasmic changes occurring during autophagy, the cell's organelles remain intact and functional. Mitochondria appear intact and maintain ATP-levels required for the completion of autodigestion (Lang-Rollin et al, 2003).

During autophagy, caspase activity is not needed to cause the distinct phenotype seen in this type of death. A class of cysteine proteases called cathepsins is activated during autophagy and will be discussed in more detail later, but briefly these enzymes reside within lysosomes and their proteolytic activity can degrade proteins as well as activate several caspases. The activity of these enzymes is restricted not only to autophagy but can also be seen in apoptosis and necrotic cell death (Turk et al, 2001; Turk and Gunčar, 2003; Yu et al, 2004).

Autophagic death and apoptosis are not mutually exclusive as it has been found that both types of death can occur simultaneously in tissues and the dying cells can share apoptotic and autophagic characteristics (Xue et al, 1999; Bursch, 2001; Lockshin and Zakeri, 2004; Edinger and Thompson, 2004). This may be a feature of what we see in influenza induced cell death as suggested by our data, presented in the next section.

2.2.3. Necrosis

In contrast to physiological cell death, necrosis appears to be death out of control, with the damage to the cell membrane as its major marker, leading to the loss of membrane integrity and ion homeostasis (Syntichaki and Tavernarakis, 2002). Necrotic cell death has been presumed to be unregulated and not under genetic control. However, it has been found that necrosis may not be completely unregulated as first suspected (Kitanaka and Kuchino, 1999; Syntichaki and Tavernarakis, 2002; Okada and Mak, 2004). Generally necrosis is thought to be a passive process that does not require energy or new protein or mRNA synthesis (Nicotera et al, 1999; Van Cruchten and Van Den Broeck, 2002). For example in humans, necrosis has been found during hypoxia, toxin exposure, ischemia and amyotrophic lateral sclerosis (Walker et al, 1988; Price et al, 1999). Necrosis is a pathological form of cell death that results from massive cellular trauma. Cells swell and lyse, thereby releasing their cytoplasmic contents, which often cause inflammatory responses and organ damage. Clumpy, ill-defined aggregation of chromatin and random length DNA fragments also occur in necrotic cells. Most organelles of the dying cell show signs of membrane permeabilization and rupture. It has been shown that mitochondria, the endoplasmic reticulum (ER) and lysosomes are altered in necrotic cells (Ferri and Kroemer, 2001; Ziegler and Groscurth, 2004). Low ATP concentrations or impaired ATP generation can push the morphology of cell death toward necrosis indicating that mitochondrial dysfunction is of importance during necrosis. The dilation and increased permeability of mitochondria during necrosis can contribute to the

decline in ATP (Nicotera et al, 1998; Leist and Jaattela, 2001). Ribosomes may dissociate and ER sequestered Ca^{++} may be released into the cytoplasm, thereby increasing cytoplasmic levels of Ca^{++} and activating calpain, a protease that can activate other proteases (Syntichaki and Tavernarakis, 2002). Lysosomes or "suicide bags" as they are sometimes called, contain over 80 types of hydrolytic enzymes. When these enzymes are released due to lysosomal membrane permeabilization or rupture, necrotic cell death occurs in heart and brain ischemic injuries (Adamec et al, 2000). Cells undergoing apoptosis can convert to necrosis, which is referred to as secondary necrosis (Muppidi et al, 2004).

2.2.4. Other Types of PCD

As mentioned above, cells can die by any of the three major types of death as apoptosis, necrosis and autophagy, each of which leads to different morphological and biochemical characteristics. However cells may also undergo cell death that is different from the three major types. There are many intermediate types of cell death that can occur and most likely there is a continuum between the major pathways of cell death. Intermediates could be variations in the degree of chromatin condensation and margination or the extent of blebbing (Leist and Jaattela, 2001; and see review Lockshin and Zakeri, 2002).

The variants have been termed apoptotic-like or necrotic-like cell death. The characteristic of apoptosis-like cell death involves chromatin condensation that is less compact or complete, electron dense and complex than that seen in apoptosis. The

display of the phagocytosis recognition signal molecules nevertheless occurs before lysis of the plasma membrane (Hirt et al, 2000). Other features of apoptosis can occur at various degrees and combinations. As mitochondria lose their membrane potential ($\Delta\Psi_m$) the release of AIF (apoptosis inducing factor) into the cytoplasm can trigger apoptosis-like cell death (Lorenzo et al, 1999; Susin et al, 1999). Depletion of heat shock protein – 70 (Hsp-70) in MCF-7 cells can activate apoptosis-like cell death (Nylandsted et al, 2000). During apoptosis-like cell death the activation of caspases does not occur instead other proteases are activated such as cathepsins, calpains and serine proteases (Leist and Jaattela, 2001; Abraham and Shaham, 2004). Apoptosis-like cell death is regarded to as being caspase-independent cell death because cells can die without the activation of caspases.

Another alternative type of cell death is defined as necrotic-like cell death. Here the cell dies in the absence of chromatin condensation or clustering of the chromatin to form speckles (Leist and Jaattela, 2001). Varying degrees of apoptosis-like features can occur such as externalization of phosphatidylserine prior to cell lysis. Necrotic-like cell death involves caspase-independent pathways. However, activation of caspase – 1 and – 8 may occur (Leist and Jaattela, 2001). Necrotic-like cell death has been classified as "aborted apoptosis" (Mathiasen and Jaattela, 2002) and is the result of active cellular processes that are interrupted with oxygen-radical scavengers (Vercammen et al, 1998), inhibition of the DNA repair protein poly(ADP)-ribose polymerase (PARP) (Ha et al, 1999) or mutations in intracellular signaling molecules (Holler et al, 2000).

Characterization of the different modes of cell death by the identification of the varying degrees in biochemical and morphological markers allows a better understanding

of the mechanism of cell death. The mode of cell death could have a differential effect on surrounding tissues and organs (Savill and Fadok, 2000) and may control the horizontal spread of oncogenic inflammation and infection (Boise and Collins, 2001). Here, we are investigating the mechanism of influenza induced cell death. Identifying the mode of cell death in our model systems is crucial to determine the mechanism by which the virus kills the cell.

2.3. Pathways Involved in Cell Death

As the number of identified gene products associated with cell death increases so does the complexity of their interactions. The gene products go through specific independent signaling pathways that lead to induction and progression of cell death. Activation of these death pathways can either be initiated from within (intrinsic) or from the outside (extrinsic). There are many components identified in the different pathways leading to cell death and some of them pertinent to our investigation will be discussed below.

2.3.1. Extrinsic Pathway:

The extrinsic pathway is defined by the involvement of an external stimulus that acts upon the cell, thereby activating an internal cellular response, which results in the activation of the cell's innate cell death machinery. The external death signal is propagated within the cell by specific death receptors that are found on the outer plasma

membrane of the cell. The death cue is actually the ligand of the death receptor and the interaction of the two activates the receptor. The activation of the receptor transmits the death cue inside the cell and initiates the recruitment of cell death components, which in turn activate a proteolytic cascade that kills the cell. The details of this pathway are discussed in more detail below.

2.3.1.1. Death Receptors and Their Action:

The tumor necrosis factor (TNF) family of receptors (TNFR) is characterized by homology in the extracellular domains. At least 16 members of the TNF ligand family have been identified. Some of these receptors initiate apoptosis, some initiate cell proliferation and some initiate both (Schultz and Harrington, 2003). The cell surface receptors that transmit apoptotic signals initiated by ligation with a specific antibody or by the natural ligands are called death receptors (DR) and play a central role in induction of apoptosis (Schultz and Harrington, 2003; Porter and Dhakshinamoorthy, 2004).

Six different DRs characterized by a conserved extracellular cysteine-rich motif are known: Fas, TNFR1, DR3, DR4 (TRAIL-R1), DR5 (TRAIL-R2), and DR6 (Rossi and Gaidano, 2003). The ligands of these receptors form a family of related cytokines also named TNF family, containing TNFα, lymphotoxin (LTα), Fas-Ligand (FasL), Apo3-Ligand (Apo-3-L), and TRAIL (TNF-related apoptosis-inducing ligand) (Rossi and Gaidano, 2003) (Figure 1, see pg 53).

The activation of the apoptotic pathway is initiated by the trimerization of the DR to its specific protein ligand. Upon activation, these DRs transmit signals via a death

domain (DD) (80-amino-acid domain) in their cytoplasmic tail and by the recruitment of specific adaptor proteins activate cytosolic cysteine proteases (caspases), as described below. Besides carrying the DD, adaptor proteins also contain a death effector domain (DED), which is involved in the next step of apoptotic signaling along the extrinsic pathway described in the next paragraph.

The FasR-FasL and TRAIL-DR4/DR5 pathways represent two specific examples of the extrinsic apoptotic signaling pathway in cells. The Fas receptor (FasR) is a 319-amino acid type 1 transmembrane glycoprotein, with broad distribution on both lymphoid and nonlymphoid cells (Itoh et al, 1991; Debatin, 2004). FasL is a version of the general class of FasR, and is a trimeric type 2 transmembrane protein that is primarily expressed by activated $CD4^+$ and $CD8^+$ T cells. It is released in soluble form after cleavage from its membrane site by metalloproteinases before binding FasR (Suda et al, 1993; Tanaka, et al 1995). The FasR is crucial for the signaling of apoptosis as well as the activation of the transcription factor nuclear factor (NF)-κB (Rossi and Gaidano, 2003). An apoptotic signal is initiated in target cells when FasR is joined by its natural ligand FasL or by agonistic antibodies. The interaction may occur on the effector cell, or in some cases, on the same cell (Zimmermann et al, 2001). The FasR-FasL interaction causes receptor oligomerization and the DD of the receptor then recruits adaptor proteins that also have DDs. One such protein is Fas-Associated Death Domain (FADD) protein, which has a DD at its C-terminus and a second protein-protein interaction domain called the Death Effector Domain (DED), at its N-terminus (Chinnaiyan et al, 1996; Muzio et al, 1996; Okada and Mak, 2004) (Figure 1). Other adaptor proteins include TRADD (TNF receptor

associated DD), DAXX, RIP (receptor interacting protein kinase), and RAIDD (RIP associated protein with a DD) (Degterev et al, 2003) (Table 1).

Death Receptors	Death Ligands	Adaptor Proteins
FasR	FasL	FADD
TNFR1	TNFα	TRADD
DR3	lymphotoxin (LTα)	DAXX
DR4 (TRAIL-R1)	TRAIL	RIP
DR5 (TRAIL-R2)	Apo-3-L	RAIDD
DR6		

Table 1. Receptors, ligands and adaptors used during extrinsic cell death pathways. Abbreviations: FasR, Fas receptor, TNFR1, tumor necrosis factor receptor 1; DR, death receptor; FasL, Fas-Ligand; TRAIL, TNF-related apoptosis-inducing ligand; FADD, Fas-Associated Death Domain; TRADD, TNF receptor associated DD; RIP, receptor interacting protein kinase; RAIDD, RIP associated protein with a DD; DD, death domain

The DED in the adaptor protein binds to the DED that is located in the prodomain of an inactive initiator caspase (or procaspase) and forms a complex called the death inducing signaling complex (DISC). The result is the activation of the initiator caspase and the

start of the proteolytic cascade. For example, FADD recruits the initiator procaspase-8 by homophilic interactions between the death effector domains of each protein (Rossi and Gaidano, 2003). The activation of caspase-8 then activates a series of downstream caspases that result in cleavage of structural and regulatory intracellular proteins, ultimately leading to apoptosis.

TRAIL, like FasL, is primarily expressed as a membrane protein. However there is evidence that a soluble form may also exist (Wajant et al, 2002). TRAIL can interact with five distinct death receptors belonging to the TNFR family. Two of these receptors, DR4 and DR5, both contain a cytoplasmic DD and can elicit apoptosis when activated by TRAIL. Both TRAIL and the DR4 and DR5 receptors are widely expressed in tissues. Activation of the DR4 and DR5 receptors by TRAIL results in the formation of the DISC complex through recruitment of FADD and subsequent activation of caspase-8, which in turn initiates the proteolytic caspase cascade. The activation of the proteolytic cascade can also be activated by an intrinsic cell death pathway, which will be discussed below.

2.3.2. Intrinsic Pathways:

The intrinsic pathway involves an internal stimulus such as DNA damage, withdrawal of growth factors, or chemotherapeutic agents all of which induce cell death by the participation of mitochondria. Mitochondria provide an intrinsic connection for the activation of the proteolytic cascade or the activation of a pathway independent of caspases. At the initiation of apoptosis, mitochondria can release into the cytoplasm several pro-apoptotic factors sequestered within the inner mitochondrial space, such as

cytochrome c. Cytochrome c can participate in the activation of procaspase-9, which subsequently activates procaspase-3, -6 and –7. Mitochondrial function is regulated by the Bcl-2 family members, which exhibit either pro- or anti-apoptotic properties and represent a pathway independent of caspases. Mitochondria are not the only organelles involved in the intrinsic pathway; lysosomes may be involved as well. Within lysosomes are a set of proteases called cathepsins that are mediators of caspase-independent cell death. The different components of the intrinsic pathway will be discussed in more detail below.

2.3.2.1. Mitochondria and Bcl-2 Family

Mitochondria are known to be key players in apoptotic cell death (Mattson and Kroemer, 2003; Goldenthal and Marin-Garcia, 2004; Polster and Fiskum, 2004). Mitochondria provide an intrinsic connection for the activation of the proteolytic cascade or the activation of a pathway independent of caspases. Mitochondria have two membranes with an intermembrane space between the outer and inner membrane. Between these mitochondrial membranes is an electrical potential generated by the actions of the proton pumps embedded in the inner mitochondrial membrane. Inside the intermembrane space are a variety of proteins that are involved in cell death. Also many proteins that are integrated in the outer membrane have a role during cell death (Alberts et al, 2002).

Beside changes in the nucleus during apoptosis, the mitochondria undergo some changes as well. For the most part the structure of the mitochondria remains normal to

slightly shrunken; they do not swell during apoptosis (Sesso et al, 2004). However mitochondria in dying cells exhibit increased permeability of the inner membrane resulting in the loss of mitochondrial membrane potential ($\Delta\Psi_m$) and depolarization and uncoupling of oxidative phosphorylation (Kroemer et al, 1995; Zamzami et al, 1995; Düßmann et al, 2003; Perl et al, 2004). As a consequence of this mitochondria can release into the cytoplasm several pro-apoptotic factors sequestered within the inner mitochondrial space, such as cytochrome c (Jiang and Wang, 2004), apoptosis-inducing factor (AIF) (Zamzami et al, 1996; Daugas et al, 2000; Cregan et al, 2004), second mitochondrial activator of caspases (Smac) (Wilkinson, 2004), direct IAP binding protein with Low pI (Diablo) (Verhagen et al, 2000), high temperature requirement (HtrA2) or Omi (Suzuki et al, 2001), endonuclease G (Arnoult et al, 2003), caspase-2 (Enoksson, 2004) and caspase-9 (Ravagnan et al, 2002; Debatin, 2004), and in turn these factors aid in the destruction of the cell by blocking anti-apoptotic factors, activating caspases (Hill et al, 2003; Lorenzo and Susin, 2004; Polster and Fiskum, 2004) and degrading DNA (Liu, 2004) (Figure 2, pg 56). Normally, cytochrome c is localized in the intermembrane space, loosely attached to the outer surface of the inner mitochondrial membrane and released when the membrane permeability of the mitochondria increases (Hancock et al, 2001). The release of cytochrome c into the cytosol triggers the formation and activation of the apoptosome complex, which includes the apoptotic protease activating factor-1 (Apaf-1) bound to cytochrome-c and procaspase-9 (Ravagnan et al, 2002).

The activation of the apoptosome activates caspase-9, which in turn activates caspase-3. Smac/Diablo and Omi/HtrA2 promote caspase activation by neutralizing the inhibitory effects on inhibitory apoptosis proteins (IAPs), while AIF and endonuclease G

cause DNA condensation (Debatin, 2004). The mechanism of how sequestered factors are released from the mitochondria is unclear but two models have been proposed. The first argues that during apoptosis a megapore, called the mitochondrial permeability transition (MPT) pore, is formed that spans the inner and outer mitochondrial membranes. The inner membrane is characterized by a transmembrane potential ($\Delta\Psi_m$) generated through the activity of proton pumps of the respiratory chain. $\Delta\Psi_m$ dissipates after the cells are induced to die (Zamzami and Kroemer, 2001; Kroemer, 2003). The MPT includes the voltage-dependent anion channels (VDAC) in the outer membrane and the adenine-nucleotide translocase (ANT) in the inner membrane (Jiang and Wang, 2004). This pore allows solutes and water to enter causing the mitochondrion to swell and rupture its outer membrane, thus releasing its contents. Opening of the MPT pore causes increased permeability of the inner membrane, loss of mitochondrial membrane potential ($\Delta\Psi_m$), depolarization and uncoupling of oxidative phosphorylation and the release of cytochrome c (Kroemer, 2003). The second model states that proapoptotic Bcl-2 family members, such as Bax and Bak, form a channel and selectively mediate the release of cytochrome c into the cytosol without causing mitochondrial swelling and alteration of function (Mattson and Kroemer, 2003).

Induction of the mitochondrial membrane permeabilization (MMP) is a major event in apoptosis (Kroemer, 2003). The MMP precedes other, non-mitochondrial signs of apoptosis. Thus, the dissipation of the mitochondrial transmembrane potential ($\Delta\Psi_m$) is an early event of cell death (Kroemer, 2003). Cells that have disrupted their $\Delta\Psi_m$ are irreversibly committed to undergo death, even when the apoptosis-inducing trigger is

withdrawn. MMP (and in particular the $\Delta\Psi_m$ collapse) marks the point-of-no-return of cell death.

Bcl-2 (B-cell lymphoma-2) family proteins play a pivotal role in the regulation of the mitochondrial pathway, since these proteins localize to intracellular membranes, in particular the mitochondrial membrane (Antonsson and Martinou, 2000). Bcl-2 was first discovered as a proto-oncogene in follicular B-cell lymphoma. Subsequently, it was identified as a mammalian homologue to the apoptosis repressor *ced-9* in *C. elegans*. Since then, at least 19 Bcl-2 family members have been identified in mammalian cells. These members possess at least one of four conserved motifs known as Bcl-2 homology domains (BH1-BH4). The Bcl-2 family members can be subdivided into three categories according to their function and structure (Adams and Cory, 2001; Zimmermann, 2001; Sprick and Walczak, 2004):

(1) Anti-apoptotic members, such as Bcl-2, Bcl-XL, Bcl-w, Mcl-1, A1 (Bfl-1), NR-13, and Boo (Diva), all of which exert anti-cell death activity and contain at least BH1 and BH2 (those most similar to Bcl-2 contain all four BH domains). Viral members of this group include E1B-19K, BHRF1, KS-Bcl-2, ORF16, and LMW5-HL.

(2) Pro-apoptotic members, such as Bax, Bak, and Bok (Mtd), which share sequence homology in BH1, BH2, and BH3, but not in BH4.

(3) BH3-only pro-apoptotic members, which include Bid, Bad, Bim, Bik, Blk, Hrk (DP5), Bnip3, BimL, and Noxa, and possess only the central short BH3 domain.

Upon induction of apoptosis, pro-apoptotic Bcl-2 proteins with multidomains such as Bax translocate from the cytoplasm to the outer mitochondrial membrane, where some argue that they oligomerize to form a pore-like structure, thereby promoting cytochrome-c release (Debatin, 2004). Bcl-2 or Bcl-XL exert their anti-apoptotic function, at least in part, by sequestering BH-3 domain-only proteins in stable mitochondrial complexes, thereby preventing activation and translocation of Bax or Bak to mitochondria (Cheng, et al 2001). In addition, Bcl-2 and Bcl-XL block apoptosis by preventing cytochrome-c release through a direct effect on mitochondrial channels such as VDAC or MPT (Kroemer and Reed, 2000; Martinou and Green, 2001).

The extrinsic and intrinsic apoptotic pathways are intimately connected. For example, caspase-8 generated by the extrinsic pathway activates, by proteolysis, the pro-apoptotic BH-3 only domain protein, Bid. Upon cleavage, the truncated Bid protein translocates to mitochondria, induces cytochrome c release and thus leads to the formation of the apoptosome (Rossi and Gaidano, 2003). The intrinsic cell death pathway can also be activated by the involvement of the tumor suppressor gene, p53.

2.3.2.2. p53

Apoptotic cell death may occur in either a p53-dependent or independent manner depending on the type of stimulus (Reviewed in Zhou and Elledge, 2000). More than 50% of human cancers carry p53 deletions or mutations (Serrano et al, 1997). As a tumor suppressor gene, p53 plays a crucial role in the execution of different forms of apoptosis (Ferri and Kroemer, 2001; Haupt et al, 2002; Borresen-Dale, 2003).

Under most conditions, p53 pathways start from DNA damage. In response to the signal emanating from the damage, the normally low levels of p53 increase (Lowe et al, 1993). Two types of events can be triggered by p53 activation: growth arrest and cell death, depending on the stage of the cell cycle as well as the cell type. In early G1, p53 may trigger a checkpoint that blocks further progression through cell cycle. This checkpoint works by inducing p21 (Ko and Prives, 1996; Sphyris et al, 2004), an inhibitor of cyclin dependent kinases (cdks), to allow damaged DNA to be fixed before entering S phase. If a cell is already in a later phase (S, G2 or M) when its DNA is damaged, p53 will stimulate cell death through transcriptional activation of several pro-apoptotic proteins, such as Bax, Fas/CD95, death receptor 4 (DR4), DR5 and Bid (Vousden and Lu, 2002). P53 is involved in both the extrinsic and the intrinsic pathways of apoptosis by initiating apoptosis through mitochondrial depolarization and sensitizing cells to inducers of apoptosis (Hofseth et al, 2004). Other p53 transcriptional activated proteins include PUMA (p53-upregulated modulator of apoptosis) (Yu et al, 2001; Cregan et al, 2004), NOXA (Yakovlev et al, 2004), APAF-1 (Moroni et al, 2001) and the serine protease PRSS25 (also known as HTRA2). Recently, the gene encoding phosphatase PAC1 has also been identified as a target of p53; this gene is induced following the binding of p53 to a novel palindromic binding site in response to oxidative stress (Yin et al, 2003).

P53 can also promote apoptosis through transcription independent mechanisms (Haupt et al, 2003). Activated p53 can directly or indirectly modulate the expression of both anti-apoptotic (Bcl-2 and Bcl-XL – Vogelstein et al, 2000) and pro-apoptotic (Bax, Bak, Bid, NOXA and PUMA) proteins and control mitochondrial membrane

permeability. It can modulate the release of mitochondrial proteins such as cytochrome c, SMAC, AIF and endonuclease G during apoptosis (Hofseth et al, 2004). Recently, a limited number of whole molecules of the p53 protein was shown to allow permeabilization of the outer mitochondrial membrane directly by forming complexes with, and inhibiting, the protective Bcl-XL and Bcl-2 proteins, leading to the release of cytochrome c (Mihara et al, 2003). It therefore seems that p53 induces several MMP-inducing proteins that might act redundantly or, alternatively, might be involved specifically in particular cell types undergoing p53-dependent cell death.

After the activation of the intrinsic pathway, the signals converge, as in the extrinsic pathway, a caspase cascade.

2.3.2.3. Caspases

Although different signaling pathways exist in response to different stimuli, they usually converge to a common mechanism leading to cell death and the dismantling of a dying cell. Cysteinyl aspartate-specific proteases, caspases, are the main enzymes involved in this process. To date, the growing family of caspases consists of 14 mammalian members, of which 11 human enzymes have been identified (caspases 1-10 and caspase 14) (Pistritto et al, 2002; Degterev et al, 2003). Based on phylogenetic analysis the caspase gene family is divided into 2 subfamilies, which are related either to the ICE-like group, homologous to IL-1 beta-converting enzyme (ICE) (caspases-1, -4, -5, -13) or to the mammalian counterparts of the *C. elegans* protease called CED-3 (Cell Death Defective-3) (caspases-2, -3, -6, -7, -8, -9, -10) (Nicholson, 1999). These groups

differed in function, those activated during apoptosis (caspases-2, -3, -6, -7, -8, -9, -10) and those implicated in the pro-inflammatory response (caspases-1, -4, -5, -13) (Creagh and Martin, 2001).

All caspases share a number of distinct features. These include the catalytic triad residues, consisting of the active site Cys285, which is a part of the conserved QACXG pentapeptide sequence, His237 and the backbone carbonyl of residue 177 (caspase-1 numbering) (Degterev et al, 2003). A prominent feature of the caspase family is its specificity for substrate cleavage C-terminal to an Aspartate residue, which is unique among mammalian proteases, except for the serine protease granzyme B. All caspases are synthesized as inactive precursor proteins or zymogens containing a prodomain followed by a large (p20) and small (p17) subunit (Concha and Abdel-Meguid, 2002). The activation of the zymogen precursor or procaspase is mediated by a series of cleavages, the first being the separation of the large and small subunits, followed by the removal of the prodomain (Degterev et al, 2003). The active caspase is a tetra homodimer, with each monomer consisting of a large and a small subunit.

During cell death caspases have evolved to link distinct upstream signaling pathways to downstream execution steps. These upstream family members are termed initiator caspases and possess long prodomains containing one of two characteristic protein-protein interaction motifs: the death effector domain (DED) (caspases-8 and -10) and the caspase activation and recruitment domain (CARD) (caspases-1, -2, -4, -5, -9, -11, and –12) (Creagh and Martin, 2001). These two motifs allow the initiator caspases to interact with upstream adaptor molecules (i.e. FADD) with similar motifs during the extrinsic cell death pathways (Chen and Wang, 2002). On the other hand, caspases

involved in the downstream execution steps are termed effector caspases or executioner caspases (caspases-3, -6, and -7). These effector caspases are responsible for cleaving multiple cellular substrates, are typically processed and activated by upstream caspases, and are characterized by the presence of a short prodomain (Nicholson, 1999; Shi, 2002).

At least three distinct pathways for caspase activation exist in mammalian cells: recruitment-activation or induced proximity mechanism, transactivation, and autoactivation (Nicholson, 1999; Shi, 2004). In the first case, two examples of caspase activation following recruitment of multiple homologous proenzymes to a common site have been demonstrated. Ligation of the CD95 (Fas, APO-1) receptor, for example, recruits procaspase-8 to an oligomeric activation complex using the adapter protein FADD/MORT1 (Chen and Wang, 2002). Trans-activation of one caspase by another is a second well-established mechanism for caspase proenzyme maturation and activation. In general, upstream activator caspases (caspases-8 or -9 once they have undergone recruitment-activation) cleave and activate downstream effector caspases (caspases-3 or -7) by proteolysis of the Asp-X site between the large and small subunits. Finally, caspases can undergo autocatalytic activation, where the procaspases although inactive have a minimal amount of catalytic activity and one homodimer may cleave the other. One such mechanism that seems to exist comes from the observation that RGD peptides can directly stimulate the autoactivation of procaspase-3 (Roy et al, 2001).

It is important to establish several basic concepts when examining the role of caspases in the execution of cell death. Firstly, caspases do not generally digest other proteins to small peptide fragments (Chang and Yang, 2000). Due to their strict substrate recognition specificity, caspases cleave targets at one or a few highly selective sites in a

single protein. Secondly, even though caspases cleave some structural proteins required for the maintenance of cell structure, they also frequently target signaling proteins, such as kinases. The cleavage of such signaling molecules results in the activation or suppression of specific downstream pathways, which in turn execute cell death (Shi, 2002). Therefore, caspases serve as signaling mediators that orchestrate a complex web of downstream execution pathways. Close to 100 substrates have been identified thus far (Utz and Anderson, 2000; Degterev et al, 2003). Caspase targets can be subdivided into six major categories: (1) proteins directly involved in the regulation of apoptosis, (2) proteins mediating/regulating apoptotic signal transduction, (3) structural and essential function proteins, (4) proteins required for cellular repair, (5) proteins regulating the cell cycle and (6) proteins involved in human pathologies (Degterev et al, 2003).

During the activation of the extrinsic cell death pathway adaptor molecules bound on the cytoplasmic end of the death receptors recruit initiator procaspases (e.g. caspases-8 and –10). Upon recruitment, the initiator procaspases become activated and begin the propagation of the cell death proteolytic cascade. These upstream caspases activate effector or executioner caspases (caspases-3 and –7). The executioner caspases target a multitude of substrates; the cleavage of these substrates produces the morphological and biochemical characteristics of cell death.

Caspases are activated not only in the extrinsic cell death pathway but also in the intrinsic cell death pathway. The proteolytic cascade is primed to begin by the release of cytochrome c from dysfunctional mitochondria and association of cytochrome c to Apaf-1 (apoptotic protease activating factor-1). The binding of cytochrome c activates Apaf-1, which subsequently binds to procaspase-9 to form the apoptosome complex. As a result

caspase-9 is activated and activates the executioner caspase-3. Both the extrinsic and intrinsic pathways converge to caspase-3, which is downstream of the apoptotic signal. However both pathways are linked much earlier. The cleavage of cytosolic BID, a BH3-only domain pro-apoptotic protein, by caspase-8 to form a truncated form, which translocates to the mitochondria and induces cytochrome c release, provides this linkage.

Caspases are not the only proteases involved in cell death. Lysosomal cathepsins have been found to play a major role in cell death by activating either caspase dependent or independent cell death.

2.3.2.4. Lysosomal proteases: Cathepsins

As mentioned before, lysosomes and more specifically their proteases called cathepsins have been implicated during autophagic cell death. About 500-600 proteases have been identified in the human genome (Lopez-Otin and Overall, 2002). Of these, about 60 are lysosomal proteases (Mason, 1995), which include a group of about a dozen papain-like lysosomal cysteine proteases. All known lysosomal cysteine proteases are cathepsins, but not all cathepsins are lysosomal or cysteine proteases (Turk and Gunčar, 2003). There are 11 human enzymes currently known (cathepsins B, C, F, H, L, K, O, S, V, X and W - Turk et al, 2000; Turk et al, 2001). Cathepsins are synthesized as monomeric inactive precursors, except for cathepsin C, which is a tetrameric protein, and are activated by the proteolytic removal of a N-terminal propeptide. Removal of the propepetide may be facilitated either by the activation of other proteases or by autocatalytic activation at acidic pH. Cathepsins are optimally active in the slightly

acidic, reducing milieu in lysosomes (Turk et al, 2001). Due to their very destructive nature cathepsins are regulated by endogenous protein inhibitors called cystatins, and not by pH (Turk et al, 1993).

Cathepsins play an important role in many physiological processes (Turk et al, 2001; Turk et al, 2002), such as protein degradation (Turk et al, 2000), prohormone processing (Tepel et al, 2000), processing of the MHC class II-associated invariant chain (cathepsins-S, -L, -B, -D), which is essential for the normal functioning of the immune system (Shi et al, 2000; Watts, 2001), normal bone remodeling (cathepsin-K) (Kakegawa et al, 1993), and tumor invasion and metastasis (cathepsins-B, -D, -L) (Sloane et al, 1994; Kos and Lah, 1998).

The deletion of cathepsins has been shown to cause several genetic disorders. Pycnodysostosis, an autosomal recessive osteochondrodysplasia characterized in humans by severe bone abnormalities, was found to be associated with the loss-of-function mutation of cathepsin K (Gelb et al, 1996), while loss-of-function mutation in the cathepsin C gene leads to Papillon-Lefevre syndrome, an autosomal recessive disorder characterized in patients by palmoplantar keratosis and severe early-onset periodontitis (Toomes et al, 1999; Hart et al, 2000; Marazita et al, 2000).

Besides their involvement during physiological processes and disease, cathepsins, specifically cathepsins –B, -D and –L act as mediators of cell death in several cell types (Guicciardi et al, 2000; Foghsgaard et al, 2001; Kägedal et al, 2001; Bidère et al, 2003; Johansson et al, 2003). For example, microinjection of cathepsin-D into human fibroblast cells induces cell death (Roberg et al, 2002).

Cathepsins play a major role during necrosis by the degradation of cellular components (e.g. organelles), but have also been implicated during apoptosis (caspase-independent cell death) and autophagy (Cuervo, 2004; Edinger and Thompson, 2004). The link to apoptosis is that cathepsins are able to activate caspases and affect the function of mitochondria. For instance, cathepsin L activates caspase-3 in digitonin-treated lysosomal fractions (Ishisaka et al, 1998, 1999; Katunuma et al, 2001). Also, cathepsin D mediates cytochrome c release and caspase activation in human fibroblast apoptosis induced by staurosporine (Johansson, 2003).

Cathepsins can affect the activity of Bcl-2 members and mitochondrial function. For example, cathepsin D can activate cytosolic Bax, which in turn can translocate to the mitochondria and selectively release AIF in T lymphocytes entering the early commitment phase to apoptosis (Bidere et al, 2003). The pro-apoptotic Bcl-2 family member, Bid, is cleaved to its active form in the presence of lysosomal extracts, suggesting the possible involvement of lysosomal proteases in apoptosis (Stoka et al, 2000). In TNF-α treated hepatocytes, the activation of caspase-8 induces the release of cathepsin B from lysosomes, which mediates the release of cytochrome c from mitochondria (Guicciardi et al, 2000).

Cathepsins do not always activate apoptosis in cells but can also protect cells against apoptosis. For instance, cathepsin B can be a negative regulator of apoptosis. Overexpression of cathepsin B in PC12 cells lowered their sensitivity to apoptosis induced by serum deprivation, while inhibition of cathepsin B had the opposite effect (Shibata, 1998).

The collection of data on cathepsins has shown that they are an important part of a cell's arsenal for self-destruction and, like caspases, are essential. With the wealth of information known, we come back to our original question: how can influenza viruses induce cell death and activate the death machinery?

2.4. Virus Induced Cell Death

Although it has been known for many years that many viruses cause programmed death of the host cell, the molecular mechanism remains unsolved. This induced cell death contributes to the cytopathogenic effects of the virus (Lyles, 2000). Although there is no obvious advantage for the induction of cell death by a cytopathogenic virus, the virus may indeed induce cell death as a method of limiting the inflammatory and immune response by the infected host to be more effective in its propagation to other cells (O'Brien, 1998). Host cells infected with bovine herpesvirus (Yazici et al, 2004), chicken anemia virus (CAV) (Noteborn, 2004), lymphocytic choriomeningitis virus (Wolfe et al, 2002), human immunodeficiency virus-1 (HIV-1) (Gil et al, 2004), alphavirus (Li and Stollar, 2004), adenovirus (Opalka et al, 2002), parvovirus (Chisaka et al, 2003), porcine reproductive and respiratory syndrome virus (PRRSV) (Labarque et al, 2003), papillomaviruses (Singh and Bhat, 2004) and influenza virus undergo apoptotic death. However, viral replication of cytopathogenic viruses (i.e. influenza virus) may also occur more rapidly than the onset or progression of the induced cell death thereby allowing the spread of the virus (Kurokawa et al, 1999).

Patients with HIV-1 infection are characterized by a selective depletion of a subset of T lymphocytes, $CD4^+$T cells, which leads eventually to immunosuppression (Chaves and Kallas, 2004). It was first proposed that the pathology of HIV disease might result from an inappropriate triggering of apoptosis (Ameisen and Capron, 1991). The induction of apoptosis via the HIV-1 Tat protein involves the upregulation of FasL, which in turn activates the Fas receptor in uninfected cells (Westendorp et al, 1995; Salmen et al, 2004). By contrast, death of HIV-infected cells seems to be Fas-independent and driven by other viral components such as vpr and HIV proteases (Dianzani et al, 2003). A key role is played by the death receptor Fas, but a role can also be played by other death receptors, such as the TNF and TRAIL receptors (Dianzani et al, 2003; Guillemard et al, 2004).

The envelope glycoprotein complex (Env) kills uninfected cells expressing CD4 and/or the chemokine receptor CXCR4 or CCR5 (Dianzani et al, 2003). The signs of Env-induced apoptosis include the loss of the mitochondrial transmembrane potential and the release of cytochrome c and AIF (Genini et al, 2001). The mechanisms of Env-triggered apoptotic MMP may involve an elevation of cytosolic Ca^{++}, reactive oxygen species and/or the transcriptional activation of p53, with the consequent expression of pro-apoptotic proteins such as Bax, which permeabilizes mitochondrial membranes (Castedo et al, 2003). Both the intrinsic and extrinsic signaling pathways can mediate cell death during HIV-1 infection (Petit et al, 2003).

In another example the prototypic alphavirus, Sindbis virus (SV), replicates lytically in a variety of mammalian cell lines and lytic replication appears to be due to the induction of apoptosis (Levine and Griffin, 1993). This induction of apoptosis also

contributes to the pathogenicity of infection. Neurons of infected neonatal mice die by apoptosis, and the mice develop a fatal encephalitis as a result of virus infection (Levine et al, 1996). The cellular pathways involved in alphavirus-induced apoptosis are complex, and much remains poorly understood. Experimental results point to the involvement of both the mitochondrial and the death receptor pathways (Li and Stollar, 2004). SV can induce apoptosis simply by the process of membrane fusion and entry, by the expression of the envelope proteins, or by the expression of the nonstructural protein, NSP2. However, viral particles are not necessary to activate apoptosis, since transfection with viral RNA or even viral RNA expressing only the nonstructural proteins will result in apoptosis.

We see many instances of viruses activating the various components of the different cell death pathways and it appears that viruses tend to activate multiple pathways instead of one. As a result the different viruses use an interplay between the activation of the extrinsic and intrinsic cell death pathways to kill a cell. In this thesis we will present our data on the involvement of the different cell death pathways during influenza induced cell death. In this introduction we will examine the number of reports by other researchers on influenza induced cell death and discuss key questions on the type of cell death induced, the possible inducers of cell death and mechanism of induction.

Takizawa and colleagues were the first to study influenza induced cell death in tissue culture cells and found the hallmark DNA laddering characteristics occurring in HeLa and MDCK cells infected with influenza A/Udorn/72 (H3N2) virus (Takizawa et al, 1993). According to Hinshaw and colleagues, a virulent avian influenza

A/Turkey/Ontario/7732/66 (Ty/Ont) virus induced severe lymphoid depletion *in vivo* and rapidly killed an avian lymphocyte cell line (RP9) *in vitro*. These authors found that, within 5h after infection, Ty/Ont virus induced fragmentation of the DNA of RP9 cells into a 200-bp ladder and caused ultrastructural changes characteristic of apoptotic cell death (Hinshaw et al, 1994). Furthermore, infection of mice with influenza virus led to cell death in bronchial epithelial and alveolar cells as indicated by a positive signal for DNA fragmentation (Mori et al, 1995). The reports suggested that influenza induced cell death was apoptotic. It was not determined what viral protein(s) were involved in the induction of influenza induced cell death. Some candidates are discussed below.

Transforming growth factor-beta (TGF-β), which can induce apoptosis in various cells (Siegel and Massague, 2003) was upregulated in MDCK cells and in mice infected with influenza virus (Schultz-Cherry and Hinshaw, 1996). This upregulation was influenced by the activity of the neuraminidase (NA) glycoprotein of influenza virus. Other evidence to support the argument that NA activity played some role during influenza induced cell death was that NA inhibitors partially abrogated apoptosis and viruses with high NA activity produced increased cell death (Morris et al, 1999). However, UV treatment of virus inhibited cell death even though NA activity was high, indicating that NA was not the sole inducer of cell death and that other pathways were involved.

Another possible candidate for the induction of influenza induced cell death was the non-structural –1 (NS-1) protein. This viral protein, normally involved in inhibiting PKR activity and regulating RNA export from the nucleus, was shown to either inhibit

(Zhirnov et al, 2002) or induce (Schultz-Cherry et al, 2001) cell death, but the reason for the contradiction was not known.

Lastly, another possible viral inducer of cell death came with the identification of PB1-F2, a new influenza virus protein expressed from a +1 reading frame of the PB1 polymerase gene segment (Chen et al, 2001). PB1-F2 induced apoptosis if added to cells, and infection with recombinant viruses lacking the protein resulted in reduced apoptotic rates in lymphocytes (Chen et al, 2001). However, most of the avian virus strains lacked the reading frame for this protein and PB1-F2-deficieny did not affect apoptosis in a variety of other host cells (Chen et al, 2001).

Thus influenza viruses induce cell death but the individual components involved in the different cell death pathways that are activated are not resolved. Preliminary data by others is available and presented below.

Initially it was found that influenza viruses were able to stimulate the production of Tumor Necrosis Factor – Alpha (TNF-α), a ligand belonging to the Tumor Necrosis Factor Family, in murine macrophages (Nain et al, 1990; Hinder et al, 1991; Peschke et al, 1993; Fujimoto et al, 1998). Influenza A virus infections were commonly associated with symptoms suggesting involvement of TNF-α (Nain et al, 1990). Messenger RNA of the TNF receptor family member, Fas, was expressed in infected HeLa cells at 3 and 4 h pi and appeared on the surface at 12 h pi (Takizawa et al, 1993; Takizawa et al, 1995; Wada et al, 1995). Saito et al showed that the fungal metabolite Brefeldin A (BFA), which blocks protein transport from the ER to Golgi apparatus, inhibited influenza induced cell death in MDCK cells (Saito et al, 1996). They proposed that BFA might act by blocking viral membrane proteins or intracellular transport of the Fas antigen.

Dying cells can activate a variety of different cell death pathways as discussed above. One such pathway involves the recruitment of adaptor proteins such as FADD (Fas-Associated Death Domain) for the activation of caspase-8. Balachandran and colleagues investigated cell death in murine embryo fibroblasts (MEF) and reported that infected FADD knockout MEF's treated with interferon had lowered levels of influenza induced cell death than wild type (WT) MEF's (Balachandran et al, 2000). They concluded that interferons potentiate influenza induced cell death through the activation of the FADD/caspase-8 extrinsic pathway.

Double stranded RNA activated protein kinase (PKR) was induced by interferons, and was thought to participate in antiviral activities (Samuel, 1991). HeLa cells with a point mutated PKR protein and infected with influenza A/Udorn/72 (H3N2) virus demonstrated a lowered expression of Fas proteins in these cells (Takizawa et al, 1996). MEF cells overexpressing PKR were more sensitive to influenza infections than WT cells (Balachandran et al, 2000). Thus PKR may participate in influenza induced cell death.

One hallmark of apoptosis is the activation of caspases. Human macrophages infected with influenza A/Beijing/353/89 (H3N2) showed activation of caspase-1 by the cleavage of proIL-1β and proIL-18 proteins (Pirhonen et al, 1999). Caspase-3-like activity can be detected in influenza A/Udorn/72 (H3N2) virus infected HeLa cells, but inhibition by a caspase-3-like inhibitor, Ac-DEVD-CHO, did not completely block influenza induced cell death, indicating that other cell death pathways may be activated (Takizawa et al, 1999). Caspases cleave cellular proteins but they can also cleave the N-terminus of influenza A and B nucleoproteins (Zhirnov et al, 1999).

Wurzer et al showed that caspase-3 was needed for the efficient propagation of an avian influenza virus (Avian A/Bratislava/79 (H7N7)) in cells by the use of small interfering RNA (siRNA) molecules (Wurzer et al, 2003). They showed that when caspase-3 was knocked down by siRNAs, viral titers increased. Caspase inhibition by zDEVD-fmk, a caspase-3 specific inhibitor, also resulted in inhibition of influenza induced cell death (Wurzer et al, 2003).

Most research has focused on extrinsic pathway of cell death during influenza induced cell death, but there is very little mention about the activation of the intrinsic pathway of cell death. In this thesis, we will explore the potential activation of the mitochondrial pathway as well as other components of the different cell death pathways during influenza induced cell death. Since the mode of cell death induced can be cell type dependent we will further investigate the mode of cell death occurring in cells that normally become infected with influenza viruses, as opposed to cells such as MDCK cells, which are commonly used as a convenient lab model even though they are not normally attached by influenza viruses.

Figure 1. Extrinsic cell death pathway.

FasR and TRAILR1/2 (DR4/DR5, respectively) are transmembrane receptors belonging to the family of death receptors. In general terms, a death receptor is composed of an extracellular domain containing the ligand binding site, a transmembrane domain and an intracellular domain, termed the death domain (DD). Engagement by a death ligand induces death receptor activation by homotrimerization. Once activated, death receptors recruit adaptor proteins through the homophilic interaction of their own DD to the DD of the adaptor proteins such as FADD. Characteristically, the adaptor protein contains an additional domain, the death effector domain (DED), necessary for procaspase recruitment. In the next step, the DED domain of the adaptor protein interacts in a homophilic manner with the DED of an initiator caspase termed procaspase-8. The formed complex is called DISC (death inducing signaling complex). Procaspase-8 is synthesized as an inactive precursor that is activated by auto-proteolytic cleavage after recruitment in the DISC. Activation of caspase-8 triggers the activation of downstream effector caspases such as caspase-3. The activation of caspase-3 leads to the proteolytic cleavage of the cellular substrates and cell death of the cell.

Extrinsic Cell Death Pathway

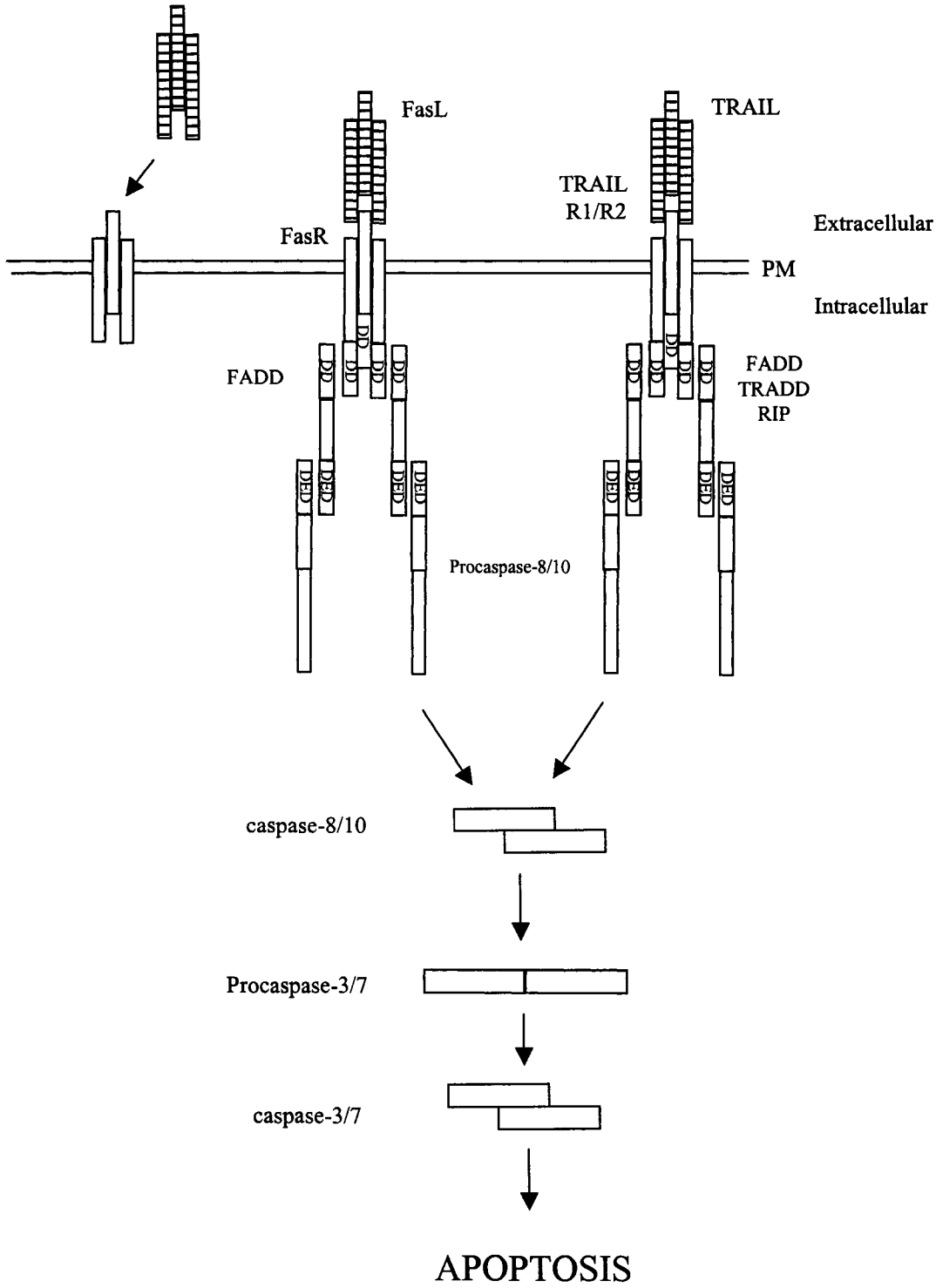

Diagram 1

Figure 2. Intrinsic cell death pathway.

Activated caspase-8 triggers the cleavage of the cytosolic Bid protein to form a truncated protein (tBid). Truncated Bid translocates to the mitochondrial membrane and stimulates the insertion or oligomerization of Bax or Bak in the outer membrane. Membrane permeabilization then causes the release of AIF, cytochrome *c*, Smac-α/DIABLO and procaspases. Cytochome c recruits the caspase adaptor molecule Apaf-1 and Apaf-1 recruits the initiator caspase procaspase-9. Together, Apaf-1 and procaspase-9 form the apoptosome enzymatic complex. The apoptosome, through the enzymatic activity of activated caspase-9, triggers the activation of the downstream effector caspase-3, inducing cell death. In response to stress, lysosomes undergo membrane permeabilization and/or local activation and release of cathepsins. Cathepsins then can cause the proteolytic activation of Bid and might have direct effects on caspases and nuclear DNA. Abbreviations: t-Bid, truncated Bid; $\Delta\Psi m$, membrane potential; MPT, membrane permeability transition; Endo G, endonuclease G; AIF, apoptosis inducing factor; (Smac)/DIABLO, second mitochondria derived activator of caspases; IAP, inhibitor of apoptosis protein.

Intrinsic Cell Death Pathway

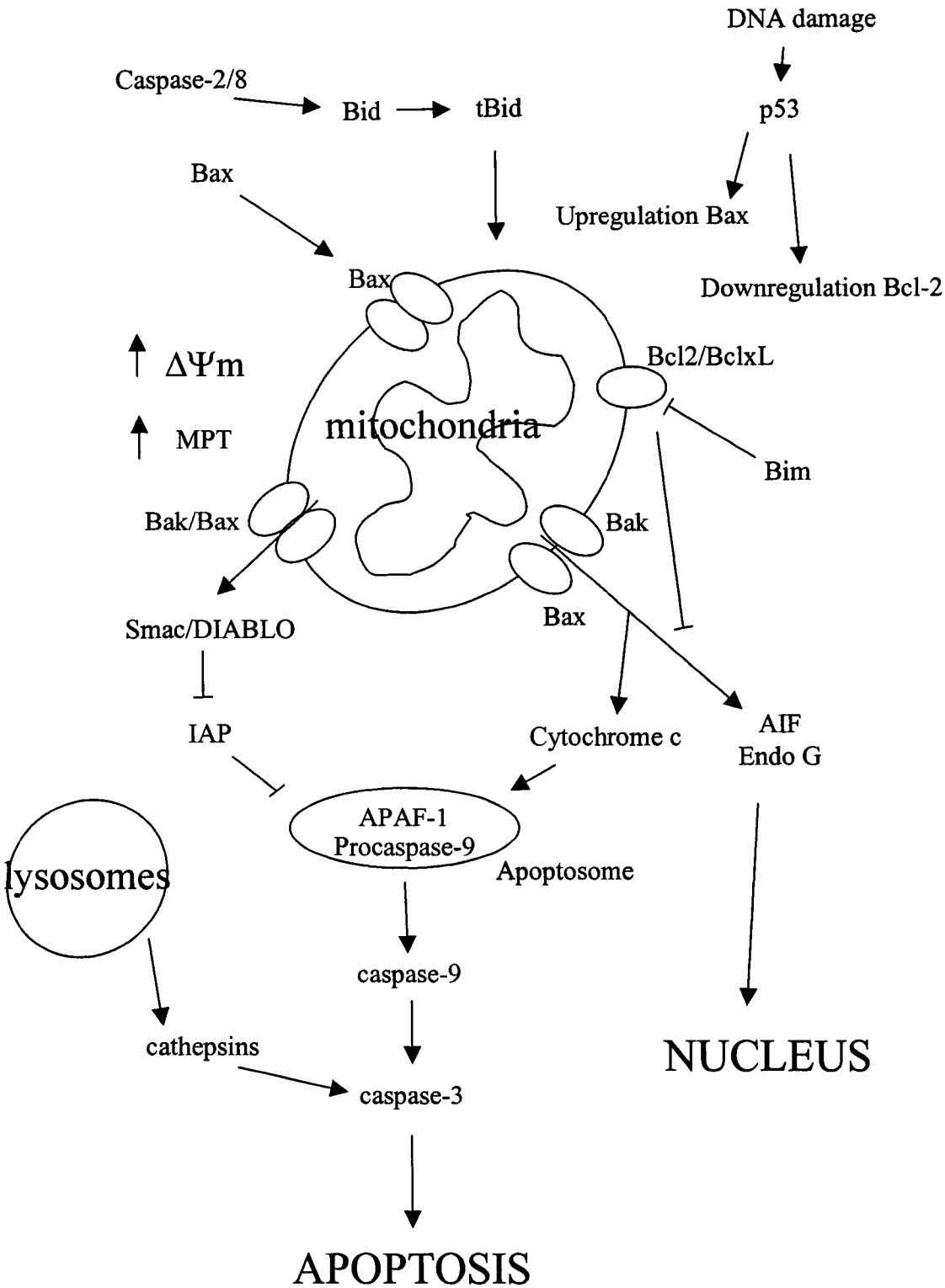

Diagram 2

Part II. Materials and Methods

MATERIALS AND METHODS

I. Cell Culture

1. Madin Darby canine kidney (MDCK) cells

MDCK cells (ATCC # CCL-34) are an immortal adherent cell line with an epithelial morphology, and are derived from normal kidney cells from *Canis familiaris* (cocker spaniel dog). These cells were a gift from Dr. Anastasia Gregoriades, Queens College.

MDCK cells were cultured in MEM (minimum essential medium Eagle, also EMEM) (Gibco, cat # 61100-061) media supplemented with 10% heat inactivated fetal bovine serum (ΔFBS) (heat inactivated at 56°C for 30 min in a water bath) (Equitech-Bio, cat # LSFB-0500), 2mM L-glutamine (Gicbo, cat # 25030-081), 1.5g/L sodium bicarbonate (Sigma-Aldrich, St Louis MO), 50U/ml penicillin (Gibco, cat # 15140-122), and 50mg/ml streptomycin (Gibco, cat # 15140-122). During the infection, infected MDCK cells were cultured in MEM media supplemented with 5 % ΔFBS 50U/ml penicillin and 50mg/ml streptomycin. The cells were incubated at 37°C in 5% CO_2 humidified condition.

Passaging of cells:

Confluent cells had their old media removed and washed with 6 ml of 1X phosphate buffered saline (PBS) (*see section on reagents*). The PBS wash was aspirated away and 1.5 ml of 2.5% trypsin/EDTA (Life Technologies, Rockville MD) was added to remove the cells off the plate. The cells were placed in a cell culture incubator (37°C) for incubation until the cells began to lift

off the flask. After trypsinization, 15 ml of warm fresh media was added to stop the action of the trypsin and the cells were split 1:10 in a new flask.

2. U937 and U937R cells

U937 cells are a human histiocytic lymphoma (macrophage) cell line with monocyte morphology in suspension. As developed in our laboratory, U937R cells are a subset of the U937 parent cell line and are less sensitive to ceramide, fas and TNF-α treatments (Karasavvas et al, 1996). U937R cells loosely adhere to tissue culture plates while U937 are grown in suspension.

Both U937 and U937R cells were cultured in RPMI 1640 media (Gibco, cat # 31800-022) supplemented with 10% ΔFBS, 2mM L-glutamine, 1.5g/L sodium bicarbonate, 50U/ml penicillin and 50mg/ml streptomycin. During the infection, infected U937 and U937R cells were cultured in RPMI 1640 media supplemented with 5% ΔFBS, 2mM L-glutamine, 50U/ml penicillin and 50mg/ml streptomycin. The cells were incubated at 37°C in 5% CO_2 humidified condition. U937R cells were passaged as stated for MDCK cells.

3. A549 cells

A549 cells (ATCC # CCL-185) are an adherent cell line with an epithelial morphology and are a continuous tumor-cell line derived from human lung carcinoma. These cells were a gift from Dr. Jeffrey A. Kazzaz (Winthrop-University Hospital).

A549 cells were cultured in Ham's F12K Nutrient medium (Gibco, cat# 211127-022) supplemented with 10% ΔFBS, 2mM L-glutamine, 1.5g/L sodium bicarbonate, 50U/ml penicillin and 50mg/ml streptomycin. During the infection, infected A549 cells were cultured in Ham's F12K Nutrient medium supplemented with 5 % ΔFBS 50U/ml penicillin and 50mg/ml

streptomycin. The cells were incubated at 37°C in 5% CO_2 humidified condition. A549 cells were passaged as stated for MDCK cells.

4. C8 and A9 cells

C8 cells are a wild type mouse embryo fibroblast line transformed with adenovirus E1A and ras and have normal levels of p53 expression [p53 +\+]. A9 cells are a mouse embryo fibroblast line transformed with adenovirus E1A and ras and are devoid of p53 expression [p53 -/-]. C8 cells grow slowly and form syncytia, while A9 cells proliferate quickly and are smaller in size than C8 cells. These cells were a gift from Dr. Scott Lowe at CSHL.

C8 and A9 cells were cultured in DMEM (Dulbecco's Modified Eagle Medium) (Gibco, cat# 12800-017) supplemented with 10% ΔFBS, 2mM L-glutamine, 1.5g/L sodium bicarbonate, 50U/ml penicillin and 50mg/ml streptomycin. During the infection, infected C8 and A9 cells were cultured in DMEM media supplemented with 5% ΔFBS, 2mM L-glutamine, 50U/ml penicillin and 50mg/ml streptomycin. Both cell lines were susceptible to cell death by serum withdrawal or reduction (1% FBS). The cells were incubated at 37°C in 7% CO_2 humidified condition. C8 and A9 cells were passaged as stated for MDCK cells.

5. Cathepsin-B -/-, -D -/-, -L -/- and WT mouse embryo fibroblast (MEF) cells

Mouse embryo fibroblast (MEF) cells harvested from transgenic mouse embryos with single knockout genotypes of cathepsin-B, -D, or -L or wild-type (WT) were immortalized with SV40. The cells were kindly provided by Dr. Marianne Boes at Harvard Medical School.

MEF cells were cultured in DMEM (Dulbecco's Modified Eagle Medium) (Gibco, cat# 12800-017) supplemented with 10% ΔFBS, 2mM L-glutamine, 1.5g/L sodium bicarbonate,

50U/ml penicillin and 50mg/ml streptomycin. During the infection, infected MEF cells were cultured in DMEM media supplemented with 5% ΔFBS, 2mM L-glutamine, 50U/ml penicillin and 50mg/ml streptomycin. The cells were incubated at 37°C in 5% CO_2 humidified condition. MEF cells were passaged as stated for MDCK cells.

6. Bak -/-, Bax -/-, Bak -/-/Bax -/- (DKO), and WT MEF cells

Mouse embryo fibroblast (MEF) cells harvested from transgenic mouse embryos with single knockout genotypes of Bak or Bax, or double knockout of Bak/Bax (DKO), or wild-type (WT) were transformed with SV40. The cells were kindly provided by Dr. Stanley Korsmeyer at Howard Hughes Medical Institute.

MEF cells were cultured in DMEM (Dulbecco's Modified Eagle Medium) (Gibco, cat# 12800-017) supplemented with 10% ΔFBS, 2mM L-glutamine, 1.5g/L sodium bicarbonate, 50U/ml penicillin and 50mg/ml streptomycin. During the infection, infected MEF cells were cultured in DMEM media supplemented with 5% ΔFBS, 2mM L-glutamine, 50U/ml penicillin and 50mg/ml streptomycin. The cells were incubated at 37°C in 5% CO_2 humidified condition. MEF cells were passaged as stated for MDCK cells.

7. PC-12 WT and PC-12 Bcl-2 overexpressing cells

PC-12 (adrenal pheochromocytoma) (ATCC CRL 1721) cells are an adherent cell line of rat origin that can be treated with NGF to differentiate into sympathetic neuron-like cells complete with neural dendritic processes. PC-12 cells overexpressing Bcl-2 were stably transfected with a plasmid containing Bcl-2. These cells were a gift from Dr. Soraya Smaili at Universidade Federal de São Paulo.

PC-12 cells were cultured in RPMI-1640 media (Gibco, cat # 31800-022) supplemented with 5% ΔFBS and 10% horse serum, 2mM L-glutamine, 1.5g/L sodium bicarbonate, 50U/ml penicillin and 50mg/ml streptomycin. During the infection, infected PC-12 WT and PC-12 Bcl-2 cells were cultured in DMEM media supplemented with 5% ΔFBS, 2mM L-glutamine, 50U/ml penicillin and 50mg/ml streptomycin. The cells were incubated at 37°C in 5% CO_2 humidified condition. PC-12 cells were passaged as stated for MDCK cells.

8. MCF-7 cells

MCF-7 (ATCC # HTB-22) cells are an adherent cell line with epithelial-like morphology and are a continuous tumor-cell line derived from human breast adenocarcinoma. They are deficient in caspase-3.

MCF-7 cells were cultured in DMEM (Dulbecco's Modified Eagle Medium) (Gibco, cat# 12800-017) supplemented with 10% ΔFBS, 2mM L-glutamine, 1.5g/L sodium bicarbonate, 50U/ml penicillin and 50mg/ml streptomycin. During the infection, infected MCF-7 cells were cultured in DMEM media supplemented with 5% ΔFBS, 2mM L-glutamine, 50U/ml penicillin and 50mg/ml streptomycin. The cells were incubated at 37°C in 5% CO_2 humidified condition. MCF-7 cells were passaged as stated for MDCK cells.

9. Mouse primary Bim -/- cells

Bim knockout mice (266/266 DEL) were provided by Dr. Philippe Bouillet of The Walter & Eliza Hall Institute of Medical Research, Australia. To obtain adult primary murine cell cultures we first dissected the Bim knockout mice (266/266 DEL) and harvested the lung and kidneys. The organs were immediately placed in ice cold PBS and were ground down with sterile

nylon strainers. The mixture of cells and PBS was centrifuged at 1,000 x g for 5 min and the supernatant aspirated. The cell pellet was resuspended with 6 ml of DMEM +10% FBS and added to 100 mm plates. The plates were incubated at 37°C in 5% CO_2 humidified condition until confluent.

II. Influenza Virus

Influenza A/WSN/33 (H1N1) (WSN)

Influenza A/WSN/33 (WSN) virus was cultured in 10-day-old embryonated chicken eggs (Charles River SPAFAS, North Franklin, CT) and incubated for 2 days post infection at 35 °C (*see below*). The allantoic fluid was collected, aliquoted and stored at –80 °C. The viral titer of the allantoic fluid was determined by the plaque assay technique. Stock titers range from 4.5 – 9 x 10^8 pfu/ml.

III. Procedure to Seed Embryonated Chick Eggs

Embryonated chicken eggs of 8-11 days old (about 2-10 eggs per virus strain) were candled to determine the viability and position of the embryo. A mark was placed between the interface of the air sac and shell membrane (injection site), avoiding any major blood vessels. For the infection dose, a 10^{-3} dilution of the viral stock was made by serial dilution with the virus diluting media (*see section on reagents*). The marked area was swabbed with ethanol and a small indent was made on the eggshell for injection of the virus. For the inoculation a 1cc sterile hypodermic syringe was used and 0.1 ml of diluted virus was injected into each egg. The injection hole was closed with either melted wax or Scotch tape. The eggs were incubated at 35-

37°C for 48 hours. After the incubation, the infected eggs were placed at 4°C overnight to solidify the membranes, kill the embryo and coagulate the blood. The tops of the eggs were opened and the infectious allantoic fluid (clear or slightly opaque liquid) was collected and placed in sterile tube on ice. RBC and yolk was avoided during the collection. The infectious allantoic fluid was spun at 1,000 x g for 5 min and the supernatant was aliquoted into cryovials. The cryovials were later placed in – 80°C freezer.

IV. Quantitation of Influenza Virus

1. Plaque Assay

The plaque assay is an infectivity assay that allows one to quantitate the number of infectious units in a virus sample. Plaques are zones of cell lysis or CPE (cytopathic effect) within a monolayer of cells. Each plaque forms from one infectious virus thus a precise calculation of the virus titer can be made. The plaque assay is more sensitive and precise as compared to the HA (hemagglutination) assay because it calculates only live viruses.

Procedure:

To determine the level of virus production in a certain cell line we infected the cells with a MOI of 0.001 to allow multiple rounds of infection. At every 24 h interval (24 – 144 h) we collected the supernatant for quantification of the virus.

MDCK cells were plated in 35 mm dishes (~ 2 x 10^6 cells/plate) overnight in order to obtain a monolayer of cells. The plated cells were washed with 1X PBS and each plate was inoculated with 0.1 ml of the appropriate virus dilution (stock virus was serially diluted to 10^{-1} -

10^{-7} with virus diluting media). The plates were incubated at room temperature (RT) for 1 hour; shake every 20 minutes to insure an even inoculation. During the viral infection, the virus overlay plaquing media (*see section on reagents*) was prepared and placed in a 37°C water bath for warming. Just before the end of the infection time, molten agar was added to the virus overlay plaquing media and mixed well. The inoculum was removed quickly before the solidification of the plaquing media and 2 ml of warmed agar overlay medium was added to each dish, avoiding unevenness and addition of bubbles. The agar was left to set and dishes were placed upside down when the agar had hardened. The dishes were incubated at 37°C in 5% CO_2 humidified condition for 2-3 days post infection for the formation of plaques. The appearance of a plaque was designated as a clear area on the plate and was counted as one plaque forming unit (pfu). After counting the number of plaques formed, plates were preserved by carefully staining the cells by removing the agar overlay and adding 2 ml of crystal violet stain (*see section on reagents*) for 10 minutes. The stain was poured off and the plate was carefully rinsed with tap water and dried upside down.

The infectivity titer was calculated as the number of plaque forming units per ml (pfu ml^{-1}) of virus by this formula: plaque number X reciprocal of dilution X reciprocal of inoculation volume in ml. To be statistically significant 20 – 100 plaques per plate were used for the plaque number. For example: We counted 32 plaques on a plate infected with a sample diluted to 10^{-4}. Our inoculation volume was 0.1 ml. We set up the calculation as follows: (32 plaques) X ($1/10^{-4}$) X (1/0.1 ml) = (32) X (10,000) X (100) = 32,000,000 pfu

2. Haemagglutination (HA) Assay

Influenza viruses possess the ability to aggregate red blood cells (RBC) by the interaction of specific glycoproteins (HA) with surface receptors present on the plasma membrane of RBCs. This effect is referred to as haemagglutination. The HA assay is an indirect method of determining virus titer because it is not a measure of infectivity, since virus replication does not occur. Instead it is a measure of virus particles in a sample. The assay is not sensitive because it requires a very large number of particles to agglutinate the RBCs, but is useful when viruses cannot form plaques.

Procedure:

We added 50 µl of undiluted virus to the first two wells of a V-shaped bottom 96 well plate. Depending on how concentrated the sample was the 8 or 12 well side was used. The addition of virus was done under the hood with aerosol resistant pipet tips. Two-fold serial dilutions of the virus with virus diluting media were carried out in all the wells (2-8 or 12) except the first well. The sample was mixed well by drawing the mixture up and down with the pipet. We added 50 µl of the sample from the second well to the third well. With a fresh tip the sample was mixed uniformly and transferred to the next well. The process was repeated until the last well (8 or 12) was reached. After the addition and mixing at the last well 50 µl was removed. We added 50 µl of 0.5% chicken RBCs (chicken, adult erythrocytes cat# 30-903J, BioWhittaker, Walkersville MD) to all the wells. The bottom of the tray was rubbed to mix the samples. The tray was placed in 4°C for 1 hour and the plate read after the incubation.

- Positive agglutination occurred when sufficient amounts of the virus formed cross-bridges between RBCs, which created a latticework structure that coated the sides of the well.

- Negative agglutination occurred when insufficient amounts of the virus were present and did not form enough cross-bridges between RBCs. The unagglutinated RBCs fell to the bottom of the well and formed well-defined RBC pellets.

A viral titer was determined by end point titration where the last dilution that showed complete agglutination by definition contained 1 HA unit. HA titer of a viral sample was the reciprocal of the highest dilution of complete agglutination divided by the inoculation volume (HA units/ml).

V. Typical Virus Infection Procedure

1. Infection of Adherent Cells

The appropriate cell line was plated in 35, 60, or 100 mm plates depending on the experiment and the number of cells needed. Typically 7-8 x 10^6 cells for 100 mm plates, 2-4 x 10^6 cells for 60 mm plates or 1-1.5 x 10^6 cells for 35 mm plates were plated overnight. The old media was removed and the cells washed with 1X PBS. The wash was aspirated away and the cells were inoculated with either: 0.1 ml for 35 mm plates, 0.25 ml for 60 mm plates or 0.5 ml for 100 mm plates of the appropriate virus dilution of the stock virus (*see below for calculation determination*). The dilution varied depending on whether a single round of infection (high multiplicity of infection, MOI) or multiple rounds of infection (low MOI) were needed. For the influenza virus a single round of replication takes approximately 8 hours. Typically a MOI of 5 was used for most infections (an MOI of 1 is 1 virus per 1 cell). Mock-infected cells were

inoculated only with the virus diluting media. The infected cells were incubated for 1 hour at RT and shook every 20 minutes. The virus was aspirated away and either: 1.5 ml for 35 mm plates, 3 ml for 60 mm plates or 6 ml for 100 mm plates of the appropriate media with reduced serum (*see cell culture for details*) was added. Plates were incubated at 37°C in 5% CO_2 humidified condition. Cells were collected at the desired time point (hours post infection).

Virus number calculation

x / # of cells = desired MOI solve for x

x = # of virus (pfu, plaque forming units) divide by inoculation volume (ml)

x = pfu/ml

Dilution of virus stock

C1V1 = C2V2 solve for V1

C1 = conc. of stock virus (pfu/ml) C2 = conc. wanted of virus (pfu/ml)

V1 = vol. of stock virus V2 = total vol. of virus needed

2. Infection of Suspension Cells (U937 cells)

Prior to infecting the suspension cells the appropriate number of cells needed for the experiment were counted on the day of the infection. Cells were added to 15 ml Falcon tubes, and centrifuged at 1,000 x g for 5 min and the supernatant aspirated away. The pellet was resuspend with 1X PBS and centrifuged at 1,000 x g for 5 min. The wash was aspirated away and the pellet was resuspended with 1ml of virus diluting media containing the appropriate virus dilution of the stock virus. Mock-infected cells were inoculated only with the virus diluting media. The infected cells were incubated for 1 hour at RT and shook every 20 minutes. After the infection the cells were washed with 4 ml of 1X PBS and centrifuged at 1,000 x g for 5 min. The virus/wash was removed and the pellet was resuspended with either: 1.5 ml for 35 mm plates, 3 ml for 60 mm plates or 6 ml for 100 mm plates of the appropriate media with reduced serum. The suspension cells were plated in the appropriate size plate and incubated at 37°C in 5% CO_2 humidified condition. Cells were collected at the desired time point (hpi).

VI. Characterization of Cell Death

Membrane Integrity (Cell Viability):

1. Trypan Blue Exclusion

Cells undergoing apoptosis or necrosis lose membrane integrity, which allows vital dyes, like trypan blue, to enter (Karasavvas et al, 1996). Virus and mock-infected cells were trypsinzed and pelleted at 1,000 x g for 5 min. The pellet was washed and thoroughly but gently resuspended with 1X PBS so as to break up any cell clumps that could make counting difficult. Cells were mixed with an equal volume of 0.4% trypan blue (0.4% trypan blue in 1X PBS,

pH7.4) (Sigma-Aldrich, St Louis MO) solution for 5 min at RT. Cell were viewed under a light microscope and counted on a hematocrit slide. At least 200 cells were counted for each time point. Cells stained blue were considered as dead while white cells were alive. The percent (%) dead cells were counted. Each assay was run in triplicate.

2. Live/Dead® Assay

The Live/Dead® Viability/Cytotoxicity assay kit (Molecular Probes, Eugene OR) was employed to assess cell viability in infected cells. Two parameters, intracellular esterase activity and plasma membrane integrity, can be used to assess cell viability. This assay utilizes calcein AM and ethidium homodimer-1 to differentiate between live and dead cell populations. Live cells have intracellular esterase activity and are able to convert the nonfluorescent calcein AM to an intense green fluorescent (ex/em ~495 nm/~515nm) polyanion. Ethidium homodimer-1 enters only cells with compromised plasma membranes and preferentially binds DNA to give an intense red fluorescence (ex/em ~495 nm/~635 nm) in dead cells. Live cells exclude uptake of ethidium homodimer-1 because they have intact plasma membranes. The Live/Dead® Viability/Cytotoxicity assay was followed as directed by the manufacturer. Briefly, cells were plated on glass coverslips overnight and infected the following day. Subsequently cells were treated with a solution containing 2 μM calcein AM and 4 μM ethidium homodimer-1 for 40 min at RT and viewed under a Leitz DMRB fluorescence microscope.

Nuclear Alterations:

1. DNA Fragmentation Analysis by Agarose Gel Electrophoresis

The desired cell line was plated in 100 mm plates at a cell density of 7 x 10^6 cells, and incubated overnight. The cells were infected as stated above and left for the desired time (hpi) for DNA extraction. The cells were scraped with a rubber policeman, washed with 1X PBS and centrifuged for 10 minutes (min) at 1,000 x g. The supernatant was aspirated and the pellet was resuspended with 1.5 ml of 1X PBS. The cells were added into a microcentrifuge tube and respun at 1,000 x g for 5 min. The wash was removed and the cell pellet was resuspended with 0.5 ml of lysis buffer (10mM Tris-HCl at pH 7.5, 10mM EDTA at pH8.0, 0.2% Triton X-100) and incubated on ice for 15 min. The lysate was centrifuged at 12,000 x g for 20 min and the supernatant was treated with 5 µl RNase A (100 µg/ml) (Sigma) and incubated at 37°C for 1 hour. DNA was purified by phenol extractions with back extractions and precipitated overnight by adding 2.5 vol. of 100% ethanol and 30µl of 5M NaCl. The DNA sample was centrifuged at 12,000 x g for 5 min and washed with 75% ethanol. The DNA pellet was dried in a Speedvac and resuspend in TE buffer (10 mM Tris-Cl, 1mM EDTA, pH 8.0) with ethidium bromide and 10X loading buffer. Resuspended DNA was run on a 2% agarose gel (ran until dye front was 2/3 down) and viewed with a UV transluminator for detection of DNA laddering.

For a more sensitive detection of fragmented DNA radioactive end labeling of DNA was performed as described previously (Karasavvas et al, 1996). Briefly, DNA was collected as mentioned above and labeled with 25µCi [α^{32}P]ddATP (3000 Ci/mmol) (Amersham, Arlington, IL) and incubated with 25 U of terminal transferase (Boehringer-Mannheim, New York) and 25mM $CoCl_2$ at 37°C for 60 min. Followed by phenol extraction and overnight ethanol precipitation. Fragmented DNA was separated on a 2% agarose gel. The gel was dried at 60 °C for 3 hrs and exposed to X-ray film for 30 min.

2. *In situ* DNA Fragmentation (TUNEL POD)

Infected cells on glass coverslips were fixed with 3% paraformaldehyde in 1X PBS for 10 min at RT, and washed with 1X PBS. End-labeling was done by using the TUNEL POD kit (Roche Molecular Biochemicals, Germany cat # 1684817) according to the manufacturer's instructions. Briefly, cells were permeabilized and incubated with 0.3% H_2O_2 in methanol to abolish endogenous peroxidase activity. Next samples were incubated for 30 min at 37 °C with a TUNEL reaction mixture containing 9 parts TUNEL label + 1 part TUNEL enzyme. The peroxidase covalently linked to 3' ends in this step (TUNEL POD) and its substrate, 3, 3'-diaminobenzidine (DAB) (Sigma-Aldrich, St Louis MO) were used for signal detection.

3. Chromatin Condensation and Fragmentation by Hoechst Staining

Chromatin condensation and fragmentation was assessed by the DNA fluorochrome *bis*benzimide (also called Hoechst 33258). Virus and mock-infected cells were trypsinzed, washed and centrifuged at 1,000 x g for 5 min. The pellet was resuspended and fixed with 100 µl of 3% paraformaldehyde (Fisher) in 1X PBS for 10 min at RT. After fixation the cells were centrifuged at 1,000 x g for 5 min. The pellet was resuspended in 40 µl of Hoechst 33258 (Sigma-Aldrich, St Louis MO) at 16µg/ml in 1X PBS for 25 min RT. Cells were washed with 1 ml of 1X PBS, centrifuged at 1,000 x g for 5 min and resuspended with the appropriate volume of 1X PBS (dependent on pellet size). Nuclei that have fragmented into small dense bodies are considered apoptotic while nuclei with evenly dispersed chromatin are non-apoptotic. Quantitation of fragmented nuclei was observed using a Leitz DMRB fluorescence microscope.

4. Quantification of Apoptosis by Flow Cytometry

Apoptosis was measured using subdiploid DNA peaks analysis after staining with propidium iodide (PI). Collected samples were fixed with a mixture of methanol:acetone (4:1) and PBS in a 1:1 ratio for 10 min at –20 °C. After fixation the samples were sent to our collaborator Dr. Serafina Oliverio at the University of Rome, Italy for further processing as discussed below. For subdiploid DNA evaluation cells were washed twice in PBS after incubation and resuspended in 0.75 ml hypotonic fluorochrome solution containing 50μg/ml PI (Calbiochem, La Jolla, CA) in 0.1% sodium citrate plus 0.1% Triton x-100 (Sigma, St. Louis, MO) in polypropylene tubes (Nunc). The tubes were placed at 4°C in the dark overnight before the flow-cytometric analysis. The PI fluorescence of individual nuclei was determined using a XL flow cytometer (Coulter, Hialeah, FL.) and the percentage of apoptotic nuclei was determined on the basis of the number of cells in the subdiploid DNA peak in the DNA fluorescence histogram.

Morphology:

Electron microscopy (EM)

Plates seeded with MDCK and A549 cells with a density of 1.5 x 10^6 were infected with WSN virus at a MOI of 5. At various hours post infection (h pi) cells were fixed in 0.5% glutaraldehyde in 1X PBS, pH 7.4 for 10 min. The cells were gently scraped off with a rubber policeman and centrifuged in microcentrifuge tubes at 12,000 x g for 5 min. The centrifuge tube with pellet was sliced with a razor to 1 mm sections and placed in 1 ml of 2.5% glutaraldehyde in 1X PBS, pH 7.4 overnight at RT. The slices containing the cells were washed 3 times with 1X PBS, pH 7.4 for 5 min each. The secondary fixation was with 1% osmium tetroxide for 3 hours

at 4 °C, after which the cells were washed 3 times with 1X PBS, pH 7.4 for 5 min each and dehydrated through ascending ethanol concentrations (50% - 100%) for 10 min each. The samples were sent to Dr Daniela Quaglino at the University of Modena, Italy for further processing. Samples were embedded in Spurr resin, sectioned with the Reichert-Jung Ultracut E microtome and stained with lead citrate and aqueous uranyl acetate. High resolution images were taken with a JOEL JEM-1200 EX electron microscope. All reagents were purchased from Electron Microscopy Sciences, Fort Washington PA.

Measurement of mitochondrial function was performed in several ways:

1. Measurement of Mitochondrial Membrane Potential

Rhodamine-123 (Sigma-Aldrich, St Louis MO) is a cationic fluorescent dye that is readily taken up by actively respiring mitochondria and commonly used in membrane depolarization analysis during cell death. A loss in fluorescence signal represents a disruption in the mitochondrial transmembrane potential. Rhodamine-123 is dissolved in dimethylsulfoxide at a stock concentration of 1 mM.

Cells were plated at a concentration of 2 x 10^6 cells in 60 mm plates overnight. As described previously (Goldstein and Korczack, 1981), cells were loaded with 1 μM of rhodamine-123 (Sigma-Aldrich, St Louis MO) during the last 45 min of the infection at 37 °C in the dark. Subsequently cells were scraped, washed with 1X PBS, centrifuged at 1,000 x g at 5 min and the pellet lysed with 1 ml of isobutanol for 5 min. The mock-infected cells were used for the basal level of fluorescence. Fluorescence intensity of rhodamine-123 extracted by isobutanol

was quantified on a Perkin Elmer MPF-66 fluorescence spectrophotofluorometer at 508 nm excitation and 536 nm emission. The slits were set at 5 nm (excitation) and 10 nm (emission).

2. MitoTracker Red

Conventional fluorescent stains for mitochondria, such as rhodamine 123, are readily sequestered by functioning mitochondria, but are subsequently washed out of the cells once the mitochondrion's membrane potential is lost. MitoTracker Red is a mitochondrion-selective stain that is concentrated by active mitochondria and retained during cell fixation. MitoTracker Red contains a mildly thiol-reactive chloromethyl moiety. The chloromethyl group appears to be responsible for keeping the dye associated with the mitochondria after fixation.

Prior to collection, cells plated on coverslips (35 mm plates) were treated with 20 nM of MitoTracker Red (stock: 100 μm in DMSO) (Molecular Probes, Eugene OR) for the last 30 min of the experiment. The cells were washed with PBS and fixed with 3% paraformaldehyde (Fisher) in 1X PBS for 10 min at RT. The fixed samples were analyzed on a Leitz DMRB fluorescence microscope with a Rhodamine filter set.

3. MTT Assay

The MTT (3- (4,5-dimethylthiazol-2-yl)-2,5-diphenyltetrazolium bromide) assay measures the enzymatic activity of the succinate-tetrazolium reductase system (EC 1.3.99.1), which belongs to the mitochondrial respiratory chain and is a good marker for measuring cell viability since activity is present only in viable cells. The assay also measures the state of the mitochondrial respiratory chain within mitochondria.

Cells were plated at a concentration of 1.5 x 10^6 in 35 mm plates overnight. A 37.5 µl aliquot of a 5mg/ml stock solution of MTT (Sigma) was added to the plate, which were incubated for 1 hr at 37°C. Cells were scraped off the plate, washed once with 1X PBS and centrifuged for 6 min at 1,000 x g. Tetrazolium salts when reduced form a purple colored water-insoluble formazan precipitate that can be solubilized and quantitated spectrometrically. The pellet was resuspended with 0.1 N acidic isopropanol (1N HCl) and centrifuged for 5 min at 1,000 x g. The supernatant was analyzed by a spectrometer and the difference between the absorbance of 570nm (background) and 690nm of each sample was measured.

4. Isolation of Cytosolic and Mitochondrial Fractions of Cytochrome c

Cells were washed once with 1X PBS and centrifuged at 1,000 x g for 5 min. The pellet was resuspended in CLAMI buffer (250 mM sucrose, 70 mM KCl, 50 mg/ml digitonin in 1X PBS, protease inhibitor cocktail (1 tablet/ 10 ml CLAMI buffer)) and incubated on ice for 5 min. The cells were pelleted at 12,000 x g for 5 min at 4°C. The supernatant (cytoplasmic fraction) was removed and the pellet was resuspended with universal immunoprecipitation buffer (IP) (50mM Tris-HCl at pH 7.4, 150 mM NaCl, 2mM EDTA, 2mM EGTA, 0.2% Triton X-100, 0.3% NP-40, protease inhibitor cocktail (1 tablet/ 10 ml IP buffer) (Boehringer Mannheim, Germany)) and incubated on ice for 30 min. The samples were centrifuged at 12,000 x g for 10 min at 4°C and the supernatant collected (represents the mitochondrial fraction).

Mitochondrial and cytoplasmic fractions (30 µg total protein loaded per lane) were separated on 15% SDS-PAGE and electroblotted onto nitrocellulose membranes (*see below for further detail on Western blotting*). Cytochrome c was detected by a monoclonal antibody [1:500 dilution] (Pharmingen). Secondary goat-antimouse horseradish peroxidase-labeled

antibody [1:10,000 dilution] (Amersham Pharmacia Biotech) was detected by enhanced chemiluminescence.

Measurement of Lysosome Activity:

1. *In situ* analysis of Acid Phosphatase Activity in Lysosomes (qualitative)

Cells were grown on coverslips overnight, infected as described above and samples were collected at various hours post infection. The coverslips were placed in a coplin jar and citrate fixation solution (18 mM citric acid, 9 mM sodium citrate, 12 mM NaCl) was added and left for 30 seconds. The coverslips were washed for 1 min with dH_20. An acid phosphatase solution (*see section on reagents*) was added to the coplin jar and incubated for 1 h at 37°C. Coverslips were gently washed with running tap water for 2 min and air dried. A methylene blue (1.4% [w/v] in ethanol) counter stain was added for 10 sec and coverslips were rinsed twice with dH_2O. The coverslips were mounted onto slides with crystal mount solution.

2. *In vitro* analysis of Acid Phosphatase Activity in Lysosomes (quantitative)

Cells were plated at 2 x 10^6 cells in 60 mm plates overnight, infected as described above and samples were collected at various hours post infection. Cells were carefully scraped with a rubber policeman, transferred to an ice-cold disposable culture tube and spun for 10 min at 1,000 x g at 4 °C. The pellet was washed with ice cold 1X PBS, transferred to a ice cold microcentrifuge tube and spun for 10 min at 1,000 x g at 4 °C. The pellet was resuspended with 100 µl of 1X PBS, mixed with 0.5 ml of p-nitrophenol phosphate (substrate) (*see section on reagents*) and 0.5 ml citrate buffer (*see section on reagents*) on ice. The sample was vortexed

very well and incubated at 37°C for 1 h. Following incubation, the reaction was terminated by the addition of 5 µl 1 N NaOH and vortexed. When made alkaline, nitrophenol was converted to a yellow precipitate complex and measured at 410 nm. The intensity of color formed was proportional to enzyme activity.

VII. Protein Analysis

1. Protein Extraction with RIPA Buffer

The desired cell line was plated overnight in 100 mm plates and the cells were infected with an MOI of 5 the following day. The cells were carefully scraped with a rubber policeman, transferred to an ice cold disposable culture tube and spun for 10 min at 1,000 x g at 4 °C. The supernatant was aspirated away and the pellet was washed with ice cold 1X PBS. The resuspended cells were transferred to a ice cold microcentrifuge tube and spun for 10 min at 1,000 x g at 4 °C. The pellet was resuspended with 50-200 µl (depending on size of pellet) of RIPA buffer (10 mM Tris-HCl pH 7.4, 150 mM NaCl, 1% Triton X-100, 0.1% SDS, 0.5 mM EDTA) with protease inhibitor cocktail (1 tablet per 10 ml RIPA buffer) (Boehringer Mannheim, Germany) and incubated on ice for 30 min. Lysate was spun at 12,000 x g for 20 minutes. The supernatant was transferred to a new microcentrifuge tube and stored at –20 or –80 °C.

2. Western Blotting

The Bio-Rad protein assay (Bradford method) (Bio-Rad Lab., Hercules CA) was used to determine protein concentrations in the samples. Equal amounts of total protein (30 µg) were resolved on 7%, 10% or 15% SDS-polyacrylamide gels (gel percentage dependent on molecular

size of protein of interest) and transferred onto Hybond supported nitrocellulose membranes (Amersham Pharmacia Biotech) by semi-dry electroblotters. The blots were blocked for 1 h in 5% nonfat dry milk in 1X PBS + 0.1% Tween 20 (PBST) at RT and then incubated with primary antibodies in blocker (5% nonfat dry milk in PBST) overnight at 4 °C. Primary antibodies used were: caspase-8 [1:1000 dilution] and caspase-3 [1:1000 dilution] gift from Donald Nicholson (Merck Frosst, Canada), cytochrome c [1:500 dilution] (Santa Cruz Biotechnology), Bid [1:500 dilution] (Santa Cruz Biotechnology) and PARP [1:500 dilution] (Santa Cruz Biotechnology). After 3 washes with PBST blots were exposed to goat anti-rabbit or, for Bid, donkey anti-goat conjugated with horseradish peroxidase (HRP) secondary antibody [1:10,000] for 1 h at RT and followed with an additional 3 washes with PBST. The blots were incubated with the ECL Plus chemiluminescence Western blotting detection reagent (Amersham Pharmacia Biotech) and exposed to Kodak BioMax film (Sigma-Aldrich, St Louis MO) for visualization.

3. Immunocytochemistry

The desired cell line was plated in 35 mm plates with glass coverslips at a cell density of 1.5×10^6 cells, and incubated overnight. The cells were infected as stated above and left for the desired time (h pi). Supernatants from the plates were collected, centrifuged, washed with 1X PBS and the cell pellet resuspended and fixed with 3% paraformaldehyde (Fisher) in 1X PBS for 10 min at RT. At the same time the plates were also washed with 1X PBS and fixed with 3% paraformaldehyde (Fisher) in 1X PBS for 10 min at RT. Cells collected from supernatant were spread onto poly-L-lysine coated microscope slides and the coverslips were permeabilized with PBS + 0.1% Triton X-100 for 5 min at RT in coplin jars. Both slides and coverslips were washed once with PBS and blocked with 5% goat serum for 1 h at RT. Blocking serum was removed and

samples were incubated with the appropriate primary antibody at 4°C overnight in a humidified chambered box. Primary antibodies used were against caspase-3 [1:1000 dilution] (Pharmingen) and cytochrome c [1:500 dilution] (Santa Cruz Biotechnology) and antibodies were diluted with PBST with 1% goat serum. The following day the samples were washed 3 times with PBST and incubated with goat anti-rabbit (IgG [H+L]) or goat anti-mouse (IgG [H+L]) secondary antibody conjugated with Alexa Fluor® 488 (Molecular Probes) for 1 h at RT. Samples were later washed 3 times with PBST and mounted with gel mount and sealed with nail polish.

VIII. *In vitro* Caspase Inhibition

Following the one hour infection with influenza or viral diluting media the infected and mock infected cells were treated with the pan-caspase inhibitor zVAD-fmk (benzyl-oxycarbonyl-Val-Ala-Asp(Ome)fluoromethylketone) (Calbiochem, cat # 627610) with a final concentration of 50 μM. Cell samples were taken at the appropriate times (hpi).

IX. Reagents

1X Phosphate Buffered Saline (PBS)

1X PBS was made by adding 137 mM NaCl, 2.7 mM KCl, 4.3 mM $Na_2HPO_4 \cdot 7H_2O$ and 1.4 mM KH_2PO_4, pH 7.3. The solution was autoclaved. To make **10X PBS** the recipe was multiplied by 10.

100X CaMg

The CaMg solution was made by adding 1 g $CaCl_2$, 1 g $MgCl_2$ and 100 ml dH_2O. The solution was autoclaved.

Virus Diluting Media

Virus diluting media was made by adding 10 ml **10X PBS**, 0.6 ml 35% BSA, 100X P/S (penicillin/streptomycin), and 1 ml **100X CaMg**. The mixture was brought up to volume to 100 ml with dH_2O. CaMg was mixed in last; otherwise CaMg and PBS would precipitate out.

MEM mix

MEM mix was made by adding 2X Minimal Essential Medium (MEM) (cat # 12-668A) (BioWhittaker, Walkersville MD), 0.42% bovine serum albumin (BSA), 2X L-glutamine (4 mM), 100U/ml penicillin and 100 mg/ml streptomycin, 0.24% sodium bicarbonate, and 0.02M HEPES.

Virus Plaquing Media

The agar overlay medium was prepared by mixing (for 25 ml) 14 ml of **MEM mix**, 0.25 ml 1% DEAE dextran, 0.5 ml 5% $NaHCO_3$, and 2.75 ml dH_2O into a 50 ml conical centrifuge tube and placed into 37 °C water bath until needed. Right before adding overlay media over cells 7.5 ml of warmed 2% Oxoid® agar (Oxoid, Hampshire England) was added and mixed well.

Crystal Violet Staining Solution

Crystal violet staining solution was made by adding 4 ml of 1% crystal violet solution in H_2O, 8 ml methanol and 30 ml H_2O.

Acid Phosphatase Solution (Sigma, cat# 181-A)

The acid phosphatase solution was made by mixing 0.6 ml of $NaNO_3$ and 0.6 ml Fast Garnet GBC base solution (7 mg/ml in HCl) into a 50 ml Falcon tube and incubating for 2-5 min at RT. Next 22.8 ml of dH_2O was added and the mixture was warmed to 37°C. Lastly, 3 ml of acetate solution (2.5 mM pH 5.2) and 3 ml of Naphthol AS-BI phosphoric acid solution (4 g/L) was added to the entire mixture.

p-Nitrophenol Phosphate Working Solution:

The p-nitrophenol phosphate, disodium hexahydrate (Sigma, cat# N-4645) powder was added to dH_20 to a working concentration of 5 mg/ml. The solution was stored at -20°C.

Citrate Buffer:

Citrate buffer was made by adding 90 mM citrate and 10 mM NaCl, pH 4.8. The buffer was stored at 4°C.

Part III. Results and Discussion

Objective

Chapter 1. Characterization of Influenza A Virus Induced Cell Death in MDCK and A549 Cells

1.1. Determination of Viral Production and Effective MOI for Cell Killing

1.1.1. Summary and Discussion

1.2. Evaluation of the Type of Cell Death in MDCK Cells

1.2.1. Membrane Integrity

1.2.2. Nuclear Alterations

1.2.3. Morphology

1.2.4. Not All MDCK Cells Undergo Cell Death at the Same Rate

1.2.5. Summary and Discussion

1.3.Evaluation of the Type of Cell Death in A549 Cells

1.3.1. Determination of Viral and Protein Production

1.3.2. Membrane Integrity

1.3.3. Nuclear Alterations

1.3.4. Morphology

1.3.5. Summary and Discussion

1.4. Viral Replication is Required to Induce Cell Death

1.4.1. Summary and Discussion

1.5. Difference in Kinetics of Cell Death is Not Unique to Influenza Induced Cell Death

1.5.1. Summary and Discussion

Objective

Influenza virus has evolved ways to induce cell death that contributes to its pathogenesis but the details remain to be found. To determine the mechanism of induction we set on to characterize the type of cell death induced by the virus. Followed by investigating the activation and the requirement of different components of the various cell death pathways.

The first question addressed was whether influenza A/WSN/33 (WSN) virus could kill Madin Darby canine kidney (MDCK) and A549 human lung epithelial cells and if so how? As mentioned in the Introduction there are many types of cell death so characterizing the type of cell death induced in both cell lines was of importance. The characterization of the type of cell death was done by examining the cellular changes occurring within the infected cell such as alterations in membrane integrity, morphology and nuclear composition.

The next question asked was, in regard to the involvement of the different components of the cell death pathways in influenza induced cell death and whether they were required? We examined the involvement and requirement of the various components of the extrinsic and intrinsic cell death pathways.

As part of the extrinsic pathway a ligand can bind to the specific receptor and induce cell death. We asked whether the attachment of virus to the cell surface could activate the extrinsic pathway leading to cell death without viral replication. Our data present in this section showed that viral replication is required. In addition previous studies (Takizawa et al, 1993; Takizawa et al, 1995; Wada et al, 1995; Balachandran et

al, 2000) have shown that influenza viruses can upregulate the expression of the Tumor Necrosis Factor Receptor Family member called Fas in HeLa cells. The Fas receptor is important since it is activated during the extrinsic cell death pathway. We therefore evaluated the need of the Fas signaling pathway by the use of a cell line defective in Fas.

Beside the extrinsic cell death pathway the intrinsic pathway contributes to the demise of the cell. Two important components of the intrinsic pathway involve the mitochondria and p53. The mitochondria plays an important role during cell death as it can release pro-apoptotic factors into the cytoplasm that can induce a caspase dependent and caspase-independent cell death pathway. We first investigated whether the mitochondria are affected during influenza induced cell death by measuring the mitochondrial membrane potential, respiration state and release of apoptotic factors (such as cyto c) into the cytoplasm. There are many proteins belonging to the Bcl-2 family that associate with the mitochondria and modulate its activity. Therefore we next examined the requirement of pro-apoptotic (Bak, Bax and Bim) and anti-apoptotic (Bcl-2) Bcl-2 family members during influenza induced cell death by the use of knockout mouse embryo fibroblast (MEF) cells.

The p53 signaling pathway plays a crucial role in the induction of cell death (Hickman et al, 2002). Certain viruses have been shown to modulate the activity of p53 hence affecting the induction of cell death. For example, the human cytomegalovirus encodes an early gene product, IE2, which has been shown to repress p53 transcriptional activity and inhibit apoptosis (Hagemeier et al, 1994; Zhu et al, 1995). As for the influenza virus it is not known whether influenza induced cell death is p53 dependent or

independent. We therefore tested the requirement of p53 during influenza induced cell death.

As discussed in the Introduction a certain class of cysteine proteases called caspases are involved in propagating the cell death signal and degrading the cell. Although different signaling pathways can be activated by different stimuli, caspases always converge to a common point linking the extrinsic and intrinsic pathways and lead to the demise of the cell. We therefore evaluated whether caspases are activated during influenza induced cell death in A549 and MDCK cells. In addition to examining the activation of caspases we wanted to determine whether caspases are dispensable during influenza induced cell death.

The cleavage of Bid, a pro-apoptotic Bcl-2 member, by caspase-8 is another convergence point of the extrinsic and intrinsic cell death pathways. The activated truncated Bid is important since it translocates to the mitochondria and affects its function. For that reason we evaluated the cleavage of Bid during influenza induced cell death.

Besides the involvement of caspases during cell death another class of proteases implicated in cell death are the lysosomal resident cathepsin proteases. For example, in *Autographa californica* M Nucleopolyhedrovirus cathepsins have been implicated in activating the virally encoded protein, ProV-CATH, which has an essential role in host liquefaction (Hom et al, 2002). No studies to date have shown the need of cathepsins during influenza induced cell death therefore we investigated the invovlement of cathepsins during influenza induced cell death by using knockout MEF cells.

Part III. Results and Discussion

Chapter 1. Characterization of Influenza A Virus Induced Cell Death in MDCK and A549 Cells

1.1. Determination of Viral Production and Effective MOI for Cell Killing:

Prior to the evaluation of the type of cell death we measured the amount of influenza A/WSN/33 [H1N1] (WSN) virus production in MDCK cells to establish the level of a productive viral infection in our hands. We chose MDCK cells because they are used extensively in general research on the influenza virus and can efficiently replicate the virus. Viral titer was determined by the plaque assay as described in Materials and Methods and was calculated as plaque forming units per milliliter (pfu/ml) through various hours post infection (hpi). Plaques were defined as regions where cells no longer existed within a monolayer of cells and were counted as one viral particle. We found an increase of WSN virus production at 24 hpi, which began to plateau at 48 hpi and declined slightly by 144 hpi (Figure 1A, see pg 156) indicating that a productive and sustainable infection was achieved.

To establish a multiplicity of infection (MOI) or infection dose that would effectively cause a cytopathic effect in infected MDCK cells, we infected these cells with varying amounts of influenza virus. An MOI of one is equivalent to one virus per cell, regardless of volume. The higher the MOI used, the more viruses that can infect an individual cell. Varying the MOI's would also help in determining whether an increase in

viral load contributes to an overall increase in the amount of cell death or if the viral replication cycle was quicker than the progression of cell death.

The cytoplasmic affect of virus on cells was measured by the level of cell death. The level of cell death was measured by the trypan blue exclusion assay, which was a good maker for membrane integrity and an indicator of cell viability. Cells that had taken up the trypan blue dye were scored as positive for trypan blue and designated as dead or dying cells because the outer plasma membrane integrity was compromised. Cells appearing white were considered as live cells. MDCK cells were plated and infected with WSN concentrations that ranged from an MOI of 0.1 to 10. We found a direct correlation between increases in MOI at 24 hpi and the level of cell death (Figure 1B) as measured by trypan blue. A general trend could be seen in that as the MOI was increased more cells died. The number of deaths approximately doubled between a MOI of 1 and 10.

However the error bars for cell death of MDCK cells infected with an MOI of 0.1, 0.5 and 1 overlappeds suggesting that the virus replicated and spread to non-infected cells quicker than the appearance of trypan blue positive cells. At a low MOI (i.e. 0.5) not all of the cells are infected by the initial addition of the virus, but with the rapid spread of the virus the cell death percentages were similar to the cells infected with an MOI of 1, where all cells were infected.

1.1.1. Summary and Discussion:

The plaque assay showed that influenza A/WSN/33 (WSN) virus replicated very well in MDCK cells while the MOI experiments indicated that an MOI of 5 gave good

cell killing in MDCK cells that was not substantially increased by increase in MOI. Therefore MDCK cells were subsequently infected at an MOI of 5.

1.2. Evaluation of the Type of Cell Death in MDCK Cells:

1.2.1. Membrane Integrity:

MDCK cells were infected with WSN at a MOI of 5 to ensure that all the cells were infected at approximately the same exact time. Cells were collected at various hpi for the analysis of cell death. We used several methods to assess the extent and type of cell death. Trypan blue was used as a marker of membrane integrity and an indicator of cell viability. We found that percent cell death of MDCK cells increased during the infection and significantly increased by 48 hpi (Figure 2). At 48 hpi, approximately 80% of infected MDCK cells were positive for trypan blue while mock infected cells (uninfected control cells) at the same time had over 20% cell death.

1.2.2. Nuclear Alterations:

An apoptotic cell has condensed chromatin with nuclear shrinkage and fragmentation that can be detected by a fluorogenic dye called Hoechst. Fragmented nuclei appear as a cluster of spheres with intense white staining due to the condensation of the chromatin as compared to normal nuclei, which appear spread out and pale blue, as will be seen later. Only nuclei that were condensed and fragmented were scored because there were many variations in the extent of nuclear changes present. Fluorescence microscopy with Hoechst staining showed that WSN infected MDCK cells at 24 hpi

displayed many cells with fragmented and condensed nuclei as compared to the mock-infected cells (Figure 3A). A quantitative analysis of nuclear fragmentation on the same sample of cells (in Figure 2) used for trypan blue showed a steady increase in the number of cells having fragmented nuclei and the majority of MDCK cells by 48 hpi had high levels of fragmentation (Figure 3B, bars). During WSN infection, increased levels of the cytopathic effect as measured by trypan blue (Figure 3B, line) correlated with increased levels of nuclear fragmentation and condensation at 48 hpi. We see at 24 hpi approximately a 50% higher level of fragmented nuclei than trypan blue positive cells. This suggests that during WSN infection changes within the nucleus occur earlier than the disruption of the outer plasma membrane. The MDCK cells infected with varying MOI's were also quantitated for the number of cells having fragmented nuclei as seen with Hoechst staining. Although we find a direct correlation between the increases in MOI and increases of fragmented nuclei (Figure 3C) the percentage of cells with fragmented nuclei was higher than the blue cells revealed by trypan blue. The nuclear data also showed that high levels of fragmented nuclei appeared in cells infected with high MOI's, consistently approximately 40% more cells with fragmented nuclei than the picture for TB.

Nuclear fragmentation is accompanied by DNA fragmentation and the appearance of a DNA ladder, a hallmark of apoptotic cell death. MDCK cells infected with an MOI of 5 were harvested at different h pi and their DNA extracted and electrophoresed on an agarose gel for the presence of a DNA ladder. As shown in Figure 4A, gel electrophoresis of DNA taken from infected MDCK cells showed laddering was barely detected at around 8 hpi and increased with time with high levels at 24 hpi. Mock-infected MDCK

cells at 24 hpi showed no DNA fragmentation. Regardless of the level of MOI infected cells undergo characteristic DNA laddering depicting apoptotic cell death (Figure 4B). MDCK cells infected with a high MOI had a higher percentage of fragmented nuclei than cells infected with a low MOI (Figure 3C); however, regardless of MOI the DNA ladder appeared to be relatively equal in fluorescence intensity in all samples. Perhaps at higher MOI's the DNA undergoes more damage and upon processing the lower molecular weight DNA is lost as compared to samples of low MOI.

Flow cytometry has been used to detect apoptotic cells by looking at changes in morphology of the dying cell that can be detected by alterations in the light scatter properties, or by assessing cellular DNA content. In an apoptotic cell, degradation of DNA reduces the total DNA content and as a consequence, the apoptotic cell takes up less DNA binding dye and the cells are counted in a sub G0-G1 peak. As a result dying cells can be distinguished from healthy cells, based on the level of DNA present and the fluorescence emitted. This method has also been referred to as fluorescence activated cell-sorting (FACS) analysis.

To use this method in our study we first infected MDCK cells with WSN (MOI 5) and collected the cells at various h pi and fixed them with methanol:acetone (4:1). The samples were later sent to our collaborator, Dr. Serafina Oliverio at the University of Rome, Italy for FACS analysis. The cells were treated with the DNA binding dye propidium iodide (PI) and their DNA content analyzed. FACS analysis (Figure 5) of WSN infected MDCK cells correlated with the DNA fragmentation and Hoechst staining data. Dead cells were detected as early as 10 hpi. By 24 hpi a large proportion of cells underwent apoptotic cell death as indicated by an increase of the subdiploid population

(M1). This M1 population represents cells that have nuclei that are fragmented. A steady rise in cell death from 6 to 12 hpi can be seen and a second rise at 18 to 24 hpi, indicating a new round of replication.

1.2.3. Morphology:

During apoptotic cell death there are morphological changes that occur within a dying cell, such as cell rounding and shrinkage. We first analyzed these changes by light microscopy (LM) and then by electron microscopy (EM). Thick sections (1 μm thick) normally used for the evaluation of sample quality prior to EM analysis were, initially used for the morphological study. MDCK cells were infected with an MOI of 5 and examined at different h pi. For a control, mock-infected cells were used at 24 hpi. Cells were harvested at various hpi and fixed with glutaraldehyde and osmium tetraoxide and dehydrated with increasing percentages of ethanol. The samples were sent to Dr Daniela Quaglino at the University of Modena, Italy and processed for EM analysis. Mock-infected MDCK cells were slender and elongated with visible nuclei and multiple nucleoli (Figure 6A). By 8 hpi regions of infected and dying cells were detected with signs of cell rounding and intense staining of the nuclei and cells with methylene blue (Figure 6B) as compared to the mock-infected cells. Later at 24 hpi we could see massive levels of cell death as detected by cell rounding, nuclear changes and disintegration of cell structures (Figure 6C).

EM analysis showed further evidence of apoptotic cell death in infected MDCK cells. EM micrographs showed greater detail than that seen by LM in mock-infected cells (Figure 7A). An increase in the number of apoptotic cells was observed with increases in

time of infection. In the population at 24 hpi we can detect typical apoptotic morphology such as condensation of chromatin, fragmentation of nuclei and cell rounding and shrinkage as compared to the mock-infected cells (Figure 7B). The infected cells had patches of increased electron density due to dense aggregates of chromatin as well as the margination of the chromatin and alterations of the cytoplasm, namely the extensive formation of vacuoles, were present (Figure 7C). Some infected cells displayed signs of secondary necrosis indicating advanced stages of influenza induced cell death (Figure 8). The cells appeared necrotic because of the disintegration of the outer plasma membrane and the degraded and diffuse appearance of the chromatin. The EM analysis showed at a single time post infection cells undergoing different stages of cell death. Visual inspection indicated that not all infected MDCK cells died at the same time even though all MDCK cells were infected with WSN (MOI 5). The reason was not clear and will be analyzed further as discussed below.

1.2.4. Not All MDCK Cells Undergo Cell Death at the Same Rate:

MDCK cells infected with WSN do not all die at the same time. This is evident even with light microscopy examination even though all the cells were infected with the virus at the same time (Figure 9A and B). At 12 hpi, MDCK cells infected with WSN at an MOI of 5 showed many cells detaching from the plate (arrows) while a large number of infected cells still remained attached. To examine this further, during each time point the unattached cells, which were located in the supernatant, were separated from the attached cells and cell viability was measured by the trypan blue exclusion assay for both populations. Cells that were no longer attached had higher levels of trypan blue positive

cells than attached cells and the ratio increased as time progressed (Figure 10A). We also assessed cell viability of the two populations by another assay called Live/Dead® because this assay uses different parameters to evaluate cell death in cells and provides an easy colorimetric method to differentiate between live and dead cells. Also *in situ* analysis of cell death can be assessed without disturbing cell morphology, unlike trypan blue analysis where cells have to be trypsizined prior to analysis. The Live/Dead® assay measures the activity of an esterase that is active only in living cells. Cells with this activity and therefore alive are able to convert calceinAM to a fluorescent product and appear green as seen in mock-infected MDCK cells (Figure 10B). The hydrolyzed fluorescent product cannot escape intact cells. Dead cells, however, appear red due to the co-presence of ethidium homodimer, which only enters cells with compromised membranes and intercalates within the DNA. Live/Dead® analysis conferred that the floating MDCK cells infected at a MOI of 5 at 24 hpi were dead (Figure 10C) while the attached cells appeared to be alive (Figure 10D).

Quantification with Hoechst staining was also done on these two populations (Figure 11A) and the results correlated with the cell viability data. There was a clear distinction between attached versus unattached cells by 48 hpi in that 100% of unattached cells had fragmented nuclei while attached cells had very low levels of fragmentation. Mock-infected cells had normal nuclei (Figure 11B) as seen by fluorescence microscopy while the majority of unattached cells had condensed and fragmented nuclei (Figure 11C) in contrast to the attached cells, which had intact nuclei, but differed from mock-infected cells in that they began to condense (Figure 11D). Although all cells were exposed to the

virus it was apparent that they responded differently. The reason was for this differential response was not clear.

1.2.5. Summary and Discussion:

We have started to characterize influenza A/WSN/33 (WSN) virus induced cell death in Madin Darby canine kidney (MDCK) cells and have determined that cell death was apoptotic by a variety of methods. We see at 48 hpi, approximately 80% of infected MDCK cells were positive for trypan blue, indicating that the outer plasma membrane was compromised. An apoptotic cell often has condensed chromatin with nuclear shrinkage and fragmentation. A quantitative analysis of nuclear fragmentation showed a steady increase in the number of cells having fragmented nuclei and the majority of MDCK cells by 48 hpi had high levels of fragmentation. During WSN infection, increased levels of the cytopathic effect correlated with increased levels of nuclear fragmentation and condensation at 48 hpi. This suggested that during WSN infection changes within the nucleus occur earlier than the disruption of the outer plasma membrane.

A hallmark of apoptotic cell death is the fragmentation of DNA into oligonucleosomal fragments as detected by gel electrophoresis. DNA fragmentation was detected slightly at around 8 hpi and increased with time with high levels already at 24 hpi. Mock-infected MDCK cells at 24 hpi show no DNA fragmentation.

The morphology of MDCK cells infected with WSN was analyzed by electron microscopy. In the population at 24 hpi we can detect typical apoptotic morphology such as condensation of chromatin, fragmentation of nuclei and cell rounding and shrinkage as

compared to the mock-infected cells. The infected cells had patches of increased electron density due to dense aggregates of chromatin and alterations of the cytoplasm, namely the formation of vacuoles. The cell shape of dying cells was no longer elongated as the mock infected cells but now round in appearance. Our data presented here indicates that WSN viruses kill MDCK cells by a classical apoptotic morphology. Further analysis of the individual components of the various cell death pathways, such as caspases would give further evidence of apoptotic cell death in MDCK cells and will be discussed later.

Besides the observation of classical apoptotic phenotypes in WSN infected MDCK cells we saw a correlation between infection dose and cell death. A general trend could be seen in that as the multiplicity of infection (MOI) was increased more MDCK cells infected with WSN showed higher trypan blue positive levels and increased numbers of condensed and fragmented nuclei as measured by Hoechst staining.

Also our examination of cells by light and electron microscopy showed that MDCK cells infected with WSN do not all die at the same time, even though all the cells were infected with the virus at the same time. During the influenza infection MDCK cells detached from the plate with increasing numbers as time progressed. There was a clear distinction between attached versus unattached cells by 48 hpi in that close to 100% of unattached cells had fragmented nuclei and trypan blue positive while attached cells had very low levels of fragmentation and good viability. It was not clear why MDCK cells died at different rates.

Since MDCK cells are not generally infected by influenza we used a human lung epithelial cell line to better mimic the cells involved during the infection process.

1.3. Evaluation of the Type of Cell Death in A549 Cells:

MDCK cells are a good cell line for evaluating influenza induced cell death because WSN replicates very well and the cells are easy to handle and manipulate. However these cells are kidney cells and are not normally involved and infected during an influenza infection. We wanted to use a cell line model system that would resemble the cells that are primarily involved in an influenza infection. In humans, influenza A viruses normally infect cells throughout the respiratory system. We chose the A549 human lung epithelial cell line because these cells are typically involved during an infection.

1.3.1. Determination of Viral and Protein Production:

Even though A549 cells were lung cells we still wanted to test whether the human lung epithelial cell line was suitable for analysis of virus-induced cell death. It was important to show that A549 cells were permissive for replication of influenza A/WSN/33 (WSN) virus and could sustain productive infections. The plaque assay (Figure 12A) showed that A549 cells could support replication of WSN since the viral titer increased through time and began to plateau by 72 hours post infection (hpi). As compared to MDCK cells, which are permissive to WSN, A549 cells somewhat more resistant, producing slightly less than 5% of the plaque forming units/ml (pfu/ml) produced by MDCK cells at 144 hpi. However, at 24 hpi MDCK cells produced almost 4000x more pfu/ml than A549 cells. MDCK cells were more efficient in viral replication but A549 cells could still produce high titers of virus.

In order to determine whether viral proteins were synthesized in A549 cells we incubated the cells in media enriched with radioactive amino acids at several 24 hour intervals after infection. Labeling infected cells with ^{35}S methionine demonstrated that in A549 cells (Figure 12B) host protein synthesis was almost completely shut off by 24 hpi and at that time viral protein production was high. Influenza proteins such as the nucleoprotein (NP), nonstructural-1 (NS-1) protein and hemagglutanin (HA) were actively synthesized at 24 hpi but at later times production was much less as visible on the autoradiograph. This reduction in radioactive signal meant that viral protein synthesis was declining and that maximal viral protein production occurred somewhere between 24 and 48 hpi.

1.3.2. Membrane Integrity:

The level of cell death was measured by trypan blue and the percentage of trypan positive cells steadily increased through the infection (Figure 13A). Forty-eight hours after the initial infection only 24% of infected A549 cells were positive, but by 144 hpi the number climbed to approximately 90%. This indicated that a longer infection time was needed before significant levels of cell death can be seen in A549 cells. The extent of cell viability of infected A549 cells was also conferred by the Live/Dead® assay. At 72 hpi mock-infected cells fluoresced green (Figure 13B and C) while at the same time 50% of infected A549 cells fluoresced both green and red (Figure 13D and E), which correlated with the trypan blue data.

1.3.3. Nuclear Alterations:

As mentioned before, during apoptotic cell death the chromatin condenses and the nucleus shrinks and fragments. As seen by Hoechst staining, infected A549 cells that had taken up trypan blue showed very little nuclear fragmentation (Figure 14A) even at 144 hpi. Nuclei from mock-infected A549 cells were large and mostly oval in shape with the chromatin being loosely packed (Figure 14B). At 96 hpi nuclei from infected A549 cells were not fragmented as seen in MDCK cells but the nuclei were round and the chromatin condensed as detected by Hoechst staining (Figure 14C). It is possible that, because the rate of cell death was much slower in A549 cells we missed the population of cells undergoing nuclear fragmentation.

A disparity can be seen in infected A549 cells in that lowered levels of cell viability did not correlate to increased levels of nuclear fragmentation (Figure 15). At 144 hpi, 10% of infected cells had nuclear changes, but at the same time 90% of the cells had compromised outer plasma membranes. This suggests that a dying A549 cell does not manifest marked changes within the nucleus and that the virus affects different cells differentially but ultimately the end result remains the same; the cell dies.

The fragmentation of DNA into oligonucleosomal fragments as detected by gel electrophoresis and TUNEL (Terminal deoxynucleotidyl transferase (TdT)-mediated dUTP Nick End Labeling) assay represents a hallmark of apoptotic cell death. DNA isolated from infected A549 cells lacked the characteristic laddering as seen on agarose gels after 96 hpi or 144 hpi (Figure 16A). These data correlate with the Hoechst analysis data in that low levels of fragmentation were detected in infected A549 cells. The lack of DNA fragmentation could result from a lack of nucleases degrading the DNA in A549 cells or the insensitivity of the method. Employing a radioactive DNA end labeling

technique we can easily test the latter possibility (Zakeri et al, 1993). To evaluate the sensitivity of the assay we labeled isolates of DNA from infected cells at different h pi with ^{32}P ATP and ran it on a gel. The autoradiograph showed the characteristic laddering beginning at 48 hpi and becoming more intense at 144 hpi (Figure 16B). By 96 hpi, large MW DNA fragments were no longer detected in the gel while smaller MW DNA fragments increased by 144 hpi. Nevertheless the labeling at 144 hpi represents only a small fraction of cells undergoing nuclear fragmentation. The results indicate that A549 cells do display the hallmark DNA laddering pattern seen during apoptosis, but more importantly the low level could indicate that other nucleases (e.g. EndoG nuclease) other than CAD (caspase activated DNase), the main nuclease for causing the DNA laddering phenotype, were activated or that nucleases in general become activated very late in the infection.

We employed the TUNEL assay. The terminal deoxynucleotidyl transferase enzyme tags newly generated free 3' OH DNA ends with a modified dUTP nucleotide (digoxigenin-11-dUTP) and can be detected with an antidigoxigenin antibody conjugated with either a peroxidase or fluorescein molecule. TUNEL analysis of infected A549 cells showed that about 40% of the infected population at 144 hpi was TUNEL positive (Figure 17A and B). TUNEL positive cells do not necessarily have nuclei that are fragmented, but that the cells at least have nicked DNA that exposes 3'-OH ends.

1.3.4. Morphology:

Light and electron microscopy analysis was performed on infected A549 cells to identify any morphological changes that occur during influenza induced cell death. As

mentioned before an apoptotic cell displays cell rounding, chromatin condensation and fragmentation as well as margination of chromatin. For light microscopy (LM), mock-infected A549 cells appeared elongated, wide and having distinctly stained nucleoli (Figure 18A). Infected A549 cells at 24 hpi (Figure 18B) and 72 hpi (Figure 18C) became thinner and more heavily stained but did not completely round up and remained elongated. Compared to mock-infected A549 cells by EM (Figure 19A) infected cells at 72 hpi (Figure 19B) and 144hpi (Figure 19C) had condensed fragmented marginated chromatin that was not very electron dense. However the EM micrographs confirmed the LM data in that the cytoplasm did not completely condense. There were signs of infected A549 cells undergoing secondary necrosis and displaying poorly stained chromatin, indicating degradation (Figure 19D). We also observed that the cytoplasm of some infected A549 cells showed extensive vacuolization as evident at 72 hpi (Figure 20).

1.3.5. Summary and Discussion:

As with MDCK cells we have also characterized cell death induced by influenza virus in the A549 human lung epithelial cell line, and found that they die by apoptosis. At 48 hpi, infected A549 cells were 24% positive for trypan blue in comparison to about 80% of infected MDCK cells, but by 144h pi infected A549 cells reached 80% cell death. Thus, before a sizable amount of infected A549 cells turned trypan positive it took an extra 96 hpi. This disparity between the cells will be addressed in more detail in the next sections below. Thus relative to MDCK cells they were delayed approximately 96 h.

A large proportion of dying infected MDCK cells have condensed and fragmented nuclei while on the other hand infected A549 cells that took up trypan blue showed much less nuclear fragmentation.

As mentioned before, a hallmark of apoptotic cell death is the fragmentation of DNA into oligonucleosomal fragments as detected by gel electrophoresis and TUNEL. DNA isolated from infected A549 cells lacked the characteristic laddering as seen on agarose gels after 144 hpi. A more sensitive assay with labeled DNA with ^{32}P ATP showed the characteristic laddering beginning at 48 hpi and becoming more intense at 144 hpi. Similarly, the TUNEL analysis data of infected A549 cells showed that about 40% of the infected population at 144 hpi was TUNEL positive, indicating that infected A549 cells at least had DNA that was nicked with exposed 3'-OH ends. Nevertheless the labeling at 144 hpi indicated that 60% of infected cells were not TUNEL positive.

A possible reason for the low level of DNA fragmentation in A549 cells may be that A549 cells lack either ICAD (Inhibitor of Caspase-Activated DNase) or CAD (Caspase-Activated DNase) proteins. ICAD acts as a chaperone protein that helps in the proper folding of CAD and is required for the efficient function of the CAD protein. The association of ICAD with CAD inhibits its nuclease activity. Cells deficient in ICAD show reduced chromatin condensation and a delay in cell death as compared to wild type cells (Zhang and Xu, 2002). Upon activation of caspase-3, ICAD is cleaved and CAD becomes activated. CAD is the main nuclease that is involved in producing the DNA ladder pattern seen on agarose gels. It has been shown that lungs cells do not express CAD mRNA (Mukae et al, 1998).

Beside the reduced level of DNA fragmentation, A549 cells had low levels of nuclear fragmentation, which made sense since extensive internucleosomal DNA fragmentation correlates with the collapse of the chromatin structure (Walker and Sikorska, 1998). Prior to nuclear fragmentation the DNA must first be degraded to allow destabilization of the chromatin structure. Rusnak et al used DU-145 human prostatic cancer cells to establish a temporal correlation between DNA and nuclear fragmentation since these cells undergo apoptosis and produce high molecular weight DNA fragments but not the low molecular weight DNA ladder fragments (Rusnak et al, 1996). They showed that attached cells accumulated DNA fragments of the size of 450-600 kilobase pairs (kbp) and prior to detachment the accumulation of some smaller DNA sizes (30-50 kbp). Upon detachment, the nuclear and chromatin morphology of the cells changed significantly with increases in the smaller fragments (Rusnak et al, 1996). Our data showed similar results in that MDCK cells had extensive DNA and nuclear fragmentation in the detached cell population whereas the majority of A549 cells remained attached and had very reduced DNA and nuclear fragmentation. The low level of nuclear changes found within A549 cells could also be speculated as a reduction in the level of degradation of the nuclear cytoskeleton (e.g. cleavage of nuclear lamina).

Lastly, morphological data showed that WSN infected A549 cells displayed condensed and marginated chromatin, and extensive cytoplasmic vacuolization. Infected A549 cells showed limited rounding at 72 (Figure 19B and 20) or 144 hpi (Figure 19C) as compared to MDCK cells (Figure 7 and 8, see pg 168 and 170).

Based on the above data A549 cells display some apoptotic characteristics but further evidence will be presented later. In examining the characteristics of cell death in

A549 cells we see differences in kinetics of cell death and nuclear changes between MDCK and A549 cells. The differences seen between the cells come from their intrinsic characteristics since the inducer of cell death is the same for both cells. It is of great interest to understand and identify the unique features within the individual cells that allow the virus to affect the cells differently and display contrasting features. If for example a cell lacking caspase-3 dies then one can speculate that other executioner caspases are activated or that death is caspase independent. Unfortunately the scope of this thesis will not address this important part since there are general characteristics occurring during influenza induced cell death and the aim of the project is to identify the common features that occur during influenza induced cell death. However, the intrinsic features found within MDCK and A549 cells will be addressed later in future work and provide valuable data on this complex process.

1.4. Viral Replication is Required to Induce Cell Death:

As mentioned in the Introduction a cell death response can be initiated by the binding of a ligand to its appropriate receptor complex to transmit the death signal within a cell. An excellent example of this type of activation is nicely exemplified by the Fas-FasL cell death pathway. In the case for viruses, a virus may enter a cell by first binding onto its proper receptor and later be internalized by either receptor mediated endocytosis or fusion of the outer plasma membrane with the viral membrane. With this one can think of the virus as a ligand binding onto its appropriate receptor and possibly activating a signal transduction pathway.

We asked if viral attachment and internalization alone was sufficient to elicit a cell death response or whether viral replication was needed to initiate cell death. To test this question we UV inactivated the virus because UV inactivation disrupts the viral genome and does not allow viral replication to occur but does permit internalization of the virus. For example, UV inactivation of lyssavirus prevents decapsidation and replication of the virus and in turn inhibits TRAIL induced cell death (Kassis et al, 2004). In contrast, sindbis virus appears to induce apoptosis simply by the process of membrane fusion and entry (Bobak et al, 1997, Li and Stollar, 2004). Virus was inactivated by irradiating the viral stock with UV light at 254 nm (50 J/m^2), following which we infected the cells with the irradiated virus. MDCK cells infected with UV treated virus neither showed the typical DNA laddering characteristic of apoptosis at 24 hpi by gel electrophoresis (Figure 21A) nor did the virus kill the cell as measured by trypan blue analysis (Figure 21B). However, untreated viruses produced strong DNA laddering and killing in MDCK cells. Because hemagglutinin (HA) proteins are responsible for allowing the virus to bind to the cell irradiated viral samples were tested by the Haemagglutination assay as mentioned in the Materials and Methods to determine whether WSN viruses still retain active HA molecules. If this protein is not functional then the virus will not bind and become internalized. The Haemagglutination assay showed an HA titer of 80 HA units per ml and confirmed that activity was retained but lowered as compared to non-irradiated viruses (5120 HA units per ml).

1.4.1. Summary and Discussion:

These results showed that viral replication was an important step in inducing influenza induced cell death, but that the mere attachment and internalization of the virus was not sufficient enough to elicit a cell death response. Binding of the virus to the cell surface was similar to a ligand binding to its receptor, but in this case the virus did not initiate a death signal; viral RNA and proteins were needed to start the induction of cell death within a cell. The signal for death by the virus occurs within the cell and not externally. However, as mentioned in the Introduction the influenza virus stimulates the synthesis of Fas molecules, which can potentially bind to surface receptors and activate a cell death response. Data to be presented later suggests that Fas is not the main initiator of cell death and that other players also contribute to the activation of cell death.

1.5. Difference in Kinetics of Cell Death is Not Unique to Influenza Induced Cell Death:

We have shown that influenza induced cell death appears to be apoptotic and proceeds in a dose dependent manner. However the kinetics of cell death are different in the two cell lines examined in that A549 cells required 144 hpi for 80-90% cell death whereas MDCK cells reached this level of cell death after 48 hpi. To investigate if this was intrinsic to the cell type we used another cell death inducer. We chose the protein synthesis inhibitor, cycloheximide (CHX) as an alternative cell death inducer because during influenza infections the virus shuts off host protein synthesis so CHX may mimic this viral process although our concentration was much higher than that needed for blocking of protein synthesis. CHX has been used extensively in cell death studies and has been found to induce cell death in many cell types.

Trypan blue and Hoechst staining were used to assess the level of cell death in the treated cells. MDCK cells either exposed to with 100 μg/ml of CHX (Wu et al, 2004) or infected with WSN (MOI 5) had comparable percentages of cell death (35% and 30%, respectively) at 24 hpi (Figure 22A) as measured by trypan blue. By 48 hpi, 95% of CHX treated MDCK cells were trypan blue positive as compared to 85% for WSN infected MDCK cells indicating that host protein synthesis was not required to kill MDCK cells.

Hoechst staining revealed high levels of fragmented nuclei in both CHX and WSN treated MDCK cells at 48 hpi, but initially at 24 hpi CHX treatments yielded a higher percentage of fragmented nuclei (Figure 22B). Overall the level of fragmentation was similar in both treatments and the difference seen at 24 hpi probably occurred because the virus may delay the fragmentation process since viral replication occurs within the nucleus of the infected cell.

In A549 cells we saw a difference in cell death kinetics with both treatments. At 96 hpi, 50% of WSN infected A549 cells were positive for trypan blue while CHX yielded only 24% positive cells (Figure 23A). By 144 hpi the level of cell death was elevated in both WSN and CHX treated A549 cells with 89% and 78% trypan blue positive cells, respectively (Figure 23A). Progression of trypan blue positive cells differed between the two treatments indicating that plasma membrane changes as well as death of the cell occurred more quickly in infected A549 cells than in CHX treated cells. Hoechst staining showed that the level of fragmented nuclei fell way below the level of trypan blue positive cells in both treatments, but CHX treated A549 cells had higher numbers of fragmented nuclei at 144 hpi than WSN infected A549 cells (Figure 23B).

1.5.1. Summary and Discussion:

The difference in cell death seen between WSN infected MDCK and A549 cells was not specific to infection but were based on intrinsic differences between the two cell types. Even though the rate of death differed between CHX treated and WSN infected A549 cells the time course was similar and by 144 h the level of cell death in both treatments was comparable. In MDCK cells the level of cell death was relatively similar as well as the time course of death since at 48 h a difference of 10% can be seen between both treatments.

MDCK cells were killed almost three times as fast as A549 at similar MOI. The difference did not derive from a lower initial production of virus in A549 cells since high levels of viral protein were detected by ^{35}S methionine labeling (see Figure 12B, pg 178). The same differential in time-to-death was observed when cells were exposed to cycloheximide, indicating that intrinsic features of the cell line determine its response. As mentioned previously, we see again that the intrinsic features of the cells greatly determine the outcome even if different inducers of cell death were used. Future studies of the intrinsic features will greatly provide better insight into influenza induced cell death. However, in order to answer whether specific cell death components must be needed during influenza induced cell death we employed various cell lines to address the need of each component. The data collected provide a general idea of the mechanism of influenza induced cell death.

It is known that the inhibition of cellular processes by viruses can indirectly induce cell death. Since influenza shuts off host protein synthesis this means that the cell death machinery needed to kill the cell is already made and available for activation. This

can also be said to be somewhat the core for CHX treated cells although our doses are much higher than what is required to stop protein synthesis. Another possibility is that by shutting off protein synthesis labile anti-apoptotic proteins will not be present to block cell death so instead cell death could be initiated (Griffin and Hardwick, 1997).

Objective

Chapter 2. Pathways Altered During Influenza A Virus Induced Cell Death

2.1. Extrinsic Pathways

2.1.1. Fas Receptor: Reduction of Fas Alters the Level of Influenza Induced Cell Death

2.1.1.1. Summary and Discussion

2.2. Intrinsic Pathways

2.2.1. Alterations in Mitochondrial Function During Influenza Induced Cell Death

2.2.1.1. Mitochondrial Membrane Potential

2.2.1.2. Mitochondrial Respiration

2.2.1.3. Mitochondrial Redox Potential

2.2.1.4. Release of Cytochrome c from Mitochondria

2.2.1.5. Summary and Discussion

2.2.2. Mitochondria Associated Proteins – Bcl-2 Family Members

2.2.2.1. Pro-Apoptotic Members – BAK and BAX

2.2.2.1.1. Summary and Discussion

Objective

Beside the extrinsic cell death pathway the intrinsic pathway contributes to the demise of the cell. Two important components of the intrinsic pathway involve the mitochondria and p53. The mitochondria plays an important role during cell death as it can release pro-apoptotic factors into the cytoplasm that can induce a caspase dependent and caspase-independent cell death pathway. We first investigated whether the mitochondria are affected during influenza induced cell death by measuring the mitochondrial membrane potential, respiration state and release of apoptotic factors (such as cyto c) into the cytoplasm. There are many proteins belonging to the Bcl-2 family that associate with the mitochondria and modulate its activity. Therefore we next examined the requirement of pro-apoptotic (Bak, Bax and Bim) and anti-apoptotic (Bcl-2) Bcl-2 family members during influenza induced cell death by the use of knockout mouse embryo fibroblast (MEF) cells.

The p53 signaling pathway plays a crucial role in the induction of cell death (Hickman et al, 2002). Certain viruses have been shown to modulate the activity of p53 hence affecting the induction of cell death. For example, the human cytomegalovirus encodes an early gene product, IE2, which has been shown to repress p53 transcriptional activity and inhibit apoptosis (Hagemeier et al, 1994; Zhu et al, 1995). As for the influenza virus it is not known whether influenza induced cell death is p53 dependent or independent. We therefore tested the requirement of p53 during influenza induced cell death.

As discussed in the Introduction a certain class of cysteine proteases called caspases are involved in propagating the cell death signal and degrading the cell. Although different signaling pathways can be activated by different stimuli, caspases always converge to a common point linking the extrinsic and intrinsic pathways and lead to the demise of the cell. We therefore evaluated whether caspases are activated during influenza induced cell death in A549 and MDCK cells. In addition to examining the activation of caspases we wanted to determine whether caspases are dispensable during influenza induced cell death.

The cleavage of Bid, a pro-apoptotic Bcl-2 member, by caspase-8 is another convergence point of the extrinsic and intrinsic cell death pathways. The activated truncated Bid is important since it translocates to the mitochondria and affects its function. For that reason we evaluated the cleavage of Bid during influenza induced cell death.

Besides the involvement of caspases during cell death another class of proteases implicated in cell death are the lysosomal resident cathepsin proteases. For example, in *Autographa californica* M Nucleopolyhedrovirus cathepsins have been implicated in activating the virally encoded protein, ProV-CATH, which has an essential role in host liquefaction (Hom et al, 2002). No studies to date have shown the need of cathepsins during influenza induced cell death therefore we investigated the invovlement of cathepsins during influenza induced cell death by using knockout MEF cells.

Chapter 2. Pathways Altered During Influenza A Virus Induced Cell Death

The data presented above demonstrates that WSN infected MDCK and A549 cells proceed to die in an apoptotic manner, indicating that the induction of cell death by the virus uses common cell death pathways. It is not known what pathways are activated and what components are involved during WSN induced cell death. In the next section we will present data on the various cell death components found in the extrinsic and intrinsic cell death pathways that are involved during WSN induced cell death.

2.1. Extrinsic Pathways:

As discussed in the Introduction cells may activate either an extrinsic or intrinsic pathway to initiate cell death. The activation of the extrinsic cell death pathway involves the binding of a ligand to its appropriate receptor, which in turn recruits certain adaptor molecules and in turn activates the initiator caspases. One very well studied extrinsic pathway is the Fas/FADD/Caspase-8 pathway. Briefly it involves the trimerization of the Fas receptor with FasL, the ligand, and recruitment of the death domain (DD) containing FADD adaptor protein. These DD's on FADD recruit procaspase-8, which also has the DD's and allows cleavage of procaspase-8 to active caspase-8 by transactivation. As a consequence the activation of caspase-8 begins the proteolytic cascade seen during apoptosis by activating caspase-3. We wished to evaluate the need for Fas during influenza induced cell death since others had implicated Fas as an agent in influenza infected cells.

2.1.1. Fas Receptor: Reduction of Fas Alters the Level of Influenza Induced Cell Death:

It has been reported previously that influenza induced cell death proceeds by the activation of the Fas/FADD/Caspase-8 signaling pathway in mouse embryo fibroblast (MEF) cells (Balachandran et al, 2000). Others have reported that influenza virus induced a transient but noticeable increase in Fas antigen mRNA early after infection, followed by the expression of Fas on the cell surface of HeLa cells (Takizawa et al, 1993). To explore the potential need for the activation of the Fas cell death pathway during influenza induced cell death we employed a human cell line called U937R.

The U937R cell line was developed in our laboratory by Dr Nicos Karasavvas and was selected as a subset from the human histiocytic lymphoma (macrophage) cell line designated U937. The U937R cells were isolated during ceramide induced cell death studies in which a population of cells was found to be resistant to ceramide induced cell death. Hence the designation U937R, where the "R" means resistance (Karasavvas et al, 1996). The cells were also found to be resistant to Fas and TNFα treatment. Another striking feature was that the cells changed from being normally a suspension cell line to one that was able to adhere to plates. As measured by RT-PCR, U937R cells appeared not to express or had very low levels of Fas mRNA as determined by Dr Andreas Cossarizza of the University of Modena, Italy. The cells also had a delayed response and lowered sensitivity to treatment with anti-Fas antibody (acts as FasL) as compared with the parental U937 cell line that was very sensitive to the anti-Fas antibody.

U937 and U937R cells were infected with WSN at an MOI of 5 and assayed for cell death at selected h pi. Initially both U937 and U937R cells had similar levels of cell death at 24 and 48 hpi as measured by trypan blue, but by 72 hpi there was a significant difference between the two (Figure 24A). U937 cells were almost all positive for trypan blue while only 76% of the U937R cell population were dying. This suggested that the lowered level of Fas expression present in the U937R cells did not hinder the activation of influenza induced cell death since at 24 and 48 hpi cell death was comparable to the U937 cells, which do express Fas. However the data at 72 hpi indicates that U937R cells may activate an alternative cell death pathway and that the activation of the Fas pathway appears to lead to a more effective cell killing as seen in infected U937 cells. Hoechst staining of both cells showed that U937R cells initially had more fragmented nuclei than U937 cell at 24 hpi, but at 48 hpi the difference narrowed and by 72 hpi nearly all the U937 cells had fragmented nuclei (Figure 24B). This further illustrates that U937 and U937R cells activate different pathways or that initially they activate the same pathway but since U937R cells lack Fas cell death diverges and continues on through a different pathway. The type of cell death occurring during influenza induced cell death in U937R cells was assessed by DNA fragmentation analysis. At 24 hpi we observed the classical DNA laddering pattern in both infected U937 and U937R cells indicating that death was apoptotic in nature (Figure 24C).

2.1.1.1. Summary and Discussion:

Our data show that a cell defective for Fas can still die when infected with WSN, but with a reduction in the total number of dying cells as compared to the parental cell

line. This could suggest that Fas is not required during influenza induced cell death but the presence of Fas increases the number of dying cells. It appears that infected cells may not only activate one cell death pathway but several and the impairment of one may only delay or reduce the level of cell death but not eliminate it from happening. Evidence of other pathways will be presented later.

2.2. Intrinsic Pathways:

As stated in the Introduction, mitochondria play a role in the intrinsic cell death pathway. Mitochondrial function and associated proteins have been implicated in the induction and progression of cell death. Here we present data on the mitochondrial alterations that occur during influenza induced cell death and the possible involvement of the various mitochondrial proteins, referred to as Bcl-2 family members. Beside mitochondria there are other components involved in the intrinsic cell death pathways. We determined the need for p53 during influenza induced cell death because many viruses affect the function of p53 protein.

2.2.1. Alterations in Mitochondrial Function During Influenza Induced Cell Death:

During cell death the mitochondria undergo many internal changes. One such change involves the loss of membrane potential between the inner mitochondrial plasma membrane and as a result the proton gradient across this inner membrane becomes disrupted. This loss of potential causes a disruption in the synthesis of ATP. The exact

mechanism for the loss of membrane potential is under debate but in general the mitochondrial membranes become more permeable allowing greater movement of solutes across them. We measured the membrane potential ($\Delta\Psi_m$) and permeability of mitochondria during influenza virus infection by using a cationic lipophilic dye called Rhodamine 123 (Rh123), which remains within the mitochondria when a potential exists between the inner membrane space and matrix. Loss of membrane potential engenders a loss in fluorescence and an increase in membrane permeability of mitochondria. This loss in membrane potential results in the release of pro-apoptotic factors like cytochrome c, apoptosis inducing factor (AIF), endonuclease G, and SMAC/DIABLO into the cytoplasm, and in turn these factors aid in the destruction of the cell by blocking anti-apoptotic factors, activating caspases and degrading DNA.

2.2.1.1. Mitochondrial Membrane Potential:

To measure the mitochondrial membrane potential WSN infected A549 cells prior to harvesting were incubated with the fluorescent probe, Rh123. Mitochondrial membrane potential was determined by the fluorescence signal emitted by retained Rh123 within the functional mitochondria and detected by a Perkin Elmer MPF-66 spectrophotofluorometer. Mitochondria in infected A549 cells showed a drop in membrane potential by a loss in measured fluorescence at 24 hpi (Figure 25A) and continued to substantially decrease through 96 hpi. Of course these are aggregate measurements of many cells. At 48 hpi infected A549 cells showed a 30-fold loss in membrane potential, but with only 20% dead cells indicating that mitochondrial dysfunction may not necessarily dictate increased levels of death. Infected MDCK cells

showed no loss in fluorescence at 24 hpi as compared to mock-infected cells, but by 48 hpi the potential dropped substantially (Figure 25B). The decrease in fluorescence signal at 48 hpi correlated with the poor viability and indicated that mitochondrial changes occurred when the outer membrane was compromised. It was not clear whether the loss of potential preceded the increased induction of cell death as measured by trypan blue (loss in membrane integrity) (see Figure 2, pg 158) or that as a result of the poor viability of the cell the mitochondria became dysfunctional. Being that the measurements represent the whole cell population perhaps a few cells have collapsing membrane potentials while others are normal. The Rh123 data however suggests that during influenza induced cell death the timing of mitochondrial membrane potential loss coincides with increased levels of cell death as measured by trypan blue as seen in the A549 and MDCK experiments. For example, in A549 cells we see a gradual increase in cell death and a gradual decline in membrane potential. As the cell membrane increases to be compromised we see a decrease in membrane potential. *In situ* measurements of individual cells will be described shortly since the membrane potential measurements taken so far represent membrane potentials of the whole cell population.

2.2.1.2. Mitochondrial Respiration:

Mitochondrial function can also be determined by the reduction of MTT by the enzymatic activity of succinate-tetrazolium reductase, which occurs only in respiring mitochondria and is a good marker of cell viability and status of the electron transport chain and oxidative phosphorylation process. The reduction of MTT produces a purple precipitate inside a cell that can be solubilized and mitochondrial respiration can be

measured by the change in optical density (OD^{570}) of the sample as compared to the control. Samples were normalized for OD^{570} per microgram of total protein ($OD^{570}/\mu g$). Mitochondrial respiration in infected A549 cells gradually dropped from an empirical value of 0.70 during the infection with the decrease in activity becoming significant by 96 h pi with a value of 0.32 as compared to mock-infected cells, which was 0.97 (Figure 25C). As for infected MDCK cells, mitochondrial respiration drastically collapsed from 1.36 as seen in mock-infected cells to 0.29 by 48 h pi (Figure 25D), a result correlating with the Rh123 data (see Figure 25B). For infected A549 cells we see a gradual deterioration of mitochondrial respiration that correlates with the gradual drop of viability and mitochondrial potential seen during the infection. While in infected MDCK cells a sudden collapse is seen that corresponds with the drastic drop of viability and mitochondrial potential seen at 48 hpi.

2.2.1.3. Mitochondrial Redox Potential:

Many mitochondrial probes are not retained long in mitochondria and are readily washed out when the potential is lost, but we employed a mitochondrial probe called MitoTracker Red that remains fixed in the cell allowing further processing of the samples. We used the probe to do *in situ* labeling of the mitochondria with visualization under a fluorescence microscope. The ability of the dye to be fixed within the mitochondria is dependent on the redox state inside the organelle. We used this dye to evaluate mitochondrial stress in A549 cells induced to die by viruses.

In mock-infected A549 cells at 144 hpi the majority of the fluorescence signal was concentrated in filamentous strands within the cytoplasm, thus represented the

normal arrangement of mitochondria in the cells (Figure 26, white arrows). As the infection progressed the arrangement and distribution of mitochondria drastically changed. The fluorescence signal was more diffuse and spread out within the cytoplasm and the filamentous strands were lost as seen at 96 or 144 hpi (Figure 26, green arrows), indicating that the mitochondrial membrane was probably more permeable and the dye could readily move out of the mitochondria.

2.2.1.4. Release of Cytochrome c from Mitochondria:

A third major indicator of alterations in mitochondrial function during cell death is the release of cytochrome c from the mitochondrial pellet (P) into the cytoplasm or supernatant fraction (S). The release of cytochrome c into the cytoplasm is an important step during the intrinsic cell death pathway and allows the amplification of the proteolytic cascade. Caspase-3 can be activated by the apoptosome, which is made up of caspase-9 and apaf-1 linked with cytochrome c. In infected MDCK cells, Western blotting using an antibody against cytochrome c showed a strong reaction in the pellet fraction (P) at 4 hpi with little reactivity in the supernatant fraction (S) (Figure 27A). As the cells die we find an increase in the release of cytochrome c into the supernatant fraction (S) by 18 hpi. Cytochrome c release appears before we detect substantial levels of cell death as measured by trypan blue (see Figure 2B). We can therefore conclude that the release of cytochrome c preceded the drop in mitochondrial membrane potential and mitochondrial collapse and other morphological events seen during cell death. We detect in A549 cells a release of cytochrome c into the cytoplasm by 24 hpi (Figure 27B).

Another method for determining the release of cytochrome c is by immunocytochemistry. Cells plated on coverslips were infected with WSN (MOI 5), collected at 24 h intervals and fixed with paraformaldehyde. The samples were triple labeled with an antibody against cytochrome c (green fluorescence), MitoTracker Red (red fluorescence) and Hoechst dye (blue fluorescence). In mock-infected A549 cells that the green cytochrome c signal was punctate (Figure 27C) indicating that cytochrome c was localized within mitochondria. In contrast, infected A549 cells showed a diffuse fluorescence signal (Figure 27D) suggesting that cytochrome c was released into the cytoplasm. The MitoTracker probe used to visualize the mitochondrial pattern in mock-infected and infected A549 cells, respectively (Figure 27E and F) showed a diffuse fluorescence signal indicting mitochondrial membrane alterations.

2.2.1.5. Summary and Discussion:

Mitochondria play an important role during cell death in that the loss of mitochondrial membrane potential ($\Delta\Psi_m$) can influence their function and can release pro-apoptotic factors like cytochrome c, AIF, endonuclease G, and SMAC/DIABLO into the cytoplasm, which in turn help the progression of the death signal within the cell.

Mitochondria were analyzed by several means to measure transmembrane potential and function. Mitochondrial transmembrane potentials were altered early in the infection cycle of A549 cells. There was a severe drop in potential in infected cells at 48 hpi (Rh123) but percent cell death at 48 hpi was slightly above 25%, suggesting that most cells were viable but with dysfunctional mitochondria. Also the respiration within the mitochondria, as measured by MTT, showed a gradual decrease in A549 cells indicating

an increase in the number of cells of the total cell population with lowered respiration. As the $\Delta\Psi_m$ and enzyme activity decreased during the infection the cell viability decreased as well. There was also an inverse relationship between caspase activity and $\Delta\Psi_m$. This suggests that the activation of caspases and loss of $\Delta\Psi_m$ are coupled in A549 cells. The individual cell (in situ) and total cell population data are consistent in that the release of cytochrome c and the alterations in mitochondrial membrane potential in infected A549 cells (Figure 27 C-F).

It appears that caspases, not mitochondrial dysfunction may be the main driving force for killing A549 cells. We saw that mitochondrial dysfunction as measured by Rh123 and MTT occurred early during the infection while levels of trypan blue positive cells were low. It was not until we saw many cells expressing active caspase-3 as determined by immunocytochemistry that we observe higher levels of trypan blue positive cells. A general outline of these events can be illustrated below:

mitochondrial dysfunction → active caspase-3 → significant levels of trypan blue positive cells

→ nuclear changes

Mitochondrial dysfunction such as loss of $\Delta\Psi_m$, increase in membrane permeability and loss of enzyme activity occurred suddenly in MDCK cells much later in the infection (48 hpi) when cell death was high. Prior to that the mitochondrial membrane

potential was similar to that of mock infected cells (24 hpi) and cell death as measured by trypan blue was low. The high levels of cell death at 48 hpi could be attributed to mitochondrial malfunction and not only the activity of caspases because we find at 24 hpi that caspases were active while the level of trypan blue positive cells was at 30% and mitochondria appeared to function normally as in mitochondria of mock-infected cells. This suggested that caspase activation came before mitochondria dysfunction, but significant levels of cell death correlated with the loss of the membrane potential. Infected MDCK cells released cytochrome c at 18 hpi when caspases were active, but release of cytochrome c does not always involve membrane potential loss and may involve members of the Bcl-2 family. It appears that mitochondrial changes occurred later on in the infection process for MDCK cells.

2.2.2. Mitochondria Associated Proteins – Bcl-2 Family Members:

2.2.2.1. Pro-Apoptotic Members – BAK and BAX:

As mentioned previously, mitochondria can release several factors into the cytoplasm, but the mechanism of how sequestered factors are released is unclear and two models have been proposed. The first argues that during apoptosis a megapore, called the mitochondrial permeability transition (MPT) pore, is formed that spans the inner and outer mitochondrial membranes. This pore allows solutes and water to enter causing the mitochondrion to swell and rupture its outer membrane, thus releasing its contents. Opening of the MPT pore causes increased permeability of the inner membrane, loss of mitochondrial membrane potential ($\Delta\Psi_m$), depolarization and uncoupling of oxidative

phosphorylation. The second model states that pro-apoptotic Bcl-2 family members, such as BAK and BAX, form a channel and selectively mediate the release of cytochrome c into the cytosol without causing mitochondrial swelling. Mitochondrial function is regulated by the interactions of various members of the Bcl-2 family and the difference in ratios of both pro- and anti-apoptotic members can determine the fate of the mitochondria and the cell. To evaluate the role of Bcl-2 family members such as BAK and BAX in influenza induced cell death we used mouse embryo fibroblast (MEF) cells knocked out for BAK and BAX.

At 24 h pi infected BAK knockout (BAK -/-) cells showed more than about a 10% increase in the level of cell death as compared with BAX knockout (BAX -/-), BAK -/- / BAX -/- double knockout (DKO) and wild type (WT) MEF cells (Figure 28A) as measured by trypan blue. By 48 h pi BAK -/-, BAX -/-, and DKO cells show more sensitivity to the viral infection than WT cells. BAK -/- cultures had approximately 80% dead cells while WT cells had only 15% dead cells. The lowered percentage in cell death in WT cells may be accounted by the high mitotic rate of the cells and low rate of death. However once cell death is activated the destruction of the cell could be rapid and complete so upon trypan analysis there is little of the cell left for quantification.

We exposed all the MEF cells to 100 μg/ml of cycloheximide (CHX) and assessed their viability by trypan blue. We used another death inducer to test the sensitivity of the MEF WT cells to apoptosis. The deletion of BAK or BAX should confer some resistance to the cells from cell death while the WT cells should be more sensitive to the treatment.

BAK -/- and DKO cells were protected against CHX treatment while survival of BAX -/- cells indicated a partial requirement for BAX in CHX induced death (Figure 28B). WT cells however were very sensitive to CHX treatment, with 80% dead cells at 48 hpi indicating that WT cells were not defective in cell death. WT cells responded as predicted to CHX treatment in that cell death was high while single and double knockout MEF's were resistant to CHX-induced death.

The reason for the reduced level of cell death in WSN infected WT cells is not clear, but CHX induces cell death by a mechanism other than inhibition of protein synthesis otherwise 1 μg/ml should induce apoptosis. However in comparison to WT cells the deletion of BAK or BAX results in increased induction of virus induced cell death as seen in our data (see Figure 28A and B). The deletion of BAK or BAX appears to create an environment within the cell to promote WSN induced cell death.

To determine whether viral production may be affected by BAK and BAX we used the plaque assay to assess viral replication in the various MEF cells. WT cells showed high levels of viral production and was used as our control (Figure 28C). Interestingly these cells produce many viruses while the level of death appears low when compared to the knockout cells. This means that low cell death is not attributable to a nonproductive infection or poor replication. Both BAK -/- and DKO cells had higher viral titers than WT cells throughout the infection whereas BAX -/- cells showed lower levels of viral production than the WT cells. However this lower level of virus production does not appear to hinder its ability to die as reflected at 48 hpi where 69% of cells die (see Fig. 28A). Based on these data it appears that the BAK protein alone may affect WSN virus production, but this interference and lowered production does not perturb the

virus induced cell death process. The WT and BAX -/- cells demonstrate that an increase in production of WSN virus does not necessarily guarantee high levels of cell death. It appears that BAK and BAX alone are not completely required for influenza induced cell death since cell death is close to 80%. However if both proteins are deleted there was about a 20% reduction in cell death, which means that the proteins play some role in influenza induced cell death but are not the main players and perhaps other similar proteins can do this job.

2.2.2.1.1. Summary and Discussion:

Mouse embryo fibroblast (MEF) cells with either BAK or BAX knockout showed a higher degree of cell death at 48 hpi than wildtype (WT) cells (see Table 1). WT cells treated with 100 μg/ml cycloheximide were readily killed so it is not clear why WT cells are not sensitive to influenza. The low level of cell death did not result from inadequate viral replication because viral titers were higher than in BAX knockout (BAX -/-) cells. WT cells have a high mitotic rate (seen during cell culturing) and death progression could be rapid enough that cells disintegrate before quantification by trypan blue. Interestingly, BAX -/- cells had high cell death coupled with the lowest titer of virus of the MEF's, which can be speculated that the deletion of BAX might allow BAK to interact with a certain protein and potentiate the induction of influenza induced cell death. There is a report that an influenza protein overlapping the PB1 open reading frame (designated PB1-F2) can localize in the inner mitochondrial membrane and impact function (Gibbs et al, 2003). Another possibility is that the alternative spliced PB1 protein may interact with BAK and BAX and that these proteins may have some inhibitory effect on PB1-F2, but

when either one of the mitochondrial proteins are knockedout PB1-F2 can replace their functions and cause mitochondrial dysfunction. Without both BAK and BAX PB1-F2 can insert itself into the mitochondrial membrane and disrupt its function as seen in the DKO cells. The increased number of dying cells may contribute to the reduction of viral titer or BAK itself could interfere with viral replication by affecting the mitochondria and possibly lowering the level of ATP thus providing less energy for the virus to use for itself. Even though WT cells have BAK present, its ability to affect viral replication could be blocked by its interaction with BAX. BAK knockout cells also had cell death, which could indicate that BAX can also potentiate viral induced cell death, but BAX appears not to alter viral replication.

		Trypan Blue Positive	
MEF cells	WSN Production	WSN	CHX
BAX -/-	+++	+++	+
BAK -/-	+	+++	–
DKO	+++	++	–
WT	++	+	+++

Table 1. Summary of WSN virus production and level of trypan blue positive cells in MEF cells. The deletion of either BAK or BAX alone does not hinder cell death, but the deletion of both lowers cell death. Also, WSN replication does not correlate with the number of trypan blue positive cells. For example: BAK -/- cells have high levels of

trypan positive cells but low WSN production while WT cells have low number of trypan positive cells and a higher production of virus. (+++, high; ++, medium; +, low; –, no death; WSN, virus; CHX, cycloheximide)

2.2.2.2. Pro-apoptotic Members – BIM:

As discussed in the Introduction there are other Bcl-2 Family proteins besides BAK and BAX that are involved in cell death induction and progression. We analyzed the need for BIM, a pro-apoptotic protein, and for BCL-2, an anti-apoptotic protein, during influenza induced cell death.

We studied the need for BIM, a BH3 only domain protein, during influenza induced cell death because it can also translocate to the mitochondria and alter the function of the organelle. Kidney and lung cells from BIM knockout (BIM -/-) mice were harvested and cultured for analysis. Primary lung BIM -/- cells were infected with WSN and by 72 hpi over 80% of the cells were trypan blue positive (Figure 29A), but only 15% of the cells had fragmented nuclei as measured by Hoechst staining (Figure 29B). This suggests that lung cells may not readily undergo fragmentation similar to A549 cells. At 24 hpi there were many infected BIM -/- cells were round and floating in the plate as compared to the mock-infected cells (Figure 29C). Primary kidney BIM -/- cells are similar to lung BIM -/- cells in that at 48 hpi over 90% of the cells were positive for trypan blue (Figure 30A). At 48 hpi the cells were destroyed and appeared to undergo secondary necrosis (Figure 30B). The data indicated that BIM is not needed for influenza

induced cell death because in both cell types cell death percentages as measured by trypan blue were very high.

2.2.2.3. Anti-apoptotic Members – BCL-2:

Up to this point we have concentrated only on Bcl-2 proteins that have pro-apoptotic properties so the next question we asked was, could anti-apoptotic Bcl-2 family members prevent influenza induced cell death? We examined the prototypical anti-apoptotic Bcl-2 family member protein called BCL-2. To test the effect of this protein we infected both naïve PC-12 cells, which constitutively overexpress BCL-2 (PC-12 bcl2 +) and the parental cell line (PC-12 WT) with WSN at a MOI of 5. At 24 hpi both cell lines had similar levels of cell death as measured by trypan blue indicating no protection, but at 48 hpi we found there to be a limited amount of protection ($P<0.038$) against influenza induced cell death (Figure 31). Longer infection times resulted in higher percentages of death in mock-infected cells, which made calculating the overall value of cell death difficult since mock-infected cell death values were subtracted from the WSN infected cell death values and percent cell death was expressed as percent of control and represented cell death due only to the virus. Mock-infected cells showed high death rates because of the low serum amount present in the media. Influenza viruses were not strong inducers of cell death in either of these cells because cell death percentages did not go above 45%. BCL-2 offers very slight protection against influenza virus indicating that Bcl-2 proteins can affect influenza induced cell death as supported by others (Olsen et al, 1994). It also suggests that the mitochondria in PC12 cells are not the main driving force for cell death activation because BCL-2 has so little impact.

2.2.3. Deletion of P53 Does Not Prevent the Induction of Influenza Induced Cell Death:

As mentioned in the Introduction exposure to UV light normally damages the genomic DNA whereupon p53 senses the damage and activates a p53 transcription dependent cell death pathway. This intrinsic pathway has been shown to enhance the effects of apoptosis by also activating a transcription independent mitochondrial pathway (Mihara et al, 2003). As a result many viruses (i.e. adenovirus) have encoded proteins that act upon the p53 protein by either activating or suppressing its function. Since p53 is involved in apoptotic cell death and viruses can affect its function we asked whether p53 dependent cell death is involved in influenza induced cell death. We used MEF cells that either have normal levels of p53 expression, designated as C8 (p53 +/+), or devoid of p53 expression, designated as A9 (p53 -/-) and determined if influenza induced cell death is altered or suppressed by the lack of expression of p53. Prior to the infection studies we evaluated the response of the MEF cells to ultraviolet (UV) light to determine that A9 cells are indeed resistant to UV.

The MEF cells were exposed to UV light (50 J/M^2) and thier viabilities assayed by trypan blue. With a few seconds of exposure massive numbers of C8 cells were trypan blue positive 24 h later indicating extreme sensitivity to UV and activation of p53 (Figure 32). However, A9 cells had significantly lower percentages of cell death than C8 cells thereby showing that the lack of p53 hampered cell killing in a dose dependent manner. The UV light experiments showed that A9 cells were a good model system to test the need for p53.

Both C8 and A9 cells were infected with WSN at a MOI of 5 and cell death was analyzed by trypan blue and DNA fragmentation. By 24 hpi C8 and A9 cells were very sensitive to the influenza virus as indicated by the high number of dead cells present (Figure 33A). However there was a 17% reduction of cell death seen in A9 cells ($P < 0.001$) indicating that p53 activation during influenza induced cell death may enhance cell killing but was not a major factor because over 80% of infected A9 cells were dead. DNA samples taken from infected C8 and A9 cells showed DNA laddering at 24 hpi (Figure 33B). Mock-infected A9 cells showed slight DNA laddering due to the low serum during the infection. Nonetheless the amount of fragmentation in A9 cells was comparable to C8 cells. This finding supports the fact that p53 was not completely required for influenza induced cell death.

2.2.3.1. Summary and Discussion:

The deletion of p53 in A9 cells does not hinder the induction of cell death since the level of trypan blue positive cells was over 80%, but in comparison to the C8 cells, which have p53, the data indicated that p53 had the potential to potentiate the induction of cell death. The induction of apoptosis in both cells by WSN was demonstrated by DNA laddering (Figure 33B), which indicated that p53 was not essential. P53 may increase the level of cell death in cells by its ability to upregulate BAX, NOXA and PUMA (Ferri and Kroemer, 2001), since BAX was dispensable during influenza induced cell death further work is needed.

Since the influenza virus can affect transcription in a cell, the p53 transcription dependent cell death pathway may not be involved, but instead the transcription

independent mitochondrial pathway may be activated and contribute to the induced cell death seen in cells. To test this idea one could measure mitochondrial function and release of cytochrome c in both A9 and C8 cells.

2.3. Connections Between the Extrinsic and Intrinsic Cell Death Pathways:

2.3.1. Cleavage of BID:

The extrinsic and intrinsic cell death pathways are not mutually exclusive and a link between the two exists. The pro-apoptotic Bcl-2 family member named BID, a BH3 only domain protein, bridges the activation of the extrinsic pathway to the eventual activation of the intrinsic pathway. Normally BID resides in the cytoplasm but, when cleaved by caspase-8 to a 15 kDa truncated protein (tBID), translocates to the mitochondria (Tang et al, 2000). This relocation of tBID aids in the permeabilization of the mitochondrial membrane and release of cytochrome c, which can occur early in the death of a cell.

Western blots of protein lysates from infected A549 cells showed that BID cleavage occurred at 96 hpi (Figure 34). By the time we observed cleavage of BID 50% of WSN infected A549 cells were trypan blue positive and mitochondrial changes (i.e. membrane potential loss) occurred prior to this detectable cleavage. This indicated that tBID is not likely to be responsible for the alterations in mitochondrial function and that other factors are likely to be involved. BID was cleaved in A549 cells during WSN infection but it was not clear how much of an impact the cleavage had on induction of cell death. It is possible that the level of cleaved BID was too low to detect by Western

blot in the early hours of infection, but nevertheless effective. We were unable to detect BID cleavage in MDCK cells because the antibody did not recognize dog BID.

2.3.2. Caspases and Influenza Induced Cell Death:

2.3.2.1. Activation of Caspases:

One of the events that indicate commitment to death is the activation of the caspase cascade. Caspases are cysteine proteases that target cellular substrates that collectively affect the cell shape; their digestion generates the apoptotic phenotype and demise of the cell. Caspase-8 (FLICE, Mach-1) activation was tested because it is one of the first caspases to be activated in the extrinsic protease cascade. Protein lysates from infected cells were run on SDS-PAGE gels for western blotting using an antibody that detects both the inactive proenzyme and active form of caspase-8. Western blot showed the appearance of the p25 cleaved fragment (20-25 kDa)(Zhang et al, 2004), which indicates activation of caspase-8, started by 10 hpi and continued to increase in MDCK cells through 24 hpi (Figure 35A). In A549 cells, the p25 cleavage fragment was detected at 24 hpi, but little increase was seen even after 96 hpi (Figure 35B).

With the activation of caspase-8 we look downstream of the caspase cascade to one of the effector caspases. Caspase-3 activation was examined since it is an important executioner protease that degrades many cellular substrates. An antibody that detects only the active form of caspase–3 showed by Western blotting that caspase-3 was also activated in MDCK and A549 cells by 24 hpi (Figure 36) as evident by the detection of the p17 cleavage product (Kamada et al, 2004).

The activation of caspase-3 was further confirmed by immunohistochemistry. As mentioned in the Materials and Methods, cells were grown on coverslips, infected with virus (MOI 5) and the samples fixed at different hpi. After incubation with the primary caspase-3 antibody the samples were incubated with a fluorescent tagged secondary antibody for visualization under a fluorescence microscope. We found caspase-3 activity in infected MDCK cells with increases in the number of positive cells by 24 and 48 hpi (Figure 37). The most intense and frequent staining was seen in the detached cells with a high percentage of dead cells with almost 1:1 correlation with fragmented nuclei and positive for trypan blue. The attached cells showed either no or lowered level of active caspase-3. There appeared to be a faint signal in the adherent MDCK cells at 48 hpi, but we believe it to be mostly background fluorescence. Hoechst staining showed that infected MDCK cells had nuclei that were condensed but not fragmented.

The caspase inhibition experiment showed that MDCK cell detachment was a direct consequence of caspase-3 since the abolishment of caspase-3 activity resulted in the cells remaining attached. High levels of caspase-3 activity were detected only in cells that were detached and floating. The infection process (the virus) activated caspase-3, but the activity of caspase-3 targeted substrates in MDCK cells that were needed for cell attachment. It appears that the virus itself does not directly affect the adhesion of the cells, but that this was a result of caspase-3 activation. Evidence of this will be presented below, but briefly the inhibition of caspases blocked the detachment of infected MDCK cells. The loss of caspases resulted in infected MDCK cells remaining attached even though the inhibitors did not affect the virus replication. If the virus were the direct cause

of the detachment, the cells then would have detached during the inhibition studies. In contrast, a different result was seen with infected A549 cells as will be mentioned below.

In A549 cells the majority of infected cells remain attached during the infection and any cell that detached disintegrated. We detect very few cells that have activated caspase-3 at 24 and 48 hpi as compared to the many cells attached to plate as seen by Hoechst staining (Figure 38). As the infection progresses we see more and more cells fluorescing green and by 144 hpi the majority of A549 cells have active caspase-3 with fluorescence at different intensities indicating variable levels of activation. We see activation of caspase-3 in approximately 3.8% of mock-infected A549 cells only because by 144 hpi there is cell death due to the loss of serum (Figure 38).

Even though we detect levels of caspase-3 activity by 72 hpi the majority of the cells remain attached. This suggests that the adhesion molecules in A549 cells are not targeted by caspase-3 or if A549 lack another protease and, for instance, can't cleave adhesion molecules. This result seems to contradict the MDCK cell data. However MDCK and A549 cells are different cells located in different body locations so they will have a different repertoire of adhesion molecules.

To further evaluate the activation of caspase-3, we looked for the cleavage of poly(ADP-ribosyl) polymerase (PARP), which is one of the substrates of caspase-3. PARP is normally found as a 116 kDa protein which upon cleavage by caspase-3 yields an 85 kDa fragment. PARP cleavage in MDCK cells began at 8 hpi and by 18 hpi full length PARP is completely cleaved into the 85 kDa fragment (Figure 39A) as seen by Western blotting. This result suggests that enough caspase-3 is activated in infected MDCK cells to cleave PARP, but significant nuclear changes occur much later in the

infection and when levels of active caspase-3 are high. By 24 hpi PARP cleavage can be seen in infected A549 cells, but only a small percent of the total PARP is affected and the level of cleaved PARP appeared not to increase even at 144 hpi (Figure 39B). It is not clear why complete cleavage of PARP is not seen during WSN induced cell death in A549 cells. However it has been shown that the activity of PARP consumes ATP stores, which leads to cell death (Nanavaty et al, 2002; Soldani and Scovassi, 2002). The virus requires ATP for its own use so this depletion of ATP by PARP may affect the infection. In the case for MDCK cells, PARP is completely cleaved and WSN replicates very well and death is quick.

2.3.2.2. Caspase Activity is Dispensable for Influenza Induced Cell Death:

Although caspases may be activated by a death inducer they may or may not be needed to kill a cell. To examine whether caspase activity was needed for viral replication or for the induction of cell death by influenza viruses we employed two approaches. First, we used a broad-spectrum caspase inhibitor, zVAD-fmk (benzyl-oxycarbonyl-Val-Ala-Asp(Ome)fluoromethylketone), to block the activation of the procaspases, and second, we used a cell line, MCF-7, that lacks caspase-3.

For the inhibition studies, zVAD was added directly into the media right after the standard one hour infection period so that cells were essentially always exposed to the inhibitor. Infected MDCK cells exposed to 50 μM of zVAD showed protection from virus induced cell death as compared to untreated cells at 48 hpi (Figure 40A) ($P < 0.004$). There was a drop of about 15% in cell death as compared to untreated cells, and overall over 70% of infected zVAD treated cells were trypan blue positive. Treated

MDCK cells, however, had a complete reduction of fragmented nuclei as detected by Hoechst staining (Figure 40B) indicating a correlation between caspase activation and nuclear fragmentation, which has also been shown by others (Perfettini and Kroemer, 2003). MDCK cells treated with zVAD (Figure 40D) morphologically differed from mock-infected (Figure 40C) and untreated infected cells (Figure 40E) that a large majority of cells remained attached as opposed to the untreated infected cells, in which were completely detached.

To determine that the ability of zVAD to protect was not due to insufficient inhibition of caspases by the inhibitor we evaluated whether caspases were activated. Western blotting showed that activation of caspase-8 could not be detected in zVAD treated cells, but in untreated cells the p25 cleavage fragment was found (Figure 41A). Immunocytochemistry confirmed no activation of caspase-3 in zVAD treated infected MDCK cells (Figure 41B). Furthermore replication of influenza virus was not hindered in zVAD treated cells compared to untreated cells (Figure 42).

We next determined the effect of zVAD on A549 cells after virus infection. Initially, infected A549 cells exposed to 50 μM of zVAD were protected at 48 hpi as compared to untreated cells ($P < 0.0004$) (Figure 43A). However by 144 hpi, the level of cell death was comparable in both treated and untreated infected cells ($P < 0.42$). We did not count fragmented nuclei in zVAD treated infected A549 cells due to of the low basal level of fragmentation established previously in these cells. Cell morphology was also analyzed and at 144 hpi untreated infected cells showed signs of cytopathology such as loss of cell numbers and cell shrinkage (Figure 43B) while zVAD treated cells showed less changes in cell structure (Figure 43C). Mock-infected cells appeared confluent and

healthy (Figure 33D). The inhibitor did not effectively block influenza induced cell death, but did prevent severe changes in cell structure. We also did not detect caspase-3 activation in zVAD treated infected A549 cells (Figure 44). Since cell death was delayed but not effectively blocked by zVAD treatment, other, caspase independent pathways were presumably activated.

The second method we employed to test the need for caspases for virus induced cell killing was the use of MCF-7 cells. The mammary carcinoma cell line, MCF-7, is devoid of caspase-3 expression due to a deletion in the *Casp3* gene (Jänicke et al, 1998; Slee et al, 1999). We first established whether the MCF-7 line was permissive to infection and could produce a productive infection. The plaque assay (Figure 35A) showed that MCF-7 cells produced levels of influenza viruses similar to A549. Cell viability studies with trypan blue showed that about 80% of infected MCF7 cells died at 96 hpi (Figure 35B, line) and close to 35% of infected MCF-7 cells had fragmented nuclei as seen with Hoechst staining (Figure 45B, bar). The interesting event is that at 48 hpi the majority of infected cells began to round up and become detached (Figure 45C and D), but they did not lose membrane integrity and did not stain positive with trypan blue.

2.3.2.3. Summary and Discussion:

One crucial event in a cell that indicates commitment to death is the activation of the cysteine proteases called caspases, which target cellular substrates resulting in cells displaying an apoptotic phenotype. Our Western blot data indicated that both caspase-8 and –3 were activated in MDCK and A549 cells by 24 hpi during influenza induced cell

death. Since caspase-3 is an important executioner caspase we also determined the activity of caspase-3 by immunocytochemistry, which would indicate activation in individual cells.

For A549 cells, we saw very few infected A549 cells having activated caspase-3 by 24 hpi, but as time progressed the number of infected A549 cells displaying a positive signal increased. The increased level of active caspase-3 correlated with an increase in cell death as measured by trypan blue. By 144 hpi, most infected A549 cells had active caspase-3 while cell death was over 80%. MDCK cells, that detached had high levels of activated caspase-3 as opposed to MDCK cells still remaining attached. Trypan blue analysis showed that attached cells with little active caspase-3 had high viability whereas detached cells with active caspase-3 were nearly all dead. This indicated that there was a differential expression of active caspase-3 in infected cells and that caspase-3 was probably involved in disrupting adhesion of MDCK cells.

To test the requirement of caspases during influenza induced cell death we first used a broad-spectrum caspase inhibitor, zVAD, to block the activation of the procaspases and secondly used a cell line devoid of caspase-3. Treatment with zVAD did not block influenza induced cell death in infected MDCK and A549 cells but merely delayed it. The first piece of supporting evidence to verify proper and efficient caspase inhibition was that Western analysis showed no activation of caspase-8 as determined by the lack of formation of the p25 cleavage fragment. Secondly, immunocytochemistry indicated that caspase-3 was not activated in zVAD treated MDCK and A549 cells. Also Hoechst staining showed a complete reduction in the number of MDCK cells with fragmented nuclei as compared to untreated cells. The lack of nuclear fragmentation

confirmed caspase inhibition because caspase-3 is the main protease involved in this process.

As stated above, this was in contrast to what others have found in that inhibition of caspases by zVAD reduced the number of dead cells by effectively inhibiting influenza induced cell death (Wurzer et al, 2003). Here we show partial protection but the majority of the cells still died. This led us to believe that other cell death pathways were activated during the infection and required additional time for cell killing.

Wurzer et al looked only at a 24 hpi time point while we examined the cell viability at later time points. Also one could possibly account for the contradicting data in that we infected MDCK and A549 cells with a human influenza virus strain, A/WSN/33 (H1N1), while Wurzer et al used an avian influenza virus strain, A/Bratislava/79 (H7N7) (Wurzer et al, 2003). It had been shown that influenza virus's differing in virulence induced differential levels of cell death in MDCK and U937 cells (Price et al, 1997). The virulent clone 7a of the influenza A/PR/8/43X A/England/939/69 (H3N2) virus produced higher levels of cell death than the more attenuated influenza A/fiji/15899/83 (H1N1) strain as indicated by nuclear morphology and flow cytometry.

In our studies we used 50 μM of zVAD as opposed to the 40 μM that Wurzer et al used (Wurzer et al, 2003). A higher dose was used since many studies have also used this dose for studying cell death. Thus incomplete suppression was not due to insufficient levels of inhibitor. The inhibition data showed that viral replication was not affected, which supported the findings of Takizawa et al (Takizawa et al, 1999), but contradicted those of others (Wurzer et al, 2003). Both Takizawa et al (Takizawa et al, 1999) and we used non-avian influenza strains, which could account for the discrepancy.

Further support our argument that caspases or specifically caspase-3 were dispensable for influenza induced cell death comes from our data with the caspase-3 deficient MCF-7 cell line. We showed that close to 80% of infected MCF-7 cells were dead as measured by trypan blue and fewer than 40% of the cells had fragmented nuclei at 96 hpi. The lowered level of nuclear fragmentation was due to the fact that caspase-3 is the leading protease involved in DNA fragmentation. The main nuclease involved during DNA fragmentation is CAD (caspase dependent nuclease) and is activated when its inhibitor called ICAD (inhibitor of caspase dependent nuclease) is cleaved by caspase-3. However fragmented nuclei were detected, so cleavage could possibly occur by means of other nucleases found in the mitochondria (endonuclease G) and/or lysosomes (DNase I).

Plaque analysis indicated that by 144 hpi that MCF-7 cells produced high titers of virus that were 2 logs lower than MDCK cells but were similar to viral yields made by the human lung epithelial A549 cell line. Indeed viral yields at 24 hpi were similar to those seen by others (Wurzer et al, 2003), but at later times we see that the titer significantly increased and influenza did not have a poor replication efficiency in MCF-7 cells.

It appears that the activation of caspases is not required for the replication of the virus and more importantly killing of the cell. It also appears that the deletion of caspase-3 does not completely block virus induced cell death and opens the possibility of other proteases being active during influenza induced cell death.

2.4. Other Proteases and Influenza induced Cell Death:

First, EM images in both MDCK and A549 cells showed the presence of many vacuoles within the cytoplasm and may as well be the formation of autophagic vacuoles indicating a role for other proteases such as found in lysosomes during influenza induced cell death. Second, in light of the fact that caspases seem to be dispensable we asked if other proteases such as cathepsins, a class of lysosomal proteases, could also play a role in influenza induced cell death. Initially we determined whether lysosomes were affected during influenza induced cell death. These organelles have been implicated in being involved in cell death as presented in the Introduction.

2.4.1. Acid Phosphatase Activity:

To test lysosomal function during influenza induced cell death we explored the role of lysosomal enzymes such as acid phosphatase. Quantitative analysis of acid phosphatase activity was determined by the decomposition of p-nitrophenol phosphate to p-nitrophenol to form a yellow supernatant. The supernatant was analyzed by a standard spectrophotometer for changes in optical density (OD^{410}) as compared to a standard sample.

At 24 hpi infected MDCK cells had an OD^{410} reading of 2.107 as compared to mock-infected MDCK cells, which had a reading of 2.112 (Figure 46A), which indicated that no significant change in acid phosphatase activity was seen. However by 48 hpi WSN infected MDCK cells had an OD^{410} reading of 2.081 while mock-infected MDCK cell OD^{410} values were 2.136. This decrease in OD^{410} signal indicated that the environment within the lysosome was becoming less favorable and enzymatic activity was declining. Additionally we qualitatively measured the activity of acid phosphatase in

MDCK cells plated on glass coverslips as indicated in the Materials and Methods section. The *in situ* analysis showed that at 24 hpi there apparently was no difference in color intensity between mock infected (Figure 46B) and WSN infected MDCK cells (Figure 46C). This finding correlated with the quantitative result at 24 hpi in that there was no noticeable change in acid phosphatase activity.

Biochemical analysis of acid phosphatase activity in infected A549 cells showed that at 24 hpi there was a minor drop in enzyme activity, but as the infection progressed the activity significantly declined by 120 hpi (Figure 47A). The *in situ* results supported the quantitative measurements in that mock-infected A549 cells (Figure 47B) had a more intense purple-red staining than infected cells (Figure 47C) at 72 hpi.

Taken together our data suggests that lysosomes are affected during influenza induced cell death since acid phosphatase activity is lowered, but it is not known whether the changes within the lysosomes contribute to cell death progression and the demise of the cell or is it a consequence of the cell being highly damaged and is a secondary effect.

2.4.2. Role of Cathepsins -B, -D and –L:

To investigate cathepsins during influenza induced cell death we used a different strategy. We examined the need for specific individual cathepsins for viral induced cell death. We employed mouse embryo fibroblast (MEF) cells that have cathepsin -B, -D or -L deleted. At 24 hpi, close to 80% of infected wild type (WT) and cathepsin-B knockout (cathepsin-B -/-) cells were trypan blue positive (Figure 48A) whereas infected cathepsin-D knockout (cathepsin-D -/-) and cathepsin-L knockout (cathepsin-L -/-) cells had 80% and 70% of the WT deaths, respectively. By 48 hpi, all three knockout cell lines had

similar levels of cell death, differing only by approximately 5% from each other with close to or over 70% of the infected cells being trypan blue positive. Infected WT cells had close to 90% cell death at 48 hpi.

The data indicates that the loss of cathepsin-D ($P<0.0025$) and –L ($P<0.0005$) as compared to the WT cells at 24 hpi had a delayed induction of cell death, but by 48 hpi a large percentage of infected cells are dying. The result is similar to the zVAD data in that partial protection is seen in MDCK cells but eventually the treated cells had levels of death comparable to the untreated cells.

It is known that cathepsins play an essential role during a virus's life cycle. For example, reovirus uncoating is a critical step for the life cycle of this virus and cathepsin L is required for virion disassembly in murine L929 cells (Golden et al. 2002). It is not known if cathepsins play a role for influenza virus replication so we asked whether cathepsins affect the efficiency of viral replication. To test this we measured the production of virus in these various MEF cells. Looking at viral replication at 24 hpi, all three knockout cell lines had equivalent viral titer levels and by 144 hpi viral production reached levels similar to those seen in MDCK cells (Figure 48B). However, the production of virus should be compared only to its parental cell line since the virus can produce different titers in other cell types. The WT cells would represent the baseline of viral production. In contrast, WT cells had much less virus produced even at 144 hpi, showing that cathepsins are able to hamper influenza virus production in MEF cells. It appears that cathepsins negatively affect influenza virus replication and as long as one of the three cathepsins (-B, -D, -L) is taken out, viral production can occur more efficiently. The connection between the three cathepsins is not known, but the data suggests that the

removal of one of them disrupts the link and allows an increase in influenza virus replication. The reduced production of influenza virus in WT cells however does not hinder virus induced cell death since death was higher in WT cells than in the knockout cells. This suggests that cathepsin function by limiting the production of viruses, aids in the cell death pathway. By increasing cell death levels virus production can be restricted.

Based on the viability and plaque assay data it appears that cathepsins play a role in influenza induced cell death, but are not major players since cell death is relatively high in the initial stages of the infection (24 hpi). However cathepsins do hinder efficient influenza virus production. Cathepsin-L -/- cells at 24 hpi had the lowest level of death and one of the highest viral titers, suggesting that cathepsin-L may play an important role in enhancing influenza induced cell death and a key part in blocking WSN virus production.

2.4.3. Summary and Discussion:

Electron micrographs of infected MDCK and A549 cells showed typical apoptotic morphologies at 24 and 144 hpi, respectively, such as cell rounding, chromatin condensation and margination, but it was also apparent that vacuolization occurred within the cytoplasm of the dying cell. The formation of vacuoles occurs in a type of cell death called autophagy, where alterations in lysosomal function and activation of lysosomal proteases such as cathepsins contribute to the killing of a cell. Cathepsin activation has been implicated in caspase dependent and independent cell death. It is not clear whether this alternative cell death pathway could contribute to influenza induced cell death. Our initial results indicated that infected MDCK cells at 48 hpi had changes within lysosomes

since that acid phosphatase activity dropped significantly by 48 hpi as compared to mock-infected cells. We tested whether cathepsins alter virus induced cell death by infecting MEF cells with cathepsin-B, -D, and –L knockout. Infected MEF cells by 48 hpi had elevated levels of death, but significantly lower than the WT cells. However cathepsin-L knockout (cathepsin-L -/-) cells at 24 hpi initially showed a delay in virus induced cell death by a approximately 50% reduction of trypan blue positive cells when compared to WT cells. Cell death increased by 48 hpi but was still significantly lower than WT cells. The deletion of cathepsin-B, -D, and –L resulted in a considerable increase in viral production compared to WT cells, indicating that these proteases are linked together in a pathway that negatively influences influenza virus production. Cathepsin-L may be a key protease in the pathway because cathepsin-L -/- cells had the highest viral titer and the lowest percentage of cell death. Cathepsin-L appears to potentiate cell death in infected cells, but the combination of cathepsin-B, -D, and –L limits the replication of influenza virus. This data suggest that cathepsins as well as caspases are important in influenza induced cell death. It would be of interest to see how deregulation of both would work, i.e. blocking caspase activity in cathepsin -/- cells. One would speculate that a reduction in the level of cell death would be seen.

CONCLUSION

Conclusion

It has been shown by many groups that certain viruses are able to induce cell death. It is this induction of cell death that contributes to the pathogenesis of the virus. Influenza is a virus that has the ability to induce cell death, but its mechanism of induction is not completely understood.

In the study presented in this thesis, we first provided data on the characterization of influenza A/WSN/33 (WSN) virus induced cell death in Madin Darby canine kidney (MDCK) cells. Even though prior data had been shown that influenza induced cell death in MDCK cells with other influenza viruses (Takizawa et al, 1993; Hinshaw et al, 1994), a study by Price et al showed that viruses with differing virulence induced cell death differently (Price et al, 1997). WSN infected MDCK cells died with classical apoptotic characteristics, but many cells had extensive vacuolization in their cytoplasm indicating that autophagy may play some part during influenza induced cell death.

Second, most studies used cells not normally found in influenza infections. We characterized and established that WSN infected human lung epithelial (A549) cells (the normal hosts for influenza) died by the activation of apoptosis. We provided detailed quantitative and qualitative data on the kinetics of cell death and morphologies seen in dying infected A549 cells. As with MDCK cells there was also extensive vacuolization in the cytoplasm of some cells, indicating that cells may progress through different stages. We secondly saw cells that were apoptotic, highly vacuolated and secondarily necrotic. Cell death is a continuum with varying characteristics so it is possible that influenza induced cell death also progresses through a continuum of differing phenotypes because different cell death components can be activated at various times.

Third, we showed the activation of caspases in both infected MDCK and A549 cells but more importantly we discovered that inhibiting the activation of caspases only delayed the onset of influenza induced cell death and did not block it as others have found (Wurzer et al, 2003). Thus other cell death pathways were activated independent of caspases during influenza induced cell death. Even the deletion of caspase-3, a main executioner protease, did not block massive cell death in WSN infected MCF-7 cells.

It had also been suggested that the Fas pathway, an extrinsic cell death pathway, was activated during influenza induced cell death and contributed to the demise of the cell (Takizawa et al, 1993; 1995; Balachandran et al, 2000). We determined by the use of a Fas defective cell line that the overall level of cell death was lowered as compared to the parental line, but cell death was still not impaired indicating the activation of alternative cell death pathways. Based on our UV inactivation virus data it appears that replication of the virus is needed and attachment and internalization is not enough for the onset of viral induced cell death. Taken together these results indicate that the main activation of cell death happens within the cell and not externally.

These findings led us to investigate the involvement of other cell death components that may be involved during influenza induce cell death. Mitochondria are an integral part of the intrinsic cell death pathway and we determined that during WSN induced cell death in both MDCK and A549 cells mitochondrial function and membrane potential were disrupted. We also saw the release of cytochrome c, which indicated a disturbance in the mitochondrial membrane and the potential to activate caspase-9. Mitochondrial dysfunction contributes to the demise of the cell by the loss of energy production and the release of pro-apoptotic factors into the cytoplasm.

Concerning the pro-apoptotic Bcl-2 family member proteins associated to the mitochondria, the deletion of BAK, BAX, and BIM did not block the induction of cell death, however the presence of BAK without BAX appeared to lower WSN production, but why this occurred was not apparent. What was apparent was that deleting both BAK and BAX (DKO cells) delayed WSN induced cell death but unfortunately did not block it. The lowered level of cell death did not contributed to a reduction in WSN production because DKO cells had higher levels of virus compared to BAK -/- cells. This suggests that there was no correlation between virus production and cell death. BAK -/- cells had higher levels of cell death and lower levels of virus while the opposite was seen in DKO cells.

We also examined whether p53 had any role during influenza induced cell death since many investigators have shown p53 to modulate cell death in cells. As with the other knockout studies, the deletion of p53 did not block cell death but merely delayed the number of dying cells as compared to the parental cell line. This indicates that p53 is not required in WSN induced cell death and that p53 probably only enhances the killing of the cell.

Since cell death was not completely blocked by zVAD and electron micrographs showed cytoplasmic vacuolization we next looked into the function of lysosomes because they have been implicated during autophagy and contain another class of proteases called cathepsins. Quantitative and qualitative data indicated changes within lysosomes confirming validity to what we see in the electron micrographs. Our cathepsin data indicated that the deletion of either cathepsin –B, -D or –L significantly lowered the level of cell death in the mouse embryo fibroblast cells but did not stop it. However, the

deletion of any cathepsin resulted in a substantial increase in viral production as compared to the wild type (WT) cell line. This indicated that cathepsins –B, -D or –L may have a negative effect on viral production and are somehow linked. As in the WT cells, cathepsins probably increase the progression of cell death in the cells and thereby not giving the virus a chance to replicate thereby lowering the yield. It appears that the various cell death components not only modulate cell death but also affect viral replication. However the latter could be a secondary effect because a dying cell can lack resources and functional cellular machinery needed for the virus.

The mechanism for influenza induced cell death may involve not only the activation of the Fas/FADD/Caspase-8 pathway, but our findings indicate that other components involved in cell death are also implicated in influenza induced cell death. Activation of caspases may be the primary route during influenza induced cell death, but additional pathways are activated along side caspases and may require longer times for efficient cell killing. It has been shown that caspases are activated and not completely necessary for influenza induced cell death, but other proteases such as cathepsins influence viral replication and cell death.

Our data suggests that incidence or level of cell death does not correlate with the level of viral production. Viral production is needed to initiate cell death as evidenced from the UV result but the activation of the individual cell death components dictates the level of cell death.

The bottom line is that once a cell becomes infected with the influenza virus it will eventually die since multiple cell death pathways can be activated. Even if some pathways were blocked the signal to die would proceed by another way, which may delay

cell death but not stop it. The cell would eventually die anyway even if all cell death pathways were blocked because the virus exploits all the cells resources and the budding process removes the outer membrane. The general idea is that the influenza virus activates many different cell death components and depending on the intrinsic features within the cell will dictate the level of cell death induction and replication efficiency of the virus.

Figures and Figure Legends

Figure 1. Determination of Viral Production and Effective MOI for Cell Killing

A. Time course of influenza A/WSN/33 (WSN) virus replication in Madin Darby Canine Kidney (MDCK) cells. As described in the Materials and Methods, samples of media from infected MDCK cells were collected and analyzed by the plaque assay (MOI 0.001). The assay showed a swift increase in viral production that produced high viral titers. Values are the means ±S.D. of 3 independent experiments.

B. MDCK cells were infected with influenza A/WSN/33 (WSN) virus at increasing multiplicities of infection (MOI). As MOI increased the percentage of dead cells at 24 hours post infection (hpi) as seen by trypan blue increased. Values are the means ±S.E.M. of 3 independent experiments.

A

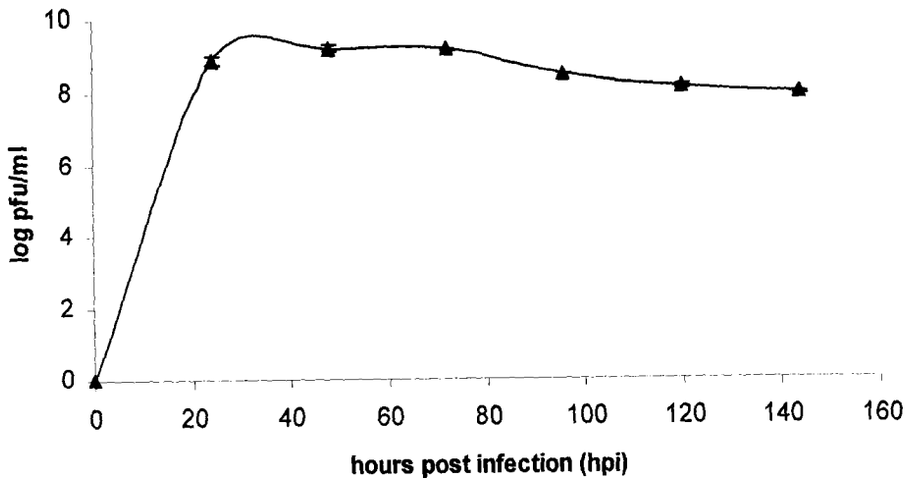

B

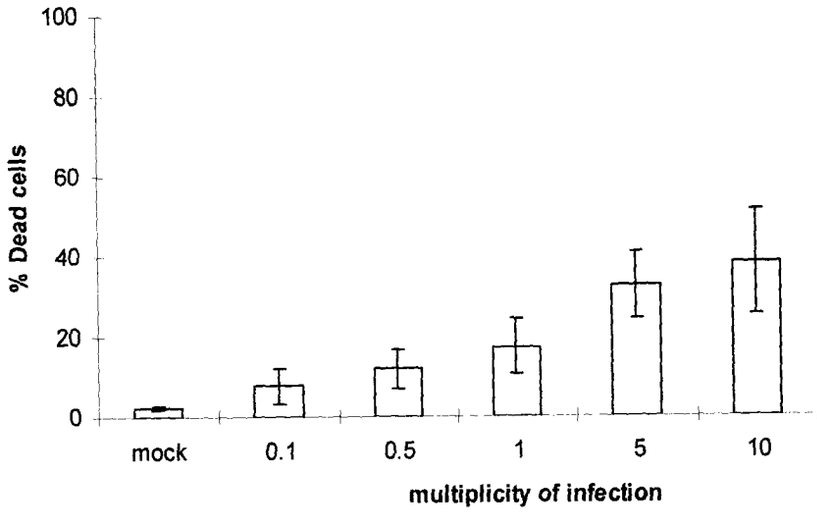

Figure 1

Figure 2. Cell death time course in WSN infected MDCK cells as measured by trypan blue analysis.

MDCK cells were infected with a multiplicity of infection (MOI) of 5 and showed high levels of dead cells at 48 hours post infection (h pi). Values are the means ±S.E.M. of at least 3 or more independent experiments.

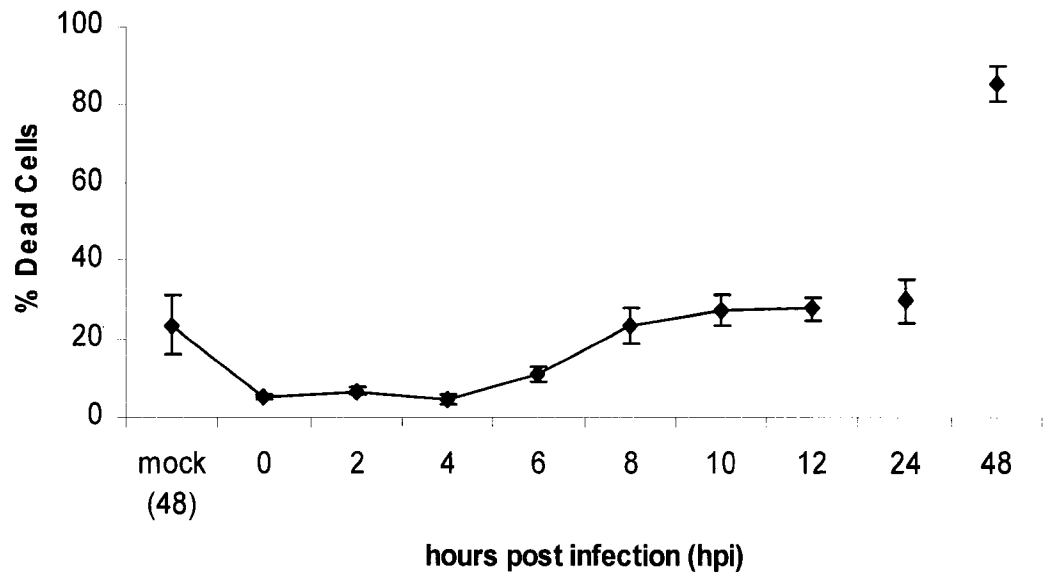

Figure 2

Figure 3. Nuclear and DNA changes during WSN infection in MDCK cells.

A. Fluorescence microscopy confirmed the quantification data by showing high levels of fragmentation in infected MDCK cells as measured by Hoechst staining. Mock-infected cells had round nuclei while dying cells at 24 hpi had fragmented and condensed nuclei. Arrows show fragmented nuclei.

B. Cell death and nuclear fragmentation time course in WSN infected MDCK cells. Infected MDCK cells showed high levels of dead cells (line, from Figure 2) and an increase in the number of fragmented nuclei (bars) as measured by trypan blue and Hoechst staining, respectively. By 48 hpi, the percentage of dead cells and fragmented nuclei were nearly the same whereas at 24 hpi the number of fragmented nuclei was twice the level as dead cells. Values are the means ±S.E.M. of at least 3 or more independent experiments.

C. MDCK cells were infected with influenza A/WSN/33 (WSN) virus at increasing multiplicities of infection (MOI). As MOI increased the number of fragmented nuclei (bars) as assayed by Hoechst increased at 24 hpi. Also the number of dying cells increased as the MOI increased at 24 hpi (points, from Figure 1B) as measured by trypan blue. Values are the means ±S.E.M. of 3 independent experiments.

A

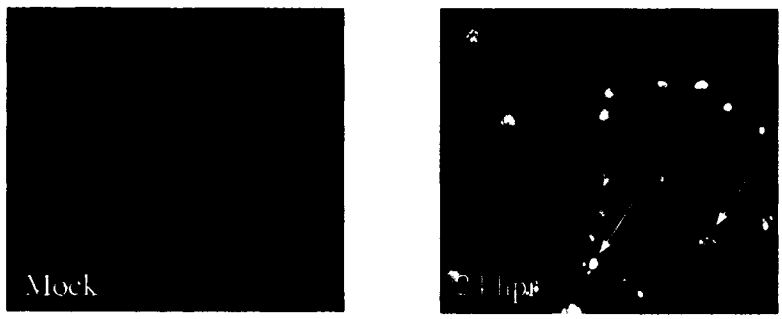

B

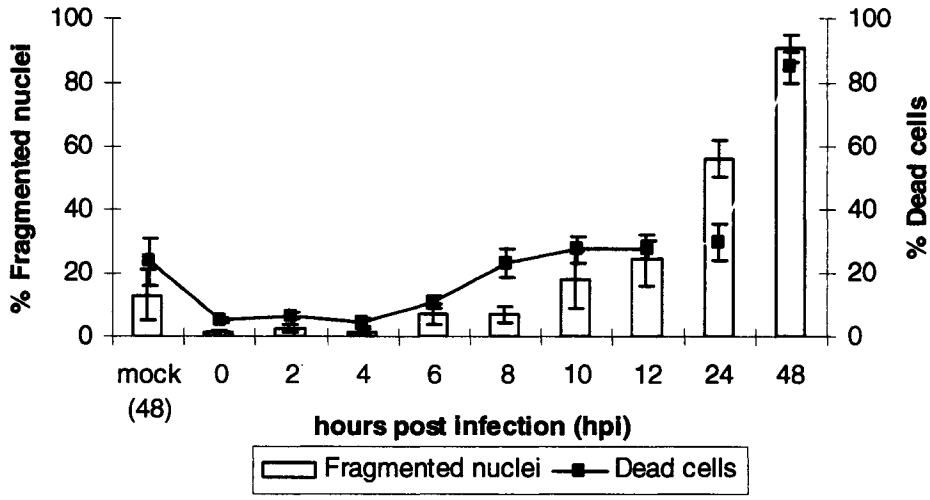

C

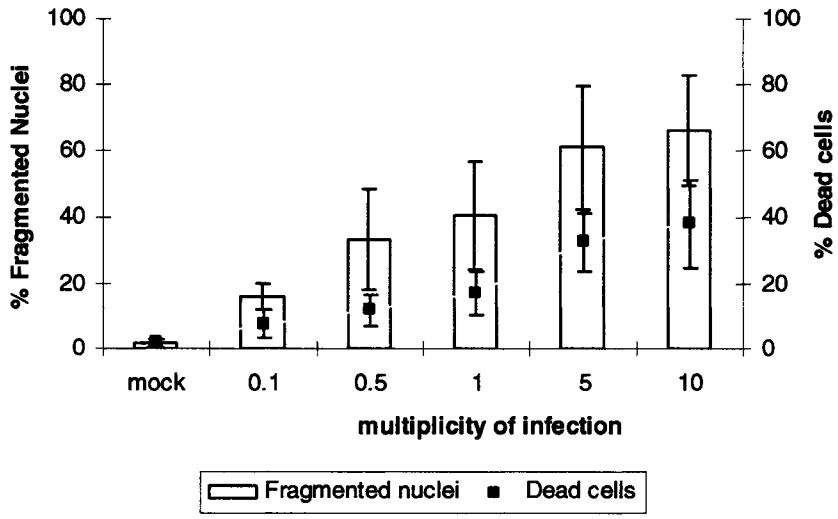

Figure 3

Figure 4. DNA changes during WSN infection in MDCK cells.

A. DNA from WSN and mock infected MDCK cells were collected at various h pi and electrophoresed on a 2% agarose gel to show the characteristic DNA laddering during apoptosis. A substantial level of DNA laddering occurred at 18 and 24 hpi. Numbers above gel indicate hpi.

B. DNA from WSN infected MDCK cells at various MOI's were collected at 24 hpi and electrophoresed on a 2% agarose gel to show the characteristic DNA laddering during apoptosis. Regardless of the MOI used infected MDCK cells showed extensive DNA laddering at 24 hpi

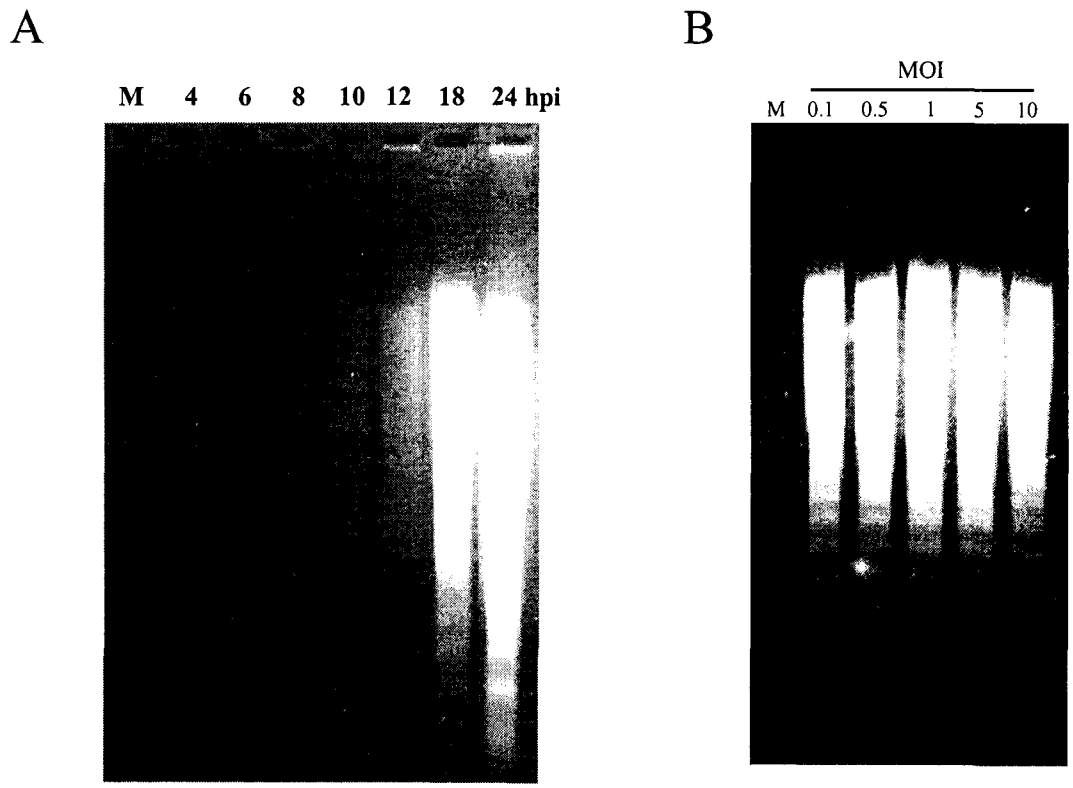

Figure 4

Figure 5. Quantification of cell death in WSN infected MDCK cells by FACS analysis.

MDCK cells were infected with a MOI of 5 and samples were collected at 0, 2, 4, 6, 8, 10, 12, 18, and 24 hpi. Mock-infected cells were collected at 24 hpi. M1 = subdiploid (apoptotic) population.

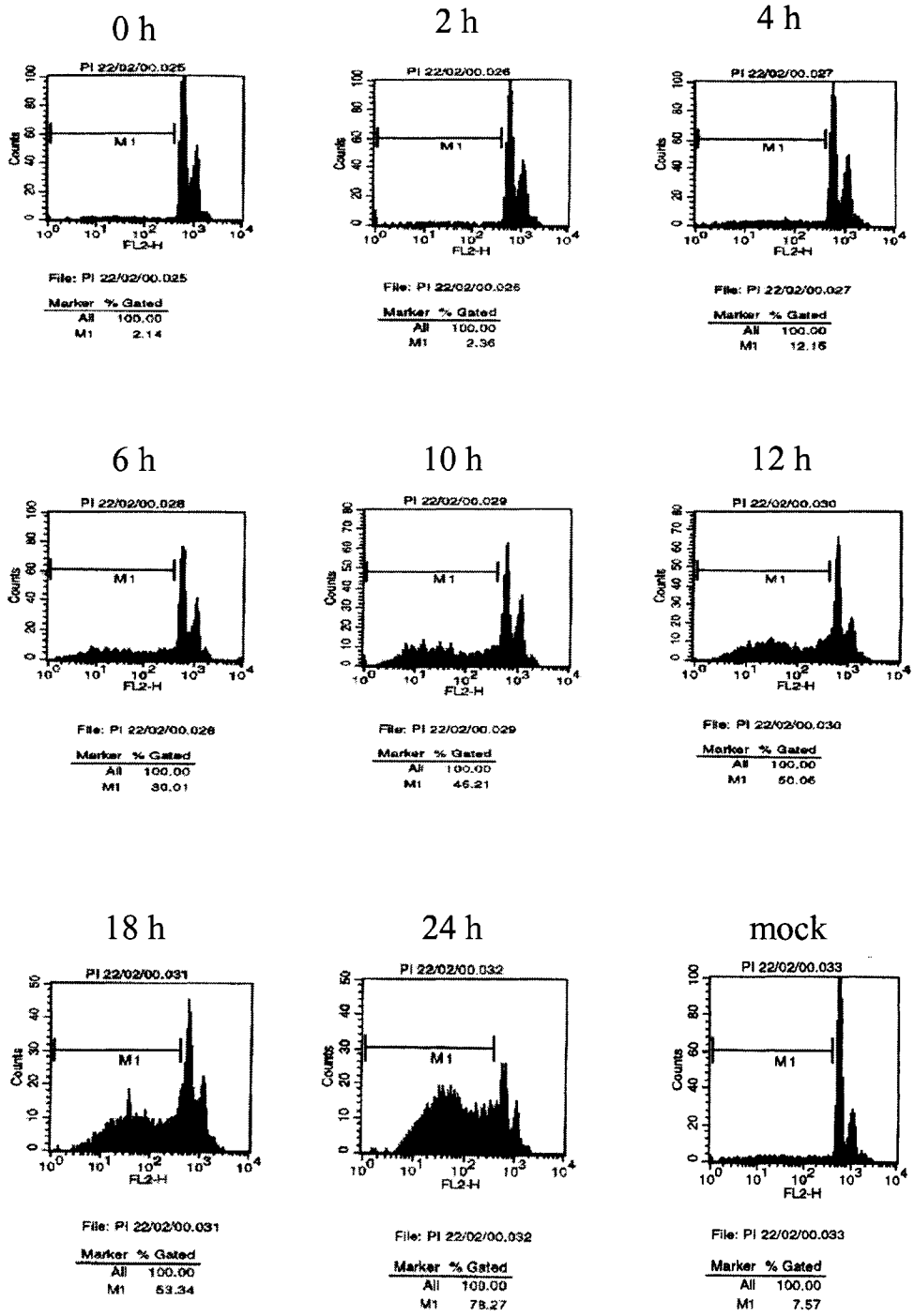

Figure 5

Figure 6. Effect of influenza virus on MDCK cell morphology as visualized by light microscopy.

MDCK cells were infected with a MOI of 5 and incubated for 8 and 24 hpi. Cells were fixed with 3% paraformaldehyde and stained with methylene blue.

A. Mock infected cells showed normal cell morphology. A, 100X, Bar = 50 μm

B. At 8 hpi, infected MDCK cells began to show signs of cell rounding and cell death. Arrow indicates a patch of dying cells. B, 100X, Bar = 50 μm

C. At 24 hpi, infected MDCK cells showed increased levels of cell rounding, loss of membrane integrity and intense methylene blue staining. Arrows indicate dying cells. C, 100X, Bar = 50 μm

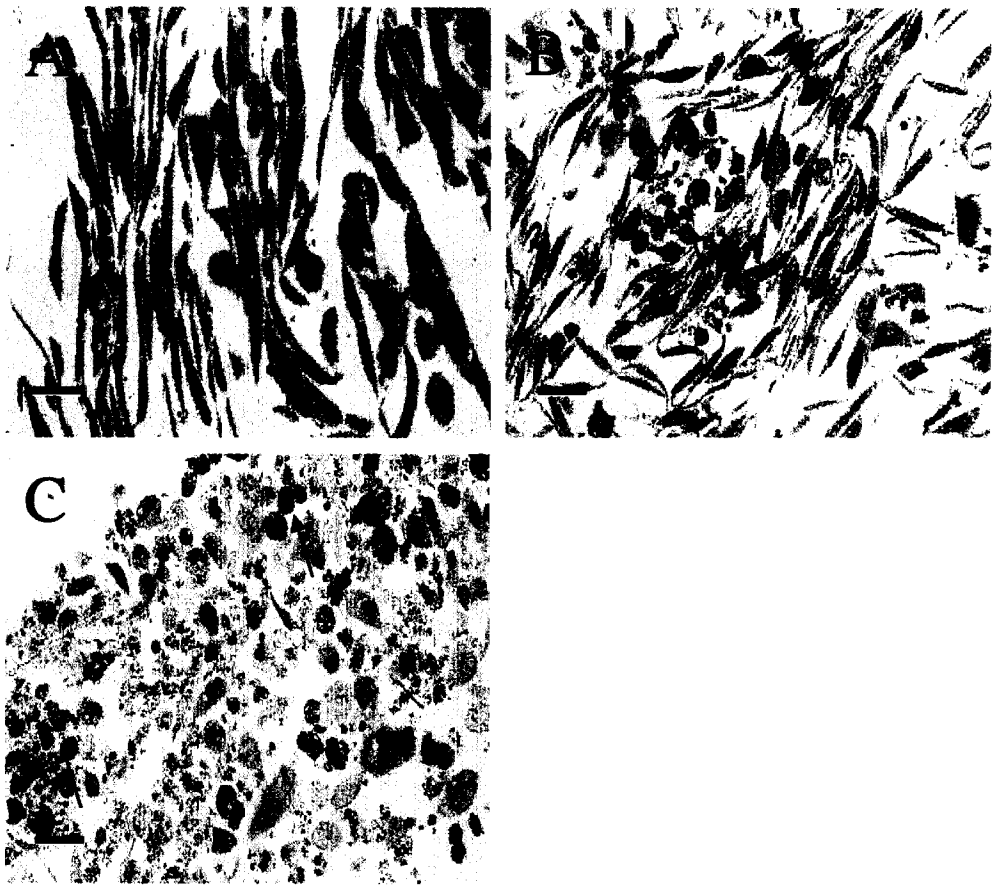

Figure 6

Figure 7. Morphological analysis of apoptosis by electron microscopy.

As described in the Materials and Methods, infected MDCK cells at 24 hpi were fixed for electron microscopy.

A. Mock-infected MDCK cells were elongated and showed large normal nuclei.

B. Infected MDCK cells showed cytoplasmic shrinkage, fragmentation and condensation of the chromatin and increased electron density.

C. Infected cells also show increased vacuolization in the cytoplasm

N: nucleus, C: cytoplasm, *: condensed and fragmented chromatin, V: vacuoles

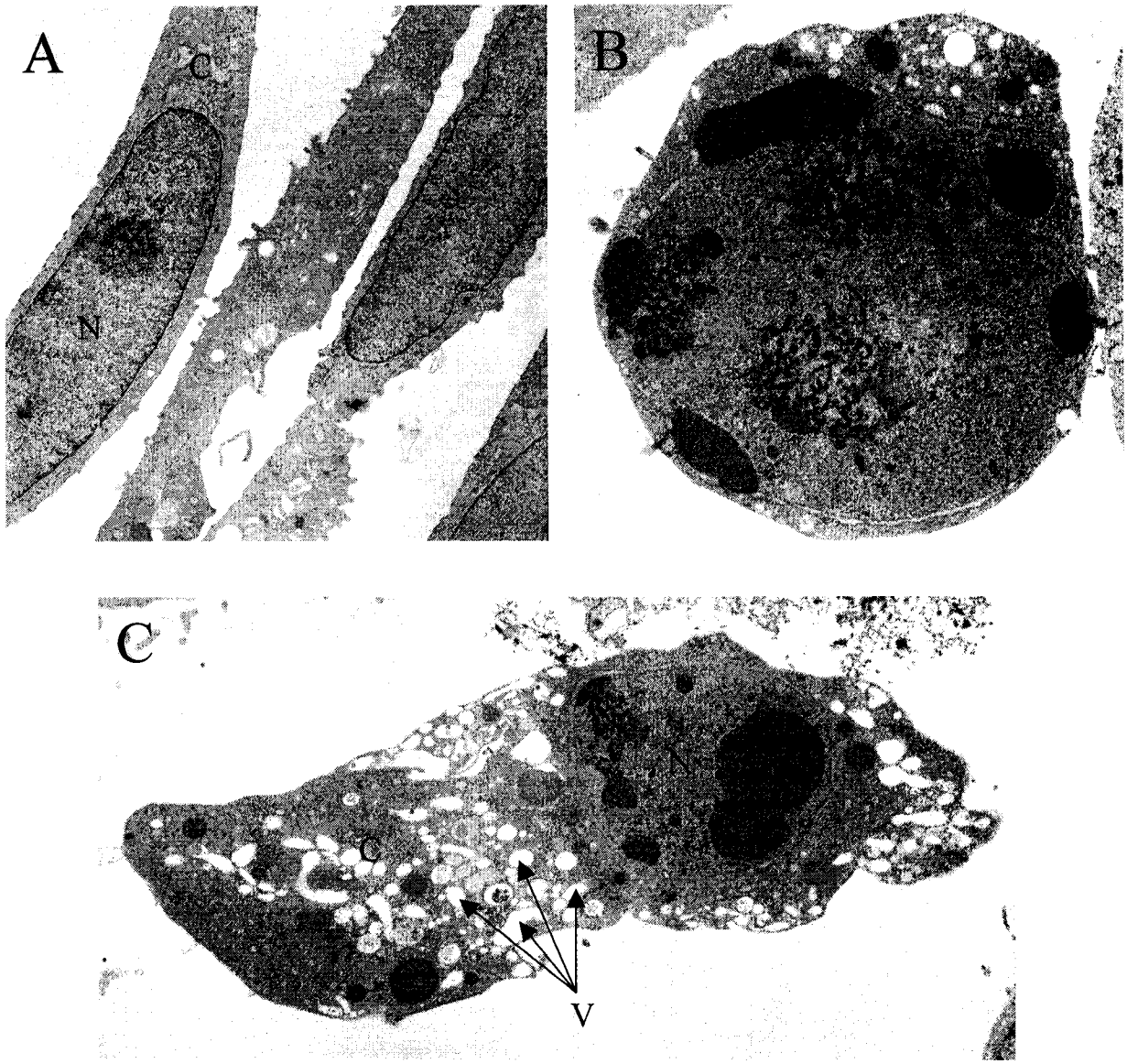

Figure 7

Figure 8. Morphological analysis of apoptosis by electron microscopy.

An electron micrograph showed many cells displaying classical apoptotic features as well as massive vacuolization and secondary necrosis in more advanced dying cells. An apoptotic cell has a condensed nucleus and cytoplasm while the chromatin is fragmented. For a necrotic cell, the outer membrane and nucleus has disintegrated while the cytoplasm is not electron dense.

N: nucleus, C: cytoplasm, *: condensed and fragmented chromatin, V: vacuoles

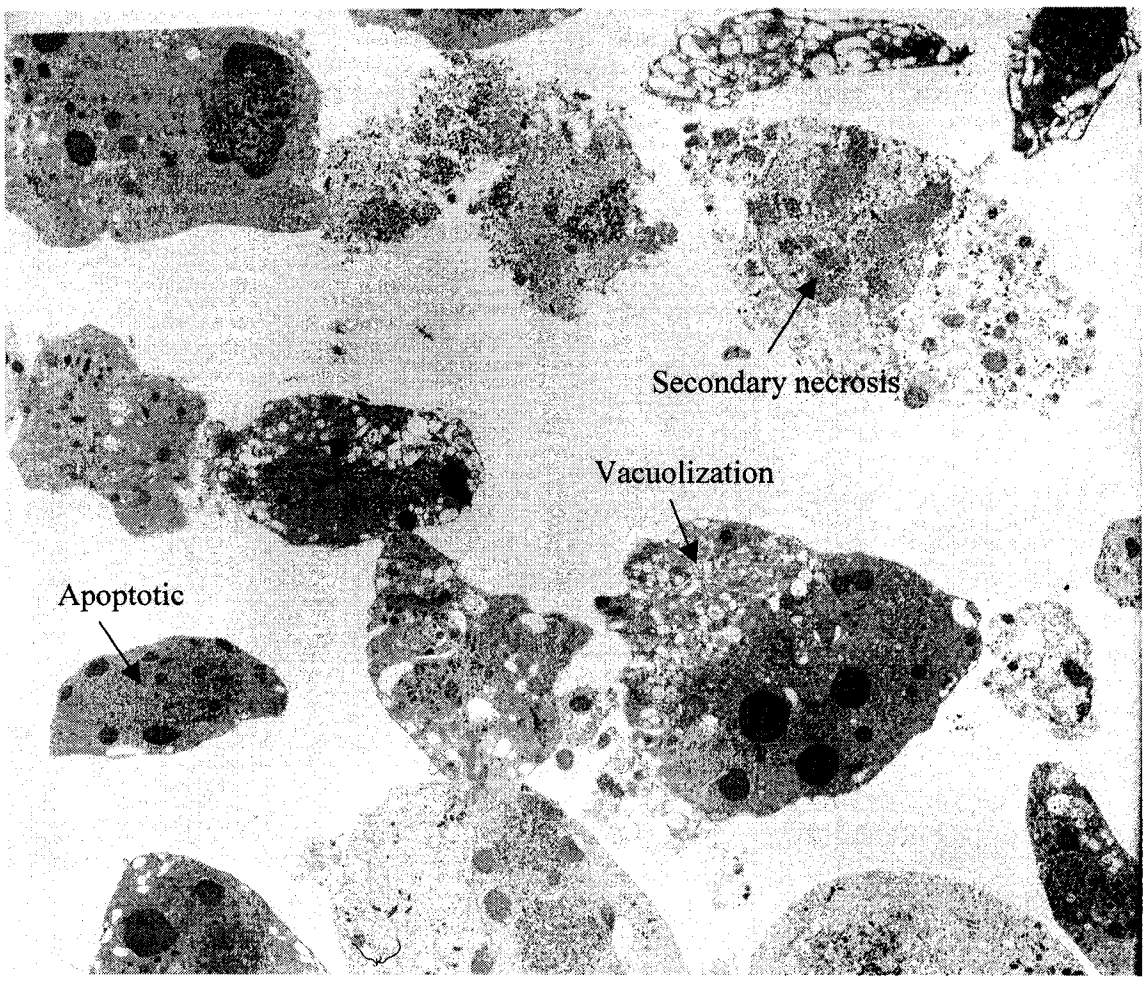

Figure 8

Figure 9. Cytopathology of influenza virus infection as seen by light microscopy.

A. Mock-infected MDCK cells at 12 hpi

B. At 12 hpi, MDCK cells showed signs of cytopathology by WSN. Clusters of cells are seen detaching off the plate (arrows).

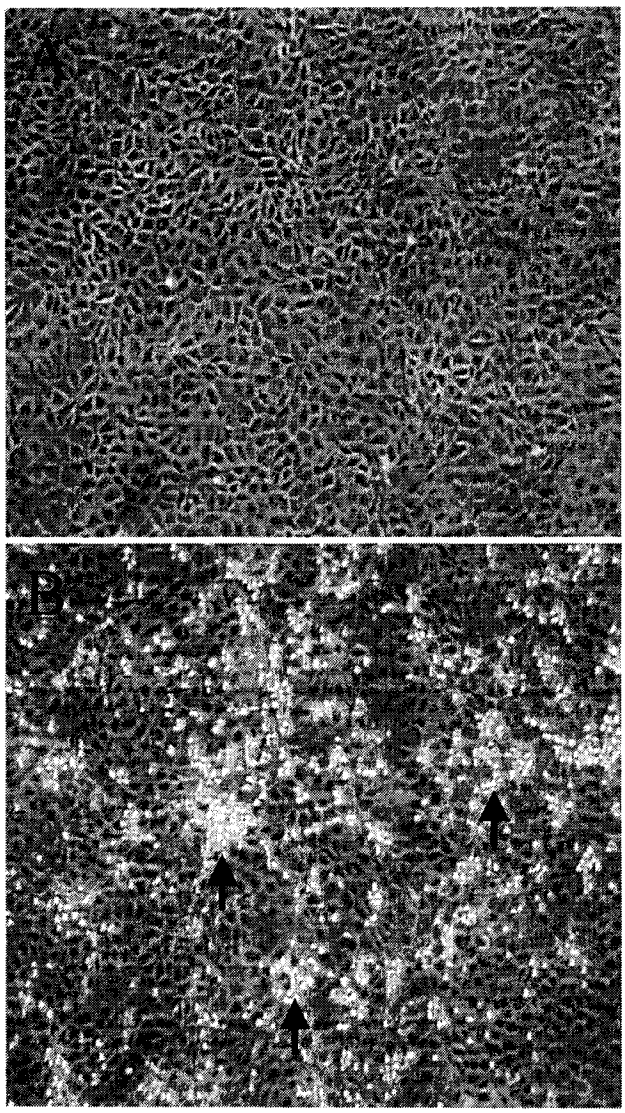

Figure 9

Figure 10. Differential differences in cell death between adherent and floating infected MDCK cells.

Both populations, adherent and floating, were analyzed for membrane integrity and cell viability by trypan blue and the Live/Dead assay.

A. Trypan blue analysis showed that detached cells (solid line) had higher levels of cell death than adherent cells (dashed line). Values are the means ±S.E.M. of 3 independent experiments.

B. Mock-infected cells fluoresce green with the hydrolysis of calcein AM, which only occurs in living cells (48 hpi). B, 400X, Bar = 12.5 μm

C. At 48 hpi, adherent MDCK cells fluoresce yellow-green as a result of the hydrolysis of calcein AM and the incorporation of ethidium bromide, which fluoresces red. C, 400X, Bar = 12.5 μm

D. Floating cells fluoresce red due to the intercalation of ethidium bromide and only appear in dying cells (48 hpi). D, 400X, Bar = 12.5 μm

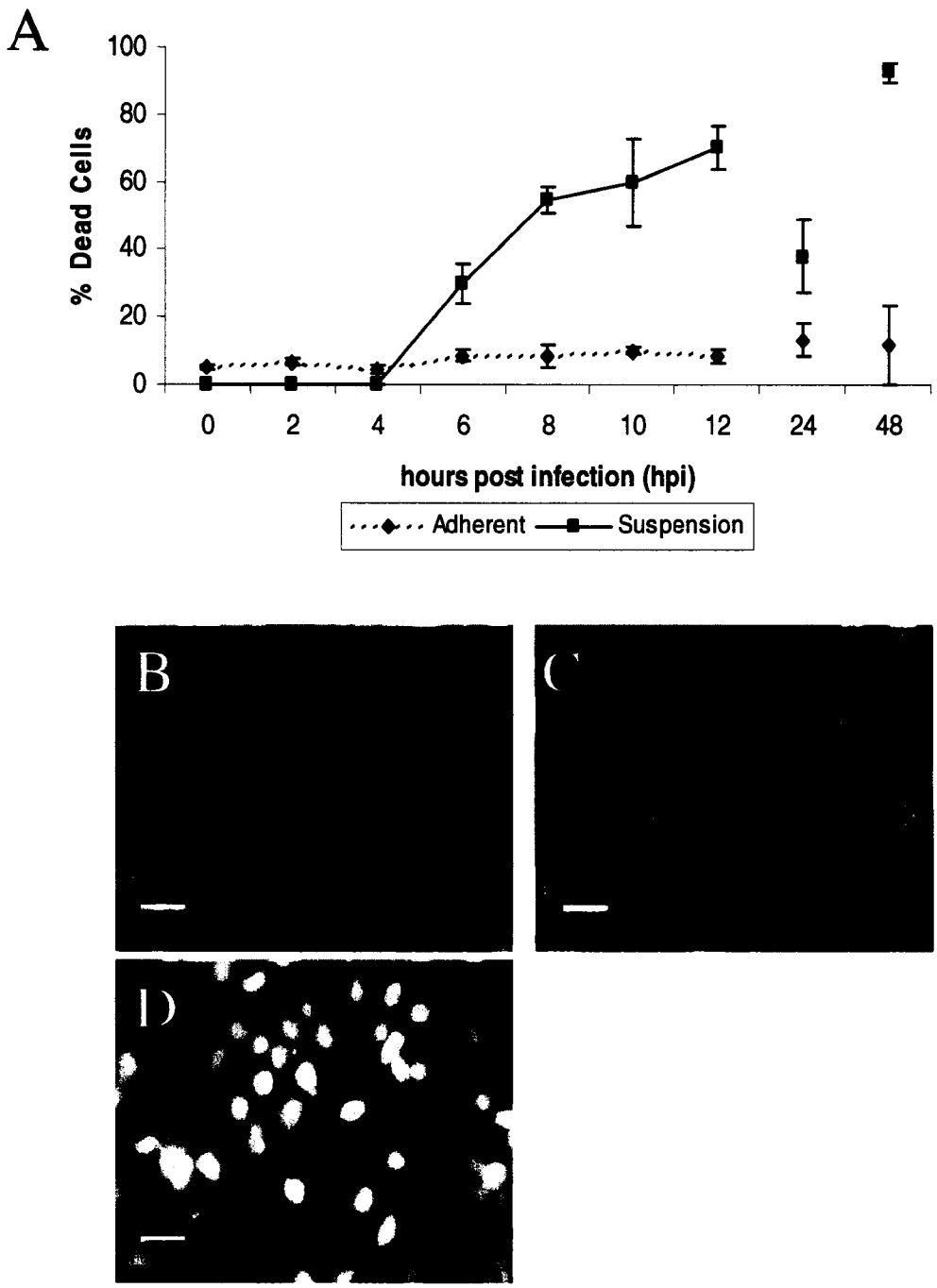

Figure 10

Figure 11. Differential differences in cell death between adherent and floating infected MDCK cells.

Both populations, adherent and floating, were analyzed for nuclear changes as measured by Hoechst staining.

A. Hoechst staining showed that detached cells (solid line) had higher levels of nuclear fragmentation than adherent cells (dashed line). Values are the means ±S.E.M. of 3 independent experiments.

B. Mock-infected cells have normal shaped nuclei (48 hpi). B, 400X, Bar = 12.5 μm

C. At 48 hpi, adherent infected cells show the starting of chromatin aggregation. C, 400X, Bar = 12.5 μm

D. Late stages of apoptosis appear in the floating infected MDCK cells (48 hpi). D, 400X, Bar = 12.5 μm

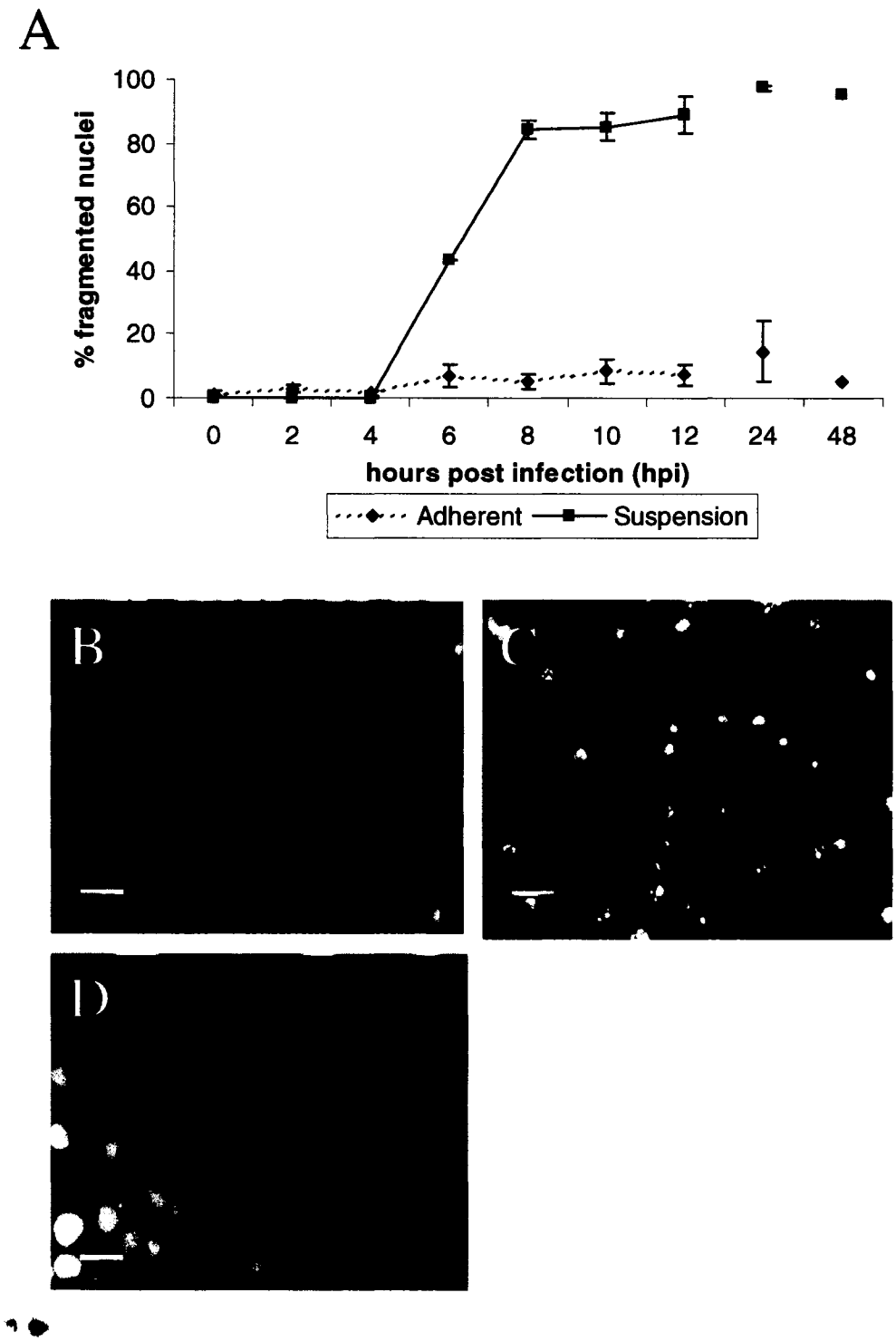

Figure 11

Figure 12. Time course of influenza A/WSN/33 (WSN) virus replication and viral protein production in A549 cells.

A. As described in the Materials and Methods, samples of media from infected A549 cells were collected and analyzed by the plaque assay (MOI 0.001). The assay showed an increase in viral production that produced high viral titers. Values are the means ±S.D. of 3 independent experiments.

B. ^{35}S Methionine labeled protein from WSN and mock infected A549 cells were resolved on a 10% SDS-PAGE gel at various hours post infection (h pi) as indicated above the gel. Host protein synthesis is shut down in the cell line as compared to the mock-infected (M) cells and viral protein production (i.e. NP) in A549 cells declines after 24 hpi. The coomassie brilliant blue stained gel shows equal loading of the samples.

A

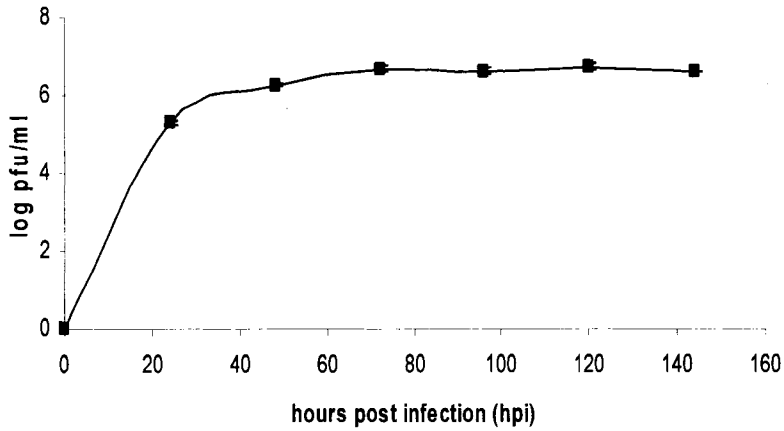

B

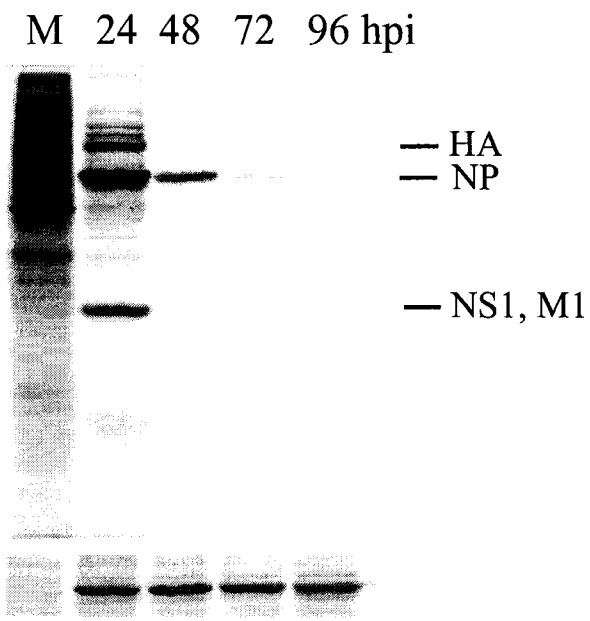

Figure 12

Figure 13. Cell death time course in WSN infected A549 cells as measured by trypan blue and the Live/Dead assays.

A. A549 cells were infected with a multiplicity of infection (MOI) of 5 and showed high levels of dead cells at 144 hpi. Values are the means ±S.D. of 3 independent experiments.

B & C. Mock-infected cells at 96 hpi for the most part fluoresce green with the hydrolysis of calcein AM, which only occurs in living cells. B, 100X, Bar = 50 μm; C, 400X, Bar = 12.5 μm

D & E. At 96 hpi, 50% of infected A549 cells fluoresce red, which is an indication of a dying cell due to the incorporation of ethidium bromide. B, 100X, Bar = 50 μm; C, 400X, Bar = 12.5 μm

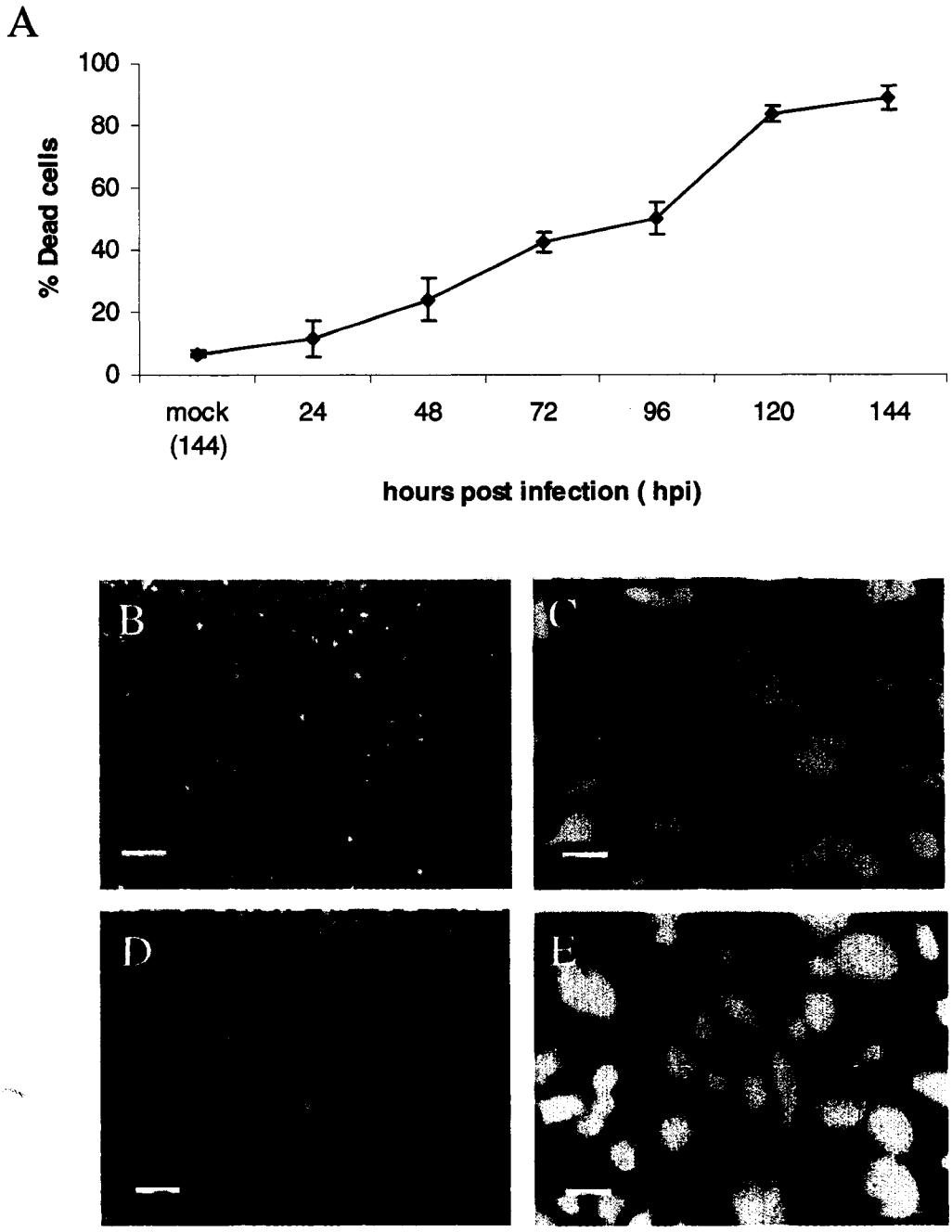

Figure 13

Figure 14. Nuclear and DNA changes during WSN infection in A549 cells.

A. As analyzed by Hoechst staining, A549 cells showed low levels of nuclear fragmentation even at 144 hpi during the infection. Values are the means ±S.D. of 3 independent experiments.

B & C. Fluorescence microscopy confirmed the quantification data that nuclear fragmentation occurred at low levels in A549 cells as measured by Hoechst staining. Mock-infected cells (B) had large round nuclei while infected cells (C) at 96 hpi had nuclei that were condensed as seen by a brighter fluorescence signal but did not fragment. B, 400X; C, 400X, Bar = 12.5 μm

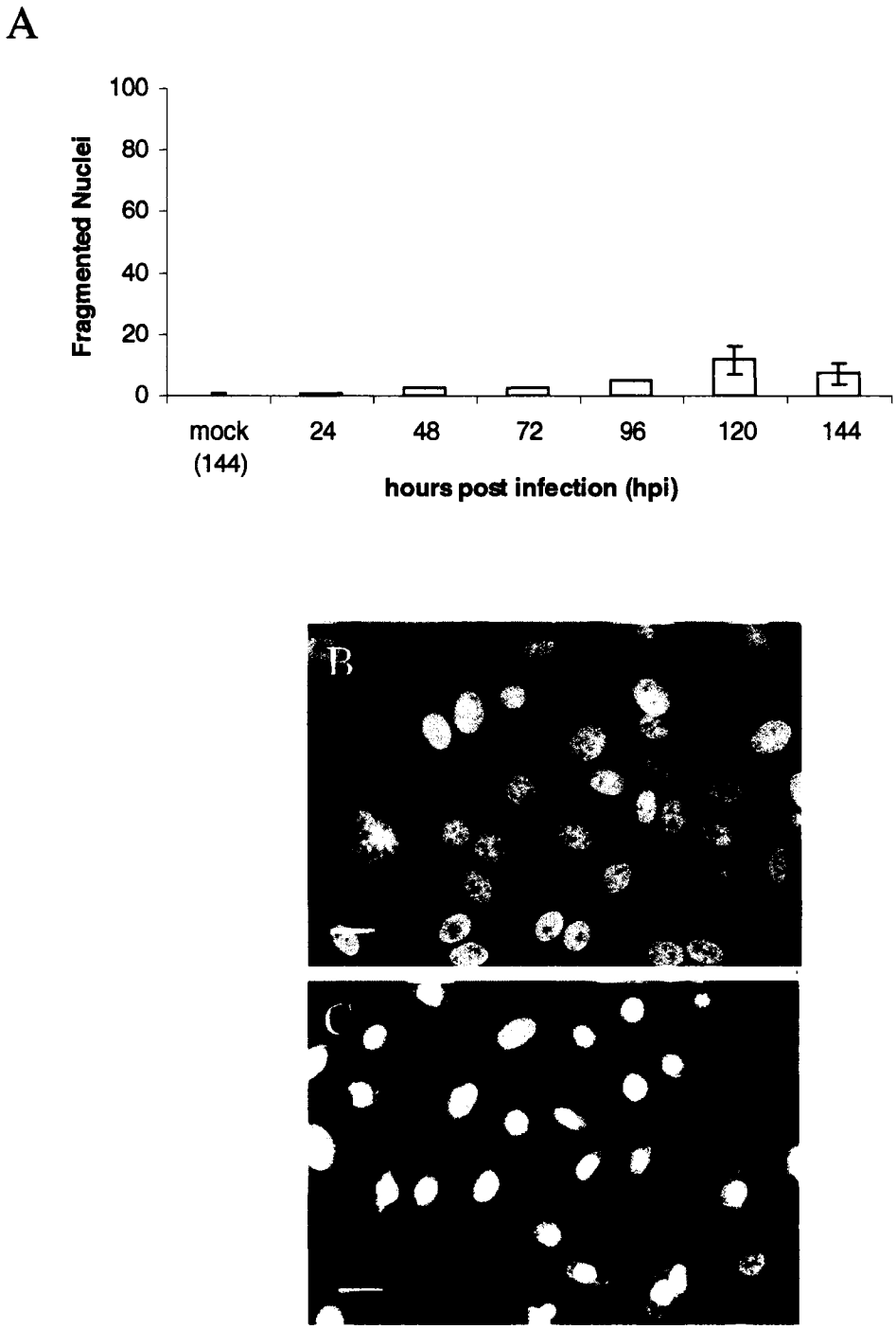

Figure 14

Figure 15. Cell death and nuclear fragmentation time course in WSN infected A549 cells.

Infected A549 cells showed high levels of cell death (line) at 144 hpi even though the level of fragmented nuclei (bar) at that time was below 20% as measured by trypan blue and Hoechst staining, respectively.

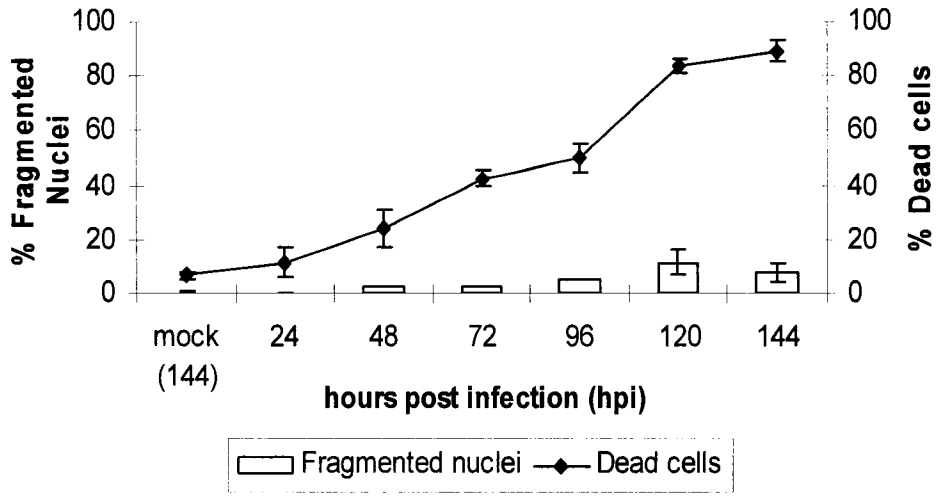

Figure 15

Figure 16. A lack of DNA fragmentation in A549 cells as measured by gel electrophoresis.

A. Infected A549 cells showed no DNA laddering even at 168 hpi while the MDCK control showed strong laddering at 24 hpi. A549 cells treated with 100 μg/ml of cycloheximide (CHX) did not display the characteristic DNA laddering pattern that occurs during apoptosis.

Lane 1: mock infected MDCK, 24 hpi
Lane 2: WSN infected MDCK, 24 hpi
Lane 3: mock infected A549, 168 hpi
Lane 4: WSN infected A549, 24 hpi
Lane 5: WSN infected A549, 48 hpi
Lane 6: WSN infected A549, 72 hpi
Lane 7: WSN infected A549, 96 hpi
Lane 8: WSN infected A549, 120 hpi
Lane 9: WSN infected A549, 168 hpi
Lane 10: 100 μg/ml CHX, 120 h
Lane 11: 100 μg/ml CHX 144 h

B. A more sensitive method utilizing radioactive $\alpha^{32}P$ end labeling detected DNA laddering in A549 cells. Laddering became more pronounced at 48 hpi and greatly intensified at 144 hpi. Lane 1, WSN 24 hpi; Lane 2, WSN 48 hpi; Lane 3, WSN 96 hpi; Lane 4, WSN 120 hpi; Lane 5, WSN 144 hpi.

A

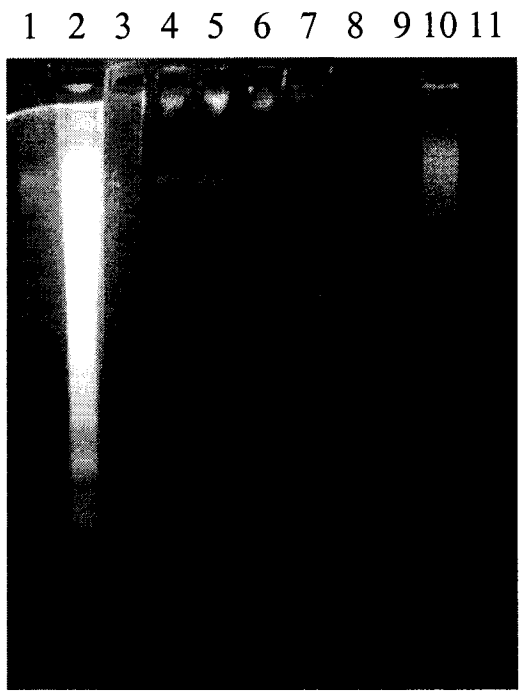

B

Figure 16

Figure 17. TUNEL labeling in A549 cells.

A. A549 cells infected with WSN showed increased levels of fragmented DNA as compared to mock-infected cells as measured by the TUNEL assay. Arrows indicate TUNEL positive cells.

B. Quantitation of the fragmentation showed that 40% of infected cells at 144 hpi were TUNEL positive. Numbers above the time points indicate percentage of TUNEL positive cells.

A

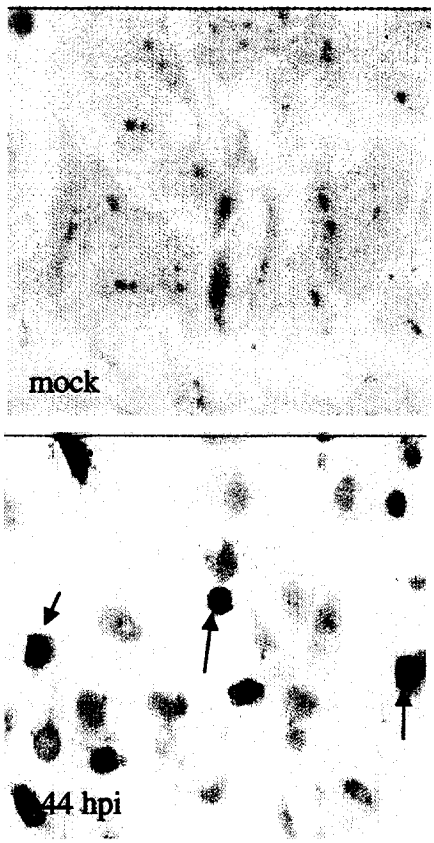

B

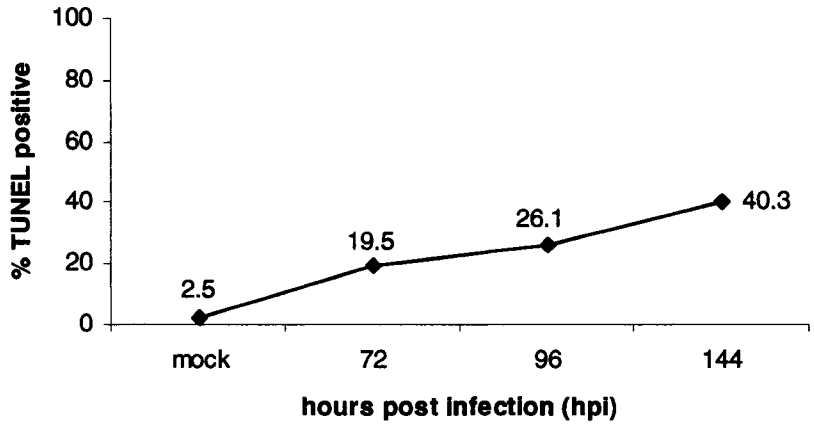

Figure 17

Figure 18. Effect of influenza virus on A549 cell morphology as visualized by light microscopy.

A549 cells were infected with a MOI of 5 and incubated for 24 and 72 hpi. Cells were fixed with 3% paraformaldehyde and stained with methylene blue.

A. Mock infected cells showed normal cell morphology. A, 100X, Bar = 50 μm

B. At 24 hpi infected A549 cells began to show cell structure changes and appear thinner than mock-infected cells. B, 100X, Bar = 50 μm

C. At 72 hpi, infected A549 cells showed increased numbers of cells with altered cell structures but overall the cells do not appear to undergo cell rounding and advanced stages of membrane integrity loss. Some cells do however take up more dye and are interpreted as dying cells. Arrows indicate cells with heavier staining. C, 100X, Bar = 50 μm

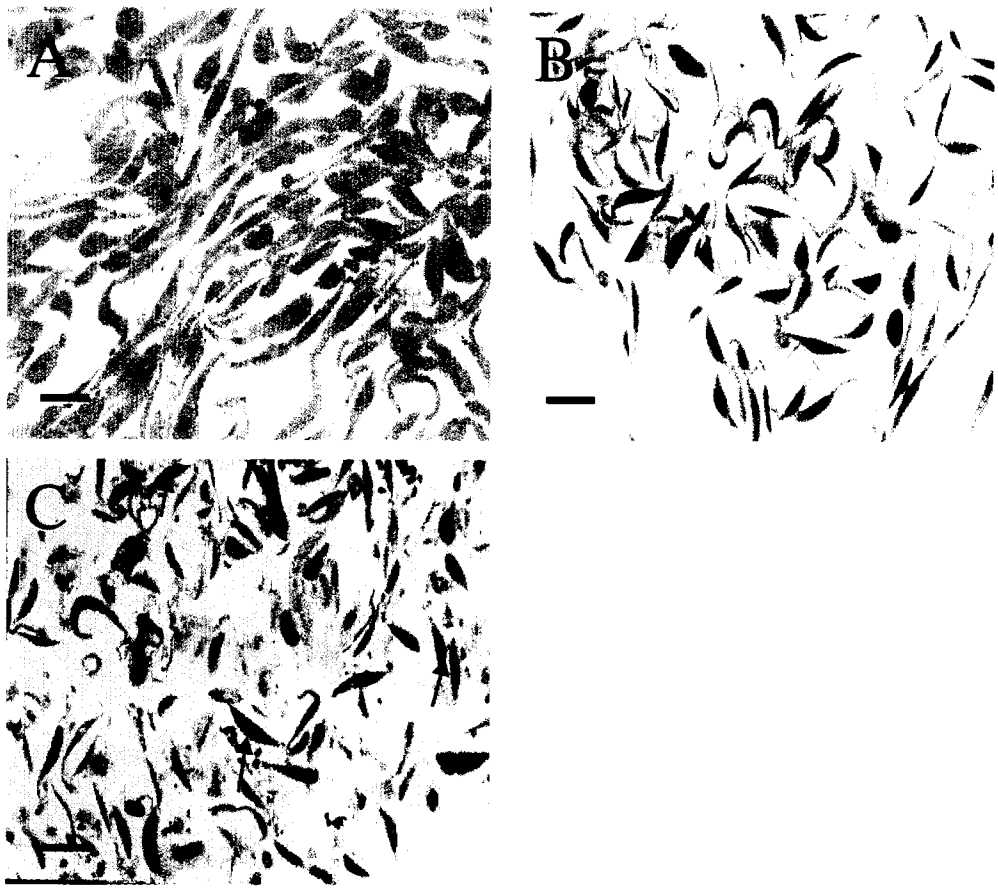

Figure 18

Figure 19. Morphological analysis of infected A549 cells by electron microscopy.

As described in the Materials and Methods, infected A549 cells at 72 and 144 hpi were fixed for electron microscopy.

A. Mock-infected A549 cells were elongated and showed large normal nuclei.

B. Infected A549 cells at 72 hpi did not display complete cytoplasmic shrinkage, but the chromatin was condensed, fragmented and marginated. The nucleus however did not appear to round up. Arrows show influenza viruses around the plasma membrane.

C. Infected cells at 144 hpi show phenotypes similar to those of 72 hpi cells.

D. At 72 hpi, infected A549 cells that are in advanced stages of cell death undergo secondary necrosis.

N: nucleus, C: cytoplasm, *: condensed and fragmented chromatin

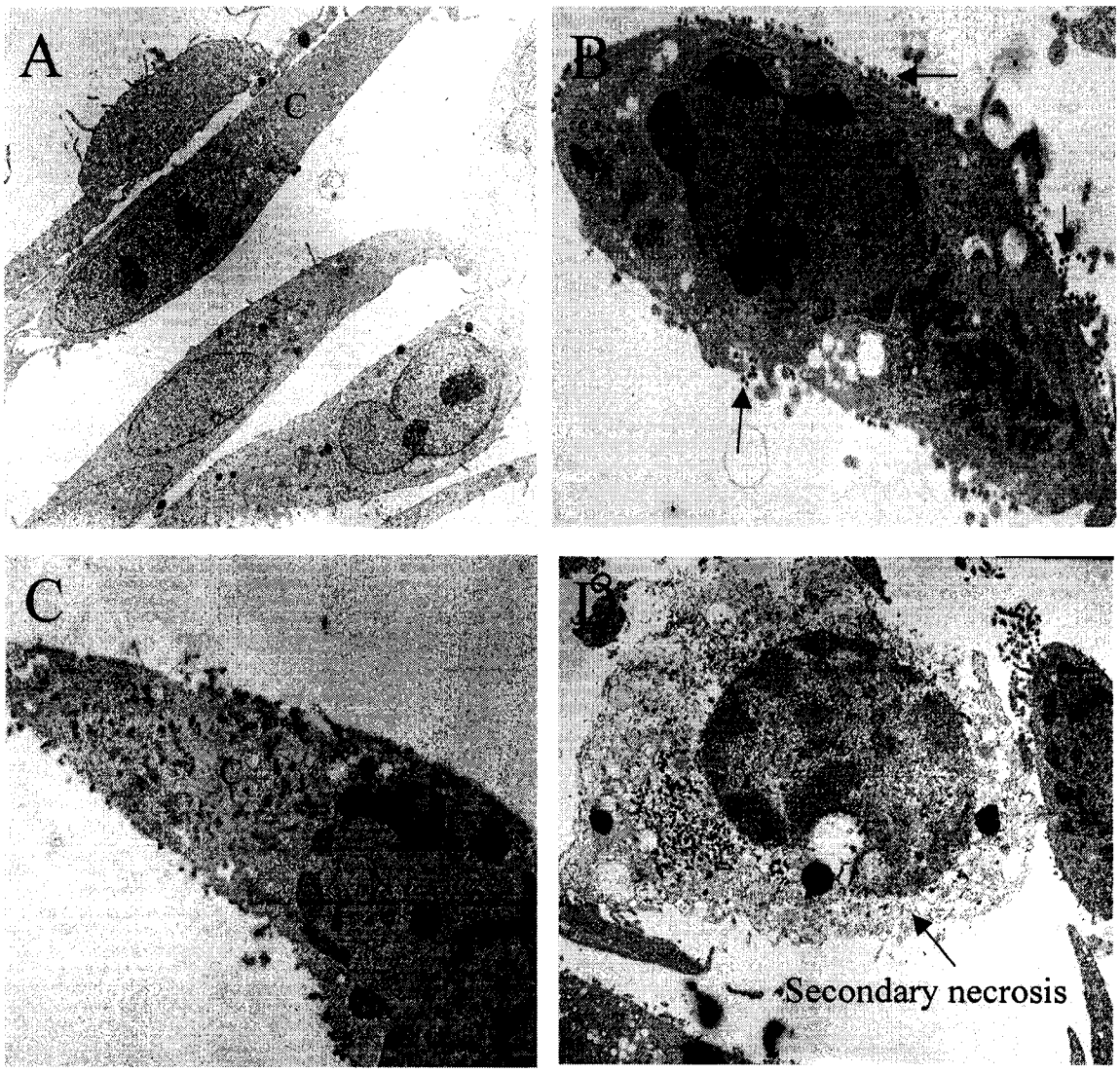

Figure 19

Figure 20. Morphological analysis of infected A549 cells by electron microscopy.

Besides the condensation of chromatin and a lack of cell rounding infected A549 cells at 72 hpi showed extensive vacuolization in the cytoplasm (arrows).

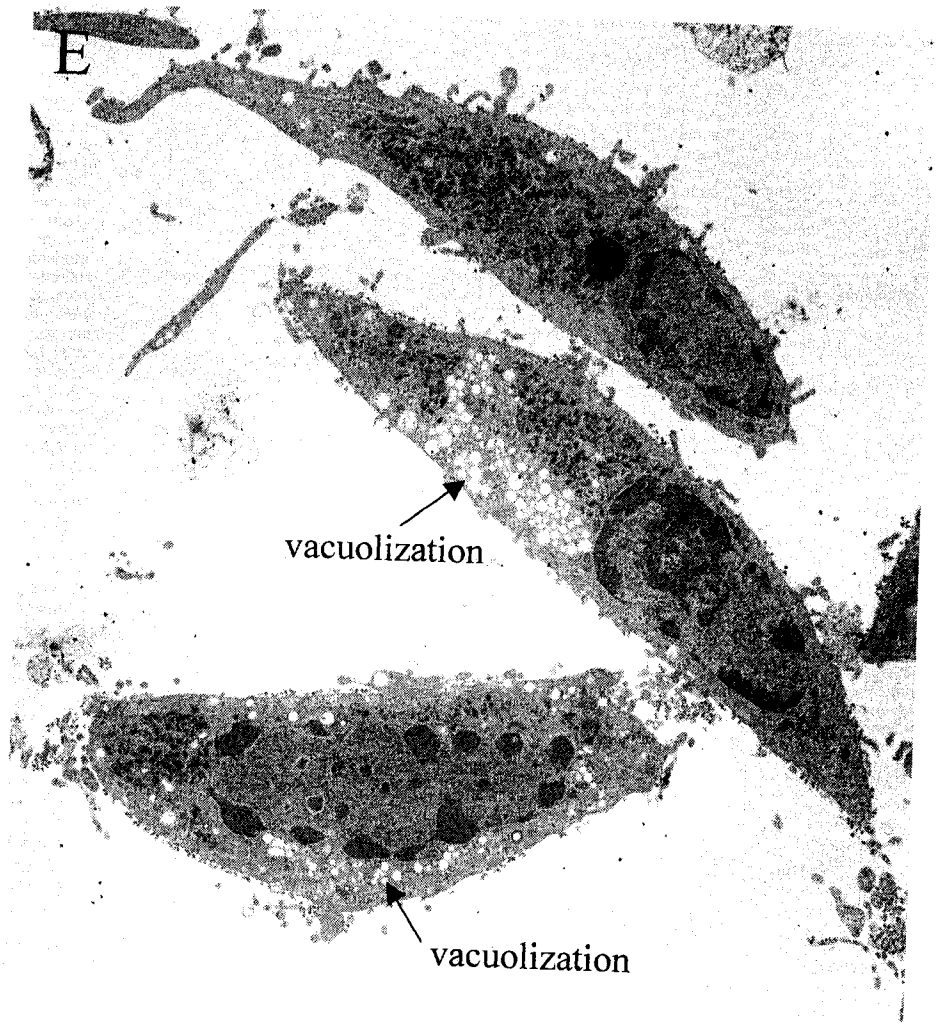

Figure 20

Figure 21. Ultraviolet inactivated WSN virus does not trigger virus induced cell death.

WSN viruses were irradiated with 254 nm UV (50 J/m^2) for 14 min and used to infect MDCK cells at an MOI of 5.

A. UV inactivated WSN virus did not induce DNA laddering in MDCK cells at 24 hpi.

B. Trypan blue analysis showed that UV treated viruses did not induce cell death in MDCK cells since the level of death was similar to that seen in mock-infected cells whereas untreated virus caused cell death at 24 hpi.

A

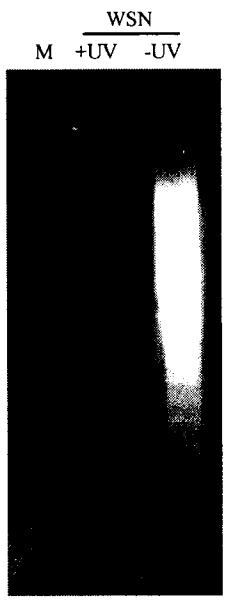

B

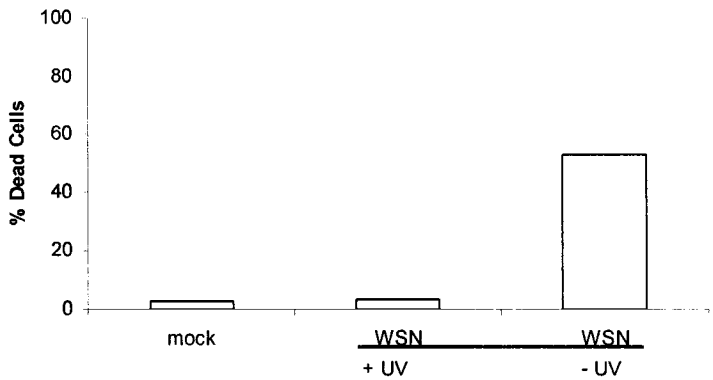

Figure 21

Figure 22. Cell death and nuclear changes in cycloheximide treated and WSN infected MDCK cells.

MDCK cells were treated with 100 μg/ml of cycloheximide (CHX) and analyzed by trypan blue and Hoechst staining at various hours post treatment.

A. Trypan blue analysis showed that CHX treated MDCK cells had comparable levels of cell death with WSN infected MDCK cells at 24 and 48 hpi. MDCK cells treated with both death inducers had similar time courses of cell death. Values are the means ±S.D. of 3 independent experiments.

B. At 24 hours, CHX treated MDCK cells had higher levels of nuclear fragmentation than WSN inflected MDCK cells but at 48 hours both treated and infected cells had similar levels of fragmentation as analyzed by Hoechst staining. Values are the means ±S.D. of 3 independent experiments.

A

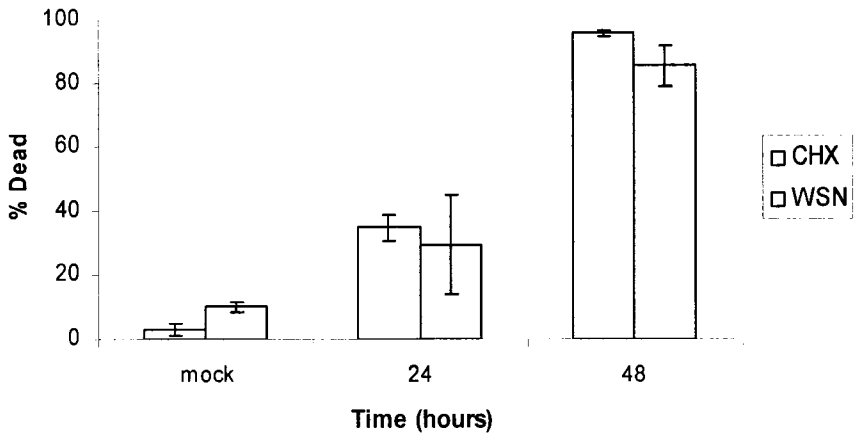

B

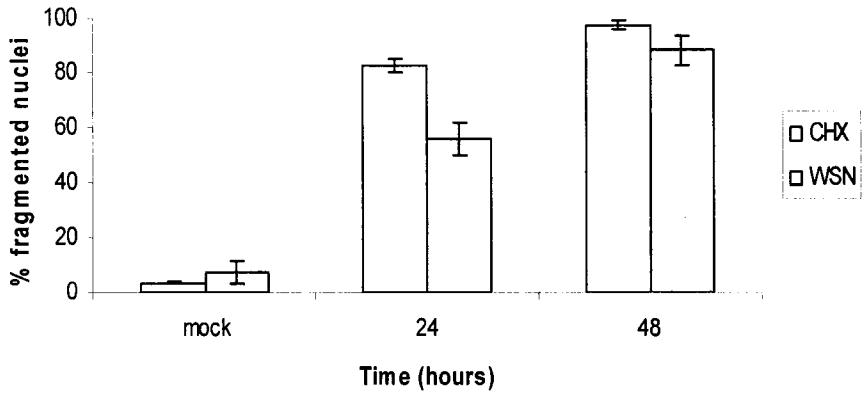

Figure 22

Figure 23. Cell death and nuclear changes in cycloheximide treated and WSN infected A549 cells.

A549 cells were treated with either 100 μg/ml of cycloheximide (CHX) or WSN (MOI 5) and analyzed by trypan blue and Hoechst staining at various hours post treatment.

A. Trypan blue analysis showed that CHX treated A549 cells (solid line) had comparable levels of cell death with WSN infected A549 cells (dash line) at 144 hpi but the rate of appearance of cell death was different. Values are the means ±S.D. of 3 independent experiments.

B. CHX treated A549 cells (solid line) at 144 hours had higher levels of nuclear fragmentation than WSN inflected A549 cells (dash line) but the overall percentage of fragmentation was well below 50% as analyzed by Hoechst staining. Values are the means ±S.D. of 3 independent experiments.

A

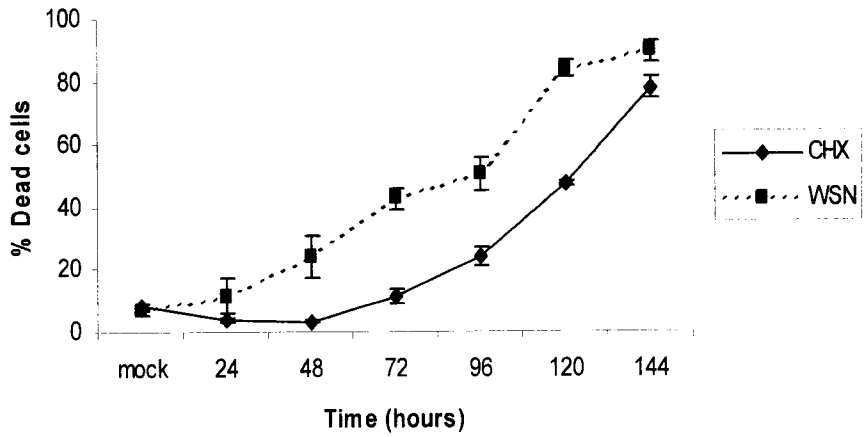

B

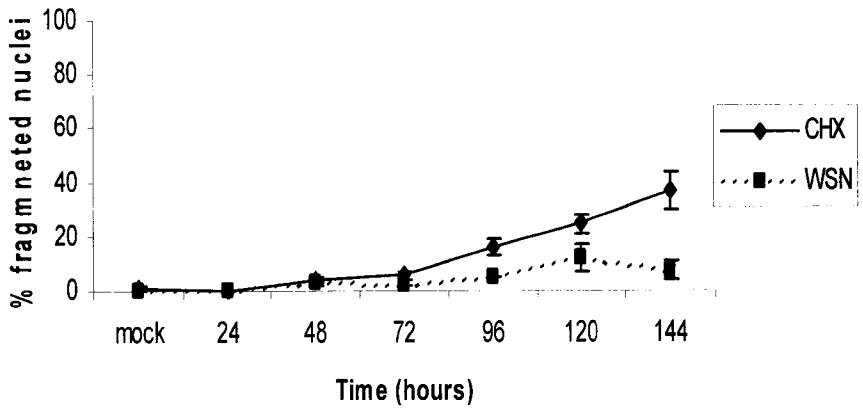

Figure 23

Figure 24. Loss of Fas reduces the extent of influenza induced cell death.

Both U937 and U937R cells were infected with influenza A/WSN/33 at a MOI of 5.

A. By 72 hpi U937 cells had higher numbers of dying cells than U937R cells indicating that Fas was needed for increasing the extent of influenza induced cell death. Values are the means ±S.D. of 3 independent experiments.

B. Hoechst analysis indicated elevated numbers of fragmented nuclei in both cells, but as with the trypan blue data U937 cells had many more fragmented nuclei than U937R cells. Values are the means ±S.D. of 3 independent experiments.

C. DNA fragmentation analysis showed the hallmark DNA laddering pattern in both infected U937 and U937R cells at 24 h pi. Lanes 1& 2, U937 cells and Lanes 3 & 4, U937R cells. Lane 1, Mock; Lane 2, WSN; Lane 3, Mock; Lane 4, WSN.

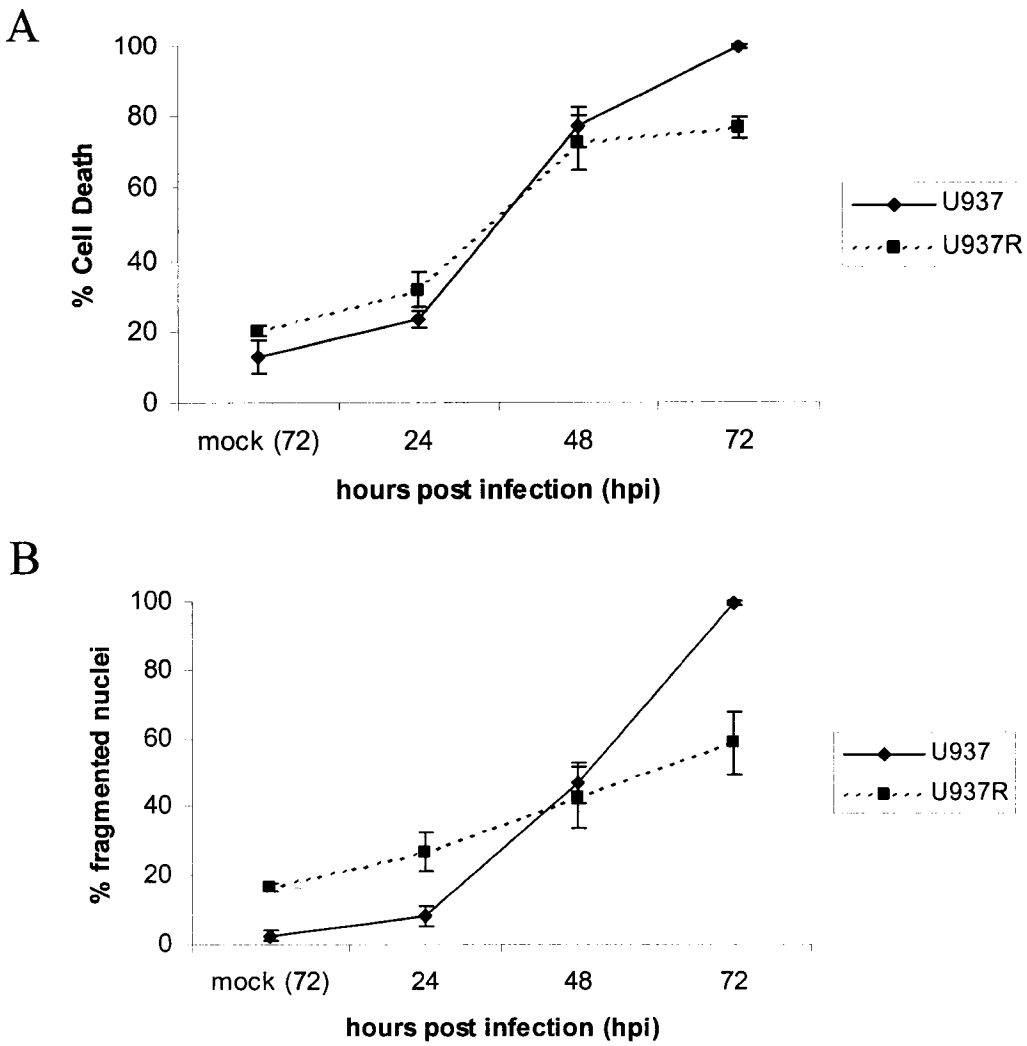

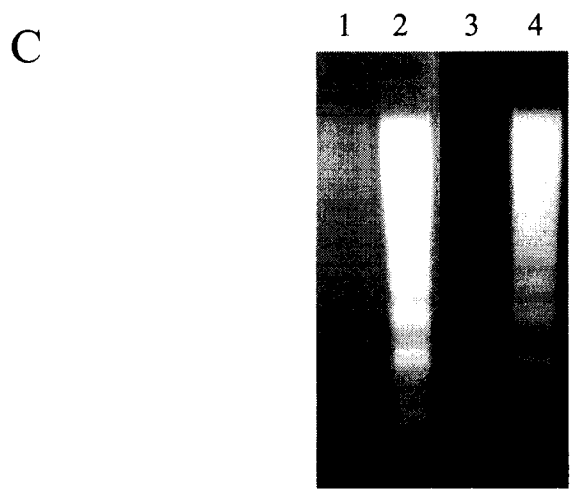

Figure 24

Figure 25. Mitochondrial dysfunction occurs in infected A549 and MDCK cells.

A & B. Infected A459 (A) and MDCK (B) cells showed a loss in mitochondrial membrane potential by a decrease in fluorescence signal of Rhodamine 123. Values are the means ±S.D. of 3 independent experiments.

C & D. MTT was used to assess mitochondrial enzyme activity in infected cells. Infected A549 (C) and MDCK (D) cells both showed a decline in the reduction of MTT indicating that the environment inside the mitochondria was becoming less favorable. Values are the means ±S.D. of 3 independent experiments.

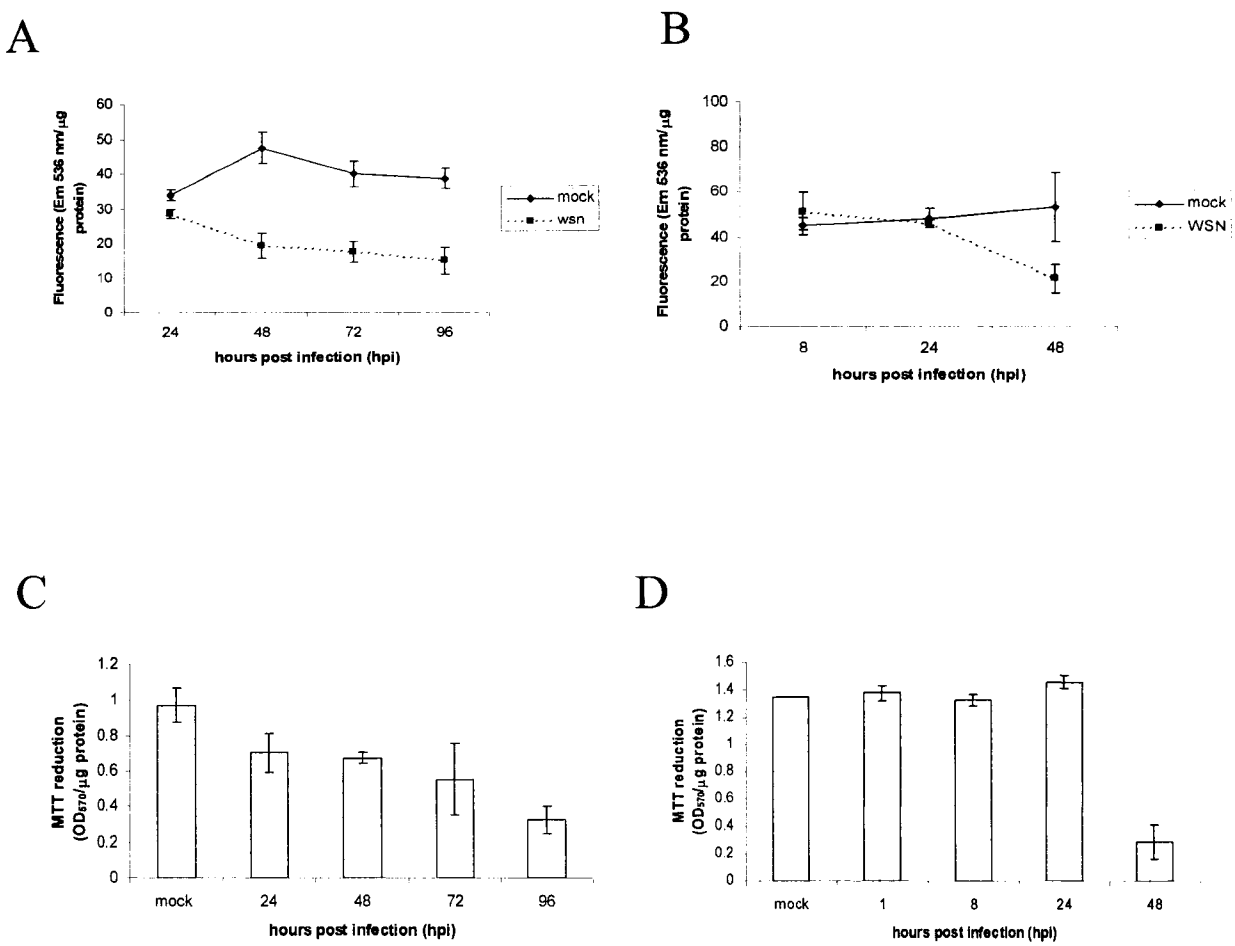

Figure 25

Figure 26. Changes occur in mitochondrial shape and distribution during influenza induced cell death in A549 cells.

We used the MitoTracker Red probe to label the mitochondria with visualization under a fluorescence microscope. The ability of the dye to be fixed within the mitochondria is dependent on the redox state inside the organelle.

We see that infected A549 cells no longer had the filamentous distribution of mitochondria seen in mock-infected cells (white arrows) but showed greater dispersion and the mitochondria retained less dye (green arrows). Right column of panels show nuclear state of A549 cells with Hoechst staining. Images at 1000X, Bar = 5 μm

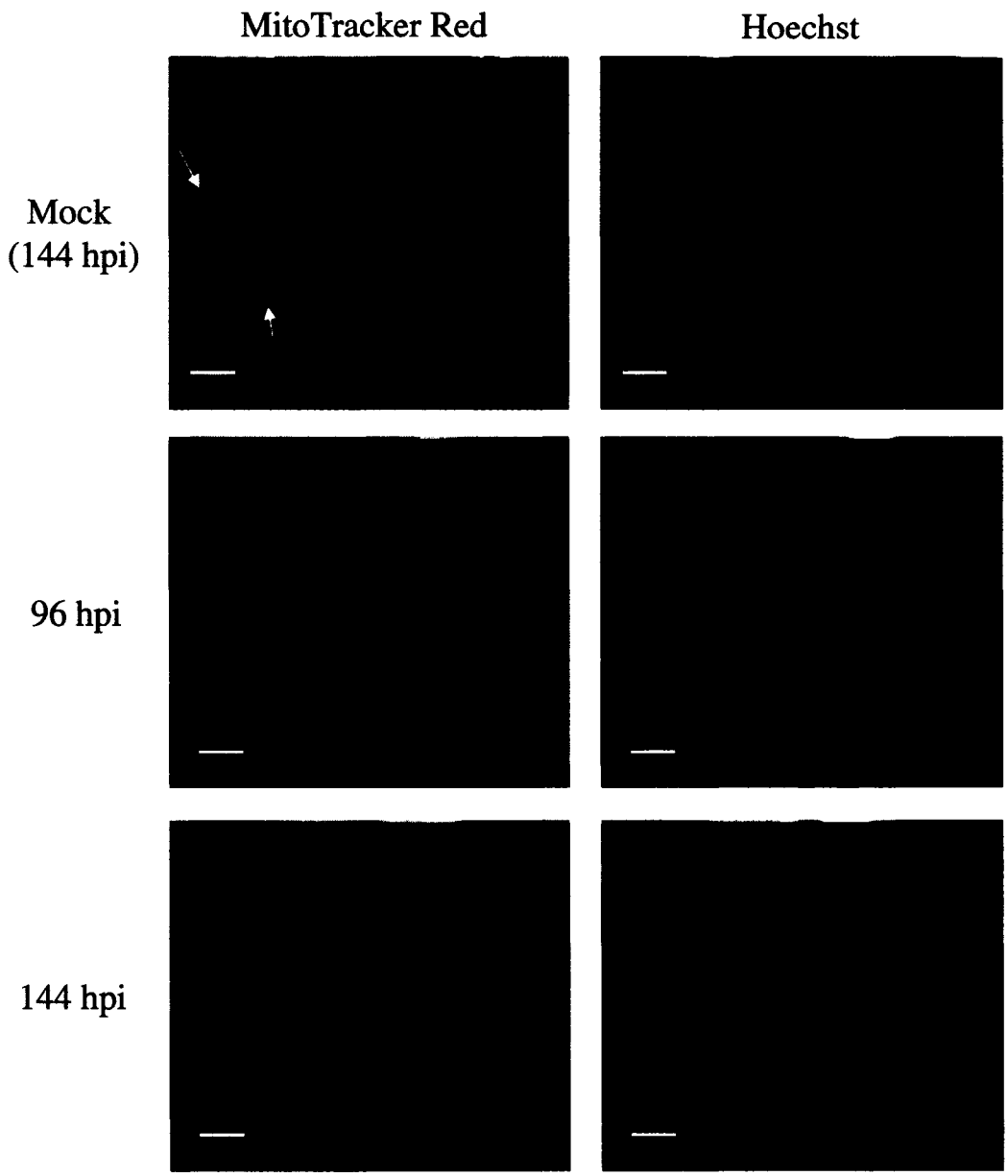

Figure 26

Figure 27. Cytochrome c is released in WSN infected cells.

Cell lysates were fractionated into the mitochondrial fraction (P) and the supernatant fraction (S) and blotted for the presence of cytochrome c.

A. Western blot analysis showed a release of cytochrome c from mitochondria into the cytoplasm in infected MDCK cells by 18 hpi.

B. In infected A549 cells cytochrome c was detected in the cytoplasm by 24 hpi.

C & D. *In situ* labeling of cytochrome c in A549 cells showed a punctate pattern in mock-infected cells (C) while diffuse staining was seen infected A549 cells at 144 hpi (D). C, 7000X; D, 7000X, Bar = 0.71 μm

E & F. MitoTracker Red staining showed the filamentous distribution of mitochondria in mock-infected A549 cells (E) while WSN infected A549 cells (F) had a red fluorescence signal that was diffuse out. E, 7000X; F, 7000X, Bar = 0.71 μm

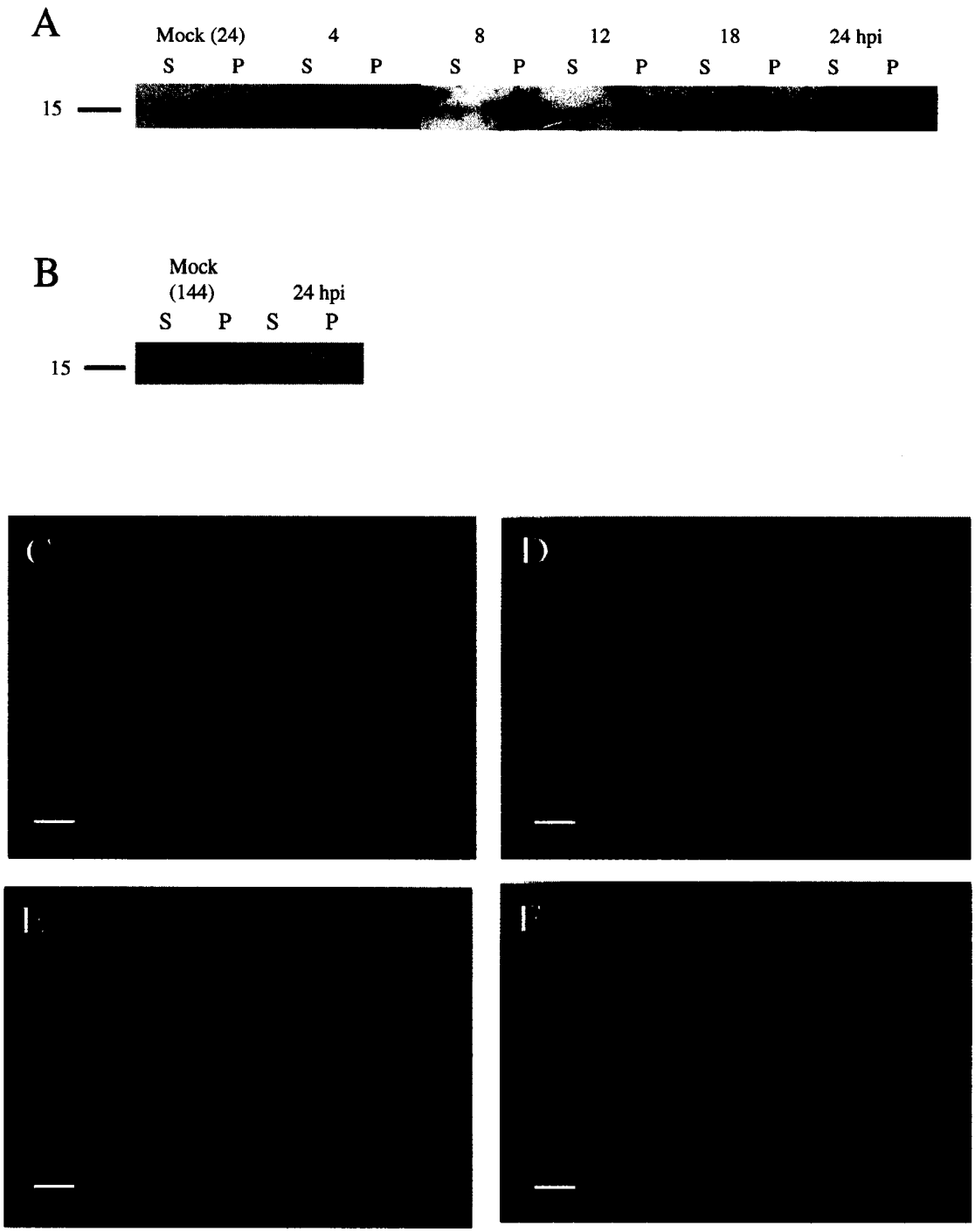

Figure 27

Figure 28. Deletion of BAK and BAX appears not to lower influenza induced cell death, but may affect viral replication.

A. Bak, Bax and double knockout (DKO) MEF cells survived less well than WT cells as measured by trypan blue at 48 hpi. The basal level of cell death seen in mock-infected cells (control) was subtracted from the WSN infected cell death values and percent cell death was expressed as percent of control and represented cell death due only to the virus. Values are the means ±S.D. of 3 independent experiments.

B. Treatment of MEF cells with 100 μg/ml of CHX showed that wild type (WT) cells were extremely sensitive while the knockout cells were protected against cell death as indicated by trypan blue analysis. The basal level of cell death seen in mock treated cells (control) was subtracted from the CHX treated cell death values and percent cell death was expressed as percent of control and represented cell death due only to CHX. Values are the means ±S.D. of 3 independent experiments.

C. The plaque assay showed that all MEF's produced high titers except for the BAK -/- cells, which produced a lower viral titer (MOI 0.001).

A

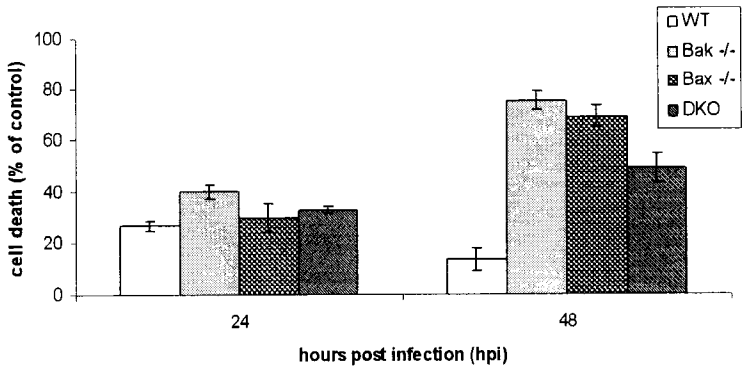

B

C

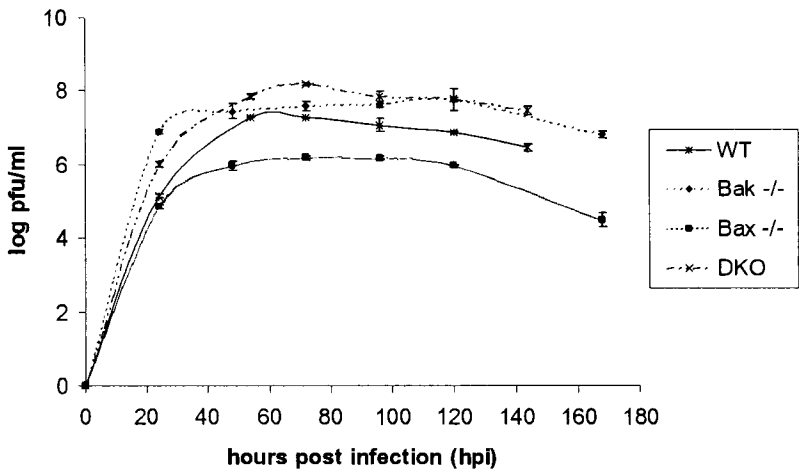

Figure 28

Figure 29. BIM not needed for influenza induced cell death in adult BIM knockout lung mouse cells.

To assess the need for BIM during influenza induced cell death we used primary adult BIM knockout (BIM -/-) lung cells harvested from BIM -/- mice.

A. Trypan blue analysis showed over 80% of infected BIM -/- lung cells were dying by 72 hpi.

B. Nuclear fragmentation levels were very low in infected BIM -/- lung cells as measured by Hoechst staining.

C. Light microscopy showed that by 24 hpi infected BIM -/- lung cells showed extreme signs of cytopathology by the virus as compared to mock-infected cells. Images at 100X, Bar = 50 μm

A

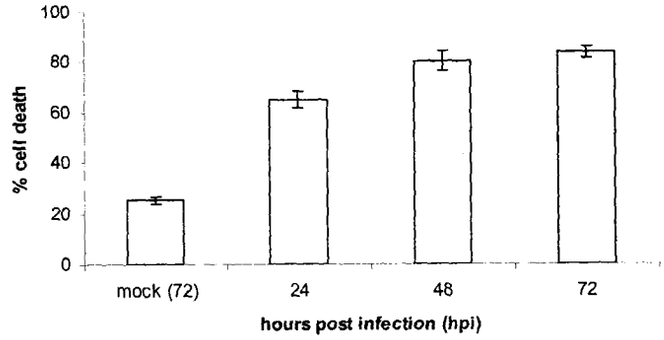

B

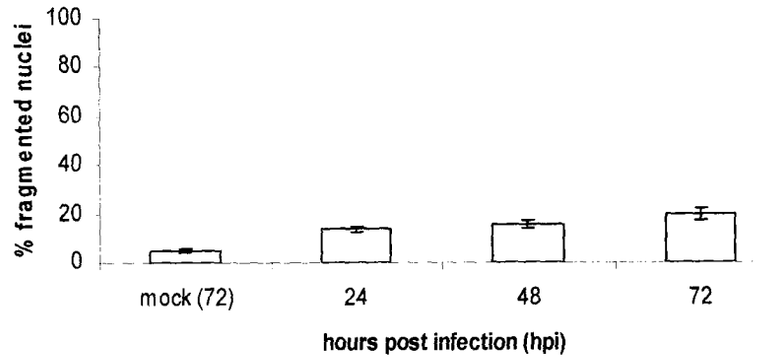

C

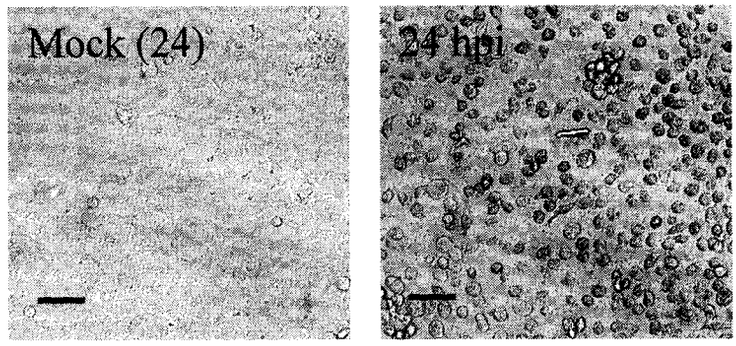

Figure 29

Figure 30. BIM not needed for influenza induced cell death in adult BIM knockout kidney mouse cells.

To assess the need for BIM during influenza induced cell death we used primary adult BIM knockout (BIM -/-) kidney cells harvested from BIM -/- mice.

A. Trypan blue analysis showed that over 90% of infected BIM -/- kidney cells were dying by 48 hpi.

B. Light microscopy showed that by 48 hpi infected BIM -/- kidney cells showed extreme signs of cytopathology by the virus as compared to mock-infected cells and appeared necrotic. Images at 100X, Bar = 50 μm

A

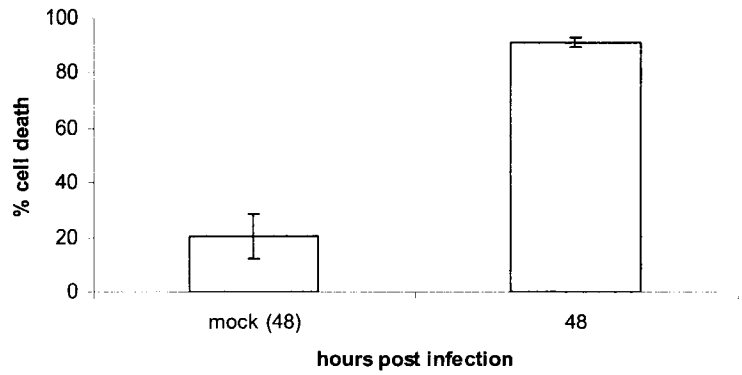

B

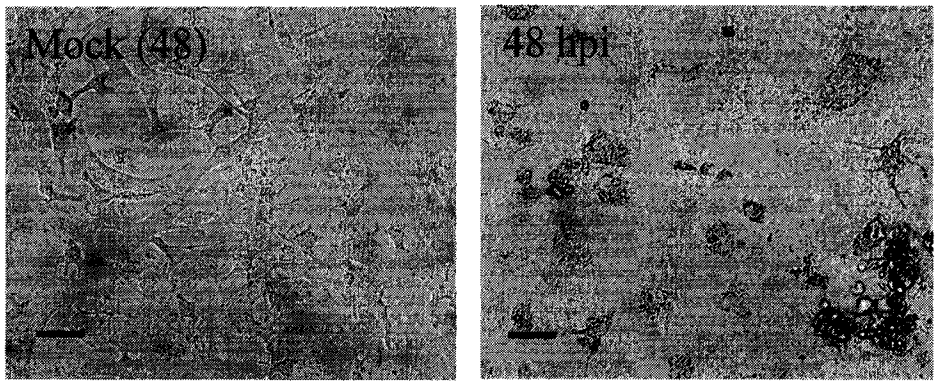

Figure 30

Figure 31. BCL-2 has limited protection against WSN induced cell death.

To evaluate whether BCL-2 can protect cells against influenza induced cell death we used PC-12 cells that constitutively overexpress BCL-2 (PC-12 bcl2 +) and compared the level of cell death to the parental cell line (PC-12 WT) when infected with WSN.

PC-12 bcl2 + cells had a lower percentage of trypan blue positive cells ($P < 0.038$) than PC-12 WT cells, but the difference although barely significant was not large indicating limited protection against WSN induced cell death. The basal level of cell death seen in mock-infected cells was subtracted from the WSN infected cell death values and percent cell death was expressed as percent of control and represented cell death due only to the virus. Values are the means ±S.D. of 3 independent experiments.

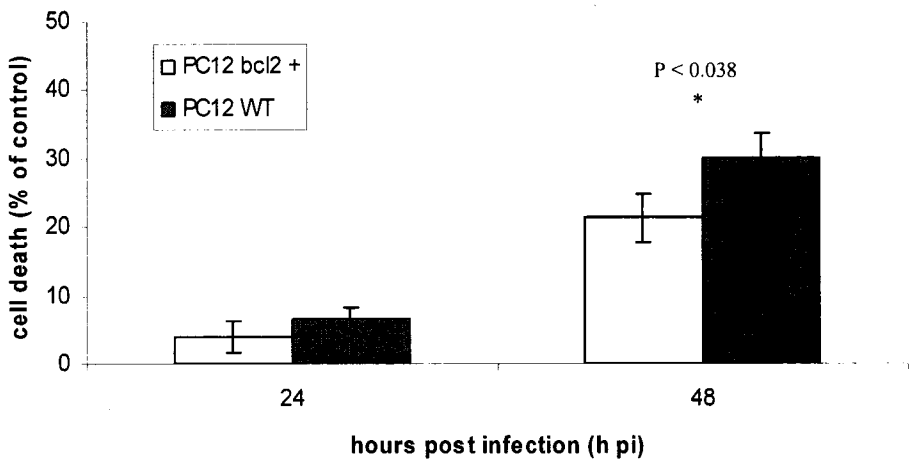

Figure 31

Figure 32. Deletion of p53 confers increased resistance to UV light induced cell death.

To determine whether deletion of p53 protects cells against cell death, we used two cells lines. C8 were (p53 +/+) while A9 were (p53 -/-). The cells were exposed to 254 nm of UV light (50 J/m^2) for various lengths of time and cell viability was assayed 24 h later by trypan blue.

The majority of C8 cells were trypan blue positive when exposed to UV light for as little as seconds while A9 cells had significantly lowered levels of cell death, which increased only with exposure time.

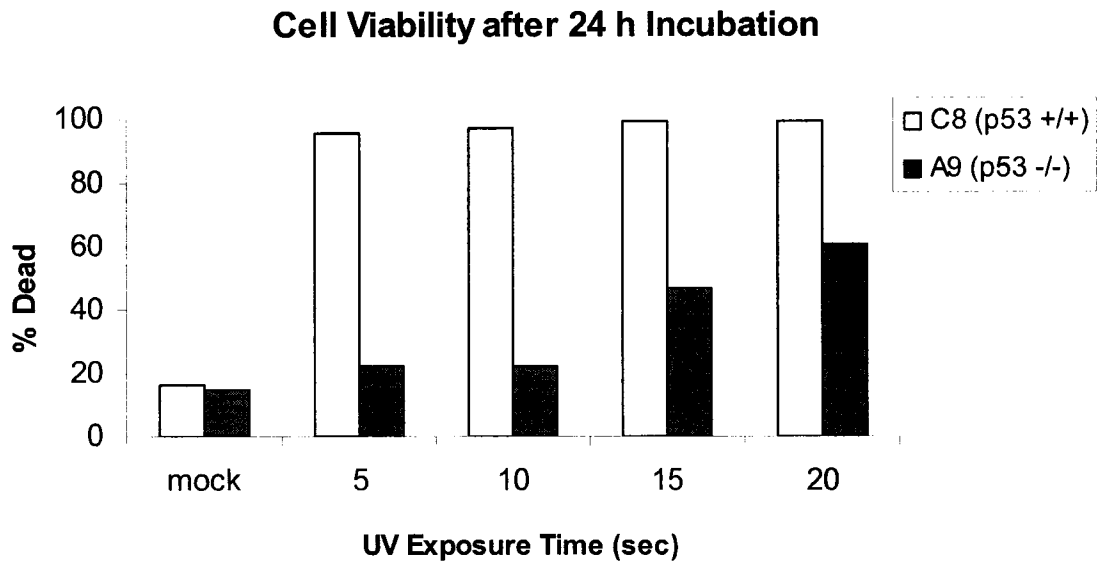

Figure 32

Figure 33. P53 not essential for influenza induced cell death.

A. Trypan blue analysis showed that at 24 h pi infected C8 (p53 +/+) cells had close to 100% cell death as compared to infected A9 (p53 -/-) cells, of which 83% were dead, indicating that p53 enhances influenza induced cell death but is not required for the induction and progression of cell death in infected cells.

B. Agarose gel electrophoresis of DNA samples of infected C8 and A9 cells showed intense DNA laddering at 24h pi. The slight laddering appearing in mock-infected A9 cells was due to serum withdrawal cell death because A9 cells have a high rate of division and require ample levels of growth factors for survival. Lanes 1 & 3, C8 cells and Lanes 2 & 4, A9 cells. Lanes 1 & 2, mock infected and Lanes 3 & 4, WSN infected.

A

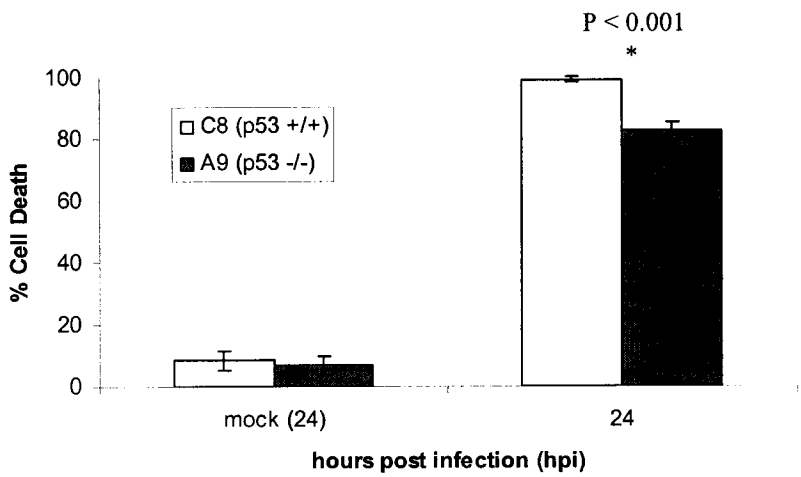

B

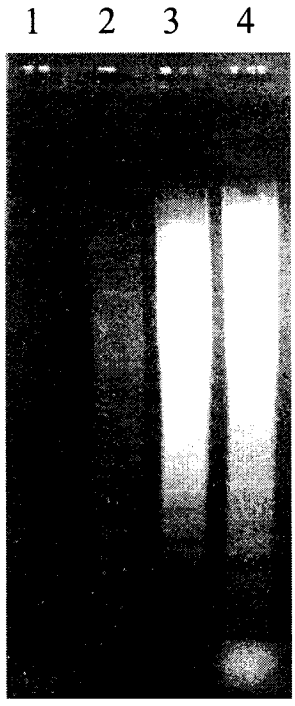

Figure 33

Figure 34. The cleavage of full length BID into a truncated version in WSN infected A549 cells.

The BH3 only domain protein called BID was analyzed by Western blotting and showed that by 96 hpi full length BID (25 kDa) was cleaved into a truncated version that was 15 kDa in WSN infected A549 cells.

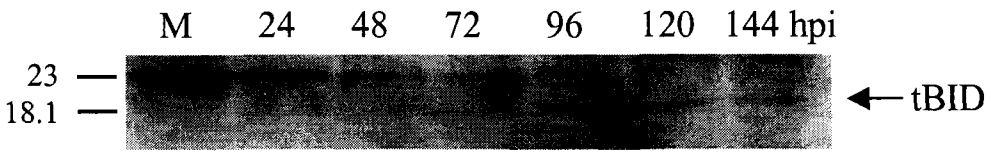

Figure 34

Figure 35. Caspase – 8 is activated during influenza induced cell death in MDCK and A549 cells.

The 44 kDa procaspase-8 protein is cleaved to form two peptides, which are 25 and 17 kDa, as detected by western blot analysis.

A. Western blot of MDCK cells indicting that during WSN infection cleavage and activation of caspase – 8 started at 12 hpi and continued to increase by 24 hpi as evident by the formation of the p25 and p17 fragments. Mock infected cells (M) only showed the procaspase – 8 form. Arrows show p25 and p17 fragments.

B. Infected A549 cells showed that cleavage of procaspase – 8 to the p25 fragment occurred at 24 hpi while mock infected (M) samples had caspase – 8 in its procaspase form. Arrow shows p25 fragment.

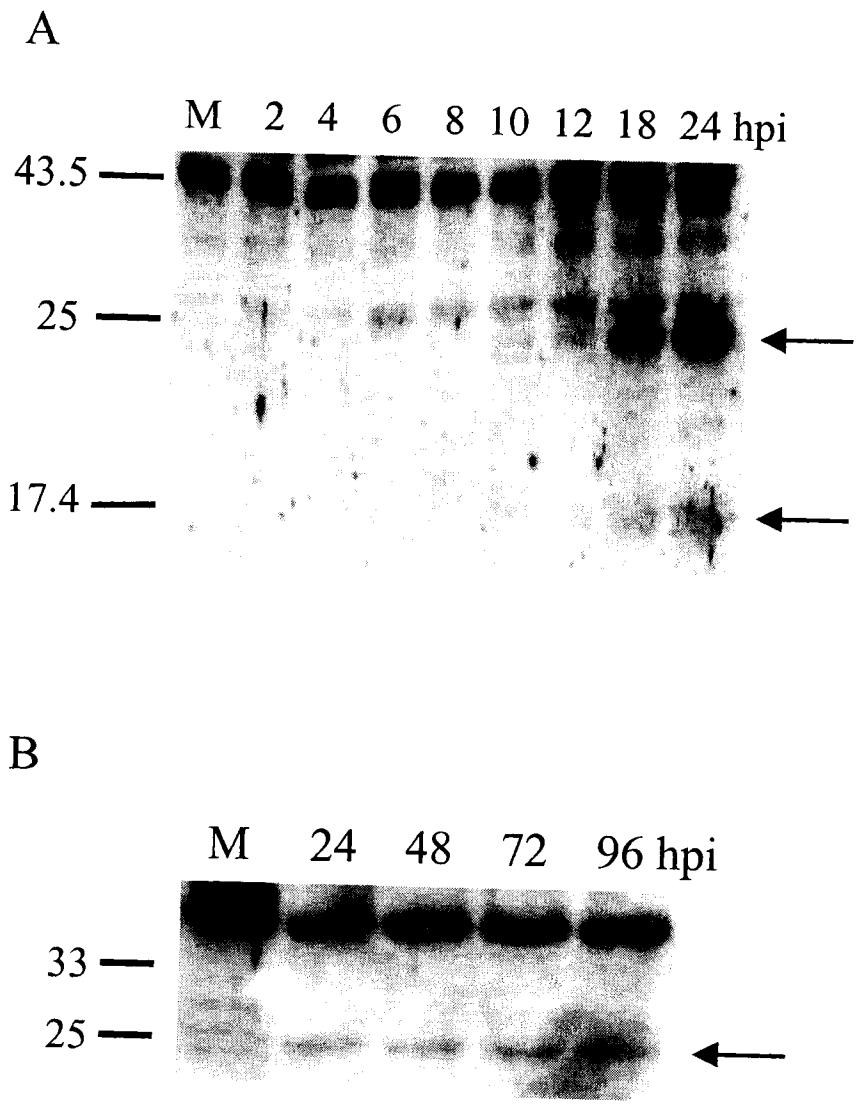

Figure 35

Figure 36. Caspase – 3 is activated during influenza induced cell death in MDCK and A549 cells.

Western blot analysis for caspase – 3 activation showed that both MDCK and A549 cells had active caspase – 3 at 24 hpi as evident by the formation of the p17 fragment. Mock-infected (M) samples did not show the procaspase form since the antibody was specific for only active caspase – 3.

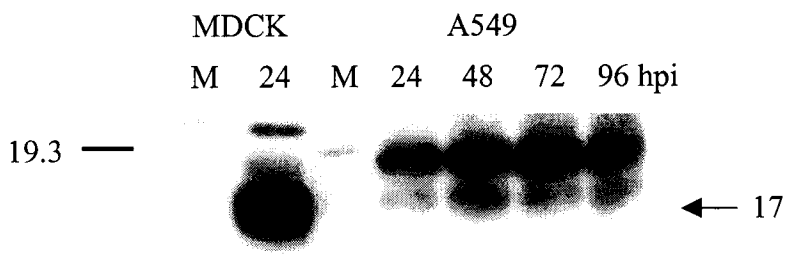

Figure 36

Figure 37. *In situ* detection of caspase – 3 activation in infected MDCK cells.

Immunocytochemistry with an antibody directed only toward active caspase-3 showed extensive activation of caspase – 3 at 24 and 48 hpi (S) in MDCK cells that were detached and floating. In contrast, adherent cells at 24 and 48 hpi (A) had few cells that fluoresced green indicating active caspase – 3. Arrows show cells with active caspase – 3 (green signal). Hoechst analysis showed the number of cells present and the extent of nuclear fragmentation. Arrows show corresponding cells with active caspase – 3. 400X, Bar = 12.5 μm

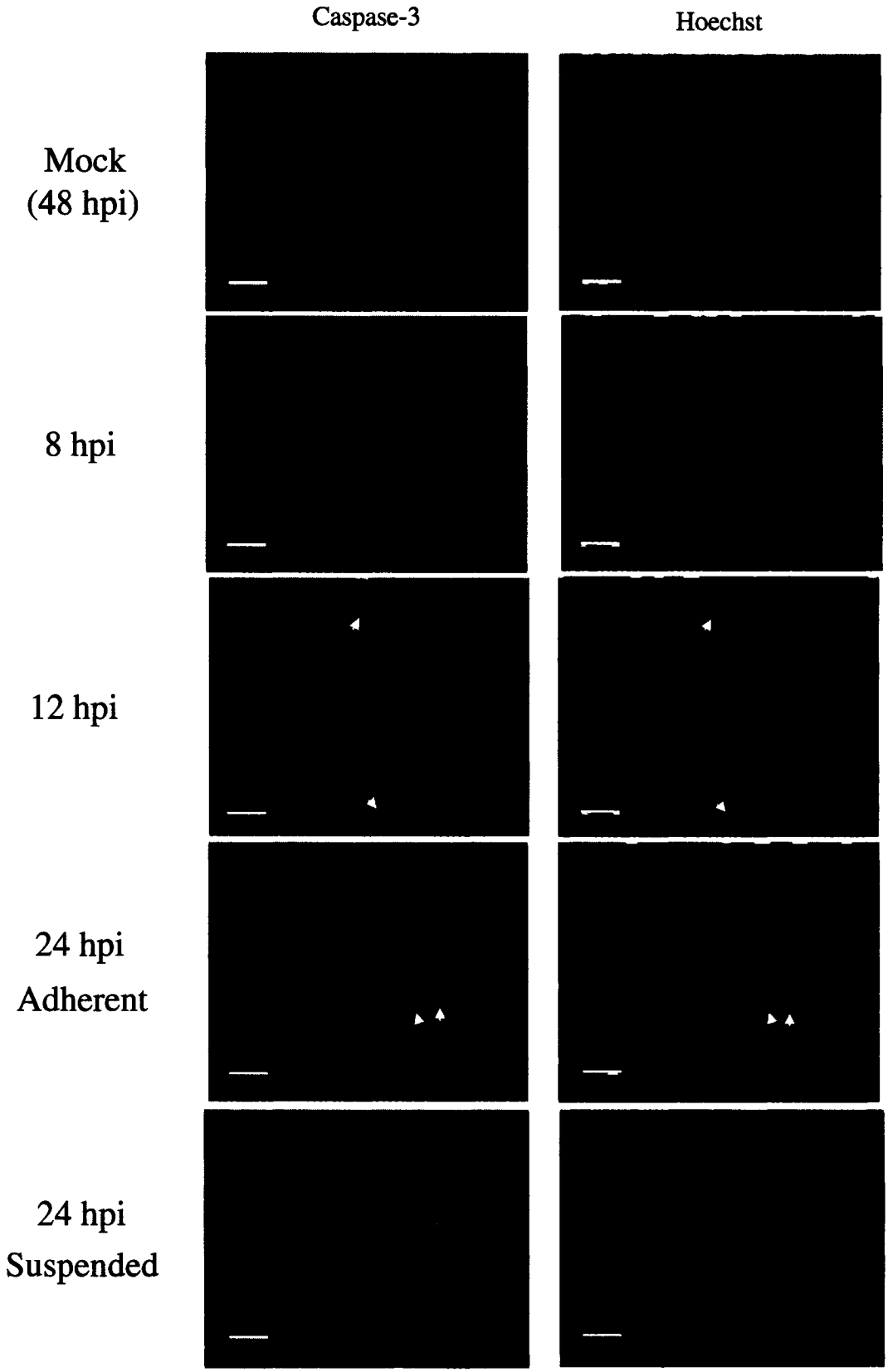

Figure 37

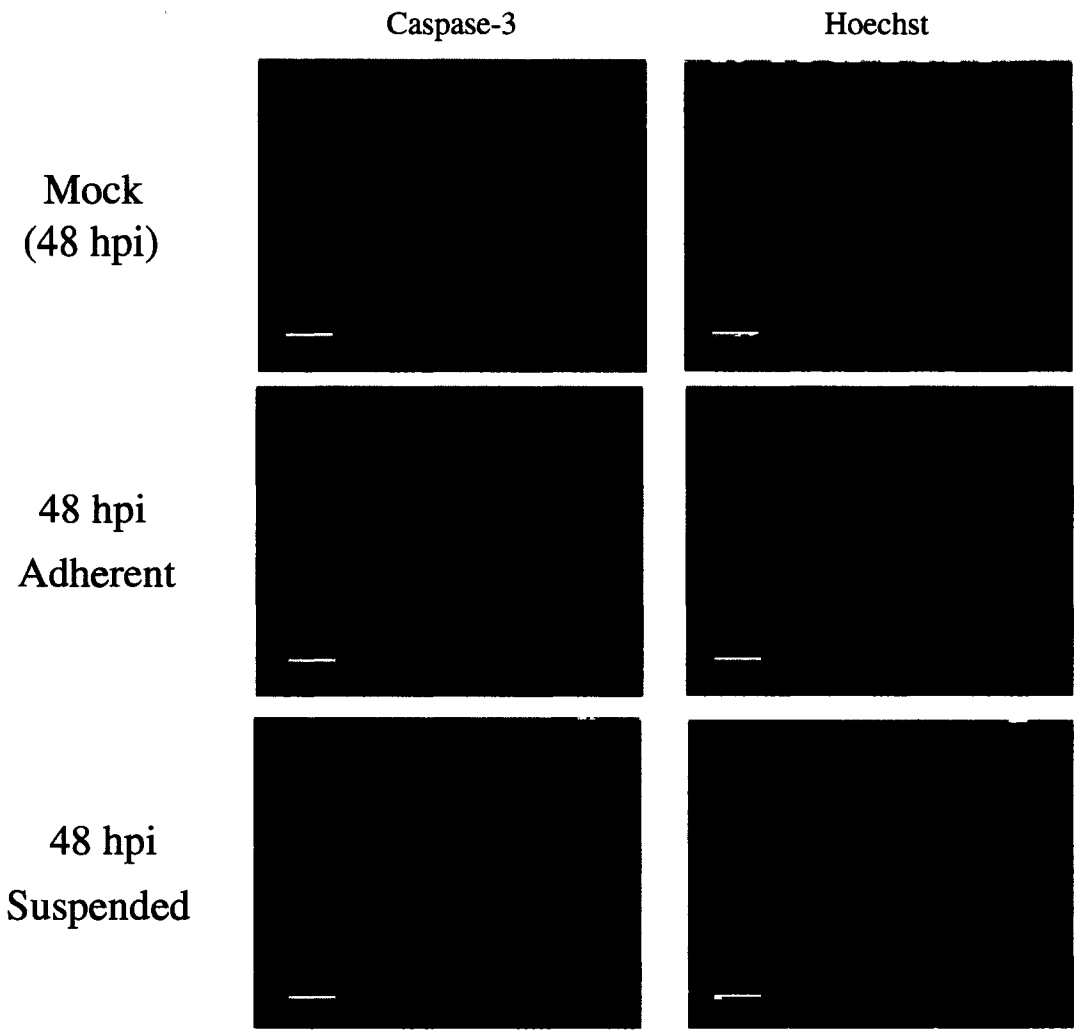

Figure 37, cont'd

Figure 38. *In situ* detection of caspase – 3 activation in infected A549 cells.

Immunocytochemistry on infected A549 cells with an antibody specific for active caspase – 3 showed widespread activation of the caspase in A549 cells as early as 72 hpi with some cells displaying intense green fluorescence indicating active caspase – 3. The majority of infected A549 cells at 144 hpi were positive for the activation of caspase – 3 since most fluoresced green. However at 24 h pi a limited number of cells had active caspase – 3. Arrows show cells with active caspase – 3 (green signal). *In situ* Hoechst staining showed the number of cells and extent of nuclear condensation and fragmentation. Arrows show corresponding cells with active caspase – 3. 400X, Bar = 12.5 μm

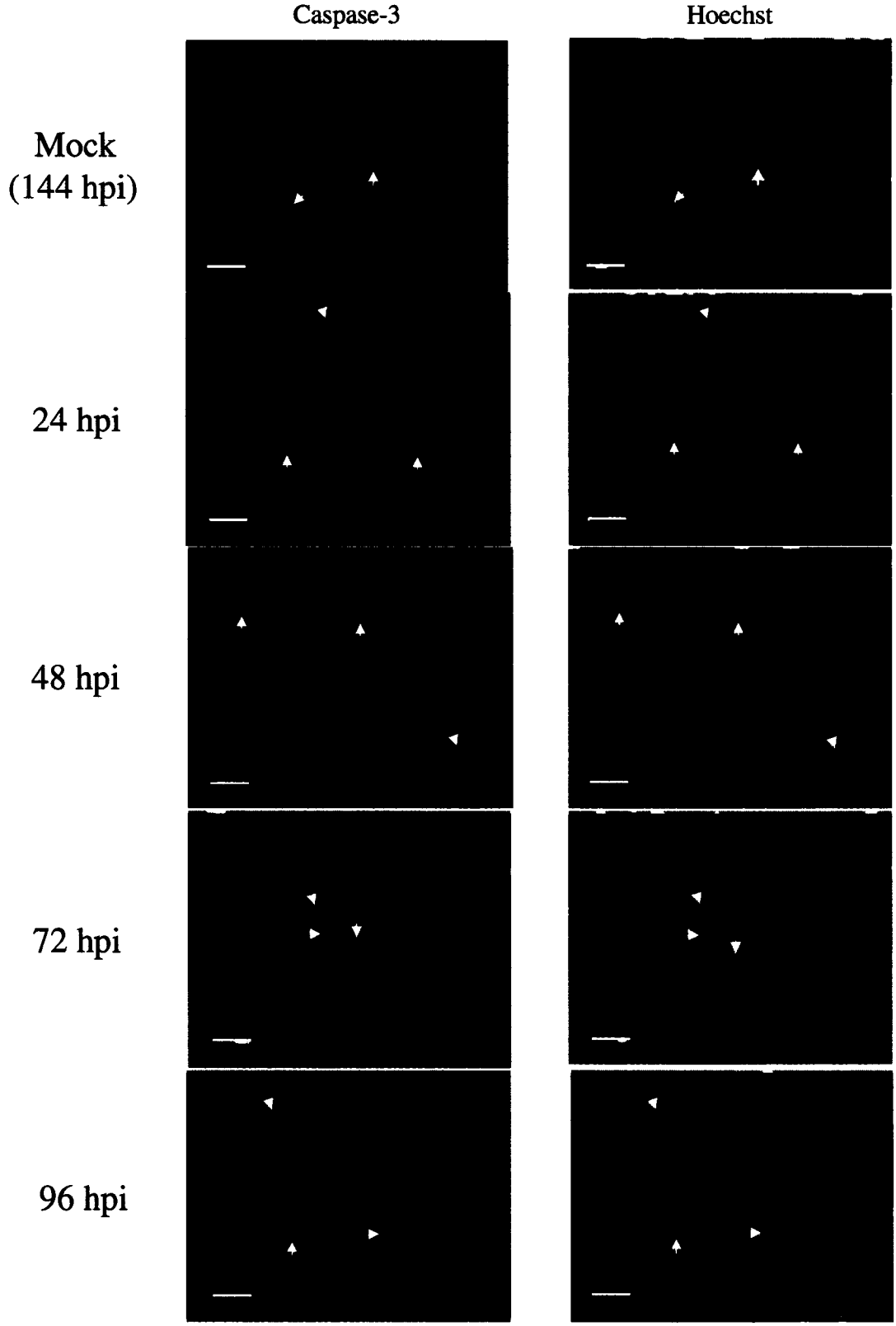

Figure 38

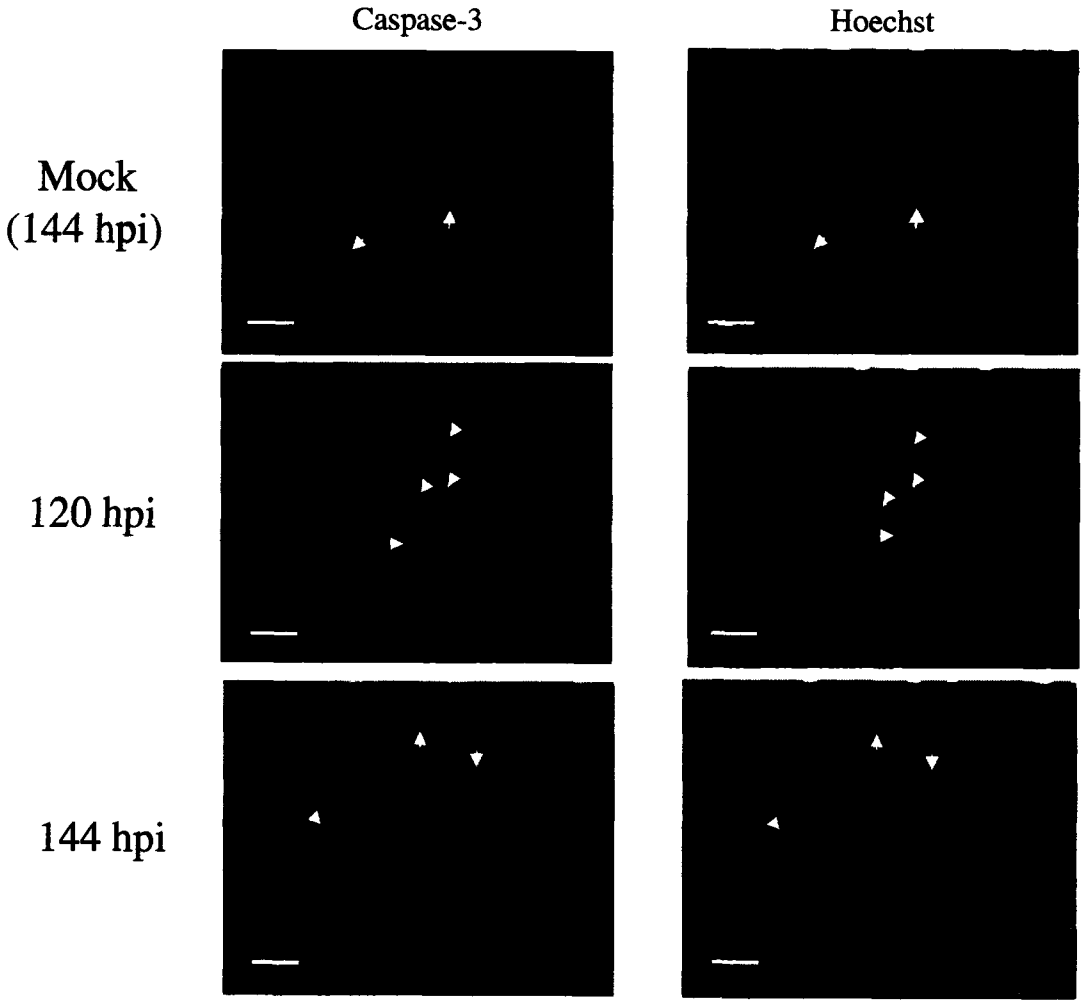

Figure 38, cont'd

Figure 39. PARP cleavage occurs in infected MDCK and A549 cells indicating active caspase – 3.

A. Protein lysates from infected MDCK cells run on 8% SDS-PAGE gels showed complete cleavage of the 116 kDa PARP protein to an 85 kDa fragment at 10 hpi.

B. A549 cells only had a minor amount of PARP cleaved even at 144 hpi. PARP was slightly cleaved in mock-infected cells (M).

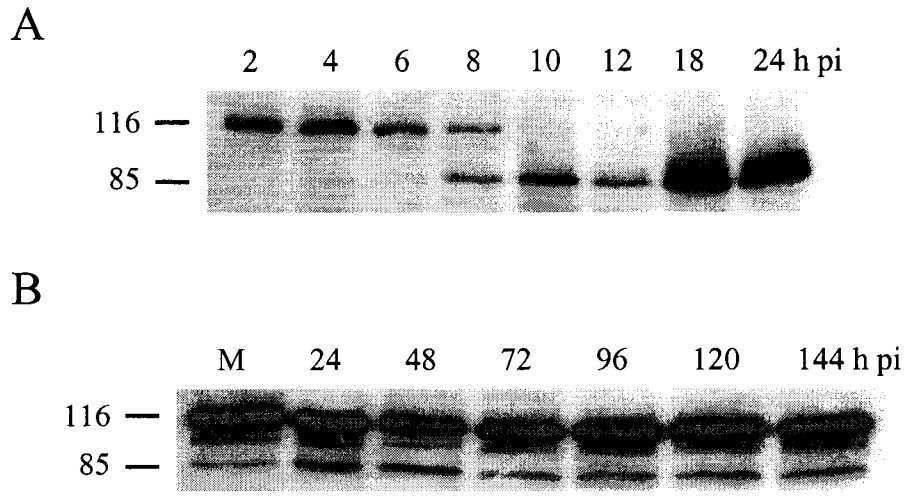

Figure 39

Figure 40. Inhibition of caspases in WSN infected MDCK cells does not inhibit influenza induced cell death.

A. Infected MDCK cells treated with 50 μM of zVAD-fmk at 48 hpi showed a reduced level of cell death as compared to the untreated infected cells as measured by trypan blue ($P<0.004$). Values are the means ±S.D. of 3 independent experiments.

B. The pan-caspase inhibitor completely blocked nuclear fragmentation in WSN infected MDCK cells. Values are the means ±S.D. of 3 independent experiments.

C, D & E. Light microscopy showed that mock-infected cells were healthy and attached (C) whereas at 48 hpi zVAD-fmk treated infected MDCK cells (D) were mostly attached to the plate. In comparison untreated infected cells (E) were completely detached and floating. C, 400X; D, 400X; E, 400X, Bar = 12.5 μm

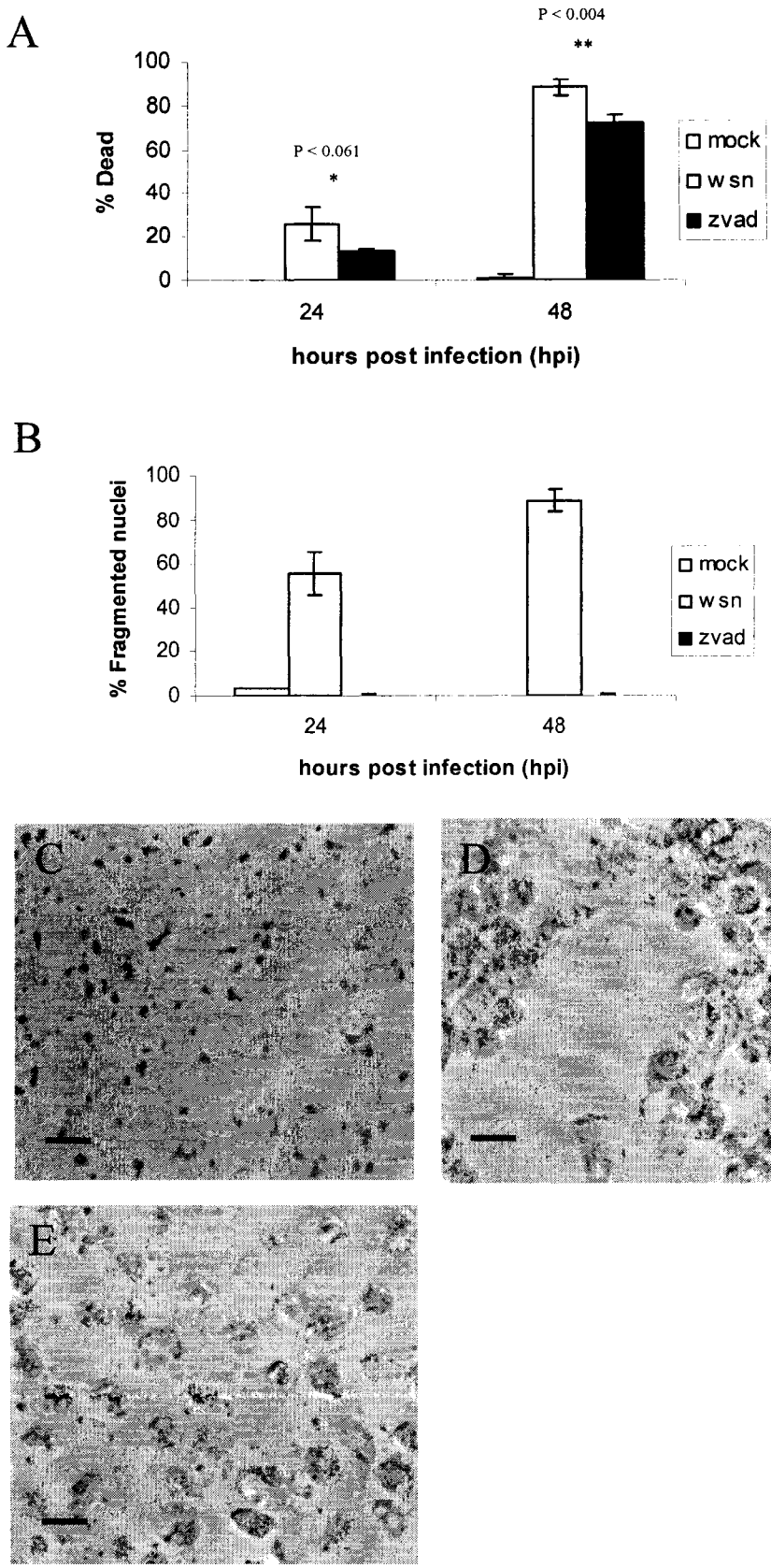

Figure 40

Figure 41. Caspase – 8 and – 3 in WSN infected MDCK cells are inhibited by the broad-spectrum inhibitor, zVAD-fmk.

A. Infected MDCK cells treated with 50 μM of zVAD-fmk for 24 h showed inhibition of caspase – 8 activation by the lack of the p25 cleavage fragment as seen by Western blot analysis. Untreated cells showed the formation of the p25 cleavage fragment (arrow).

B. Immunocytochemistry indicated that activation of caspase – 3 did not occur in zVAD-fmk treated infected MDCK cells at 24 hpi. Untreated cells fluoresced green indicating active caspase – 3. Hoechst staining shows the number of cells and extent of nuclear condensation and fragmentation. B, 400X, Bar = 12.5 μm

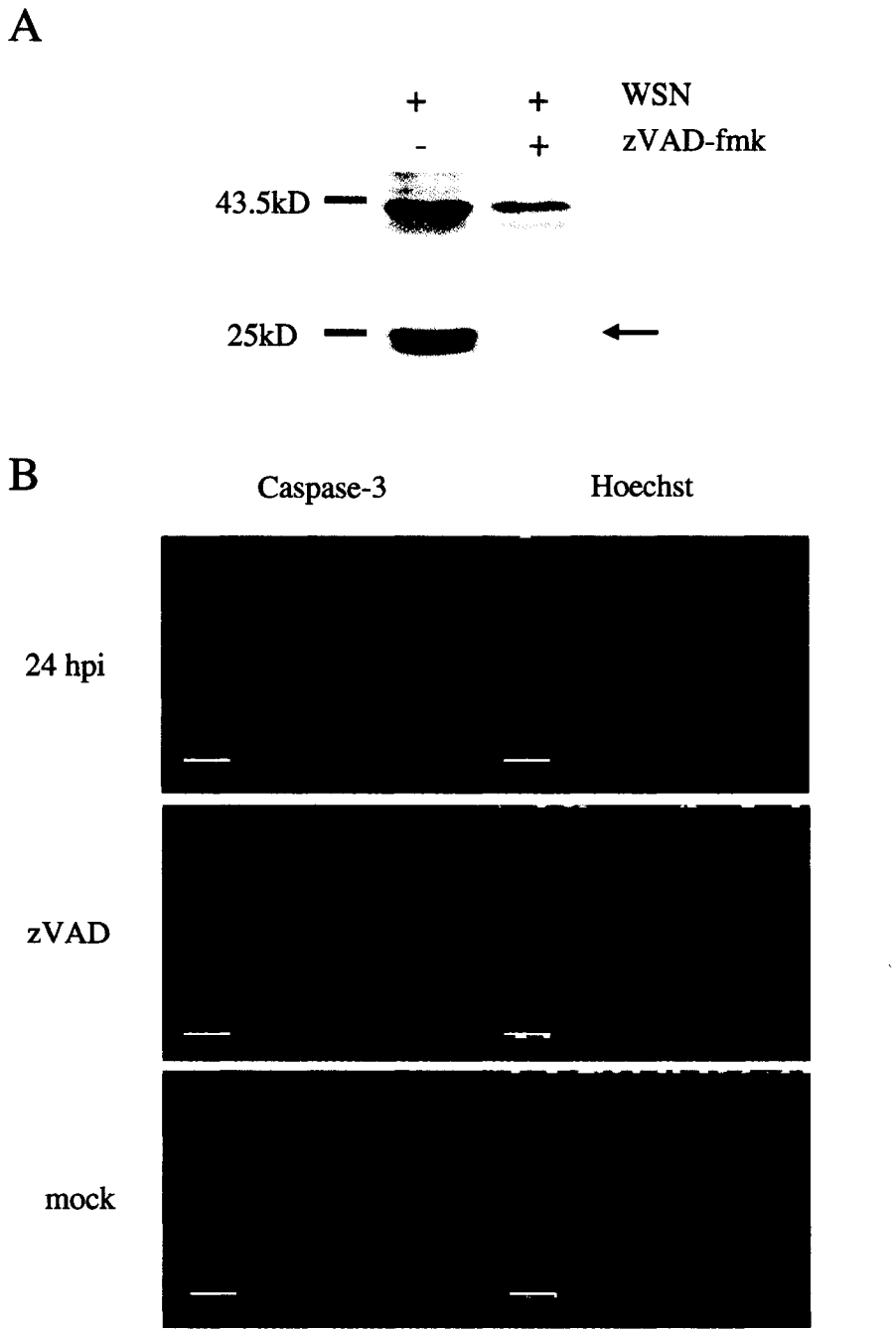

Figure 41

Figure 42. zVAD treatment does not alter influenza A virus replication in MDCK cells.

Plaque assay results indicated that zVAD-fmk treated cells replicated with an equivalent titer of virus as compared to untreated infected cells.

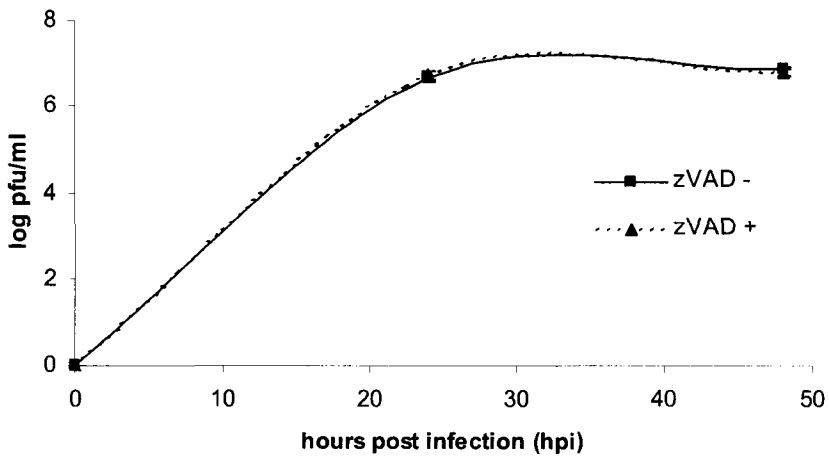

Figure 42

Figure 43. Inhibition of caspases in WSN infected A549 cells does not inhibit influenza induced cell death.

A. Infected A549 cells treated with 50 μM of zVAD-fmk at 48 ($P<0.0004$) and 96 hpi ($P<0.0021$) showed significantly reduced levels of cell death as compared to the untreated infected cells as measured by trypan blue indicating a protection against viral induced cell death. However by 144 hpi treated and untreated cells had similar levels of dead cells.

B, C & D. Light microscopy showed that at 96 hpi untreated infected A549 cells (B) showed signs of cytopathology such as loss of cell numbers and cell shrinkage while zVAD treated A549 cells showed less changes in cell structure (C). Mock-infected cells appeared confluent and healthy at 96 hpi (D). B, 400X; C, 400X; D, 400X, Bar = 12.5 μm

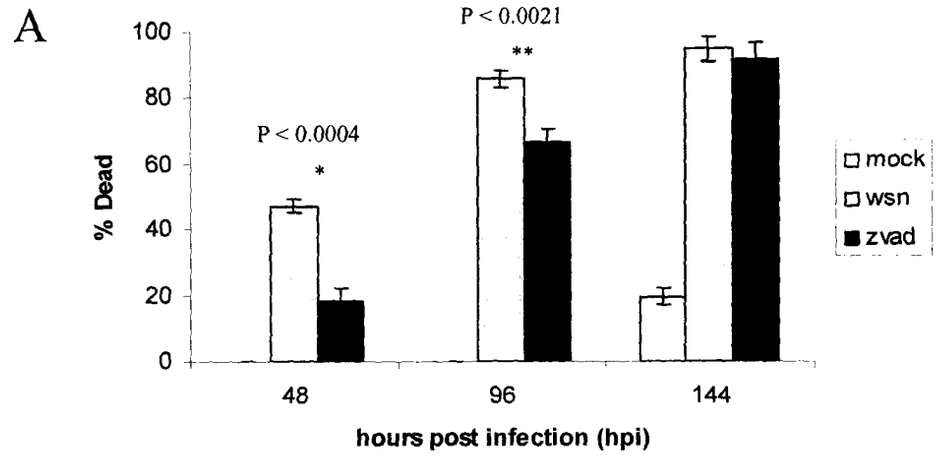

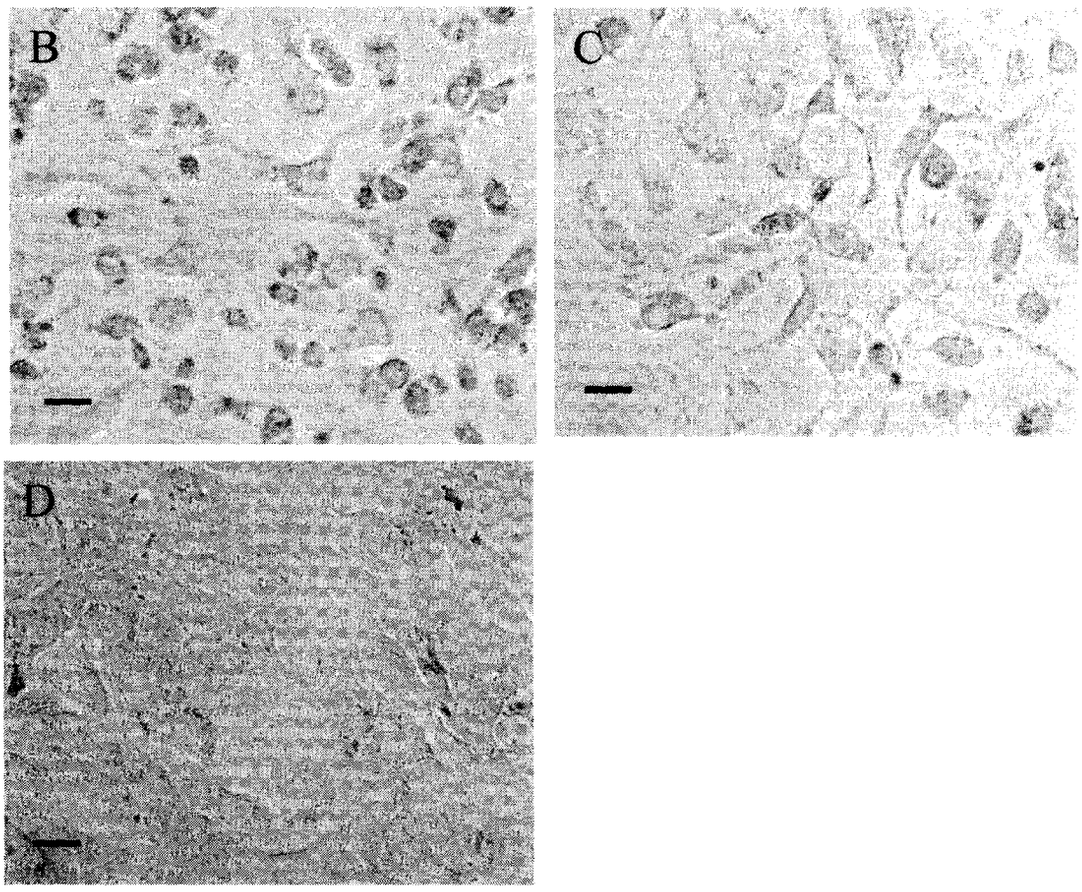

Figure 43

Figure 44. Fluorescence microscopy data confirmed that zVAD completely inhibited caspase – 3 activation in A549 cells.

Immunocytochemistry showed that caspase – 3 activation was completely blocked by zVAD-fmk in infected A549 cells by the lack of green fluorescence at 144 h pi. A549 cells not treated with zVAD-fmk showed many cells that fluoresced green indicating active caspase – 3. Hoechst staining showed the number of cells and extent of nuclear condensation. 400X, Bar = 12.5 μm

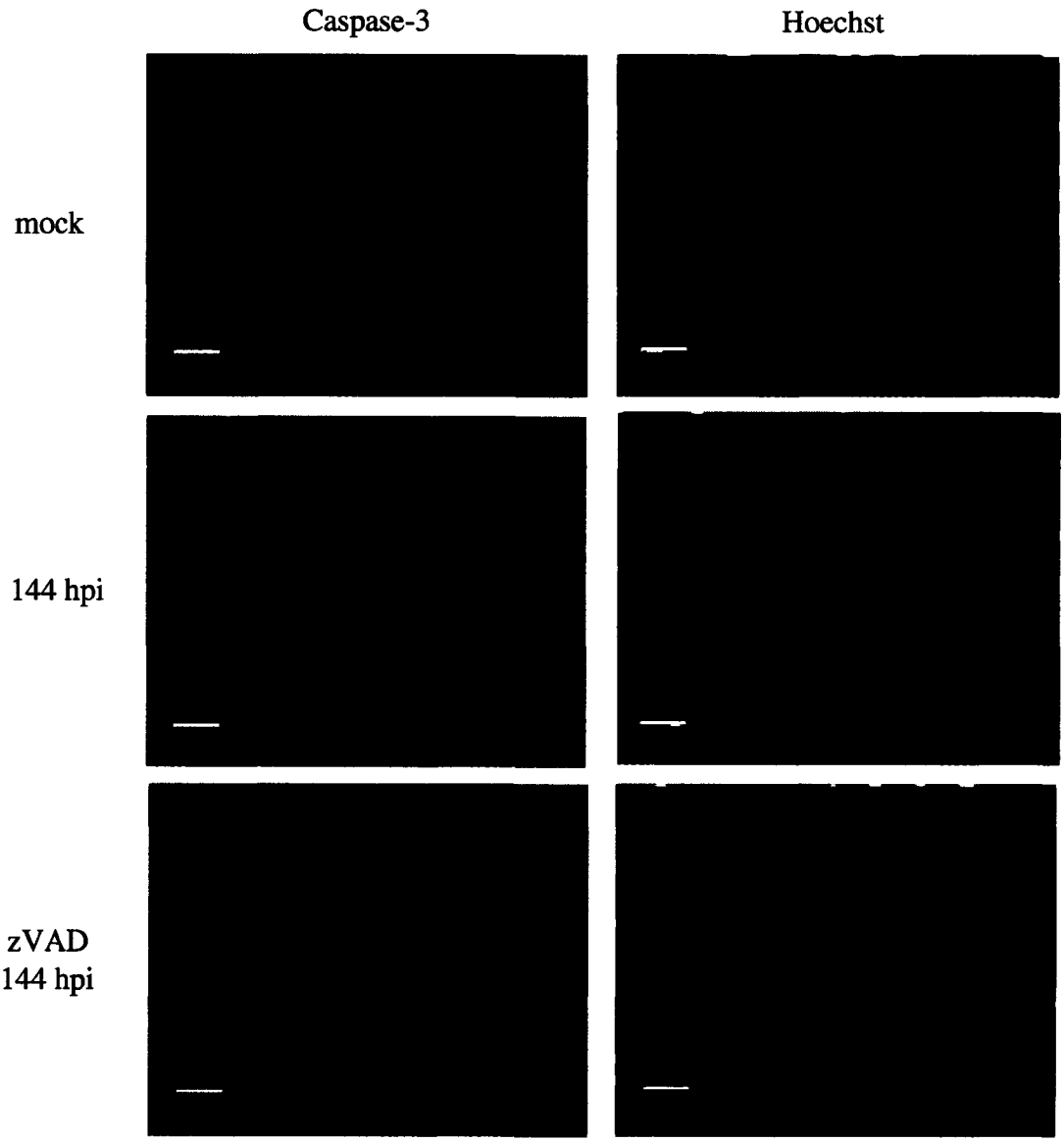

Figure 44

Figure 45. Caspase-3 not required for influenza induced cell death or replication of WSN.

MCF-7 cells, which are devoid of caspase-3 activity, were used to assess whether caspase-3 is needed for viral induced cell death.

A. The plaque assay (MOI 0.0001) showed that WSN could replicate in MCF-7 cells with levels of viral production similar to A549 cells (see Figure 12, pg 178).

B. Cell death determined by trypan blue showed an increase in the percentage of dead cells through time in infected MCF-7 cells (line). Nuclear fragmentation by Hoechst staining (bar) showed lower levels as compared to the viability data during the infection. Values are the means ±S.D. of 3 independent experiments.

C& D. Light microscopy showed that mock-infected MCF-7 cells (C) were attached and large in size while WSN infected MCF-7 cells (D) were round in appearance and floating by 48 hpi. C, 400X; D, 400X, Bar = 12.5 μm

A

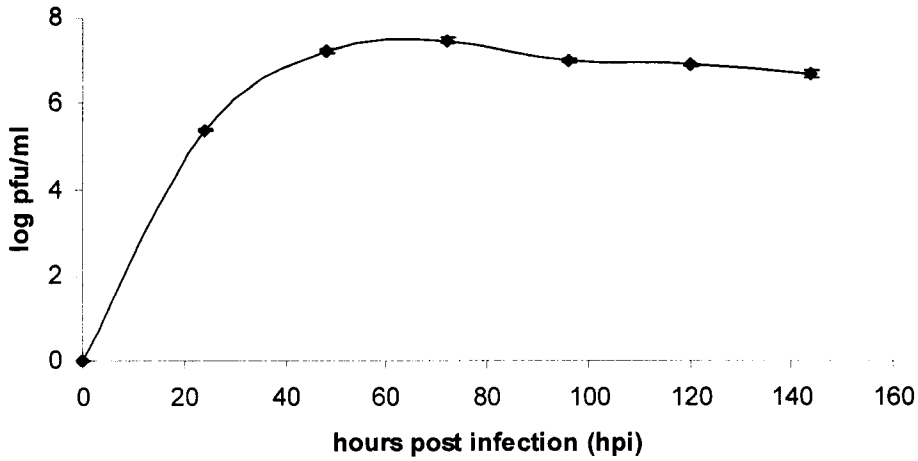

B

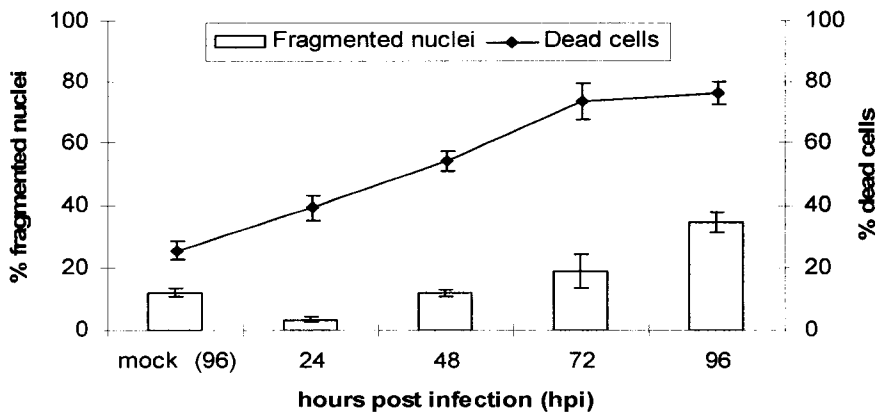

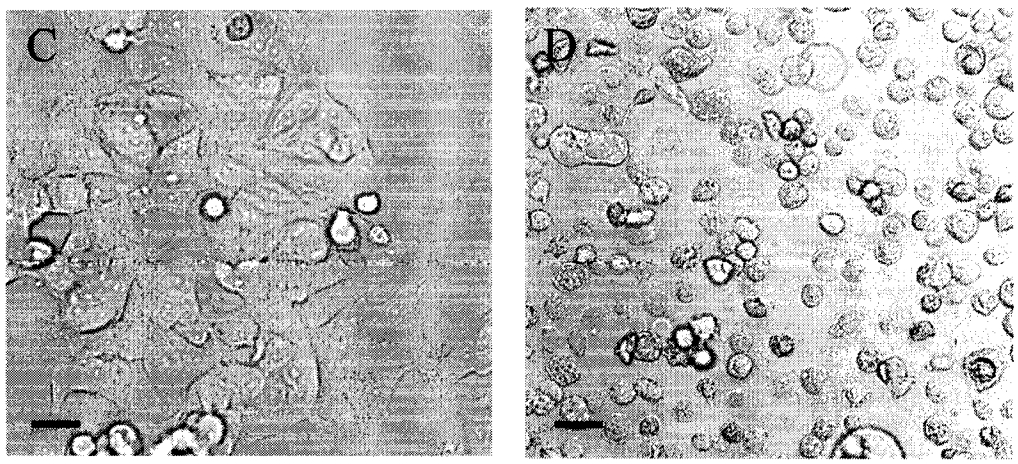

Figure 45

Figure 46. Changes within the lysosome reduced the function of acid phosphatase in WSN infected MDCK cells.

A. Quantitative analysis of activity as measured by the decomposition of p-nitrophenol phosphate showed a decline in the OD reading (410 nm) of infected MDCK cells by 48 hpi as compared to mock-infected cells. Values were normalized to total protein and the means ±S.D. of 3 independent experiments.

B & C. *In situ* analysis of acid phosphatase activity showed that mock infected (B) and WSN infected (C) MDCK cells had similar color intensities at 24 hpi, correlating with the quantitative data. B, 400X; C, 400X, Bar = 12.5 μm

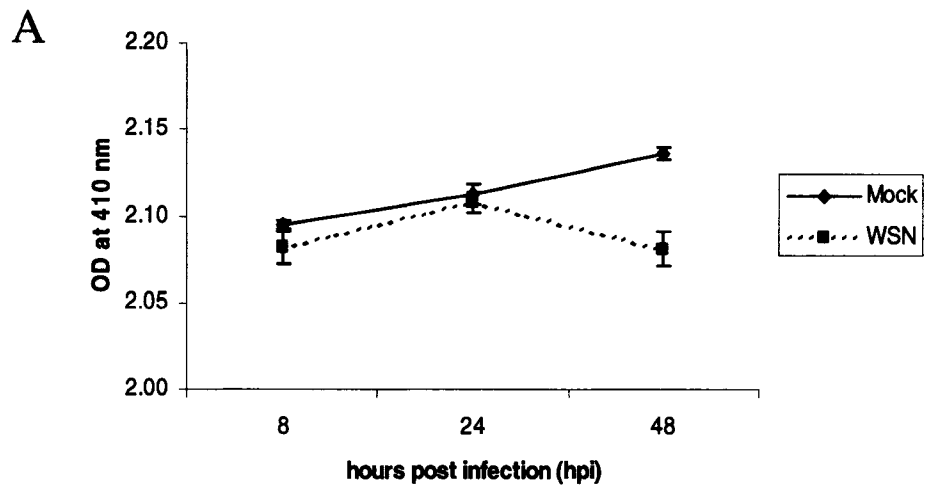

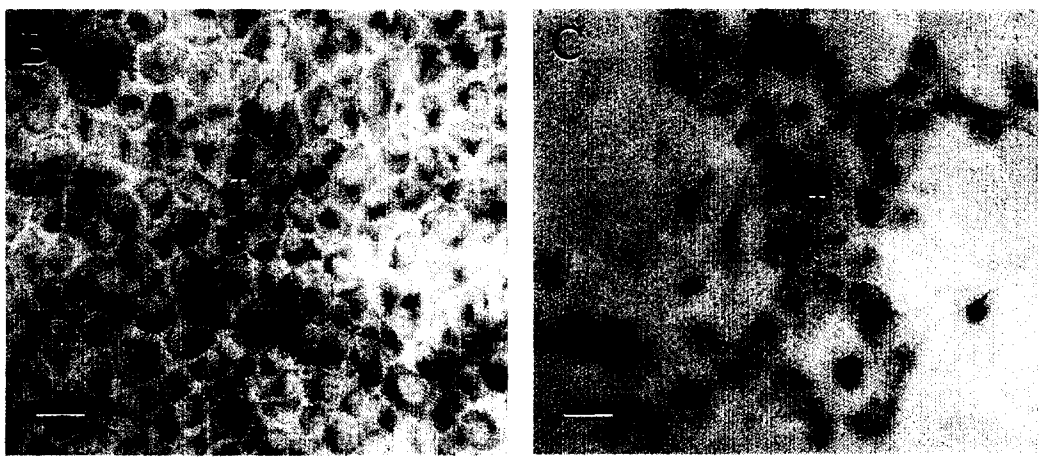

Figure 46

Figure 47. Changes within the lysosome reduced the function of acid phosphatase in WSN infected A549 cells.

A. Quantitative analysis of acid phosphatase activity in infected A549 cells showed a decline in OD signal (410 nm) starting at 24 hpi and a continued decline through 120 hpi as compared to mock-infected cells. Values are the means ±S.D. of 3 independent experiments.

B & C. *In situ* analysis of acid phosphatase activity showed that mock-infected (B) cells had a higher color intensity, which meant the presence of active acid phosphatase than WSN infected (C) A549 cells at 72 hpi, correlating with the quantitative data. B, 400X; C, 400X, Bar = 12.5 μm

A

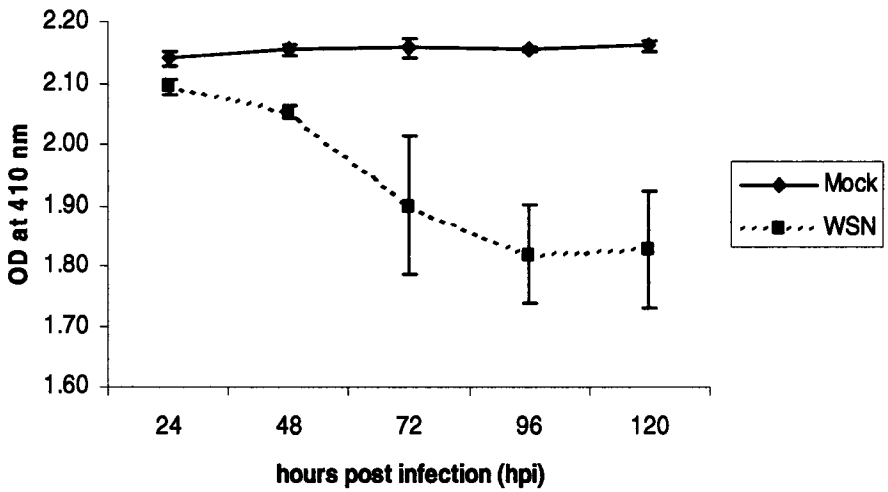

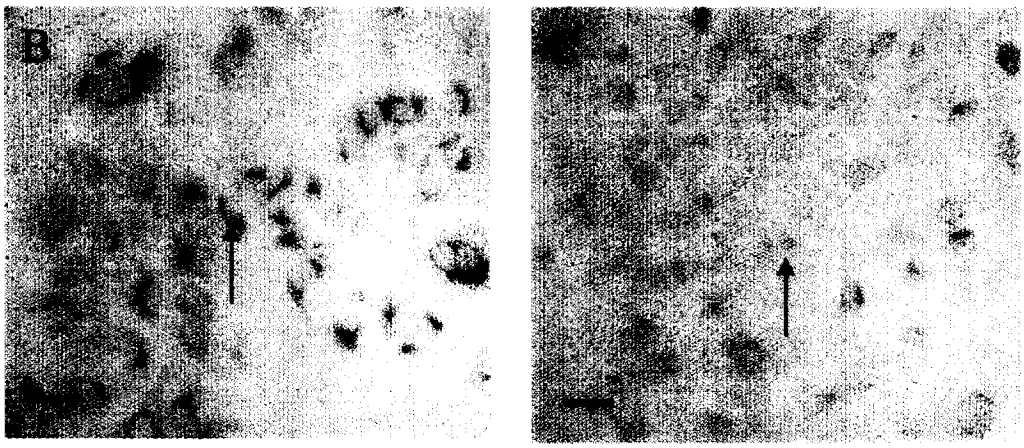

Figure 47

Figure 48. Cathepsins appear to affect influenza induced cell death and replication.

The need for cathepsins during influenza induced cell death was analyzed by using MEF's with key cathepsin knockouts.

A. At 24 hpi cathepsin B knockout (cat B -/-) cells had equivalent numbers of dead cells as measured by trypan blue as wild type (WT) cells. Cathepsin D knockout (cat D -/-) ($P< 0.027$) and cathepsin L knockout (cat L -/-) ($P< 0.003$) cells had a 20 –30 % difference in the percentage of dead cells than WT cells, respectively. However by 48 hpi cat B -/-, cat D -/-, and cat L -/- cells had similar levels of death but were lower than the WT cells. Values are the means ±S.D. of 3 independent experiments.

B. Viral titer analysis (MOI 0.001) showed that cat B -/-, cat D -/-, and cat L -/- cells had higher titers than WT cells and by 144 hpi the titers were similar to the levels seen in MDCK cells.

A

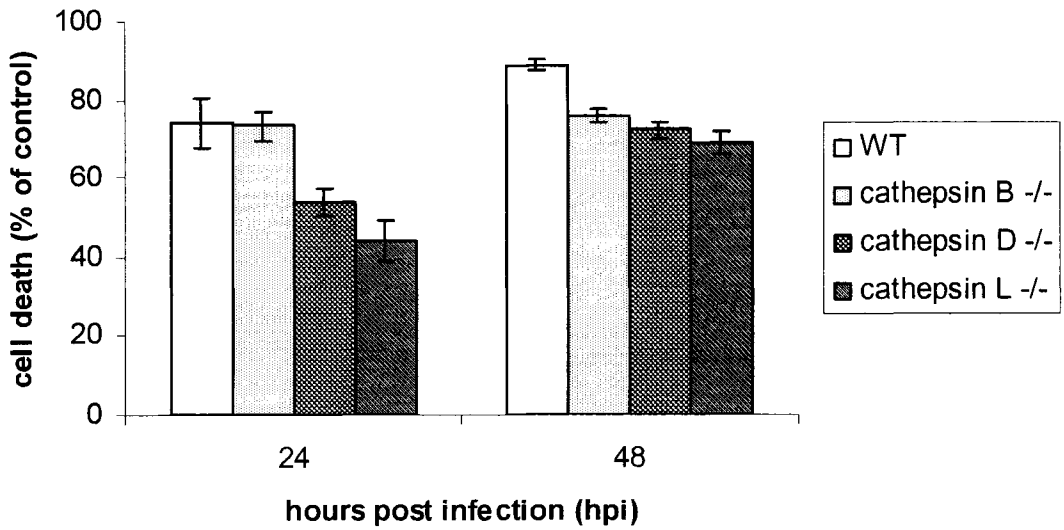

B

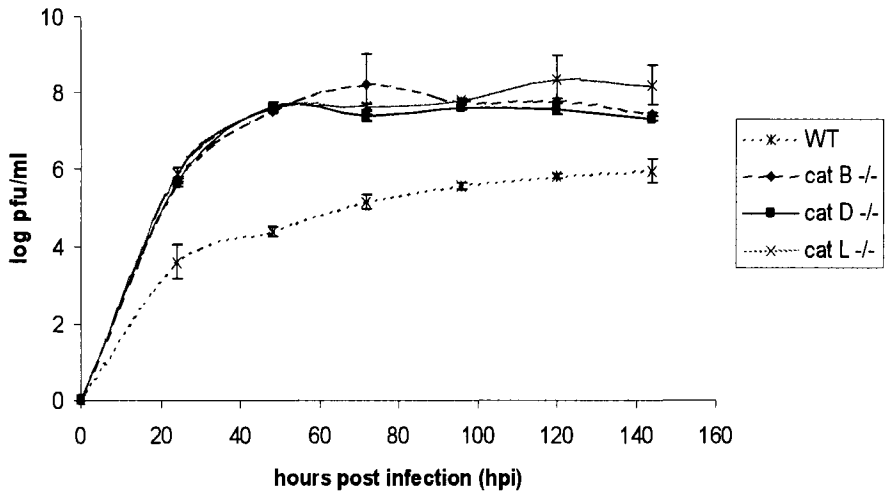

Figure 48

References

Abraham G. The effect of ultraviolet radiation on the primary transcription of influenza virus messenger RNAs. Virology. 1979 Aug;97(1):177-82.

Abraham MC and Shaham S. Death without caspases, caspases without death TRENDS in Cell Biology 2004 Vol.14 No.4 April.

Adamec E, Mohan PS, Cataldo AM, Vonsattel JP, Nixon RA. Up-regulation of the lysosomal system in experimental models of neuronal injury: implications for Alzheimer's disease. Neuroscience. 2000;100(3):663-75.

Adams JM, Cory S.Life-or-death decisions by the Bcl-2 protein family. Trends Biochem Sci. 2001 Jan;26(1):61-6.

Alberts, Bruce; Johnson, Alexander; Lewis, Julian; Raff, Martin; Roberts, Keith; Walter, Peter. Molecular Biology of the Cell. 4th ed. New York: Garland Publishing; 2002.

Allen H, McCauley J, Waterfield M, Gething MJ. Influenza virus RNA segment 7 has the coding capacity for two polypeptides. Virology 1980;107:548-551.

Alonso-Caplen FV, Nemeroff ME, Qiu Y, Krug RM. Nucleocytoplasmic transport: the influenza virus NS_1 protein regulates the transport of spliced NS2 mRNA and its precursor NS_1 mRNA. Genes Dev 1992;6:255-267.

Ameisen JC, Capron A. Cell dysfunction and depletion in AIDS: the programmed cell death hypothesis. Immunol Today. 1991 Apr;12(4):102-5.

Antonsson B, Martinou JC. The Bcl-2 protein family. Exp Cell Res. 2000 Apr 10;256(1):50-7.

Arnoult D, Gaume B, Karbowski M, Sharpe JC, Cecconi F, Youle RJ. Mitochondrial release of AIF and EndoG requires caspase activation downstream of Bax/Bak-mediated permeabilization. EMBO J. 2003 Sep 1;22(17):4385-99.

Aubert M, Blaho JA. Modulation of apoptosis during herpes simplex virus infection in human cells. Microbes Infect. 2001 Aug;3(10):859-66.

Balachandran S, Roberts PC, Kipperman T, Bhalla KN, Compans RW, Archer DR, Barber GN. Alpha/beta interferons potentiate virus-induced apoptosis through activation of the FADD/Caspase-8 death signaling pathway. J Virol. 2000 Feb;74(3):1513-23.

Bancroft CT, Parslow TG. Evidence for segment-nonspecific packaging of the influenza a virus genome. J Virol. 2002 Jul;76(14):7133-9.

Barisic K, Petrik J, Rumora L. Biochemistry of apoptotic cell death. Acta Pharm. 2003 Sep;53(3):151-64.

Beaulaton J and Lockshin RA. Ultrastructural study of the normal degeneration of the intersegmental muscles of Anthereae polyphemus and Manduca sexta (Insecta, Lepidoptera) with particular reference of cellular autophagy. J. Morphol. 1977 154: 39 – 57.

Bidere N, Lorenzo HK, Carmona S, Laforge M, Harper F, Dumont C, Senik A. Cathepsin D triggers Bax activation, resulting in selective apoptosis-inducing factor (AIF) relocation in T lymphocytes entering the early commitment phase to apoptosis. J Biol Chem. 2003 Aug 15;278(33):31401-11.

Bobak D, Moorman J, Guanzon A, Gilmer L, Hahn C. Inactivation of the small GTPase Rho disrupts cellular attachment and induces adhesion-dependent and adhesion-independent apoptosis. Oncogene. 1997 Oct;15(18):2179-89.

Boise LH, Collins CM. Salmonella-induced cell death: apoptosis, necrosis or programmed cell death? Trends Microbiol. 2001 Feb;9(2):64-7.

Borresen-Dale AL. Genetic profiling of breast cancer: from molecular portraits to clinical utility. Int J Biol Markers. 2003 Jan-Mar;18(1):54-6.

Bossy-Wetzel E, Schwarzenbacher R, Lipton SA. Molecular pathways to neurodegeneration. Nat Med. 2004 Jul;10 Suppl:S2-9.

Braithwaite AW, Russell IA. Induction of cell death by adenoviruses. Apoptosis. 2001 Oct;6(5):359-70.

Browne SE, Beal MF. The energetics of Huntington's disease. Neurochem Res. 2004 Mar;29(3):531-46.

Bucher E, Hemmes H, de Haan P, Goldbach R, Prins M. The influenza A virus NS1 protein binds small interfering RNAs and suppresses RNA silencing in plants. J Gen Virol. 2004 Apr;85(Pt 4):983-91.

Bursch W. The autophagosomal-lysosomal compartment in programmed cell death. Cell Death Differ. 2001 Jun;8(6):569-81.

Bursch W, Ellinger A, Gerner C, Frohwein U, Schulte-Hermann R. Programmed cell death (PCD). Apoptosis, autophagic PCD, or others? Ann N Y Acad Sci. 2000;926:1-12.

Bursch W, Kienzl H, Ellinger A, Török L, Walker R, Sikorska M, Pandey S and Schulte-Hermann R. Active cell death induced by antiestrogens tamoxifen and ICI 164384 in human mammary carcinoma cells (MCF-7) in culture: the role of autophagy. Carcinogenesis 1996 17: 1595 – 1607.

Campion D, Flaman JM, Brice A, Hannequin D, Dubois B, Martin C, Moreau V, Charbonnier F, Didierjean O, Tardieu S, et al. Mutations of the presenilin I gene in families with early-onset Alzheimer's disease. Hum Mol Genet. 1995 Dec; 4(12):2373-7.

Castedo M, Perfettini JL, Andreau K, Roumier T, Piacentini M, Kroemer G. Mitochondrial apoptosis induced by the HIV-1 envelope. Ann N Y Acad Sci. 2003 Dec;1010:19-28.

Chang HY, Yang X. Proteases for cell suicide: functions and regulation of caspases. Microbiol Mol Biol Rev. 2000 Dec;64(4):821-46.

Chanturiya AN, Basanez G, Schubert U, Henklein P, Yewdell JW, Zimmerberg J. PB1-F2, an influenza A virus-encoded proapoptotic mitochondrial protein, creates variably sized pores in planar lipid membranes. J Virol. 2004 Jun;78(12):6304-12.

Chaves MM, Kallas EG. Cell cycle distribution of CD4+ lymphocytes in HIV-1-infected subjects. Cytometry. 2004 Nov;62B(1):46-51.

Chen M, Wang J. Initiator caspases in apoptosis signaling pathways. Apoptosis. 2002 Aug;7(4):313-9.

Chen W, Calvo PA, Malide D, Gibbs J, Schubert U, Bacik I, Basta S, O'Neill R, Schickli J, Palese P, Henklein P, Bennink JR, Yewdell JW. A novel influenza A virus mitochondrial protein that induces cell death. Nat Med. 2001 Dec;7(12):1306-12.

Cheng EH, Wei MC, Weiler S, Flavell RA, Mak TW, Lindsten T, Korsmeyer SJ. BCL-2, BCL-X(L) sequester BH3 domain-only molecules preventing BAX- and BAK-mediated mitochondrial apoptosis. Mol Cell. 2001 Sep;8(3):705-11.

Chi S, KitanakaC,Noguchi K, Mochizuki T,Nagashima Y, ShirouzuM, FujitaH, Yoshida M, Chen W, Asai A, Himeno M, Yokoyama S and Kuchino Y. Oncogenic Ras triggers cell suicide through the activation of a caspase independent cell death program in human cancer cells. Oncogene 1999 18: 2281 – 2290.

Chinnaiyan AM, Tepper CG, Seldin MF, O'Rourke K, Kischkel FC, Hellbardt S, Krammer PH, Peter ME, Dixit VM. FADD/MORT1 is a common mediator of CD95 (Fas/APO-1) and tumor necrosis factor receptor-induced apoptosis. J Biol Chem. 1996 Mar 1;271(9):4961-5.

Chisaka H, Morita E, Yaegashi N, Sugamura K. Parvovirus B19 and the pathogenesis of anaemia. Rev Med Virol. 2003 Nov-Dec;13(6):347-59.

Clarke PG. Developmental cell death: morphological diversity and multiple mechanisms. Anat Embryol (Berl). 1990;181(3):195-213.

Colman PM. Neuraminidase: Enzyme and Antigen. In: Krug RM, ed. New York: Plenum Press, 1989;175-218.

Compans RW and Choppin PW. Reproduction of myxoviruses. In: Fraenkel-Conrat H, Wagner RR, eds. *Comprehensive Virology*, vol IV. New York: Plenum, 1975; 179-252.

Concha NO, Abdel-Meguid SS.Controlling apoptosis by inhibition of caspases. Curr Med Chem. 2002 Mar;9(6):713-26.

Cornillon S, Foa C, Davoust J, Buonavista N, Gross JD and Golstein P (1994) Programmed cell death in *Dictyostelium*. J. Cell Sci. 10: 2691 - 2704

Creagh EM, Martin SJ. Caspases: cellular demolition experts. Biochem Soc Trans. 2001 Nov;29(Pt 6):696-702.

Cregan SP, Dawson VL, Slack RS. Role of AIF in caspase-dependent and caspase-independent cell death. Oncogene. 2004 Apr 12;23(16):2785-96.

Cuervo M. Autophagy: many paths to the same end. Mol Cell Biochem. 2004 Aug;263(1-2):55-72.

Cuervo M. Autophagy: in sickness and in health. Trends Cell Biol. 2004 Feb;14(2):70-7.

Daugas E, Susin SA, Zamzami N, Ferri KF, Irinopoulou T, Larochette N, Prevost MC, Leber B, Andrews D, Penninger J, Kroemer G. Mitochondrio-nuclear translocation of AIF in apoptosis and necrosis. FASEB J. 2000 Apr;14(5):729-39.

de la Luna S, Fortes P, Beloso A, Ortin J. 1995 *J Virol* 69(4):2427-33.

Debatin KM. Apoptosis pathways in cancer and cancer therapy. Cancer Immunol Immunother. 2004 Mar;53(3):153-9.

Degterev A, Boyce M, Yuan J. A decade of caspases. Oncogene. 2003 Nov 24;22(53):8543-67.

Delgadillo MO, Saenz P, Salvador B, Garcia JA, Simon-Mateo C. Human influenza virus NS1 protein enhances viral pathogenicity and acts as an RNA silencing suppressor in plants. J Gen Virol. 2004 Apr;85(Pt 4):993-9.

Dianzani U, Bensi T, Savarino A, Sametti S, Indelicato M, Mesturini R, Chiocchetti A. Role of FAS in HIV infection. Curr HIV Res. 2003 Oct;1(4):405-17.

Donelan NR, Basler CF, Garcia-Sastre A. A recombinant influenza A virus expressing an RNA-binding-defective NS1 protein induces high levels of beta interferon and is attenuated in mice. J Virol. 2003 Dec;77(24):13257-66.

Düßmann H, Rehm M, Kögel D and Prehn JHM. Outer mitochondrial membrane permeabilization during apoptosis triggers caspase-independent mitochondrial and caspase-dependent plasma membrane potential depolarization: a single-cell analysis Journal of Cell Science 2003:116, 525-536.

Duesberg P. Distinct subunits of the ribonucleoprotein of influenza virus. J Mol Biol 1969;42:485-499.

Duhaut SD, McCauley JW. Defective RNAs inhibit the assembly of influenza virus genome segments in a segment-specific manner.Virology. 1996 Feb 15;216(2):326-37.

Duvall E, Wyllie AH, Morris RG. Macrophage recognition of cells undergoing programmed cell death (apoptosis). Immunology. 1985 Oct;56(2):351-8.

Edinger AL, Thompson CB. Death by design: apoptosis, necrosis and autophagy. Curr Opin Cell Biol. 2004 Dec;16(6):663-9.

Eefting F, Rensing B, Wigman J, Pannekoek WJ, Liu WM, Cramer MJ, Lips DJ, Doevendans PA. Role of apoptosis in reperfusion injury. Cardiovasc Res. 2004 Feb 15;61(3):414-26.

Emeny JM, Morgan MJ. Susceptibility of various cells treated with interferon to the toxic effect of poly(I)-poly(C) treatment. J Gen Virol. 1979 Apr;43(1):253-5.

Emeny JM, Morgan MJ. Regulation of the interferon system: evidence that Vero cells have a genetic defect in interferon production. J Gen Virol. 1979 Apr;43(1):247-52.

Enoksson M, Robertson JD, Gogvadze V, Bu P, Kropotov A, Zhivotovsky B, Orrenius S. Caspase-2 permeabilizes the outer mitochondrial membrane and disrupts the binding of cytochrome c to anionic phospholipids. J Biol Chem. 2004 Nov 26;279(48):49575-8.

Fadok VA, Voelker DR, Campbell PA, Cohen JJ, Bratton DL, Henson PM. Exposure of phosphatidylserine on the surface of apoptotic lymphocytes triggers specific recognition and removal by macrophages. J Immunol. 1992 Apr 1;148(7):2207-16.

Falcon AM, Marion RM, Zurcher T, Gomez P, Portela A, Nieto A, Ortin J. Defective RNA replication and late gene expression in temperature-sensitive influenza viruses expressing deleted forms of the NS1 protein. J Virol. 2004 Apr;78(8):3880-8.

Ferko B, Stasakova J, Romanova J, Kittel C, Sereinig S, Katinger H, Egorov A. Immunogenicity and protection efficacy of replication-deficient influenza A viruses with altered NS1 genes. Virol. 2004 Dec;78(23):13037-45.

Ferri KF, Kroemer G. Organelle-specific initiation of cell death pathways. Nat Cell Biol. 2001 Nov;3(11):E255-63.

Fields, BN, Knipe, DM, Howley PM. Fields Virology. Lippincott-Raven Publishers. 1996, 3rd ed.

Foghsgaard L, Wissing D, Mauch D, Lademann U, Bastholm L, Boes M, Elling F, Leist M, Jaattela M. Cathepsin B acts as a dominant execution protease in tumor cell apoptosis induced by tumor necrosis factor. J Cell Biol. 2001 May 28;153(5):999-1010.

Fortes P, Beloso A, Ortin J. Influenza virus NS1 protein inhibits pre mRNA splicing and blocks mRNA nucleocytoplasmic transport. EMBO J 1994;13:704-712.

Fujimoto I, Takizawa T, Ohba Y, Nakanishi Y. Co-expression of Fas and Fas-ligand on the surface of influenza virus-infected cells. Cell Death Differ. 1998 May;5(5):426-31.

Galati D, Bocchino M, Paiardini M, Cervasi B, Silvestri G, Piedimonte G. Cell cycle dysregulation during HIV infection: perspectives of a target based therapy. Curr Drug Targets Immune Endocr Metabol Disord. 2002 Apr;2(1):53-61.

Garcia-Sastre A, Egorov A, Matassov D, Brandt S, Levy DE, Durbin JE, Palese P, Muster T. Influenza A virus lacking the NS1 gene replicates in interferon-deficient systems. Virology. 1998 Dec 20;252(2):324-30.

Gelb BD, Moissoglu K, Zhang J, Martignetti JA, Bromme D, Desnick RJ. Cathepsin K: isolation and characterization of the murine cDNA and genomic sequence, the homologue of the human pycnodysostosis gene. Biochem Mol Med. 1996 Dec;59(2):200-6.

Genini D, Sheeter D, Rought S, Zaunders JJ, Susin SA, Kroemer G, Richman DD, Carson DA, Corbeil J, Leoni LM. HIV induces lymphocyte apoptosis by a p53-initiated, mitochondrial-mediated mechanism. FASEB J. 2001 Jan;15(1):5-6.

Gercel-Taylor C, O'Connor SM, Lam GK, Taylor DD. Shed membrane fragment modulation of CD3-zeta during pregnancy: link with induction of apoptosis. J Reprod Immunol. 2002 Jul-Aug;56(1-2):29-44.

Gibbs JS, Malide D, Hornung F, Bennink JR, Yewdell JW. The influenza A virus PB1-F2 protein targets the inner mitochondrial membrane via a predicted basic amphipathic helix that disrupts mitochondrial function. J Virol. 2003 Jul;77(13):7214-24.

Gil J, Bermejo M, Alcami J. HIV and apoptosis: a complex interaction between cell death and virus survival. Prog Mol Subcell Biol. 2004;36:117-49.

Glassford A, Lee JE, Xu L, Giffard RG. Caspase inhibitors reduce the apoptotic but not necrotic component of kainate injury in primary murine cortical neuronal cultures. Neurol Res. 2002 Dec;24(8):796-800.

Golden JW, Linke J, Schmechel S, Thoemke K, Schiff LA. Addition of exogenous protease facilitates reovirus infection in many restrictive cells. J Virol. 2002 Aug;76(15):7430-43.

Goldenthal MJ, Marin-Garcia J. Mitochondrial signaling pathways: a receiver/integrator organelle. Mol Cell Biochem. 2004 Jul;262(1-2):1-16.

Goldstein S, Korczack LB. Status of mitochondria in living human fibroblasts during growth and senescence in vitro: use of the laser dye rhodamine 123. J Cell Biol. 1981 Nov;91(2 Pt 1):392-8.

Goodkin ML, Morton ER, Blaho JA. Herpes simplex virus infection and apoptosis. Int Rev Immunol. 2004 Jan-Apr;23(1-2):141-72.

Gottschalk A. The specific enzyme of influenza virus and Vibrio cholerae. Biochim Biophys Acta 1957;23:645-646.

Green DR, Evan GI. A matter of life and death. Cancer Cell. 2002 Feb;1(1):19-30.

Guicciardi ME, Deussing J, Miyoshi H, Bronk SF, Svingen PA, Peters C, Kaufmann SH, Gores GJ. Cathepsin B contributes to TNF-alpha-mediated hepatocyte apoptosis by promoting mitochondrial release of cytochrome c. J Clin Invest. 2000 Nov;106(9):1127-37.

Guillemard E, Jacquemot C, Aillet F, Schmitt N, Barre-Sinoussi F, Israel N. Human immunodeficiency virus 1 favors the persistence of infection by activating macrophages through TNF. Virology. 2004 Nov 24;329(2):371-80.
Ha HC, Snyder SH. Poly(ADP-ribose) polymerase is a mediator of necrotic cell death by ATP depletion. Proc Natl Acad Sci U S A. 1999 Nov 23;96(24):13978-82.

Hagemeier C, Caswell R, Hayhurst G, Sinclair J, Kouzarides T. Functional interaction between the HCMV IE2 transactivator and the retinoblastoma protein. EMBO J. 1994 Jun 15;13(12):2897-903.

Halaby R, Zakeri Z, Lockshin RA. Metabolic events during programmed cell death in insect labial glands. Biochem Cell Biol. 1994 Nov-Dec;72(11-12):597-601.

Hancock JT, Desikan R, Neill SJ. Does the redox status of cytochrome C act as a fail-safe mechanism in the regulation of programmed cell death? Free Radic Biol Med. 2001 Sep 1;31(5):697-703.

Hall D, Gu G, Garcia-Anoveras J, Gong L, Chalife M and Driscoll M. Neurology of degenerative cell death in *Caenorhabditis elegans*. J. Neurosci. 1997 17: 1033 – 1045.

Hart TC, Hart PS, Michalec MD, Zhang Y, Marazita ML,Cooper M, Yassin OM, Nusier M, Walker SJ. Med. Genet 2000. 37, 95-101.

Haupt S, Louria-Hayon I, Haupt Y.P53 licensed to kill? Operating the assassin. J Cell Biochem. 2003 Jan 1;88(1):76-82.

Hay AJ, Lomniczi B, Bellamy AR, Skehel JJ. Transcription of the influenza virus genome. Virology 1977;83:337-355.

Hay AJ. The action of adamantanamines against influenza A viruses: inhibition of the M_2 ion channel protein. Sem Virol 1992;3:21-30.

Hickman ES, Moroni MC, Helin K. The role of p53 and pRB in apoptosis and cancer. Curr Opin Genet Dev. 2002 Feb;12(1):60-6.

Hill MM, Adrain C, Martin SJ. Portrait of a killer: the mitochondrial apoptosome emerges from the shadows. Mol Interv. 2003 Feb;3(1):19-26.

Hinder F, Schmidt A, Gong JH, Bender A, Sprenger H, Nain M, Gemsa D. Influenza A virus infects macrophages and stimulates release of tumor necrosis factor-alpha. Pathobiology. 1991;59(4):227-31.

Hinshaw VS, Olsen CW, Dybdahl-Sissoko N, Evans D. Apoptosis: a mechanism of cell killing by influenza A and B viruses. J Virol. 1994 Jun; 68(6): 3667-73.

Hirt UA, Gantner F, Leist M. Phagocytosis of nonapoptotic cells dying by caspase-independent mechanisms. J. Immunol. 2000:164, 6520–6529.

Hofseth LJ, Hussain SP, Harris CC. p53: 25 years after its discovery. Trends Pharmacol Sci. 2004 Apr;25(4):177-81.

Holler N, Zaru R, Micheau O, Thome M, Attinger A, Valitutti S, Bodmer JL, Schneider P, Seed B, Tschopp J. Fas triggers an alternative, caspase-8-independent cell death pathway using the kinase RIP as effector molecule. Nat Immunol. 2000 Dec;1(6):489-95

Holsinger LJ, Nichani D, Pinto LH, Lamb RA. Influenza A virus M_2 ion channel protein: a structure-function analysis. J Virol 1994;68: 1551-1563.

Hom LG, Ohkawa T, Trudeau D, Volkman LE. Autographa californica M nucleopolyhedrovirus ProV-CATH is activated during infected cell death. Virology. 2002 May 10;296(2):212-8.

Horisberger MA. The large P proteins of influenza A viruses are composed of one acidic and two basic polypeptides. Virology 1980;107: 302-305.

Hughey PG, Compans RW, Zebedee SL, Lamb RA. Expression of the influenza A virus M_2 protein is restricted to apical surfaces of polarized epithelial cells. J Virol 1992;66:5542-5552.

Inglis SC, Almond JW. An influenza virus gene encoding two different proteins. Phil Trans R Soc Lond 1980;288:375-381.

Inglis SC,Carroll AR, Lamb RA, Mahy BW. Polypeptides specified by the influenza virus genome. I. Evidence for eight distinct gene products specified by fowl plague virus. Virology 1976;74:489-503.

Ishisaka R, Kanno T, Kanematsu H, Utsumi T, Akiyama J, Horton AA, Yoshioka T. Superoxide dismutase-like activity of metal substituted lactoferrin derivatives. Physiol Chem Phys Med NMR. 1998;30(1):1-13.

Ishisaka R, Utsumi T, Kanno T, Arita K, Katunuma N, Akiyama J, Utsumi K. Participation of a cathepsin L-type protease in the activation of caspase-3. Cell Struct Funct. 1999 Dec;24(6):465-70.

Itoh N, Yonehara S, Ishii A, Yonehara M, Mizushima S, Sameshima M, Hase A, Seto Y, Nagata S. The polypeptide encoded by the cDNA for human cell surface antigen Fas can mediate apoptosis. Cell. 1991 Jul 26;66(2):233-43.

Jackson DC, Tang XL, Murti KG, Webster RG, Tregear GW, Bean WJ. Electron microscopic evidence for the association of M_2, protein with the influenza virion. Arch Virol 1991;118:199-207.

Jaeschke H, Lemasters JJ. Apoptosis versus oncotic necrosis in hepatic ischemia/reperfusion injury. Gastroenterology. 2003 Oct;125(4):1246-57.

Janicke RU, Ng P, Sprengart ML, Porter AG. Caspase-3 is required for alpha-fodrin cleavage but dispensable for cleavage of other death substrates in apoptosis. J Biol Chem. 1998 Jun 19;273(25):15540-5.

Jiang X, Wang X. Cytochrome C-mediated apoptosis. Annu Rev Biochem. 2004;73:87-106.

Jochova J, Quaglino D, Zakeri Z, Woo K, Sikorska M, Weaver V and Lockshin RA. Protein synthesis, DNA degradation, and morphological changes during programmed cell death in labial glands of *Manduca sexta*. Dev. Genet.1997 21: 249 – 257.

Johansson AC, Steen H, Ollinger K, Roberg K. Cathepsin D mediates cytochrome c release and caspase activation in human fibroblast apoptosis induced by staurosporine. Cell Death Differ. 2003 Nov;10(11):1253-9.

Kagedal K, Johansson U, Ollinger K. The lysosomal protease cathepsin D mediates apoptosis induced by oxidative stress. FASEB J. 2001 Jul;15(9):1592-4.

Kakegawa H, Nikawa T, Tagami K, Kamioka H, Sumitani K, Kawata T, Drobnic-Kosorok M, Lenarcic B, Turk V, Katunuma N. Participation of cathepsin L on bone resorption. FEBS Lett. 1993 Apr 26;321(2-3):247-50.

Kamada S, Kikkawa U, Tsujimoto Y, Hunter T. Nuclear translocation of caspase-3 is dependent on its proteolytic activation and recognition of a substrate-like protein(s). J Biol Chem. 2004 Nov 29.

Karasavvas N, Erukulla RK, Bittman R, Lockshin R, Zakeri Z. Stereospecific induction of apoptosis in U937 cells by N-octanoyl-sphingosine stereoisomers and N-octyl-sphingosine. The ceramide amide group is not required for apoptosis. Eur J Biochem. 1996 Mar 1;236(2):729-37.

Kassis R, Larrous F, Estaquier J, Bourhy H. Lyssavirus matrix protein induces apoptosis by a TRAIL-dependent mechanism involving caspase-8 activation. J Virol. 2004 Jun;78(12):6543-55.

Katunuma N, Matsui A, Le QT, Utsumi K, Salvesen G, Ohashi A. Novel procaspase-3 activating cascade mediated by lysoapoptases and its biological significances in apoptosis. Adv Enzyme Regul. 2001;41:237-50.

Kerr JF. A histochemical study of hypertrophy and ischaemic injury of rat liver with special reference to changes in lysosomes. J Pathol Bacteriol. 1965 Oct;90(2):419-35.

Kerr JF. An electron-microscope study of liver cell necrosis due to heliotrine. J Pathol. 1969 Mar;97(3):557-62.

Kerr JF. Shrinkage necrosis: a distinct mode of cellular death. J Pathol. 1971 Sep;105(1):13-20.

Kerr JF. Shrinkage necrosis of adrenal cortical cells. J Pathol. 1972 Jul;107(3):217-9.

Kerr JF, Wyllie AH, Currie AR. Apoptosis: a basic biological phenomenon with wide-ranging implications in tissue kinetics. Br J Cancer. 1972 Aug;26(4):239-57.

Khaled AR, Durum SK. Lymphocide: cytokines and the control of lymphoid homeostasis. Nat Rev Immunol. 2002 Nov;2(11):817-30.

Kitanaka C, Kuchino Y. Caspase-independent programmed cell death with necrotic morphology. Cell Death Differ. 1999 Jun;6(6):508-15.

Klenk HD, Garten W. Host cell proteases controlling virus pathogenicity. Trends in microbiology 1994;2:39-43.

Klenk HD, Rott R, Orlich M, Blodorn J. Activation of influenza A viruses by trypsin treatment. Virology 1975;68:426-439.

Ko LJ, Prives C. p53: puzzle and paradigm. Genes Dev. 1996 May 1;10(9):1054-72.

Kos J, Lah TT. Cysteine proteinases and their endogenous inhibitors: target proteins for prognosis, diagnosis and therapy in cancer. Oncol Rep. 1998 Nov-Dec;5(6):1349-61.

Kroemer G. Mitochondrial control of apoptosis: an introduction. Biochem Biophys Res Commun. 2003 May 9;304(3):433-5.

Kroemer G, Petit P, Zamzami N, Vayssiere JL, Mignotte B. The biochemistry of programmed cell death. FASEB J. 1995 Oct;9(13):1277-87.

Kroemer G, Reed JC. Mitochondrial control of cell death. Nat Med. 2000 May;6(5):513-9.

Krug RM, Etkind PR. Cytoplasmic and nuclear virus-specific proteins in influenza virus-infected MDCK cells. Virology 1973;56:334-348.

Krzyzowska M, Schollenberger A, Niemialtowski MG. How human immunodeficiency viruses and herpesviruses affect apoptosis. Acta Virol. 2000 Jun-Aug;44(3):203-10.

Kurokawa M, Koyama AH, Yasuoka S, Adachi A. Influenza virus overcomes apoptosis by rapid multiplication. Int J Mol Med. 1999 May;3(5):527-30.

Labarque G, Van Gucht S, Nauwynck H, Van Reeth K, Pensaert M. Apoptosis in the lungs of pigs infected with porcine reproductive and respiratory syndrome virus and associations with the production of apoptogenic cytokines. Vet Res. 2003 May-Jun;34(3):249-60.

Lamb RA. Genes and proteins of the influenza viruses. In: Krug RM, ed. The influenza viruses. New York: Plenum Press, 1989;1-87.

Lamb RA, Choppin PW. Synthesis of influenza virus proteins in infected cells: translation of viral polypeptides, including three P polypeptides, from RNA produced by primary transcription. Virology 1976; 74:504-519.

Lamb RA, Choppin PW, Chanock RM, Lai CJ. Overlapping genes for polypeptides NS_1 and NS_2 on RNA segment 8. Mapping of the two of influenza virus genome. Proc Natl Acad Sci USA 1980;77:1857-1861.

Lamb RA, Choppin PW. A ninth unique influenza virus-coded polypeptide. Philos Trans R Soc Land (Bioi) 1980;288:327-333.

Lamb RA, Choppin PW. The gene structure and replication of influenza virus. Ann Rev Biochem 1983;52:467-506.

Lamb RA, Lai CJ. Sequence of interrupted and uninterrupted mRNAs and cloned DNA coding for the two overlapping nonstructural proteins of influenza virus. Cell 1980;21 :475-485.

Lamb RA, Lai CJ, Choppin PW. Sequences of mRNAs derived from genome RNA segment 7 of influenza virus: Colinear and interrupted mRNAs code for overlapping proteins. Proc Natl Acad Sci USA 1981 ; 78:4170-4174.

Lamb RA, Lai CJ. Conservation of the influenza virus membrane protein (M_1) amino acid sequence and an open reading frame of RNA segment 7 encoding a second protein (M_2) in H1N1 and H3N2 strains. Virology 1981;112:746-751.

Lamb RA, Zebedee SL, Richardson CD. Influenza virus M_2 protein is an integral membrane protein expressed on the infected-cell surface. Cell 1985;40:627-633.

Lang-Rollin IC, Rideout HJ, Noticewala M, Stefanis L. Mechanisms of caspase-independent neuronal death: energy depletion and free radical generation. J Neurosci. 2003 Dec 3;23(35):11015-25.

Lazarowitz SG, Compans RW, Choppin PW. Influenza virus structural and nonstructural proteins in infected cells and their plasma membranes. Virology 1971;46:830-843.

Lazarowitz SG, Choppin PW. Enhancement of the infectivity of influenza A and B viruses by proteolytic cleavage of the hemagglutinin polypeptide. Virology 1975;68:440-454.

Lee CY, Cooksey BA, Baehrecke EH. Steroid regulation of midgut cell death during Drosophila development. Dev Biol. 2002 Oct 1;250(1):101-11.

Leist M and Jaattela M. Four deaths and a funeral: from caspases to alternative mechanisms. Nat Rev Mol Cell Biol 2: 589_598, 2001.

Levine B, Griffin DE. Molecular analysis of neurovirulent strains of Sindbis virus that evolve during persistent infection of scid mice. J Virol. 1993 Nov;67(11):6872-5.

Li ML, Stollar V. Alphaviruses and apoptosis. Int Rev Immunol. 2004 Jan-Apr;23(1-2):7-24.

Lichtenstein DL, Toth K, Doronin K, Tollefson AE, Wold WS. Functions and mechanisms of action of the adenovirus E3 proteins. Int Rev Immunol. 2004 Jan-Apr;23(1-2):75-111.

Lin BC, Lai CI. The influenza virus nucleoprotein synthesized from cloned DNA in a simian virus 40 vector is detected in the nucleus. Virol 1983;45:434-438.

Liu H, Pope RM Apoptosis in rheumatoid arthritis: friend or foe. Rheum Dis Clin North Am. 2004 Aug;30(3):603-25, x.

Lockshin RA. Programmed cell death. Activation of lysis by a mechanism involving the synthesis of protein. J Insect Physiol. 1969 Sep;15(9):1505-16.

Lockshin RA. Degeneration of insect intersegmental muscles: electrophysiological studies of populations of fibres. J Insect Physiol. 1973 Dec;19(12):2359-72.

Lockshin RA, Beaulation J. Programmed cell death. Cytochemical evidence for lysosomes during the normal breakdown of the intersegmental muscles. Ultrastruct Res. 1974 Jan;46(1):43-62.

Lockshin RA, Beaulaton J. Programmed cell death. Cytochemical appearance of lysosomes when death of the intersegmental muscles is prevented. J Ultrastruct Res. 1974 Jan;46(1):63-78.

Lockshin RA, Williams CM. Programmed cell death. IV. The influence of drugs on the breakdown of the intersegmental muscles of silkmoths. J Insect Physiol. 1965 Jun;11(6):803-9.

Lockshin RA, Zakeri Z. Physiology and protein synthesis in programmed cell death. Early synthesis and DNA degradation. Ann N Y Acad Sci. 1992 Nov 21;663:234-49.

Lockshin RA, Zakeri Z. Caspase-independent cell deaths. Curr Opin Cell Biol. 2002 Dec;14(6):727-33.

Lockshin RA, Zakeri Z. Apoptosis, autophagy, and more. Int J Biochem Cell Biol. 2004 Dec;36(12):2405-19.

Lopez-Otin C, Overall CM. Protease degradomics: a new challenge for proteomics. Nat Rev Mol Cell Biol. 2002 Jul;3(7):509-19.

Lorenzo HK, Susin SA, Penninger J, Kroemer G. Apoptosis inducing factor (AIF): a phylogenetically old, caspase-independent effector of cell death. Cell Death Differ. 1999 Jun;6(6):516-24.

Lorenzo HK, Susin SA. Mitochondrial effectors in caspase-independent cell death. FEBS Lett. 2004 Jan 16;557(1-3):14-20

Lowe SW, Schmitt EM, Smith SW, Osborne BA, Jacks T. p53 is required for radiation-induced apoptosis in mouse thymocytes. Nature. 1993 Apr 29;362(6423):847-9.

Lu Y, Qian XY, Krug RM. The influenza virus NS1 protein: a novel inhibitor of pre-mRNA splicing.Genes Dev. 1994 Aug 1;8(15):1817-28.

Lu Y, Wambach M, Katze MG, Krug RM. Binding of the influenza virus NS1 protein to double-stranded RNA inhibits the activation of the protein kinase that phosphorylates the eIF-2 translation initiation factor. Virology. 1995 Dec 1;214(1):222-8.

Lyles DS. Cytopathogenesis and inhibition of host gene expression by RNA viruses. Microbiol Mol Biol Rev. 2000 Dec;64(4):709-24.

Marino G, Lopez-Otin C. Autophagy: molecular mechanisms, physiological functions and relevance in human pathology. Cell Mol Life Sci. 2004 Jun;61(12):1439-54.

Marsh M, Helenius A. Virus entry into animal cells. Adv Virus Res 1989;36:107-151.

Martin K, Helenius A. Nuclear transport of influenza virus ribonucleoproteins: the viral matrix protein (M_1) promotes export and inhibits import. Cell 1991,67.117-130.

Martinou JC, Green DR.Breaking the mitochondrial barrier. Nat Rev Mol Cell Biol. 2001 Jan;2(1):63-7.

Mason, R.W. (1995). Subcellular Biochemistry, Vol. 27, edited by J. B. Lloyd & R. W. Mason, pp. 159-190. Dordrecht: Kluwer.

Matassov D, Kagan T, Leblanc J, Sikorska M, Zakeri Z. Measurement of apoptosis by DNA fragmentation. Methods Mol Biol. 2004;282:1-17.

Mathiasen IS, Jaattela M. Triggering caspase-independent cell death to combat cancer. Trends Mol Med. 2002 May;8(5):212-20.

Matlin KS, Reggio H, Helenius A, Simons K: The entry of enveloped viruses into an epithelial cell line. Prog Clin Biol Res 1982;91:599-611.

Mattson MP, Kroemer G. Mitochondria in cell death: novel targets for neuroprotection and cardioprotection. Trends Mol Med. 2003 May;9(5):196-205.

Mihara M, Erster S, Zaika A, Petrenko O, Chittenden T, Pancoska P, Moll UM.p53 has a direct apoptogenic role at the mitochondria.
Mol Cell. 2003 Mar;11(3):577-90.

Mikulasova A, Vareckova E, Fodor E. Transcription and replication of the influenza a virus genome. Acta Virol. 2000 Oct;44(5):273-82.

Mori I, Komatsu T, Takeuchi K, Nakakuki K, Sudo M, Kimura Y. In vivo induction of apoptosis by influenza virus. J Gen Virol. 1995 Nov;76 (Pt 11):2869-73.

Moroni MC, Hickman ES, Denchi EL, Caprara G, Colli E, Cecconi F, Muller H, Helin K. Apaf-1 is a transcriptional target for E2F and p53. Nat Cell Biol. 2001 Jun;3(6):552-8.

Morris GE. Nuclear proteins and cell death in inherited neuromuscular disease. Neuromuscul Disord. 2000 Jun;10(4-5):217-27.

Morris SJ, Price GE, Barnett JM, Hiscox SA, Smith H, Sweet C. Role of neuraminidase in influenza virus-induced apoptosis. J Gen Virol. 1999 Jan;80 (Pt 1):137-46.

Mukae N, Enari M, Sakahira H, Fukuda Y, Inazawa J, Toh H, Nagata S. Molecular cloning and characterization of human caspase-activated DNase. Proc Natl Acad Sci U S A. 1998 Aug 4;95(16):9123-8.

Muppidi JR, Tschopp J, Siegel RM. Life and death decisions: secondary complexes and lipid rafts in TNF receptor family signal transduction. Immunity. 2004 Oct;21(4):461-5.

Muster T, Rajtarova J, Sachet M, Unger H, Fleischhacker R, Romirer I, Grassauer A, Url A, Garcia-Sastre A, Wolff K, Pehamberger H, Bergmann M. Interferon resistance promotes oncolysis by influenza virus NS1-deletion mutants. Int J Cancer. 2004 May 20;110(1):15-21.

Muzio M, Chinnaiyan AM, Kischkel FC, O'Rourke K, Shevchenko A, Ni J, Scaffidi C, Bretz JD, Zhang M, Gentz R, Mann M, Krammer PH, Peter ME, Dixit VM. FLICE, a novel FADD-homologous ICE/CED-3-like protease, is recruited to the CD95 (Fas/APO-1) death--inducing signaling complex. Cell. 1996 Jun 14;85(6):817-27.

Nain M, Hinder F, Gong JH, Schmidt A, Bender A, Sprenger H, Gemsa D. Tumor necrosis factor-alpha production of influenza A virus-infected macrophages and potentiating effect of lipopolysaccharides. J Immunol. 1990 Sep 15;145(6):1921-8.

Nanavaty UB, Pawliczak R, Doniger J, Gladwin MT, Cowan MJ, Logun C, Shelhamer JH. Oxidant-induced cell death in respiratory epithelial cells is due to DNA damage and loss of ATP. Exp Lung Res. 2002 Dec;28(8):591-607.

Narayanan K, Chen CJ, Maeda J, Makino S. Nucleocapsid-independent specific viral RNA packaging via viral envelope protein and viral RNA signal. J Virol. 2003 Mar;77(5):2922-7.

Neumann G, Brownlee GG, Fodor E, Kawaoka Y. Orthomyxovirus replication, transcription, and polyadenylation. Curr Top Microbiol Immunol. 2004;283:121-43.

Nicholson DW. Caspase structure, proteolytic substrates, and function during apoptotic cell death. Cell Death Differ. 1999 Nov;6(11):1028-42.

Nicotera P, Leist M, Fava E, Berliocchi L, Volbracht C. Energy requirement for caspase activation and neuronal cell death. Brain Pathol 2000; 10: 276–282. 2000; 460: 1–15.

Nicotera P, Leist M, and Ferrando-May E. Intracellular ATP, a switch in the decision between apoptosis and necrosis. Toxicol Lett 1998 102-103: 139-142.

Nicotera P, Leist M, Ferrando-May E. Apoptosis and necrosis: different execution of the same death. Biochem Soc Symp. 1999;66:69-73

Nobusawa E Aoyama T Kato H, Suzuki Y, Tateno Y, Nakajima K Comparison of complete amino acid sequences and receptor-binding properties among 13 serotypes of hemagglutinin of influenza A viruses Virology 1991.182:475-485.

Noteborn MH.Chicken anemia virus induced apoptosis: underlying molecular mechanisms. Vet Microbiol. 2004 Feb 4;98(2):89-94.

Nylandsted, J. *et al.* Selective depletion of heat shock protein 70 (Hsp70) activates a tumor-specific death program that is independent of caspases and bypasses Bcl-2. Proc. Natl Acad. Sci. USA 2000:97, 7871–7876.

O'Brien V. Viruses and apoptosis. J Gen Virol. 1998 Aug;79 (Pt 8):1833-45.

Okada H, Mak TW. Pathways of apoptotic and non-apoptotic death in tumour cells. Nat Rev Cancer. 2004 Aug;4(8):592-603.

O'Neill RE, Talon J, Palese P. The influenza virus NEP (NS2 protein) mediates the nuclear export of viral ribonucleoproteins. EMBO J. 1998 Jan 2;17(1):288-96.

Opalka B, Dickopp A, Kirch HC. Apoptotic genes in cancer therapy. Cells Tissues Organs. 2002;172(2):126-32.

Oppenheim RW. Cell death during development of the nervous system. Annu Rev Neurosci. 1991;14:453-501.

Palese P, Tobita K, Ueda M, Compans RW. Characterization of temperature sensitive influenza virus mutants defective in neuraminidase. Virology 1974;61:397-410.

Perl A, Gergely P, Nagy G, Koncz A and Banki K. Mitochondrial hyperpolarization: a checkpoint of T-cell life, death and autoimmunity TRENDS in Immunology 20004 Vol.25 No.7 July.
Perfettini JL, Kroemer G. Caspase activation is not death. Nat Immunol. 2003 Apr;4(4):308-10.

Peschke T, Bender A, Nain M, Gemsa D. Role of macrophage cytokines in influenza A virus infections. Immunobiology. 1993 Nov;189(3-4):340-55.

Petit F, Arnoult D, Viollet L, Estaquier J. Intrinsic and extrinsic pathways signaling during HIV-1 mediated cell death. Biochimie. 2003 Aug;85(8):795-811.

Petri T, Dimmock NJ. Phosphorylation of influenza virus nucleoprotein in vivo. J Gen Virol 1981;57:185-190.

Pirhonen J, Sareneva T, Kurimoto M, Julkunen I, Matikainen S. Virus infection activates IL-1 beta and IL-18 production in human macrophages by a caspase-1-dependent pathway. J Immunol. 1999 Jun 15;162(12):7322-9.

Pistritto G, Jost M, Srinivasula SM, Baffa R, Poyet JL, Kari C, Lazebnik Y, Rodeck U, Alnemri ES. Expression and transcriptional regulation of caspase-14 in simple and complex epithelia. Cell Death Differ. 2002 Sep;9(9):995-1006.

Polster BM, Fiskum G. Mitochondrial mechanisms of neural cell apoptosis. J Neurochem. 2004 Sep;90(6):1281-9.

Pons MW, Schulze IT, Hirst GK, Hauser R. Isolation and characterization of the ribonucleoprotein of influenza virus. Virology 1969;39: 250-259.

Pons MW. Isolation of influenza virus ribonucleoprotein from infected cells. Demonstration of the presence of negative-stranded RNA in viral RNP. Virology 1971;46:149-160.

Porter AG, Barber C, Carey NH, Hallewell RA, Threlfall G, Emtage JS. Complete nucleotide sequence of an influenza virus haemagglutinin gene from cloned DNA. Nature 1979;282:471-477.

Porter AG, Dhakshinamoorthy S.Apoptosis initiated by dependence receptors: a new paradigm for cell death? Bioessays. 2004 Jun;26(6):656-64.

Price DL, Sisodia SS, Borchelt DR. Genetic neurodegenerative diseases: the human illness and transgenic models. Science. 1998 Nov 6;282(5391):1079-83.

Privalsky ML, Penhoet EE. Phosphorylated protein component present in influenza virions. J ViroI1977;24:401-405.

Ravagnan L, Roumier T, Kroemer G. Mitochondria, the killer organelles and their weapons. J Cell Physiol. 2002 Aug;192(2):131-7.

Rees PJ, Dimmock NJ. Electrophoretic separation of influenza virus ribonucleoproteins. J Gen Virol 1981;53:125-132.

Richardson JC, Akkina RK. NS_2 protein of influenza virus is found in purified virus and phosphorylated in infected cells. Arch Virol 1991; 116:69-80.

Roberg K, Kagedal K, Ollinger K. Microinjection of cathepsin D induces caspase-dependent apoptosis in fibroblasts. Am J Pathol. 2002 Jul;161(1):89-96.

Ross CA, Poirier MA. Protein aggregation and neurodegenerative disease. Nat Med. 2004 Jul;10 Suppl:S10-7.

Rossi D, Gaidano G. Messengers of cell death: apoptotic signaling in health and disease. Haematologica. 2003 Feb;88(2):212-8.

Roy S, Bayly CI, Gareau Y, Houtzager VM, Kargman S, Keen SL, Rowland K, Seiden IM, Thornberry NA, Nicholson DW. Maintenance of caspase-3 proenzyme dormancy by an intrinsic "safety catch" regulatory tripeptide. Proc Natl Acad Sci U S A. 2001 May 22;98(11):6132-7.

Rusnak JM, Calmels TP, Hoyt DG, Kondo Y, Yalowich JC, Lazo JS. Genesis of discrete higher order DNA fragments in apoptotic human prostatic carcinoma cells.Mol Pharmacol. 1996 Feb;49(2):244-52.

Saito T, Tanaka M, Yamaguchi I. Effect of brefeldin A on influenza A virus-induced apoptosis in vitro. J Vet Med Sci. 1996 Nov;58(11):1137-9.

Salmen S, Teran G, Borges L, Goncalves L, Albarran B, Urdaneta H, Montes H, Berrueta L. Increased Fas-mediated apoptosis in polymorphonuclear cells from HIV-infected patients. Clin Exp Immunol. 2004 Jul;137(1):166-72.

Samuel CE. Antiviral actions of interferon. Interferon-regulated cellular proteins and their surprisingly selective antiviral activities.Virology. 1991 Jul;183(1):1-11.

Sandvig K and van Deurs B. Toxin-induced cell lysis: protection by 3-methyladenine and cycloheximide. Exp. Cell Res. 1992; 200: 253 – 262

Sato SB, Kawilsaki K, Ohnishi S-I. Haemolytic activity of influenza virus haemagglutinin glycoproteins activated in mildly acidic environments. Proc Natl AcadSci USA 1983;80:3153-3157.

Savill J, Fadok V. Corpse clearance defines the meaning of cell death. Nature. 2000 Oct 12;407(6805):784-8.

Sawa A, Tomoda T, Bae BI. Mechanisms of neuronal cell death in Huntington's disease. Cytogenet Genome Res. 2003;100(1-4):287-95.
Schultz DR, Harrington WJ Jr. Apoptosis: programmed cell death at a molecular level. Semin Arthritis Rheum. 2003 Jun;32(6):345-69.

Schultz-Cherry S, Hinshaw VS. Influenza virus neuraminidase activates latent transforming growth factor beta. J Virol. 1996 Dec;70(12):8624-9.

Schultz-Cherry S, Dybdahl-Sissoko N, Neumann G, Kawaoka Y, Hinshaw VS. Influenza virus ns1 protein induces apoptosis in cultured cells. J Virol. 2001 Sep;75(17):7875-81.

Schweichel JU, Merker HJ. The morphology of various types of cell death in prenatal tissues. Teratology. 1973 Jun;7(3):253-66.

Searle J. Letter: Cytolysis. Cancer Res. 1975 Oct;35(10):2900-1.

Seglen PO and Jordan PB. 3-Methyladenine, a specific inhibitor of autophagic/lysosomal protein degradation in isolated rat hepatocytes. Proc. Natl. Acad. Sci. USA 1982:79: 1889 – 1892.

Seo SH, Hoffmann E, Webster RG. The NS1 gene of H5N1 influenza viruses circumvents the host anti-viral cytokine responses. Virus Res. 2004 Jul;103(1-2):107-13.

Serrano M, Lin AW, McCurrach ME, Beach D, Lowe SW. Oncogenic ras provokes premature cell senescence associated with accumulation of p53 and p16INK4a. Cell. 1997 Mar 7;88(5):593-602.

Sesso A, Marques MM, Monteiro MM, Schumacher RI, Colquhoun A, Belizario J, Konno SN, Felix TB, Botelho LA, Santos VZ, Da Silva GR, Higuchi MD, Kawakami JT. Sprick MR, Walczak H. The interplay between the Bcl-2 family and death receptor-mediated apoptosis Biochimica et Biophysica Acta 1644 (2004) 125– 132.

Sheriff A, Gaipl US, Voll RE, Kalden JR, Herrmann M. Apoptosis and systemic lupus erythematosus. Rheum Dis Clin North Am. 2004 Aug;30(3):505-27, viii-ix.

Shi GP, Bryant RA, Riese R, Verhelst S, Driessen C, Li Z, Bromme D, Ploegh HL, Chapman HA. Role for cathepsin F in invariant chain processing and major histocompatibility complex class II peptide loading by macrophages. J Exp Med. 2000 Apr 3;191(7):1177-86.

Shi Y.Mechanisms of caspase activation and inhibition during apoptosis. Mol Cell. 2002 Mar;9(3):459-70.

Shi Y.Caspase activation, inhibition, and reactivation: a mechanistic view. Protein Sci. 2004 Aug;13(8):1979-87.

Shibata M, Kanamori S, Isahara K, Ohsawa Y, Konishi A, Kametaka S, Watanabe T, Ebisu S, Ishido K, Kominami E, Uchiyama Y. Participation of cathepsins B and D in apoptosis of PC12 cells following serum deprivation. Biochem Biophys Res Commun. 1998 Oct 9;251(1):199-203.

Siegel PM, Massague J. Cytostatic and apoptotic actions of TGF-beta in homeostasis and cancer. Nat Rev Cancer. 2003 Nov;3(11):807-21.

Singh KK. Mitochondria damage checkpoint in apoptosis and genome stability. FEMS Yeast Res. 2004 Nov;5(2):127-32.

Singh S, Bhat MK. Carboplatin induces apoptotic cell death through downregulation of constitutively active nuclear factor-kappaB in human HPV-18 E6-positive HEp-2 cells.

Biochem Biophys Res Commun. 2004 May 28;318(2):346-53.

Skehel JJ, Daniels RS, Hay AJ, Ruigrok RWH, Wharton SA, Wrigley NG, Weiss W, Wiley DC. Structure changes in influenza virus haemagglutinin at the pH of membrane fusion. Biochem Soc Trans 1986;14: 252-253.

Slee EA, Adrain C, Martin SJ. Serial killers: ordering caspase activation events in apoptosis. Cell Death Differ. 1999 Nov;6(11):1067-74.

Sloane BF, Moin K, Sameni M, Tait LR, Rozhin J, Ziegler G. Membrane association of cathepsin B can be induced by transfection of human breast epithelial cells with c-Ha-ras oncogene. J Cell Sci. 1994 Feb;107 (Pt 2):373-84.

Soldani C, Scovassi AI. Poly(ADP-ribose) polymerase-1 cleavage during apoptosis: an update. Apoptosis. 2002 Aug;7(4):321-8.

Sphyris N, Morris RG, Harrison DJ. Induction of p21 and nuclear accumulation of TAp73alpha and c-abl during apoptosis of cisplatin-treated primary pancreatic acinar cells. Int J Oncol. 2004 Dec;25(6):1661-70.

Stoka V et al. Lysosomal protease pathways to apoptosis. Cleavage of bid, not pro-caspases, is the most likely route. J Biol Chem. 2001 Feb 2;276(5):3149-57.

Suda T, Takahashi T, Golstein P, Nagata S. Molecular cloning and expression of the Fas ligand, a novel member of the tumor necrosis factor family. Cell. 1993 Dec 17;75(6):1169-78.

Susin SA, Lorenzo HK, Zamzami N, Marzo I, Snow BE, Brothers GM, Mangion J, Jacotot E, Costantini P, Loeffler M, Larochette N, Goodlett DR, Aebersold R, Siderovski DP, Penninger JM, Kroemer G. Molecular characterization of mitochondrial apoptosis-inducing factor.Nature. 1999 Feb 4;397(6718):441-6.

Suzuki Y, Imai Y, Nakayama H, Takahashi K, Takio K, Takahashi R.A serine protease, HtrA2, is released from the mitochondria and interacts with XIAP, inducing cell death. Mol Cell. 2001 Sep;8(3):613-21.

Syntichaki P, Tavernarakis N. Death by necrosis. Uncontrollable catastrophe, or is there order behind the chaos? EMBO Rep. 2002 Jul;3(7):604-9.
Takizawa T, Fukuda R, Miyawaki T, Ohashi K, Nakanishi Y. Activation of the apoptotic Fas antigen-encoding gene upon influenza virus infection involving spontaneously produced beta-interferon. Virology. 1995 Jun 1;209(2):288-96.

Takizawa T, Matsukawa S, Higuchi Y, Nakamura S, Nakanishi Y, Fukuda R. Induction of programmed cell death (apoptosis) by influenza virus infection in tissue culture cells. J Gen Virol. 1993 Nov; 74 (Pt 11): 2347-55.

Takizawa T, Ohashi K, Nakanishi Y. Possible involvement of double-stranded RNA-activated protein kinase in cell death by influenza virus infection. J Virol. 1996 Nov;70(11):8128-32.

Takizawa T, Tatematsu C, Ohashi K, Nakanishi Y. Recruitment of apoptotic cysteine proteases (caspases) in influenza virus-induced cell death. Microbiol Immunol. 1999;43(3):245-52.

Tanaka M, Suda T, Takahashi T, Nagata S. Expression of the functional soluble form of human fas ligand in activated lymphocytes. EMBO J. 1995 Mar 15;14(6):1129-35.

Tepel C, Bromme D, Herzog V, Brix K. Cathepsin K in thyroid epithelial cells: sequence, localization and possible function in extracellular proteolysis of thyroglobulin. J Cell Sci. 2000 Dec;113 Pt 24:4487-98.

Testa U. Apoptotic mechanisms in the control of erythropoiesis. Leukemia. 2004 Jul;18(7):1176-99.

Toomes C et al. Loss-of-function mutations in the cathepsin C gene result in periodontal disease and palmoplantar keratosis. Nat Genet. 1999 Dec;23(4):421-4.

Turk B, Dolenc I, Turk V, Bieth JG. Kinetics of the pH-induced inactivation of human cathepsin L. Biochemistry. 1993 Jan 12;32(1):375-80.

Turk D, Guncar G. Lysosomal cysteine proteases (cathepsins): promising drug targets. Acta Crystallogr D Biol Crystallogr. 2003 Feb;59(Pt 2):203-13.

Turk B, Stoka V, Rozman-Pungercar J, Cirman T, Droga-Mazovec G, Oresic K, Turk V. Apoptotic pathways: involvement of lysosomal proteases. Biol Chem. 2002 Jul-Aug;383(7-8):1035-44.

Turk B, Turk D, Turk V. Lysosomal cysteine proteases: more than scavengers. Biochim Biophys Acta. 2000 Mar 7;1477(1-2):98-111.

Turk V, Turk B, Turk D. Lysosomal cysteine proteases: facts and opportunities. EMBO J. 2001 Sep 3;20(17):4629-33.

Ulmanen I, Broni BA, Krug RM. Role of two of the influenza virus core P proteins in recognizing cap I structures (m^7GpppNm) on RNAs and in initiating viral RNA transcription. Proc Natl Acad Sci USA 1981; 8:7355-7359.

Utz PJ, Anderson P. Life and death decisions: regulation of apoptosis by proteolysis of signaling molecules. Cell Death Differ. 2000 Jul;7(7):589-602.

Van Cruchten S, Van Den Broeck W. Morphological and biochemical aspects of apoptosis, oncosis and necrosis. Anat Histol Embryol. 2002 Aug;31(4):214-23.

Vercammen D, Beyaert R, Denecker G, Goossens V, Van Loo G, Declercq W, Grooten J, Fiers W, Vandenabeele P. Inhibition of caspases increases the sensitivity of L929 cells to necrosis mediated by tumor necrosis factor. J Exp Med. 1998 May 4;187(9):1477-85.

Verhagen AM, Ekert PG, Pakusch M, Silke J, Connolly LM, Reid GE, Moritz RL, Simpson RJ, Vaux DL. Identification of DIABLO, a mammalian protein that promotes apoptosis by binding to and antagonizing IAP proteins. Cell. 2000 Jul 7;102(1):43-53.

Verhoeyen M, Fang R, Min Jou W, Devos R, Huylebroeck D, Saman E, Fiers W. Antigenic drift between the haemagglutinin of the Hong Kong influenza strains A/ Aichi/2/68 and A/Victoria/3/75. Nature 1980; 286:771-776.

Vogelstein B, Kinzler KW. Cancer genes and the pathways they control. Nat Med. 2004 Aug;10(8):789-99.

Vogelstein B, Lane D, Levine AJ.Surfing the p53 network. Nature. 2000 Nov 16;408(6810):307-10.

Von Boehmer H. Positive selection of lymphocytes. Cell. 1994 Jan 28;76(2):219-28.

Vousden KH, Lu X. Live or let die: the cell's response to p53. Nat Rev Cancer. 2002 Aug;2(8):594-604.

Wada N, Matsumura M, Ohba Y, Kobayashi N, Takizawa T, Nakanishi Y. Transcription stimulation of the Fas-encoding gene by nuclear factor for interleukin-6 expression upon influenza virus infection. J Biol Chem. 1995 Jul 28;270(30):18007-12.

Wajant H, Pfizenmaier K, Scheurich P. Non-apoptotic Fas signaling. Cytokine Growth Factor Rev. 2003 Feb;14(1):53-66.

Walker NI, Harmon BV, Gobe GC, Kerr JF. Patterns of cell death. Methods Achiev Exp Pathol. 1988;13:18-54.

Walker PR, Sikorska M. New aspects of the mechanism of DNA fragmentation in apoptosis. Biochem Cell Biol. 1997;75(4):287-99.

Wang CW, Klionsky DJ. The molecular mechanism of autophagy. Mol Med. 2003 Mar-Apr;9(3-4):65-76.

Watts C. Antigen processing in the endocytic compartment. Curr Opin Immunol. 2001 Feb;13(1):26-31.

Westendorp MO, Frank R, Ochsenbauer C, Stricker K, Dhein J, Walczak H, Debatin KM, Krammer PH. Sensitization of T cells to CD95-mediated apoptosis by HIV-1 Tat and gp120. Nature. 1995 Jun 8;375(6531):497-500.

White S, Rosen A. Apoptosis in systemic lupus erythematosus. Curr Opin Rheumatol. 2003 Sep;15(5):557-62.

Wilkinson JC, Wilkinson AS, Scott FL, Csomos RA, Salvesen GS, Duckett CS. Neutralization of Smac/Diablo by inhibitors of apoptosis (IAPs). A caspase-independent mechanism for apoptotic inhibition. J Biol Chem. 2004 Dec 3;279(49):51082-90.

Winter G, Fields S. Nucleotide sequence of human influenza A/PR/8/34 segment 2. Nucleic Acid Res 1982;10:2135-2143.

Wolfe T, Asseman C, Hughes A, Matsue H, Takashima A, von Herrath MG. Reduction of antiviral CD8 lymphocytes in vivo with dendritic cells expressing Fas ligand-increased survival of viral (lymphocytic choriomeningitis virus) central nervous system infection. J Immunol. 2002 Nov 1;169(9):4867-72.

Wurzer WJ, Planz O, Ehrhardt C, Giner M, Silberzahn T, Pleschka S, Ludwig S. Caspase 3 activation is essential for efficient influenza virus propagation. EMBO J. 2003 Jun 2;22(11):2717-28.

Wyllie AH. Glucocorticoid-induced thymocyte apoptosis is associated with endogenous endonuclease activation. Nature. 1980 Apr 10;284(5756):555-6.

Wyllie AH. Apoptosis: cell death in tissue regulation. J Pathol. 1987 Dec;153(4):313-6.

Wyllie AH, Kerr JF, Currie AR. Cellular events in the adrenal cortex following ACTH deprivation. J Pathol. 1972 Jan;106(1):Pix

Wyllie AH, Kerr JF, Currie AR. Cell death: the significance of apoptosis. Int Rev Cytol. 1980;68:251-306.

Wyllie AH, Beattie GJ, Hargreaves AD. Chromatin changes in apoptosis. Histochem J. 1981 Jul;13(4):681-92.

Wyllie AH, Morris RG, Smith AL, Dunlop D. Chromatin cleavage in apoptosis: association with condensed chromatin morphology and dependence on macromolecular synthesis. J Pathol. 1984 Jan;142(1):67-77.

Xue L, Fletcher GC, Tolkovsky AM. Autophagy is activated by apoptotic signaling in sympathetic neurons: an alternative mechanism of death execution. Mol. Cell Neurosci. 1999: 14: 180 – 198.

Yakovlev AG, Di Giovanni S, Wang G, Liu W, Stoica B, Faden AI. BOK and NOXA are essential mediators of p53-dependent apoptosis. J Biol Chem. 2004 Jul 2;279(27):28367-74.

Yamada H, Chounan R, Higashi Y, Kurihara N, Kido H. Mitochondrial targeting sequence of the influenza A virus PB1-F2 protein and its function in mitochondria. FEBS Lett. 2004 Dec 17;578(3):331-6.

Yasuda I, Nakada S, Kato A, Toyoda T, Ishihama A. Molecular assembly of influenza virus: association of the NS, protein with virion matrix. Virology 1993;196:249-255.

Yazici Z, Baskin Y, Baskin H, Gecer O, Bahar IH, Ozkul A. Study of programmed cell death in bovine herpesvirus 1 infected MDBK cells and the possible role of nitric oxide in this process. Acta Vet Hung. 2004;52(3):287-97.

Yin Y, Liu YX, Jin YJ, Hall EJ, Barrett JC. PAC1 phosphatase is a transcription target of p53 in signalling apoptosis and growth suppression. Nature. 2003 Apr 3;422(6931):527-31.

Yu L, Lenardo MJ, Baehrecke EH. Autophagy and Caspases: A New Cell Death Program. Cell Cycle. 2004 Sep 20;3(9).

Yu J, Zhang L, Hwang PM, Kinzler KW, Vogelstein B.PUMA induces the rapid apoptosis of colorectal cancer cells. Mol Cell. 2001 Mar;7(3):673-82.

Zakeri ZF, Ahuja HS. Apoptotic cell death in the limb and its relationship to pattern formation. Biochem Cell Biol. 1994 Nov-Dec;72(11-12):603-13.

Zakeri Z, Lockshin RA. Cell death during development. J Immunol Methods. 2002 Jul 1;265(1-2):3-20.

Zakeri ZF, Quaglino D, Latham T, Lockshin RA. Delayed internucleosomal DNA fragmentation in programmed cell death. FASEB J. 1993 Mar;7(5):470-8.

Zamzami N, Kroemer G. The mitochondrion in apoptosis: how Pandora's box opens. Nat Rev Mol Cell Biol. 2001 Jan;2(1):67-71.

Zamzami N, Marchetti P, Castedo M, Hirsch T, Susin SA, Masse B, Kroemer G. Inhibitors of permeability transition interfere with the disruption of the mitochondrial transmembrane potential during apoptosis. FEBS Lett. 1996 Apr 8;384(1):53-7.

Zamzami N, Marchetti P, Castedo M, Zanin C, Vayssiere JL, Petit PX, Kroemer G. Reduction in mitochondrial potential constitutes an early irreversible step of programmed lymphocyte death in vivo. J Exp Med. 1995 May 1;181(5):1661-72.

Zebedee SL, Lamb RA. Influenza A virus M_2, protein: monoclonal antibody restriction of virus growth and detection of M_2, in virions. J Virol 1988;62:2762-2772.

Zebedee SL, Richardson CD, Lamb RA. Characterization of the influenza virus M, integral membrane protein and expression at the infected-cell surface from cloned cDNA. J ViroI1985;56:502-511.

Zhang J, Xu M.Apoptotic DNA fragmentation and tissue homeostasis.
Trends Cell Biol. 2002 Feb;12(2):84-9.

Zhang J, Leser GP, Pekosz A, Lamb RA. The cytoplasmic tails of the influenza virus spike glycoproteins are required for normal genome packaging. Virology. 2000 Apr 10;269(2):325-34.

Zhang MC, Liu HP, Demchik LL, Zhai YF, Yang da J.LIGHT sensitizes IFN-gamma-mediated apoptosis of HT-29 human carcinoma cells through both death receptor and mitochondria pathways.
Cell Res. 2004 Apr;14(2):117-24.

Zhirnov OP, Konakova TE, Garten W, Klenk H. Caspase-dependent N-terminal cleavage of influenza virus nucleocapsid protein in infected cells. J Virol. 1999 Dec;73(12):10158-63.

Zhirnov OP, Konakova TE, Wolff T, Klenk HD. NS1 protein of influenza A virus down-regulates apoptosis. J Virol. 2002 Feb;76(4):1617-25.

Zhivotovsky B, Kroemer G. Apoptosis and genomic instability. Nat Rev Mol Cell Biol. 2004 Sep;5(9):752-62.

Zhou BB, Elledge SJ. The DNA damage response: putting checkpoints in perspective. Nature. 2000 Nov 23;408(6811):433-9.

Zhu H, Shen Y, Shenk T. Human cytomegalovirus IE1 and IE2 proteins block apoptosis. J Virol. 1995 Dec;69(12):7960-70.

Ziegler U, Groscurth P. Morphological features of cell death. News Physiol Sci. 2004 Jun;19:124-8.

Zimmermann KC, Bonzon C, Green DR. The machinery of programmed cell death. Pharmacol Ther. 2001 Oct;92(1):57-70.